

UNIVERZITA PALACKÉHO V OLOMOUCI

Lékařská fakulta

**ŠTÚDIUM MOLEKULÁRNEJ PATOFYZIOLÓGIE
PRIMÁRNÝCH ERYTROCYTÓZ**

Dizertačná práca

Mgr. Barbora Kráľová

UNIVERZITA PALACKÉHO V OLOMOUCI

Lékařská fakulta

Ústav biologie



**ŠTÚDIUM MOLEKULÁRNEJ PATOFYZIOLÓGIE PRIMÁRNÝCH
ERYTROCYTÓZ**

Dizertačná práca

Mgr. Barbora Král'ová

Olomouc, 2022

Doktorský študijný program: Lékařská biologie
Školiteľ: doc. Mgr. Monika Horváthová, Ph.D.

Prehlásenie:

Týmto prehlasujem, že predloženú dizertačnú prácu som napísala samostatne, pod vedením mojej školiteľky doc. Mgr. Moniky Horváthovej, Ph.D. a s použitím citovanej literatúry.

V Bratislave

Podčakovanie:

V prvom rade by som chcela úprimne podčakovať mojej školiteľke doc. Mgr. Monike Horváthovej, Ph.D. za jej nepretržitú podporu, trpezlivosť a všestrannú pomoc počas môjho Ph.D. štúdia. Bez jej vedenia a povzbudenia by nebolo možné dokončiť moje štúdium.

Okrem toho, moja vdaka patrí doc. RNDr. Vladimírovi Divokému, Ph.D. za jeho vedecký prínos a odborné pripomienky počas môjho Ph.D. štúdia. V neposlednom rade ďakujem aj všetkým spolupracovníkom na Ústave biologie LF UPOL, ktorí ma podporovali a prispeli k môjmu výskumu. Ďakujem tiež našim klinickým spolupracovníkom z Hemato-onkologickej kliniky a Detskej kliniky FN Olomouc za podporu a spoluprácu.

Na záver moje osobitné podčakovanie patrí priateľovi a rodine, ktorí ma motivovali a boli mi veľkou oporou.

OBSAH

1. TEORETICKÝ ÚVOD.....	1
1.1 Hematopoéza	1
1.1.1 Ontogenetický vývoj hematopoézy	2
1.2 Erytropoéza	3
1.2.1 Erytroidná diferenciácia a maturácia.....	3
1.2.2 Hemoglobín a prepínanie globínovej expresie.....	5
1.2.3 Odstraňovanie erytrocytov	6
1.2.4 Molekulárna regulácia erytropoézy.....	7
1.2.5 Erythropoetín a regulácia jeho produkcie	8
1.2 EPOR/JAK2 signalizácia v erytroidných bunkách	10
1.2.1 Neerytroidná aktivácia JAK2 signalizácie	13
1.3 Poruchy hematopoézy spojené s narušením JAK2 signalizácie	14
1.3.1 Primárne erytrocytózy	14
1.3.2 Myeloproliferatívne neoplázie	17
1.4 Prepojenie erytropoézy a metabolizmu železa.....	19
1.4.1 Príjem, transport a recyklácia železa.....	19
1.4.2 Systémová regulácia metabolizmu železa hepcidínom	21
1.4.3 Regulácia produkcie hepcidínu	22
2. CIELE DIZERTAČNEJ PRÁCE.....	26
2.1 Analýza dôsledkov <i>gain-of-function EPOR</i> mutácie na erytropoézu a metabolizmus železa na myšom modeli.....	26
2.2 Štúdium vybraných hereditárnych <i>JAK2</i> mutácií	26
2.3 Kritické zhodnotenie literatúry týkajúcej sa nových poznatkov patofysiologie Ph-negatívnych MPN	26
3. METODICKÉ POSTUPY.....	27
3.1 Postupy s použitím PFCP myšieho modelu	27
3.1.1 PFCP myší model.....	27
3.1.2 Genotypizácia PFCP myšieho modelu.....	27
3.1.3 Stanovenie expozície fosfatidylserínu.....	28
3.1.4 Stanovenie parametrov železa a detekcia železa v tkanive	28
3.1.5 Izolácia RNA z tkaniva	29
3.1.6 Stanovenie hladín hepcidínu, ferritínu, EPO.....	29

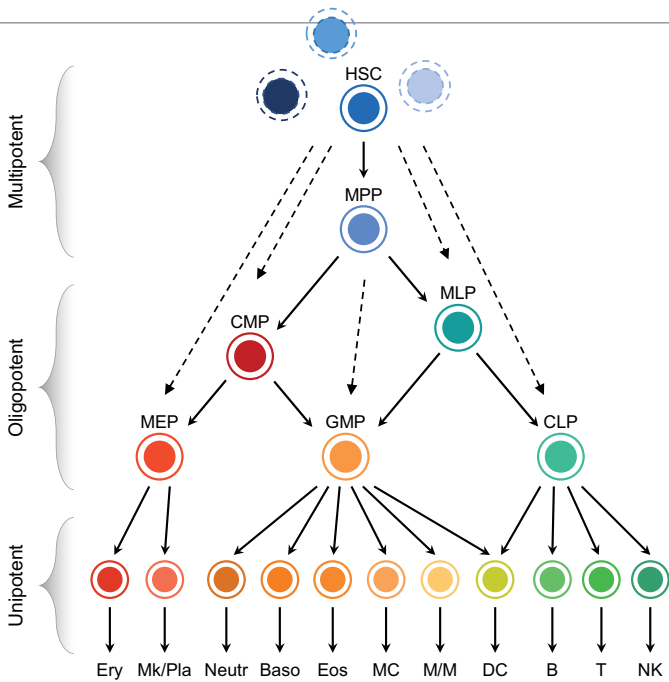
3.1.7	Kvantitatívna <i>real time</i> PCR	29
3.1.8	Analýza erytroidnej diferenciácie a maturácie pomocou prietokovej cytometrie.....	30
3.1.9	Meranie hladiny reaktívnych foriem kyslíka.....	31
3.1.10	Prežívanie erytrocytov	31
3.2	Postupy s použitím bunkového modelu	31
3.2.1	Konštrukcia vektora a mutagenéza.....	31
3.2.2	Transfekcia plazmidovej DNA do buniek Ba/F3	32
3.2.3	Test senzitivity k inhibítorm	33
3.2.4	Imunoblot	33
3.3	Postupy s použitím ľudských vzoriek	34
3.3.1	Vzorky pacientov	34
3.3.2	Izolácia DNA z periférnej krvi.....	34
3.3.3	Skríning mutácie <i>JAK2</i> R1063H pomocou T-ARMS PCR	34
3.3.4	Stanovenie <i>cis/trans</i> konfigurácie mutácií <i>JAK2</i> V617F a R1063H	35
3.4	Štatistické analýzy.....	36
4.	KOMENTÁR K PREDLOŽENÉMU SÚBORU PUBLIKÁCIÍ	37
4.1	Analýza dôsledkov <i>gain-of-function EPOR</i> mutácie na erytropoézu a metabolizmus železa na myšom modeli.....	38
4.1.1	Štúdium primitívnej erytropoézy a ranej definitívnej erytropoézy u myší s <i>gain-of-function EPOR</i> mutáciou.....	38
4.1.2	Štúdium vzťahu erytropoézy a metabolizmu železa u myší s <i>gain-of-function EPOR</i> mutáciou	41
4.2	Štúdium vybraných hereditárnych <i>JAK2</i> mutácií	51
4.2.1	Štúdium kooperácie dedičných <i>JAK2</i> E846D a R1063H mutácií	52
4.2.2	Štúdium interakcie získanej <i>JAK2</i> V617F a dedičnej <i>JAK2</i> R1063H mutácie	54
4.2.3	Skríning <i>JAK2</i> R1063H mutácie v zdravej populácii a u pacientov s myeloidnými neopláziami	56
4.3	Kritické zhodnotenie literatúry týkajúcej sa nových poznatkov patofyziológie Ph-negatívnych MPN	59
5.	SÚHRN/SUMMARY	61
6.	POUŽITÁ LITERATÚRA.....	65
7.	ZOZNAM SKRATIEK.....	77
8.	PRÍLOHY	80

1. TEORETICKÝ ÚVOD

1.1 Hematopoéza

Hematopoéza je proces tvorby krvných elementov z multipotentných krvotvorných kmeňových buniek – HSC (hematopoietic stem cells), ktorý sa v dospelosti odohráva v kostnej dreni. Avšak za patologických podmienok, počas rôznych hematologických porúch, môže dochádzať k extramedulárnej hematopoéze v slezine, pečeni alebo lymfatických uzlinách (Orkin a Zon, 2002). Nedávne zistenia o funkčných HSC osídľujúcich tkanoivo pľúc a tenkého čreva naznačujú, že HSC aktívne cirkulujú v rámci celého tela a spochybňujú konvenčnú definíciu HSC rigidne pôsobiacich v tradičných hematopoetických orgánoch (Lefrançais a kol., 2017; Fu a kol., 2019).

Nové poznatky o povrchových markeroch a transkripčnom profile jednotlivých bunkových štadií zmenili pohľad aj na klasický **hierarchický model hematopoézy**, na vrchole ktorého je umiestnená populácia HSC zahŕňajúca tzv. dlhodobé HSC – LT-HSC (long-term HSC) a krátkodobé HSC – ST-HSC (short-term HSC) (Yang a kol., 2005). Kým LT-HSC sú malou populáciou dormantných buniek s dlhodobou schopnosťou sebaobnovy, ST-HSC s krátkodobou rekonštitučnou kapacitou predstavujú hlavný zdroj hematopoézy. Ich priamym potomstvom sú multipotentné progenitory – MPP (multipotent progenitors), ktoré strácajú schopnosť sebaobnovy a diferencujú smerom k viacerým líniám cez niekoľko štadií oligopotentných a bi-/unipotentných progenitorov, ktoré nakoniec dávajú vznik zrelým hematopoetickým bunkám (Cheng a kol., 2020) (Obr. 1). V súčasnej dobe je uvedený model hematopoézy **nahradený alternatívnym modelom** považujúcim HSC za heterogénnu bunkovú populáciu zloženú z viacerých čiastočne líniovo špecifikovaných subpopulácií buniek. HSC sú schopné obísť niektoré prechodné štadiá diferenciácie a priamo vedú k vzniku bi-/unipotentných, prípadne zrelých buniek (Obr. 1) (Notta a kol., 2016). Preto HSC nepredstavujú vrchol stupňovito vetvenej hematopoézy, ale skôr kontinuum buniek podieľajúcich sa na hematopoéze flexibilným a dynamickým spôsobom (Yokota, 2019; Velten a kol., 2017). Do tohto procesu je zahrnutá kooperácia nielen známych kľúčových cytokínov, rastových a transkripčných faktorov, ale aj epigenetických zmien a aktivity rôznych miRNA (microRNA) molekúl (Mann a kol., 2022). V neposlednom rade je dôležité spomenúť hypoxiu (Dausinas Ni a kol., 2022) v asociácii s kompozíciou mikroprostredia kostnej drene (Bonaud a kol., 2021), ktoré sa rovnako podieľajú na organizácii hematopoetického systému.



Obr. 1: Klasický vs. alternatívny model hematopoézy. Podľa klasického modelu hematopoézy diferenciácia HSC prebieha kaskádovo cez jednotlivé bunkové stupne a je schematicky znázornená plnými šípkami. Alternatívny model znázornený prerušovanou čiarou popisuje HSC ako heterogénnu populáciu zloženú z rôznych frakcií čiastočne líniovo špecifikovaných buniek schopných priamej diferenciácie do zrelých bunkových foriem bez jednotlivých bifurkácií. Skratky: B (B cells) – B lymfocyty; Baso (basophils) – bazofily; CLP (common lymphoid progenitor) – spoločný lymfoidný progenitor; CMP (common myeloid progenitor) – spoločný myeloidný progenitor; DC (dendritic cells) – dendritické bunky; Eos (eosinophils) – eosinofily; Ery (erythrocytes) – erytrocyty; GMP (granulocyte/monocyte progenitor) – progenitor pre granulocyty a monocyty; HSC (hematopoietic stem cells) – hematopoetické kmeňové bunky; MC (mast cells) – mastocyty; MEP (megakaryocyte/erythroid progenitor) – progenitor pre megakaryocyty a erytrocyty; Mk/Pla (megakaryocytes/platelets) – megakaryocyty a trombocyty; MLP (multilymphoid progenitor) – multilymfoïdný progenitor; MPP (multipotent progenitor) – multipotentný progenitor; M/M (monocytes/macrophages) – monocyty a makrofágy; Neutr (neutrophils) – neutrofily; NK (natural killer cells) – natural killer bunky; T (T cells) – T lymfocyty. (Prevzaté a upravené podľa Antoniani a kol., 2017).

1.1.1 Ontogenetický vývoj hematopoézy

Počas embryogenézy sa hematopoetický systém vyvíja vo fázach **primitívnej a definitívnej hematopoézy** (Palis, 2014).

Krátko po gastrulácii, u myši okolo embryonálneho dňa – ED7,25 a u človeka približne 19 dní po oplodnení, sa v žltkovom vačku formujú krvné ostrovčeky, kde sa produkujú prvotné krvné prekurzory (Ferkowicz a kol., 2005). **Prvá vlna hematopoézy** je spojená hlavne s tvorbou primitívnych erytrocytov – EryP, ktoré sú charakteristické makrocitózou, produkciou embryonálneho hemoglobínu – Hb a tým, že v nezrelej forme vstupujú do cirkulácie, kde následne dochádza k terminálnej diferenciácii a vypudeniu jadra (Palis a kol., 1999). V menšej miere vznikajú primitívne megakaryocyty, ktoré majú v porovnaní s definitívnymi bunkami inú polyploidiu a veľkosť (Tober a kol., 2007). Naproti tomu,

primitívne formy makrofágov tiež produkovaných v tomto období sú sotva odlišiteľné od ich definitívnych bunkových foriem (Palis a kol., 1999).

Neskôr, spoločne so vznikom krvného obehu, u myši okolo ED8,25 a u človeka v rozmedzí 3. – 4. týždňa embryonálneho vývinu, je v **druhej vlne hematopoézy** primitívna hematopoéza nahradená definitívou. V žltkovom vačku vznikajú erytromyeloidné progenitory – EMP, ktoré migrujú do fetálnej pečene – FL (fetal liver), odkiaľ po dozretí v podobe definitívnych erytrocytov, makrofágov a ďalších buniek myeloidnej línie vstupujú do krvného obehu (McGrath a kol., 2015). Okrem toho, počas ED9,0 až ED9,5 sú produkované aj B a T lymfoidné progenitory (Yoshimoto a kol., 2011; Yoshimoto a kol., 2012).

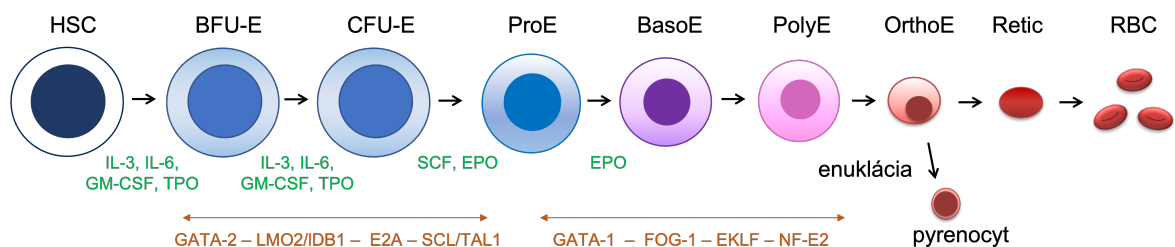
Tretia vlna hematopoézy nastupuje u myši začiatkom ED10,5 a u človeka v 5. týždni embryonálneho vývinu tvorbou HSC hlavne v oblasti aorta-gonad-mesonefros – AGM (Medvinsky a Dzierzak, 1996). Prítomnosť HSC bola pozorovaná aj v iných embryonálnych štruktúrach napr. vo viacerých artériách, či žltkovom vačku alebo placente (de Bruijn a kol., 2000; Lux a kol., 2008; Gekas a kol., 2005). Nie je však známe, či v týchto oblastiach vznikajú *de novo* alebo sa sem dostávajú prostredníctvom cirkulácie. HSC totiž štandardne opúšťajú AGM oblasť a vstupujú do cirkulácie. Ich primárnym cielom kolonizácie je pečeň, kde podstupujú masívnu expanziu. Neskôr opäť migrujú do kostnej drene a sleziny, kde u myši zotravávajú až do dospelosti a nepretržito prispievajú k hematopoéze. U človeka je finálnym miestom hematopoézy výhradne kostná dreň (Palis, 2014).

1.2 Erytropoéza

1.2.1 Erytroidná diferenciácia a maturácia

Jednu vývojovú vetvu hematopoézy tvorí erytropoéza, ktorá sa radí medzi najkritickejšie procesy, nakoľko erytrocyty sú životne dôležité pre ich schopnosť prenášať kyslík. Miestom erytropoézy sú erytroblastické ostrovčeky nachádzajúce sa blízko osteoblastickej niky a pozostávajúce z centrálnych makrofágov, ktoré obklopujú niekoľko desiatok dozrievajúcich erytroblastov. Hlavnou úlohou týchto makrofágov je udržiavanie bunkových interakcií s erytroblastami, sekrécia faktorov/cytokínov a zaistovanie železa pre hémovú syntézu, ktoré sú spoločne potrebné k správnemu chodu diferenciácie a proliferácie erytroidných buniek. Okrem toho, vyučovaním rastových faktorov akými sú napr. IGF-1 (insulin-like growth factor) a BMP-4 (bone morphogenetic protein) sú makrofágy schopné stimulovať stresom indukovanú erytropoézu (Li a kol., 2021; Paulson a kol., 2020).

Prvé bunky špecifické pre erytroidnú líniu sú skoré unipotentné progenitory – **BFU-E** (burst forming unit-erythroid), z ktorých sa vyvíjajú neskoré erytroidné progenitory – **CFU-E** (colony forming unit-erythroid) (Obr. 2). Obe formy nezrelých progenitorov tvoria heterogénnu populáciu buniek (Li a kol., 2019) schopných penetrovať do periférnej krvi a *in vitro* vytvárať kolónie v polotekutých médiách. CFU-E predstavujú prvé morfológicky odlišiteľné bunky erytroidnej línie a od terminálne diferencovaného erytrocytu ich delia ďalšie štyri mitotické delenia, počas ktorých vzniká populácia prekurzorov: **proerytroblast**, **bazofilný erytroblast**, **polychromatický** a **ortochromatický erytroblast** (Nandakumar a kol., 2016) (Obr. 2). Prechod medzi jednotlivými štádiami nie je kaskadovitý, ale v súlade s alternatívnym modelom hematopoézy postupný a plynulý (Huang a kol., 2020). Terminálna maturácia erytroblastov je asociovaná so a) znižovaním proliferatívneho potenciálu; b) hemoglobinizáciou s čím súvisí zvýšený príjem iónov železa a nadprodukcia globínových reťazcov a teda nadobudnutie acidofilie cytoplazmy; c) produkciou cytoskeletárnych, či membránových proteínov a antigénnych proteínov krvných skupín d) postupným znížením objemu cytoplazmy; e) kondenzáciou chromatínu s čím súvisí konečné zníženie génovej expresie (Dzierzak a Philipsen, 2013; Nandakumar a kol., 2016; Palis a kol., 2014). V poslednej fáze maturácie dochádza k enukleácii – vypudneniu jadra za vzniku pyrenocytu a retikulocytu (Obr. 2). Pyrenocyt je prostredníctvom expozície fosfatidylserínu – PS (phosphatidylserine) pohlený centrálnym makrofágom. Bezjadrový **retikulocyt** (Obr. 2) sa vyplavuje do krvného obehu, kde sa v priebehu 24 – 48 hodín mení na **erytrocyt**. Dozrievanie retikulocytu je charakterizované odstránením reziduálnych organel procesom autofágie alebo exocytózy, znížením objemu bunky a remodeláciou cytoskeletárnej siete zodpovednej za nadobudnutie bikonkávneho tvaru špecifického pre erytrocyt (Mei a kol., 2021).



Obr. 2: Diferenciácia a regulácia erytropoézy. Diferenciácia je znázornená cez jednotlivé differenciačné kroky od hematopoetickej kmeňovej bunky – HSC (hematopoietic stem cell) cez unipotentné progenitory BFU-E (burst forming unit-erythroid), CFU-E (colony forming unit-erythroid) a prekuzory: proerytroblast – ProE (proerythroblast), bazofilný erytroblast – BasoE (basophilic erythroblast), polychromatický erytroblast – PolyE (polychromatic erythroblast) a ortochromatický erytroblast – OrthoE (orthochromatic erythroblast) podstupujúci enukláciu za vzniku pyrenocytu a retikulocytu – Retic (reticulocyt), ktorý dozrieva do podoby

zrelej červenej krvinky – RBC (red blood cells). Extracelulárna regulácia uvedenými cytokínmi, rastovými faktormi a hormónmi je znázornená zelenou farbou. Intracelulárna regulácia uvedenými transkripčnými faktormi je znázornená oranžovou farbou.

1.2.2 Hemoglobín a prepínanie globínovej expresie

Hb je tetramér dvoch podjednotiek α globínového typu a dvoch podjednotiek β globínového typu viažúcich molekulu hému, ktorý je tvorený protoporfyrínom IX s centrálnymi atómom železa schopným viazať kyslík. Globínové reťazce sú syntetizované chronologicky v závislosti od poradia, v akom sú umiestnené v α globínovej (*HBZ*, *HBA2*, *HBA1*) a β globínovej rodine génov (*HBE*, *HBG2*, *HBG1*, *HBD*, *HBB*), ktoré sa nachádzajú na ľudskom 16. chromozóme resp. 11. chromozóme (Sankaran a kol., 2010). U myší je α -globínový klaster génov (*Hba-x*, *Hba-1*, *Hba-2*) lokalizovaný na 11. chromozóme a β globínový klaster génov (*Hbb-y*, *Hbb-bh1*, *Hbb-b1*, *Hbb-b2*) na 7. chromozóme (Blobel a kol., 2015). Expresia α -globínovej rodiny je riadená pomocou väzby špecifických transkripčných faktorov a tzv. enhancerov na *upstream* sekvenciu HS-40 (DNase I hypersensitive site-40) (Higgs a kol., 1990). Naopak, regulačnou oblasťou β globínovej rodiny génov je lokus LCR (locus control region) (Li a kol., 2002).

V priebehu ontogenézy je u ľudí syntetizovaných celkom 7 rôznych typov hemoglobínov (Tab. 1). Ich tvorba je sprevádzaná dvomi vlnami prepínania globínovej expresie tzv. ***globin switching***. Prvá vlna zmeny hemoglobínovej produkcie nastáva prechodom z embryonálnych Hb na fetálny Hb a druhá vlna začína *in utero* a je ukončená postnatálne, keď začínajú prevládať dve adultné formy Hb. Kým HbA₁ v dospelosti reprezentuje 98% celkového Hb; tak HbA₂ je v cirkulácii zastúpený menšinovo (1 – 3%). HbF je podobne ako HbA₂ detekovateľný v minimálnych množstvách (<1%), avšak za patologických podmienok môžu byť jeho hladiny zvýšené (Dzierzak a Philipsen, 2013).

Tab. 1: Typy ľudských hemoglobínov

Typ ľudského Hb	Názov Hb a zloženie globínových reťazcov
Embryonálny Hb	Hb Gower 1 – $\zeta_2 \epsilon_2$
	Hb Gower 2 – $\alpha_2 \epsilon_2$
	Hb Portland I – $\zeta_2 \gamma_2$
	Hb Portland II – $\zeta_2 \beta_2$
Fetálny Hb	Hb F – $\alpha_2 \gamma_2$
Adultný Hb	Hb A – $\alpha_2 \beta_2$
	Hb A ₂ – $\alpha_2 \delta_2$

Myšie primitívne erytrocyty exprimujú ζ , $\beta h1$ a ϵ globíny, zatiaľ čo definitívne erytrocyty exprimujú $\alpha 1$, $\alpha 2$, βmaj a βmin globíny. Prechodná vlna definitívnej erytropoézy v myšej FL sa vyznačuje expresiou adultných β -globínov spoločne s embryonálnym $\beta h1$ -globínom (McGrath a Palis, 2008).

Prepínanie globínovej expresie je komplexný proces a zahŕňa viaceré regulačné mechanizmy (Hariharan a kol., 2021). Klúčovú úlohu v druhej vlne prepínania globínovej expresie a utlmení produkcie HbF zohráva transkripčný faktor BCL11A (B-cell lymphoma/leukemia 11A), ktorý priamo reprimuje promotorovú oblast γ -globínového génu (Liu a kol., 2018).

1.2.3 Odstraňovanie erytrocytov

Životnosť ľudských červených krviniek je približne 120 dní a myších 45 dní (Wang a kol., 2010). Odbúravanie starnúcich erytrocytov z cirkulácie je prirodzený proces, ktorý prebieha prostredníctvom **erytrofagocytózy** – EPC (erythrophagocytosis) makrofágmi retikuloendotelového systému – RES v slezine, ale aj v kostnej dreni a v Kupfferových bunkách pečene (Knutson a kol., 2003). Starnutie erytrocytov súvisí s a) ich zníženou metabolickou a antioxidačnou aktivitou; b) mikrovezikuláciou (exocytóza nefunkčných proteínov); c) zníženou mierou deformateľnosti bunky (v dôsledku destabilizácie membránových proteínov); d) narušením iónovej homeostázy (strata vody a príjem Ca^{2+}) (Lutz a Bogdanova, 2013). Tieto procesy vedú k zníženej fluidite membrány, zníženej expresii povrchového markera CD47 (inhibítora EPC), zvýšenej expozícii membránového PS a väzbe imunoglobulínov G – IgG a opsonínov, čím je sprostredkovaná makrofágová eliminácia erytrocytov (Gottlieb a kol., 2012). V makrofágoch následne po pohltení erytrocytov vzniká fagolyzozóm, kde dochádza k ich rozpadu, degradácii hemoglobínu a uvoľňovaniu železa z hému. Okrem toho, makrofág je schopný endozomálne spracovať železo prijaté z voľne cirkulujúceho hému aj hemoglobínu (Nielsen a kol., 2010).

Predčasné odstraňovanie erytrocytov označované pojmom **eryptóza** je indukované osmotickým šokom, oxidatívnym stresom, intoxikáciou tiažkými kovmi a je sprievodným javom niektorých ochorení akými sú sepsa, malária, deficit železa, talasémia, MDS (myelodysplasticický syndróm) a ī. (Repsold a Joubert, 2018). Ide o aktívne regulovaný proces, ktorý sa v mnohých aspektoch podobá na apoptózu prebiehajúcu v jadrových bunkách. Základnými znakmi eryptózy sú externalizácia PS a zmršťovanie bunky, ktoré sú

spojené so zvýšenou intracelulárhou koncentráciou Ca^{2+} a destabilizáciou iónovej homeostázy (Föller a Lang., 2020).

Termínom **neocytolýza** označujeme selektívnu deštrukciu mladých erytrocytov vytvorených v hypoxickej podmienkach napr. vo vesmíre (Rice a Alfrey, 2005) alebo vo vyšších nadmorských výškach (Risso a kol., 2007) po návrate do prostredia s normálnou hladinou kyslíka. Tento proces je spojený s nadmernou produkciami reaktívnych foriem kyslíka – ROS (reactive oxygen species) (Song a kol., 2015). K neocytolýze pravdepodobne dochádza aj u novorodencov pri pôrode, kedy hypoxicke prostredie strieda normoxiu (Föller a kol., 2008).

1.2.4 Molekulárna regulácia erytropoézy

Erytropoéza je prísne regulovaný robustný dej, ktorý za jednu sekundu vytvorí až $2,4 \cdot 10^6$ červených krviniek (Palis a kol., 2014).

Pozitívna regulácia erytropoézy prebieha na extracelulárnej a intracelulárnej úrovni. **Extracelulárne faktory**, ktoré ovplyvňujú determináciu HSC smerom k erytroidnej línii a skorú erytropoézu sú predovšetkým IL-3 (interleukín), IL-6, faktor stimulujúci kolónie granulocytov a makrofágov – GM-CSF (granulocyte-macrophage colony-stimulating factor) a trombopoetín – TPO. Následná diferenciácia erytroidných buniek je riadená SCF (stem cell factor) a predovšetkým EPO, ktorý sa stáva primárnu molekulou riadiacou produkciu erytrocytov (Obr. 2) (Lodish a kol., 2010).

Prítomnosť uvedených cytokínov, rastových faktorov a hormónov vedie k aktivácii **intracelulárnych transkripčných faktorov**. Klúčovú úlohu pri tzv. *lineage commitment*, teda špecifikáciu smerom k erytroidnej línii a pri skorej erytropoéze zohráva GATA-2, ktorý sa cez proteínový mostík zložený z heterodiméru LMO2/LDB1 (LIM domain only 2/LIM domain binding 1) a E2A viaže s ďalším transkripčným faktormi SCL/TAL1 (stem cell leukemia/T-cell acute leukemia) (Mead a kol., 2001). Expresia GATA-2 sa s progresiou diferenciácie znižuje a nahradza ju expresia GATA-1 (Crispino a kol., 2005; Rodrigues a kol., 2005), ktorý sa vo väzbe s kofaktorom FOG-1 (friend of GATA protein 1) (Tsang a kol., 1998) a ďalšími transkripčnými faktormi EKLF (erythroid Krüppel-like factor) (Perkins a kol., 1996) a NF-E2 (nuclear factor erythroid-2) (Shivdasani a Orkin, 1995) synergicky podieľa na terminálnej erytropoéze (Obr. 2). Rovnováha génovej expresie je ďalej zabezpečená histón remodelujúcimi komplexami, ktoré asociujú s uvedenými transkripčnými faktormi a regulujú ich aktivitu. Počas erytropoézy napríklad dochádza

k dramatickému zníženiu aktivity histón deacetylázy – HDAC (histone deacetylase), ktorá sa podieľa na „rozvoľnení“ chromatínu a je asociovaná s iniciáciou génovej expresie. To má za následok kompletnejšiu aktiváciu GATA-1, TAL1 a KLF1 transkripčných faktorov. Naopak, naviazanie korepresorov napr. EZH2 (enhancer of zeste 2), GFI1B (growth factor independence 1b) a i. spôsobuje umlčanie tzv. *silencing* expresie niektorých génov (Mochizuki-Kashio a kol., 2011; Vassen a kol., 2014). Jedným z nich je gén *Spi-1* kódujúci transkripčný faktor PU.1 (putative oncogene Spi-1) (Dahl a kol., 2007; Kim a kol., 2020), ktorý pôsobí ako antagonist GATA-1 a zodpovedá hlavne za myeloidnú diferenciáciu (Burda a kol., 2010).

Za účelom udržania homeostázy, musí byť **erytropoéza regulovaná aj negatívne**, pričom pravdepodobne až 60% proerytroblastov podstupuje apoptózu. Tento proces je sprostredkovany napr. autokrinnou sekréciou FAS ligandu neskorými erytroblastami, čo následne vedie k aktivácii kaspáz u skorých erytroblastov exprimujúcich FAS receptor (De Maria a kol. 1999). Negatívny dopad na tvorbu červených krviniek má aj vyššia hladina faktorov imunitnej odpovede/zápalu akými sú napr. IFN- γ (interferón- γ), TNF- α (tumor necrosis factor- α), IL-6 alebo transformujúci rastový faktor – TGF- β (transforming growth factor- β) (Libregts a kol., 2011).

1.2.5 Erytropoetín a regulácia jeho produkcie

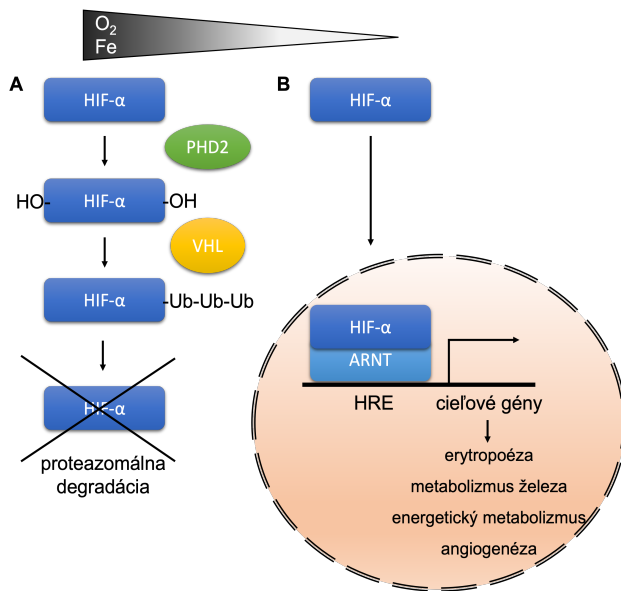
Erytropoetín je hlavným hormónom riadiacim proces erytropoézy. Ide o glykoproteín, ktorý zdieľa štruktúrnu homológiu s inými hormónmi a cytokínmi triedy I. Pôvodne sa predpokladalo, že EPO je pre líniu špecifikáciu HSC smerom k erytroidnej línii nepodstatný (Lin a kol., 1996). Ukázalo sa však, že EPO pôsobí už na úrovni MPP, u ktorých podporuje indukciu erytroidného programu a mení tak ich klonálnu kompozíciu (Grover a kol., 2014; Eisele a kol., 2022). Od štátia CFU-E sa potom stáva pre erytropoézu absolútne nevyhnutným a riadi prežívanie/proliferáciu progenitorov a kinetiku maturácie prekurzorov (Wu a kol., 1995).

Počas fetálneho vývinu je EPO produkovaný hepatocytmi pečene (Dame a kol., 1998), po narodení sú jeho primárnym zdrojom fibroblasty kortexu obličiek (Maxwell a kol., 1993). Pečeň si však zachováva schopnosť produkcie EPO aj v dospelosti a to pri stredne ľahkom až ľahkom deficite okyslienia organizmu (Semenza a Wang, 1992). Okrem toho, expresia EPO a jeho receptora bola zaznamenaná v neurónoch hippocampu a v mozgovej kôre, kde pravdepodobne plní ochrannú funkciu pred mozgovou hypoxiou a ischémiou (Brand

a Hermfisse, 1997; Bernaudin a kol., 2000). Tento typ EPO však kvôli hematoencefalickej bariére neovplyvňuje hladiny cirkujúceho EPO, takže jeho úloha v erytropoéze je vylúčená. Okrem uvedeného, *EPO* transkripty sa našli aj v tkanivách sleziny, pľúc, semenníkov alebo samotných erytroidných bunkách, ale úloha EPO v týchto orgánoch/bunkách ako aj jeho príspevok do celkovej hladiny EPO nie sú zatiaľ dobre preštudované (Weidemann a Johnson, 2009; Stopka a kol., 1998).

Expresia génu *EPO* je regulovaná na transkripčnej úrovni kyslíkovým deficitom prostredníctvom negatívnej **spätnoväzbovej slučky**, v ktorej kľúčovú úlohu zohráva transkripčný faktor HIF-2 patriaci do rodiny hypoxiou indukovaťných faktorov – HIF (hypoxia inducible factor) (Bunn, 2013).

HIF tvorí heterodimér zložený z α podjednotky (HIF α) a z konštitučne exprimovanej beta podjednotky tiež označovanej ako ARNT (aryl hydrocarbon receptor nuclear translocator). Kým podjednotky HIF-1 α a HIF-2 α sú štruktúrne aj funkčne podobné a sú aktivátormi transkripcie, tak podjednotka HIF-3 α má inhibičnú funkciu (Duan, 2016). Za normoxických podmienok je životnosť HIF- α podjednotky veľmi krátka, cyklicky dochádza k jej produkciu a následnej degradácii. Labilita HIF- α je zabezpečená prolylhydroxylázou 2 – PHD2 (prolyl hydroxylase domain), ktorá využíva železo ako kofaktor a α -ketoglutarát ako substrát pre hydroxyláciu dvoch konzervovaných prolínových zvyškov HIF- α podjednotky. Hydroxylácia je dôležitým markerom potrebným pre rozpoznanie proteínom VHL (von Hippel Lindau), ktorý s E3 ubikvitín-ligázovou aktivitou spôsobuje ubikvitináciu HIF- α podjednotky, čo vedie k jej proteazomálnej degradácii (Obr. 3A) (Semenza a Wang 1992; Warnecke a kol., 2004). Naopak, počas hypoxie je HIF- α podjednotka stabilizovaná väzbou s ARNT podjednotkou, takto vytvára heterodimér, ktorý prechádza do jadra a naviazaním sa na HRE (hypoxia responsive element) promotorové oblasti rôznych génov stimuluje ich expresiu (Obr. 3B).



Obr. 3: Hypoxická dráha znázornená počas normoxických podmienok (O_2) a dostupnosti železa (Fe) (A), kedy je podjednotka HIF-2 α (hypoxia inducible factor) označená PHD2 (prolyl hydroxylase domain 2) hydroxylázou a rozpoznaná VHL (von Hippel Lindau) E3 ubikvitín ligázou, ktorá sprostredkúva jej proteazomálnu degradáciu; znížených hladín kyslíka a železa (B), kedy dochádza k narušeniu PHD2 hydroxylačnej schopnosti a stabilizácii HIF-2 α , ktorý v jadre spolu s podjednotkou ARNT (aryl hydrocarbon receptor nuclear translocator) tvorí aktívny transkripcný faktor s multifaktoriálnym efektom regulujúcim expresiu rôznych génov zapojených do uvedených procesov.

HIF-1 a HIF-2 transkripcné faktory vykazujú odlišnú tkanivovú špecifickosť a špecifickosť vo svojich transkripcných cieľoch (Obr. 3B). Expresia génov, ktorých produkty zvyšujú lokálny príslu kyslíka do tkanív (napr. VEGF (vascular endothelial growth factor)) alebo umožňujú adaptáciu bunkového metabolizmu na podmienky s nízkym obsahom kyslíka (napr. GLUT-1 (glucose transporter-1)) je spúšťaná oboma transkripcnými faktormi. Ale napríklad väčšina génov kódujúcich glykolytické enzýmy je výhradne pod reguláciou HIF-1 transkripcného faktora (Albadari a kol., 2019). Naopak HIF-2 transkripcný faktor okrem expresie *EPO* podporuje transkripciu génov zodpovedných za príjem a spracovanie železa potrebného pre erytropoézu (napr. nižšie diskutované gény kódujúce DMT1 (divalent metal transporter 1), DCYTB (duodenal cytochrome B ferrireductase) a FPN (ferroportin)) (Mole, 2010; Shah a kol., 2014). Týmto spôsobom dochádza k jednej úrovni prepojenia hypoxickej reakcie, erytropoézy a kontroly metabolizmu železa.

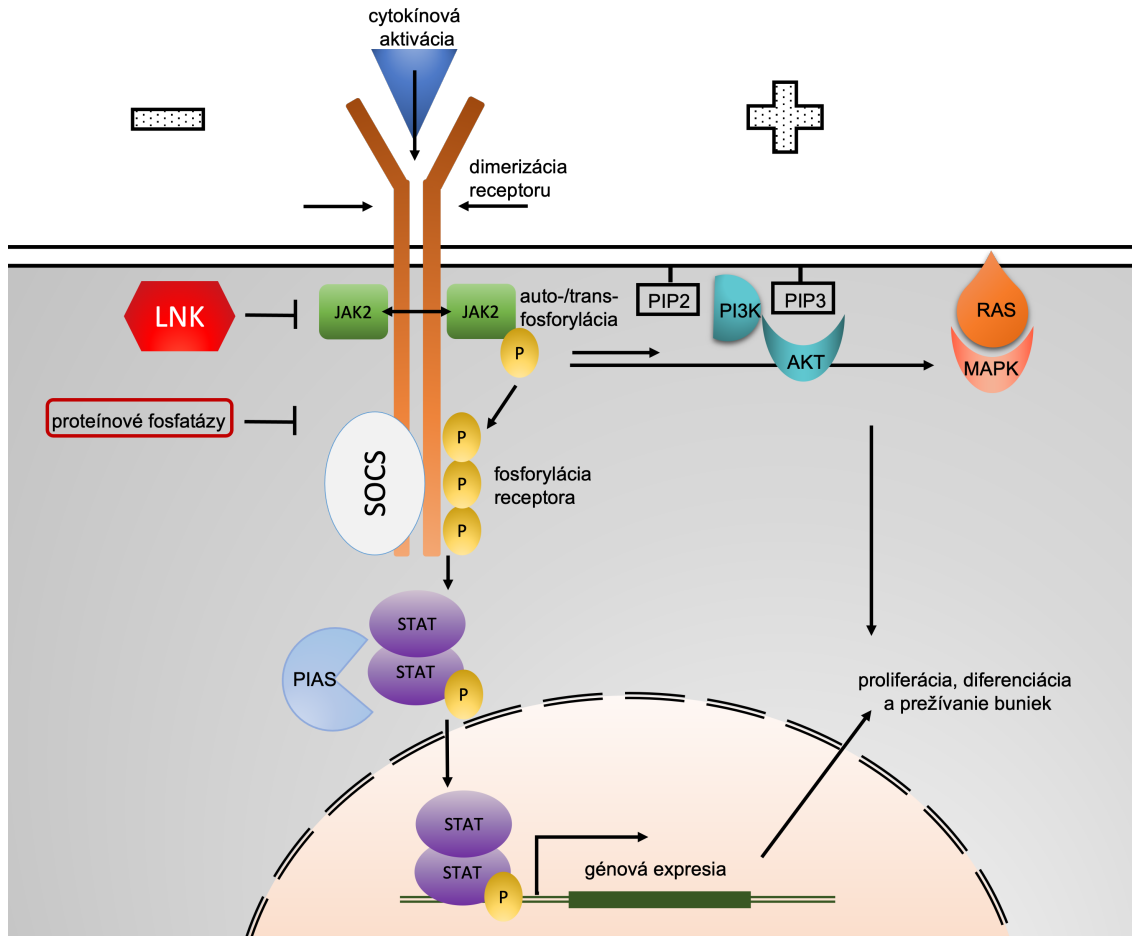
1.2 EPOR/JAK2 signalizácia v erytroidných bunkách

EPO je po endokrinnej sekrécií naviazaný na erytropoetínový receptor – EPOR lokalizovaný na povrchu erytroidných progenitorov a prekurzorov. Najvyššia koncentrácia EPOR bola zaznamenaná na povrchu CFU-E a k jej postupnému znižovaniu dochádza spoločne

s vyššou úrovňou diferenciácie. Fyziologická expresia *EPOR* podľa najnovších štúdií nie je typická len pre bunky erytroidnej línie, ale bola zaznamenaná aj v iných neerytroidných krvných elementoch (napr. HSC, MPP, megakaryocyty, makrofágy, B lymfocyty). Ektopická expresia *EPOR* môže pri vysokých hladinách EPO reprogramovať akúkoľvek hematopoetickú bunku smerom k erytroidnej línii (Zhang a kol., 2021).

EPO/EPOR signalizácia je pre erytropoézu esenciálna, nakoľko *knock-out* génu kódujúceho EPO alebo EPOR je u myší letálny (Wu a kol., 1995). U ľudí sú dedičné mutácie *EPO* alebo *EPOR* pozorované u pacientov s erytrocytózou (Lorenzo a kol., 2013; Zmajkovic a kol., 2018; Kralovics a kol., 1997 a)) (kapitola 1.3.1).

EPOR patrí do rodiny cytokínových receptorov typu I, ktoré nemajú vlastnú kinázovú aktivitu, ale sú závislé od aktivity asociovanej kinázy; v prípade *EPOR* ide o Janusovu kinázu JAK2 (Janus kinase 2) (Ihle, 1995), ktorá patrí spolu s ďalšími kinázami JAK1, JAK3 a TYK2 (Tyrosine kinase 2) do rodiny nereceptorových tyrozínskych kináz. JAK2 proteín je rozdelený do 7 konzervovaných domén – JH (JAK homology), ktoré vytvárajú 4 funkčne odlišné domény. FERM (band 4.1, ezrin, radixin, moesin) doména (JH5 – JH7) sa spolu s SH2 doménou (src homology domain) (JH3 – JH4) podieľa na nekovalentnej väzbe k cytokínovému receptoru (Haan a kol., 2001). Počas absencie ligandu je JAK2 aktivita limitovaná autofosforyláciou S523 a Y570 zvyškov v JH2 pseudokinázovej doméne. Väzba EPO na *EPOR* spôsobuje jeho homodimerizáciu a následnú konformačnú zmenu JAK2, ktorá vytvára aktivačnú slučku JH1 kinázovej domény zodpovednej za auto- a transfosforyláciu tyrozínových zvyškov (Y1007 a Y1008) nachádzajúcich sa v samotnej JH1 doméne (Saharinen a kol., 2002) (Obr. 4). Aktivovaná JAK2 vzápäť fosforyluje 8 tyrozínových zvyškov receptora, ktoré slúžia ako väzbové miesta intracelulárnych adaptoričových proteínov obsahujúcich SH2 doménu, akými sú hlavné proteíny STAT (signal transducer and activator of transcription) (Socolovsky a kol., 1999; Grebien a kol., 2008). Rodina transkripcných faktorov STAT pozostáva zo 7 proteínov schopných viazať sa na cytokínové receptory. Proteíny STAT sú počas ich aktivácie fosforylované pomocou väzby na receptor, okrem STAT1, ktorý sa viaže priamo na JAK2 (Krito a kol., 2002). Po aktivácii dochádza k ich dimerizácii a transportu do jadra, kde riadia expresiu niekoľkých génov (Obr. 4).



Obr. 4: JAK2 signalizácia vo všeobecnosti spočíva vo väzbe cytokínu s receptorom, po ktorej dochádza k trans- a autofosforylácii príslušných JAK2 (Janus kinase) kináz. Aktivované JAK2 fosforylujú tyrozínové zvyšky receptoru, ktoré poskytujú väzobné miesta pre molekuly STAT (signal transducer and activator of transcription). STAT molekuly sa po fosforylácii a dimerizácii presúvajú do jadra, kde ako transkripcné faktory spúšťajú expresiu génov zabezpečujúcich proliferáciu, diferenciáciu a prežívanie hematopoetických buniek. Popri dominantnej JAK2/STAT signálnej dráhe sa aktivujú tiež PI3K(phosphatidylinositol 3-kinase)/AKT a RAS/MAPK (mitogen activated protein kinase) signálne dráhy, čo je znázornené symbolom +. Aby nedochádzalo k nežiaducej bunkovej expanzii, musí byť JAK2 signalizácia negatívne regulovaná molekulami LNK (lymphocyte adaptor protein), SOCS (suppressors of cytokine signaling), PIAS (protein inhibitors of STATs) alebo proteínovými fosfatázami, čo je znázornené symbolom -.

EPOR preferenčne aktivuje proteíny STAT5, ktoré podporujú expresiu antiapoptotických génov *Bcl-XL* (B-cell lymphoma-extra large) (Afreen a kol., 2020) a *Mcl-1* (myeloid cell leukemia 1) (Turnis a kol., 2021), ktoré spoločne prispievajú k prežívaniu erytroidných buniek. Medzi ďalšie aktivované gény patria: *ID1* (inhibitor of DNA binding 1); *TFRC* (transferrin receptor); *TRIB3* (tribbles pseudokinase 3); a *SPI2A* (serine protease inhibitor 2A), ktorých produkty sa v uvedenom poradí podieľajú na expanzii a prežívaní erytroblastov; príjme železa; terminálnej diferenciácií erytroblastov; a antioxidačnej obrane bunky (Bhoopalan a kol., 2020). Ďalším zo STAT5 cieľových génov je *ERFE* (*Fam132b*) kódujúci hormón erytroferón, ktorý sa podieľa na systémovej regulácii metabolizmu železa

a svojím pôsobením zabezpečuje dostatočný prísun železa pre erytroidné bunky syntetizujúce Hb (Kautz a kol., 2014); bližšie je jeho efekt popísaný nižšie (kapitola 1.4.3). Väzbou ďalších adaptorov na tyrozínové zvyšky receptora sa aktivujú kanonické dráhy PI3K (phosphotidylinositol 3-kinase)/AKT a Ras/MAPK (mitogen activated protein kinase) signálna dráha, ktoré vzájomne zaistujú proliferáciu, diferenciáciu a prežívanie buniek (Obr. 4) (Jafari a kol., 2019; Kumkhaek a kol., 2013; Tóthová a kol., 2021). Navyše, jedným z hlavných cieľov PI3K/AKT signalizácie je transkripčný faktor FOXO3 (forkhead box O-3), ktorý sa významne podieľa na erytroidnej diferenciácii a maturácii a hrá dôležitú úlohu v regulácii hladiny ROS, odstraňovaní mitochondrií a enukleácie (Liang a kol., 2015; Marinkovic a kol., 2008; Menon a kol., 2018).

Na fosforylované tyrozínové zvyšky receptora sa v rovnakej miere ako pozitívne regulátory viažu aj **negatívne regulátory** zodpovedné za ukončenie **JAK2 signalizácie** (Obr. 4). Ide napr. o proteíny rodiny SOCS (suppressors of cytokine signaling), ku ktorých expresii dochádza po cytokínovej stimulácii vďaka negatívnej spätnoväzobnej slučke. Ich funkciou je zamedzenie aktivácie STAT priamo naviazaním sa na receptor (Sasaki a kol., 2000) alebo nepriamo väzbou s JAK kinázou (Jegalian a Wu, 2002). Okrem toho, spolupracujú s proteínnimi rodinami Cullin na ubikvitinácii JAK2 a jej následnej degradácii (Rawlings a kol., 2004). Proteínové fosfatázy PTP (protein tyrosine phosphatase) sa viažu na JAK2 a podieľajú na jej defosforylácii (Bourdeau a kol., 2005; Baker a kol., 2007). Ďalším SH2 doménu obsahujúcim negatívnym regulátorom je lymfocytárny adaptorový proteín – LNK (kódovaný génom *SH2B3*), ktorý väzbou s JAK2 oslabuje jej aktivitu (Tong a kol., 2005). Medzi ďalšie spôsoby utlmenia signalizácie patrí internalizácia a následná lyzozomálna degradácia receptora (Walrafen a kol., 2005) alebo inhibícia samotných transkripčných faktorov STAT prostredníctvom členov rodiny PIAS (protein inhibitors of STATs), ktoré predchádzajú ich dimerizáciu (Liu a kol., 1998) alebo spúšťajú sumoyláciu cieľových transkripčných faktorov a bránia tak celkovej génovej expresii (Palvimo, 2007). Nakoniec, aj hydroxylácia EPOR sprostredkovanaď enzymom PHD3 vedie k jeho ubikvitinácii a proteozomálnej degradácii (Heir a kol., 2016).

1.2.1 Neerytroidná aktivácia JAK2 signalizácie

Okrem EPOR, JAK2 asociouje aj s trombopoetínovým receptorom – MPL a receptorom viažucim faktor stimulujúci kolónie granulocytov – G-CSFR (granulocyte colony-stimulating factor receptor) a ako odpoveď na stimuláciu TPO alebo G-CSF (granulocyte

colony-stimulating factor) iniciuje bunkovú proliferáciu a diferenciáciu prekurzorov na zrelé trombocyty resp. neutrofilné granulocyty a makrofágy. Na celkovú JAK2 signalizáciu vplýva aj odlišná aktivácia jednotlivých STAT molekúl a ich schopnosť tvoriť homopričípadne heterodiméry v závislosti od typu asociovaného receptora (Hu a kol., 2021). Navyše bolo ukázané, že JAK2 sa dostáva do tesnej blízkosti s FAK (focal adhesion kinase) a Src kinázami (Zhu a kol., 1998; Ingle a Klinken, 2006), čo umožňuje ich krízovú fosforyláciu a aktiváciu. Prepojenie viacerých receptorov, adaptorov a signálnych dráh s JAK2 naznačuje, že tento enzým má v hematopoéze centrálné postavenie a narušenie jeho aktivity napríklad v dôsledku sporadických získaných alebo dedičných mutácií v samotnej JAK2, či MPL alebo G-CSFR vedie k abnormálnej JAK2 signalizácii a rozvoju myeloproliferatívnych neoplázií – MPN (myeloproliferative neoplasm) (kapitola 1.3.2). Okrem toho, aj určité v populácii rozšírené polymorfizmy proteínov zapojených do JAK2 signalizácie môžu byť spojené s náchylnosťou k rozvoju MPN alebo môžu ako genetické modifikátory ovplyvňovať ich fenotyp.

1.3 Poruchy hematopoézy spojené s narušením JAK2 signalizácie

Zásadná úloha JAK2 signalizácie v hematopoéze odzrkadľuje skutočnosť, že jej dysregulácia je spojená s rôznymi poruchami hematologického a imunitného systému, ktoré môžu mať charakter bud' autoimunitného ochorenia, imunodeficiencie, prípadne malígnej nadmernej tvorby krvných elementov alebo naopak deficitu krvných elementov a to v závislosti od typu mutácií. Tie sa môžu klasifikovať podľa ich dopadu na funkciu proteínov zahrnutých do JAK2 signalizácie – *gain-of-function* alebo *loss-of-function*, prípadne podľa ich spôsobu vzniku – získané alebo dedičné. V nasledujúcich kapitolách dizertačnej práce sa budem podrobnejšie venovať iba poruchám hematopoézy s narušenou JAK2 signalizáciou, ktoré priamo súvisia s predloženou dizertačnou prácou.

1.3.1 Primárne erytrocytózy

Absolútna erytrocytóza je stav, pri ktorom je trvalo zvýšené objemové percento červených krvniek v krvi, označované ako hematokrit – Hct (hematocrit); u mužov je spojená s Hct > 52% a u žien s Hct > 48% u žien po dobu najmenej 2 mesiacov. Pri diagnóze je nutné odlísiť pravú erytrocytózu od relatívnej, ktorá je spôsobená skôr zníženým objemom plazmy a je dôsledkom straty telesných tekutín. Základná klasifikácia erytrocytóz spočíva v ich rozdelení na primárne a sekundárne erytrocytózy, ktoré sa líšia v *in vitro* senzitivite

erytroidných progenitorov k EPO a v hladinách sérového EPO (Tab. 2). Prienikom týchto dvoch skupín sú erytrocytózy so znakmi ako primárnych tak sekundárnych erytrocytáz (Tab. 2) (Prchal, 2010).

Tab.2.: Klasifikácia absolútnych erytrocytáz

skupina erytrocytáz	pôvod erytrocytózy	názov/príčina	in vitro hypersenzitivita	hladiny EPO
primárne erytrocytózy	získaná	Polycytémia Vera (mutácie JAK2 a i.)	+	↓
	dedičná	Familiárna erytrocytóza typu 1 (mutácie EPOR)	+	↓
sekundárne erytrocytózy	získaná	hypoxémia asociovaná s inou klinickou patológiou	-	↑
		karboxyhemoglobinémia		
		pobyt vo vysokých nadmorských výškach		
		autonómna produkcia EPO/ exogénne podávanie EPO		
	dedičná	Familiárna erytrocytóza typu 5 (mutácie EPO)	-	↑ alebo neprimerane normálne
		Familiárna erytrocytóza typu 6-7 (mutácie Hb)		
		Familiárna erytrocytóza typu 8 (mutácie BPGM)		
sekundárne erytrocytózy so znakmi primárnych erytrocytáz	dedičná	Deficit cytochrom-b5-reduktázy	+/-	↑ alebo neprimerane normálne
		Familiárna erytrocytóza typu 2 (mutácie VHL)		
		Familiárna erytrocytóza typu 3 (mutácie EGLN1~PHD2)		
		Familiárna erytrocytóza typu 4 (mutácie EPAS1~HIF2α)		

Skratky: EEC (endogenous erythroid colonies) – erytroidné endogénne kolónie, JAK2 – Janusova kináza, EPOR – erytropoetínový receptor, EPO – erytropoetín, Hb – hemoglobín, BPGM – 2,3-bisfosfoglycerát mutáza, VHL – von Hippel Lindau, EGLN1 gén kódujúci PHD2 – prolylhydroxyláza 2, EPAS1 (endothelial PAS domain-containing protein 1) gén kódujúci HIF-2α (hypoxia inducible factor) – hypoxiou indukovaný transkripcný faktor.

Molekulárne defekty hematopoetického progenitora zodpovedné za vznik primárnej erytrocytózy spôsobujú bud' neadekvátnu odpoveď alebo úplnú nezávislosť erytroidného progenitora od rastových faktorov a jeho autonómnu nadprodukciu. Pacienti s primárhou erytrocytózou majú preto zvýšenú *in vitro* senzitivitu progenitorov k EPO, dokonca v niektorých prípadoch sú prítomné endogénne erytroidné kolónie – EEC (endogenous erythroid colonies) absolútne nezávislé od EPO (Tab.2). Ďalším diagnostickým markerom rozvíjajúcim sa v dôsledku kompenzačného efektu sú znížené hladiny EPO, ktoré sa môžu prípadne nachádzať na dolnej úrovni referenčných hodnôt (Tab.2) (Prchal, 2010).

Príkladom primárnej získanej erytrocytózy je Polycytémia vera – PV, ktorá vzhľadom na svoj malígy charakter patrí do súboru ochorení MPN, ktoré sú podrobnejšie popísané nižšie (kapitola 1.3.2).

Primárne dedičné erytrocytózy sú reprezentované primárhou familiárnou vrodenou polycytémiou – PFCP (primary familial and congenital polycythemia), ktorá je menej častá ako PV. PFCP vzniká v dôsledku zárodočných *gain-of-function EPOR* mutácií s autozomálne dominantnou dedičnosťou, no boli popísané aj prípady *de novo EPOR* mutácií. Prevažne ide o *nonsense* mutácie lokalizované v exóne 8 alebo mutácie posúvajúce čítací rámec tzv. *frame shift* mutácie, ktoré vedú k vzniku stop kodónu (Juvonen a kol., 1991; Chapelle a kol. 1993; Sokol a kol., 1995 Kralovics a Prchal, 2001; Petersen a kol., 2004; Bento a kol., 2013; Gross a kol., 2014; Chauveau a kol., 2016). Výsledkom mutácií je skrátenie receptora a strata jeho regulačnej domény, ktorá je esenciálna pre väzbu negatívnych regulátorov. Vplyvom týchto mutácií dochádza k deregulácii JAK2 signalizácie vedúcej k abnormálnej transkripcii génov a následnej nadprodukcií červených krviniek. Na výslednom fenotype sa okrem toho podieľa aj deregulácia PI3K signalizácie, ktorá normálne podporuje internalizáciu EPOR a jeho degradáciu. V dôsledku EPOR mutácií je preto degradácia receptora oslabená, s čím súvisí jeho zvýšená senzitivita k EPO (Sulahian a kol., 2009). Funkčné štúdie však poukazujú na komplexnejšie pozadie patológie EPOR mutácií. Jedna z nich popisuje myší model s kompletne eliminovanou distálou doménou EpoR, u ktorého je zachovaná bazálna erythropoéza bez rozvoja erytrocytózy (Zang a kol., 2001). Na to nadväzujú výsledky ďalšej štúdie opisujúcej nový mechanizmus pôsobenia EPOR mutácií, podľa ktorého pre rozvoj erytrocytózy nepostačuje len skrátenie receptora, ale vyžaduje sa práve prítomnosť novej aminokyselinovej sekvencie generovanej *frame shift* mutáciami. Novovzniknutý funkčne odlišný C-koniec receptora nadobúda novú funkciu, ktorá v dôsledku stabilizácie a zotrvenia EPOR na plazmatickej membráne zodpovedá za hypersenzitivitu buniek k EPO (Pasquier a kol., 2018). Na rozdiel od uvedených mutácií existuje aj taký typ mutácie, ktorý rovnako vedie k skráteniu receptora, ale nie je asociovaný s erytrocytózou. Ide o mutáciu postihujúcu extracelulárnu doménu receptora, ktorá pravdepodobne kompromituje jeho väzbu s EPO. Zvýšené hladiny EPO pozorované u nositeľov tejto mutácie sú pravdepodobne kompenzáciou hyposenzitivity erytroidných progenitorov k EPO, ktorá by pri jeho normálnych hladinách spôsobila anémiu (Oskarsson a kol., 2018).

Molekulárna patofyziológia geneticky podmienených erytrocytóz je pomerne heterogénná a zahrňa poruchy kľúčových vyššie popísaných signálnych dráh regulujúcich erytropoézu (Tab.2). Vďaka molekulárno-genetickým metódam bola odhalená veľká skupina kauzálnych mutácií, aj napriek tomu je u značnej časti pacientov etiológia neznáma a zaraďujeme ich do skupiny tzv. idiopatických erytrocytóz – IE (Girodon a kol., 2017; Camps a kol. 2016). Pribúdajúce štúdie však odhalujú aj nekanonické varianty spomenutých génov (Tab. 2) alebo varianty iných génov, ktoré môžu byť zodpovedné za rozvoj erytrocytóz. Príkladom takýchto mutácií asociovaných s IE sú *missense EPOR* varianty (Sokol a kol., 1994; Le Couedic a kol., 1996; Kralovics a kol., 1997 b); Chandrasekhar a kol., 2020), z ktorých niektoré samostatne (Peroni a kol., 2018) alebo spolupôsobením s inou kauzálnou mutáciou (Rabadan Moraes a kol., 2022) vedú k miernej ale značnej hyperaktivite JAK2 signalizácie, nadmernej proliferácii a diferenciácií erytroidných buniek. Rovnako tak novoobjavené intronické a zostrihové varianty génu kódujúceho VHL vedúce k hyperaktivácii HIF-2 (Lenglet a kol., 2018) alebo varianty v géne *PIEZ01* kódujúcom mechanosenzitívny kanál, ktorý sa aktivuje pri prechode erytrocytu krvnými mikrokapilárami (Knight a kol. 2019; Filser a kol. 2020), sú popisované u pacientov pôvodne klasifikovaných ako IE. Ďalšie zriedkavé inaktivačné varianty génov kódujúcich LNK (McMullin a Cario, 2016), IRP1 (iron regulatory protein 1) (Oskarsson a kol., 2020) a HFE (hemochromatosis protein) (Biagetti a kol., 2018; Burlet a kol., 2019) sú taktiež spojené so zvýšeným Hct, ktorý zrejme nastáva z dôvodu neadekvátnej inhibície JAK2, hyperaktivácie HIF-2, ktorý je pod translačnou reguláciu IRP1 alebo z dôvodu vyššej dostupnosti železa pre nedostatočnú stimuláciu hepcidínu proteínom HFE (kapitola 1.4.3).

1.3.2 Myeloproliferatívne neoplázie

Myeloproliferatívne neoplázie tvoria skupinu príbuzných klonálnych hematologických porúch s prekrývajúcim sa fenotypom, sú charakterizované nadprodukciou plne diferencovaných myeloidných buniek, ktorá vytláča produkciu ostatných krvných elementov, preto príznaky MPN sú dané ako nadbytkom, tak aj nedostatom krvných buniek. Okrem toho, MPN majú s progresiou ochorenia tendenciu totálneho rozvratu krvotvorby a transformácie do sekundárnej akútnej myeloidnej leukémie – sAML.

V hematopatológií v posledných rokoch došlo k značnému rozvoju poznatkov a pre potrebu upraviť klasifikáciu a donedávna používané diagnostické kritériá vznikla najnovšia klasifikácia MPN podľa Svetovej zdravotníckej organizácie – WHO (world health

organisation) (Tab. 3). Medzi klasické MPN patrí chronická myeloidná leukémia – CML s typickým Philadelphia chromozómom – Ph, ktorý vzniká recipročnou translokáciou t(9;22) (Tab. 3). Ku klasickým, ale Ph-negatívnym MPN, sú zaradené PV, esenciálna trombocytémia – ET a primárna myelofibróza – PMF (Tab. 3). Iné Ph-negatívne MPN (Tab. 3) sú zriedkavejšie a ich molekulárna príčina je často nejasná (Arber a kol., 2016).

Tab.3: Klasifikácia MPN. (Upravené podľa Arber a kol., 2016)

Subkategória MPN	Jednotlivé entity MPN
Ph-poziívne MPN	Chronická myeloidná leukémia – CML
Ph-negatívne MPN	Polycytémia vera – PV
	Primárna myelofibróza – PMF
	Esenciálna trombocytémia – ET
Iné Ph-negatívne MPN	Chronická neutrofilná leukémia – CNL
	Inak nešpecifikovaná Chronická eosinofilná leukémia
	Neklasifikovateľné MPN

Skratky: Ph – Philadelphia chromozóm, MPN – meyoproliferatívne neoplázie

Typickým znakom klasických Ph-negatívnych MPN je vo väčšine prípadov deregulácia JAK2 signalizácie v dôsledku riadiacich tzv. *driver* mutácií, najčastejšie mutácií v géne kódujúcom JAK2, MPL alebo kalretikulín – CALR (calreticulin). Ide o sporadické *de novo* mutácie s vysokou mierou penetrancie. Ph-negatívne MPN sú heterogénnou skupinou jednak po stránke klinického prejavu, tak aj po stránke histologických, cytogenetických a molekulárno-genetických nálezov (Tefferi a Pardanani, 2015). Ukazuje sa, že táto fenotypová diverzita pochádza zo súčinnosti uvedených *driver* mutácií s príavnými mutáciami somatického alebo dedičného pôvodu, ktoré sú pomerne často popisované u pacientov s MPN (Landgren a kol., 2008; Tashi a kol., 2017). Navyše za heterogenitou stojí okrem genetických činiteľov spektrum negenetických faktorov (O'Sullivan a Mead, 2019), čo odzrkadľuje komplexnosť patobiológie klasických Ph-negatívnych MPN, ktorá je podrobnejšie popísaná v predloženom súhrnnom článku *Nové poznatky v patofyziológii Ph-negatívnych myeloproliferatívnych neoplázií* (príloha 5).

Nové liečebné stratégie Ph-negatívnych MPN sú zamerané na JAK signalizáciu a podľa cieľových molekúl ich možno klasifikovať do troch typov: a) protilátky voči cytokínom alebo receptorom, b) JAK inhibítory a c) STAT inhibítory (Hu a kol., 2021); a sú využité v prípade, že pacienti nereagujú na konvenčnú liečbu. Najčastejšie sa odporúča liečba JAK inhibítormi (Harrison a kol., 2017), ktoré tvoria skupinu malých molekúl s rôznou chemickou štruktúrou schopných inhibovať ATP (adenosine triphosphate)-väzobné miesto a brániť vzniku aktívnej konformácie. Počas liečby nešpecifickým JAK inhibítorm – Ruxolitinibom dochádza k zmenšeniu sleziny, zlepšeniu krvného obrazu, ústupu

symptomatológie a jeho priaznivý efekt sa potvrdil aj na zvýšenom celkovom prežívaní, či zníženom riziku leukemickej transformácie (Grabek a kol., 2020). S postupom času hlavne z dôvodu možnosti nadobudnutia rezistencie MPN klonu na podávaný inhibítorky, alebo pre jeho niektoré nepriaznivé účinky, boli vyvinuté lepšie tolerované inhibítory ďalších generácií so selektívou špecifickosťou k jednotlivým JAK kinázam (Hu a kol., 2021).

1.4 Prepojenie erytropoézy a metabolizmu železa

Nakoľko schopnosť červených krviniek transportovať kyslík je závislá od železa nachádzajúceho sa v molekule Hb, procesy metabolizmu železa a erytropoézy sú vzájomne prepojené na viacerých úrovniach a sú vzájomne regulované. Akákoľvek odchýlka v ich koordinácii môže viesť k patologickým stavom ovplyvňujúcim hladiny železa alebo priebeh erytropoézy. Dostupnosť železa je limitujúcim faktorom erytropoézy a jeho nutričný nedostatok je najbežnejšou príčinou anémie. Na druhú stranu, železo v nadmernom množstve je pre bunku toxicke. Schopnosť železa prijímať/uvolňovať elektróny vo Fentonovej reakcii, ktorá súvisí s produkciou ROS, vysvetluje, prečo pri preťažení železom dochádza k poškodeniu buniek (Hentze a kol., 2004).

1.4.1 Príjem, transport a recyklácia železa

Denný príjem nutričného železa je za fyziologických podmienok relatívne malý (približne 1 – 2 mg železa), pričom rovnaké množstvo sa obratom z tela vylučuje stratou krvi alebo deskvamáciou epitelálnych buniek. Ďalšie dráhy exkrécie železa, okrem deskvamácie, krvácania, prípadne potenia (Collins a kol., 2008), zatiaľ neboli popísané (Byrne a kol., 2013). Železo pochádzajúce z potravy je vstrebávané v duodene prevažne v jeho hémovej forme, avšak mechanizmy jeho príjmu zostávajú nejasné. Naopak u anorganického železa vieme, že je transportované cez apikálnu membránu enterocytov pomocou transportéru DMT1 (Gunshin a kol., 2005), čomu predchádza redukcia trojmocného železa na dvojmocné za účasti DCYTB (McKie, 2008). Následne sa železo buď ukladá v enterocytoch v zásobnom proteíne – feritíne alebo vstupuje do krvného obehu cez bazolaterálnu membránu prostredníctvom FPN (Abboud a Haile, 2000; Donovan a kol., 2000). Zároveň dochádza k spätej oxidácii železa na trojmocné za účasti hephaestinu (Vulpe a kol., 1999). Po vstupe do cirkulácie sa železo okamžite viaže na proteínový prenášač transferín – Tf, ktorý okrem schopnosti transportu, znižuje riziko vzniku toxickej

radikálov udržiavaním železa v rozpustnej forme (Gomme a kol., 2005). Pri pret'ažení organizmu železom (pri transferínovej saturácii – TSAT > 60%) sa železo akumuluje v netransferínovej podobe ako NTBI (non-transferrin-bound-iron) alebo v bunkách, kde vytvára tzv. *labile iron pool* – LIP s život ohrozujúcim oxidatívnym potenciálom (Chen a kol., 2021).

Najväčším rezervoárom železa v tele je pečeň, ktorá môže vo forme feritínu uchovávať až 1000 mg železa. (Carmona a kol., 2014). Pri zvýšených požiadavkách erytropoézy sa železo z feritínu mobilizuje pomocou tzv. feritinofágie. Ide o proces degradácie feritínu v autolyzómoch iniciovaný proteínom NCOA4 (nuclear receptor coactivator 4), ktorý naviguje feritín smerom k lyzozómom (Mancias a kol., 2014), odkiaľ sa po uvoľnení do cytoplazmy dostáva cez kanál FPN do krvného obehu.

Aj keď uvedené mechanizmy prispievajú k celkovému prísunu železa pre erytropoézu, jej najhlavnejším zásobovateľom je recyklácia železa zo starnúcich alebo poškodených erytrocytov v procese erytrofagocytózy. Podobne ako pri feritinofágii, železo sa z fagolyzozómu dostáva cez cytoplazmu do cirkulácie cez FPN za súčasnej oxidácii ceruloplazmínom (Vulpe a kol., 1999). Týmto spôsobom sa takmer kompletne pokrýva denný obrat železa (20 – 25 mg) potrebného k tvorbe červených krviniek.

Cirkulujúce železo, uvoľnené z enterocytov duodena, hepatocytov alebo makrofágov je prijímané erytroblastami cez transferínový receptor 1 – TfR1 schopný vychytávať transferín s naviazaným železom – holo-transferín. Tento komplex sa dostáva do bunky prostredníctvom endozómu, ktorého okyslenie umožňuje disociáciu železa z transferínu (Fleming a kol., 1997). Následne, sa železo presúva bud' priamo (tzv. *kiss and run* transportom) (Hamdi a kol., 2016) alebo cez cytoplazmu do mitochondrií, kde je využité pri biosyntéze hému, ktorý sa po prechode do cytoplazmy spája s globínovými reťazcami a vytvára tak molekuly Hb. Okrem TfR1, sa na povrchu erytroidnej bunky nachádza aj jeho homológ TfR2, ktorý asociouje s EPOR a predpokladá sa, že je rozhodujúci pre účinný transport EPOR k bunkovému povrchu a pre terminálnu diferenciáciu erytroblastov (Forejtníková a kol., 2010; Nai a kol., 2014).

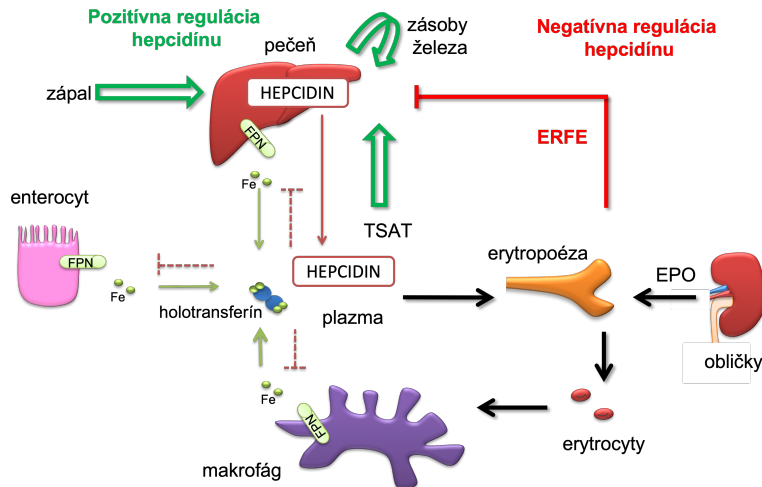
Navýše, pri znížených koncentráciách železa v organizme, TfR2 obmedzuje prechod EPOR k membráne erytroblastov, tým znižuje ich senzitivitu k EPO a v takýchto nevyhovujúcich podmienkach utlmuje erytropoézu (Khalil a kol., 2018). Nedostatok železa môže viest' k zníženiu erytropoetickej aktivity aj na úrovni renálnej produkcie EPO; a to prostredníctvom väzby IRP1 na 5' regulačnú oblast' *HIF-2α* mRNA. Tým dochádza k inhibícii *HIF-2α* translácie, zníženiu produkcie EPO a v konečnom dôsledku utlmeniu erytropoézy. Popri

tom, ako nízke hladiny železa negatívne ovplyvňujú priebeh erytropoézy, môžu pre zachovanie bazálnej erytropoézy aspoň minimálne zvýšiť tok železa potrebného pre erytropoézu napr. PHD2/HIF2- α osou. Ako už bolo uvedené, aktivita PHD2 je podmienená nielen okysličením, ale aj dostupnosťou železa (Obr. 3). Preto okrem hypoxie, aj lokálne znížené hladiny železa v tenkom čreve oslabujú PHD2 enzymatickú funkciu, čo vedie k stabilizácii HIF-2 transkripčného faktora, ktorý spúšťa expresiu cielových génov kódujúcich DMT1, DCYTB a FPN zvyšujúcich import nutričného železa (Shah a kol., 2009). Okrem toho, príjem železa enterocytmi duodena sa môže pri jeho nedostatku zvýšiť aj aktivitou IRP1 molekúl, ktoré väzbou na 3' regulačnú oblasť stabilizujú *DMT1* mRNA.

Hladiny železa ovplyvňujú samotnú erytropoetickú aktivitu a *vice versa*. Dôkazom sú myši, u ktorých po podaní EPO (Artuso a kol., 2019) alebo jeho zvýšenou expresiou (Diaz a kol., 2013) došlo k výraznej mobilizácii cirkulujúceho železa. Princíp, akým spôsobom EPO stimulovaná erytropoetická aktivita vedie k vyššiemu prísunu železa nespočíva v priamom funkčnom pôsobení EPO, ale v aktivovaných erytropoetických bunkách sekretujúcich hormón ERFE, ktorý mechanizmom popísaným nižšie reguluje metabolizmus železa (Kautz a Nemeth, 2014; Kautz a kol., 2014).

1.4.2 Systémová regulácia metabolizmu železa hepcidínom

Hepcidín, produkovaný hepatocytmi a vylučovaný obličkami, je hlavným regulátorom systémovej homeostázy železa. Riadi koncentráciu železa v plazme tak, že sa viaže na FPN umiestnený hlavne na povrchu enterocytov, hepatocytov a makrofágov, spôsobuje jeho ubikvitináciu za účasti E3 ubikvitín ligázy RNF17 (ring finger protein 17) (Ginzburg, 2019; Jiang a kol., 2021), internalizáciu a degradáciu v lyzozómoch (Kautz a Nemeth, 2014). Tým tlmí uvoľňovanie nutričného, zásobného a recyklovaného železa (Ganz a Nemeth, 2012) (Obr. 5). Pri vyšších koncentráciách môže hepcidín priamo blokovať export železa uzavorením FPN. Tento mechanizmus zabezpečuje retenciu železa v bunkách, ktoré nemajú endocytózový aparát (napr. erytrocyty) alebo za podmienok, pri ktorých je endocytóza spomalená (Aschemeyer a kol., 2018). Najnovšie sa ukázalo, že hepcidín sa preferenčne viaže len na FPN aktuálne transportujúci železo, pričom ignoruje molekuly FPN umiestnené na bunkách s nízkou transportnou aktivitou. Týmto mechanizmom sa pravdepodobne predchádza trvalému odstráneniu FPN z povrchu bunky, ktoré by si pre obnovenie transportu železa inak vyžadovalo opäťovnú biosyntézu FPN (Billesbølle a kol., 2020).



Obr. 5: Regulácia metabolizmu železa. Hepcidín produkovaný hepatocytmi sa viaže na FPN (ferroportín), ktorý exportuje železo (Fe) z hepatocytov, enterocytov a makrofágov RES (retikuloendotelový systém); spôsobuje jeho degradáciu a následné zníženie koncentrácie železa v plazme. Fibroblasty kortexu obličiek produkujú EPO (erytropoetín) ako odpoveď na hypoxiu. EPO priamo stimuluje expanziu erytroblastov v kostnej dreni a nepriamo spôsobuje zvýšenie produkcie ERFE (erytroferón), ktorý má funkciu inhibítora produkcie hepcidínu. Znížením hepcidínu dochádza k stabilizácii FPN na bunkovom povrchu a k mobilizácii zásobného, nutričného a recyklovaného železa zo senescentných erytrocytov do plazmy, kde je železo naviazané na transferín za vzniku holotransferínu. Zvýšenie cirkulujúceho železa spojené so zvýšenou TSAT (transferínová saturácia) viedie k príjmu železa diferencujúcimi erytroidnými prekurzormi. Stimulátormi produkcie hepcidínu sú naopak zápalové procesy a zvýšené hladiny cirkulujúceho/zásobného železa.

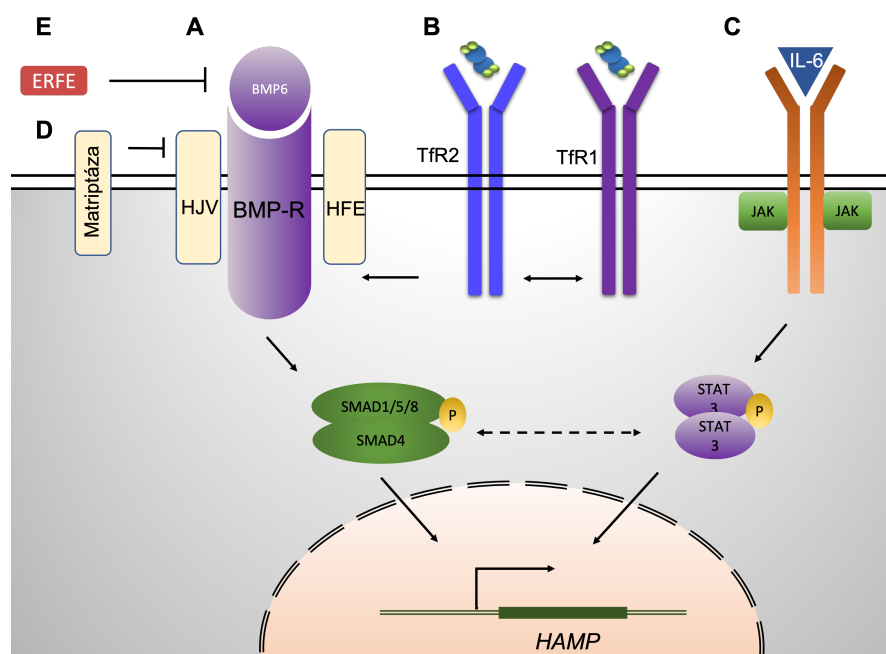
1.4.3 Regulácia produkcie hepcidínu

Ľudský gén kódajúci hepcidín (*HAMP*) je lokalizovaný na 19. chromozóme a kóduje krátky peptid zložený z 25 aminokyselín (Park a kol., 2001). Produkcia hepcidínu je regulovaná na jeho transkripcnej úrovni.

Pozitívna regulácia hepcidínu koreluje s vysokými hladinami železa (Obr. 5). Na bunkové resp. orgánové preťaženie železom sa pečeň adaptovala pomocou endogénnej sekrécie BMP ligandov, ktoré v kontexte antioxidačnej obrany aktivujú BMP/SMAD (small and mothers against decapentaplegic protein) signalizáciu. BMP6 sa spoločne s konštitutívne exprimovaným BMP2 zodpovedajúcim za bazálnu expresiu hepcidínu (Wang a kol., 2020) viaže na špecifické BMP receptory (BMPR) a spúšťa fosforyláciu intracelulárnych proteínov SMAD1/5/8, ktoré ako komplex so SMAD4 prechádzajú do jadra a spúšťajú transkripciu génu *HAMP* (Meynard a kol., 2009; Andriopoulos a kol., 2009) (Obr. 6A). Aktivácia BMPR vyžaduje dvojstupňovú kontrolu v podobne prítomnosti a) funkčného HJV (hemojuvelin), ktorý slúži ako koreceptor BMPR (Wang a kol., 2005) (Obr. 6A) a b) proteínov HFE a TfR2, ktoré sa podieľajú na správnom zostavení BMPR/HJV komplexu (Obr. 6B). Na systémovej úrovni, vysoké hladiny sérového železa a zvýšená hodnota TSAT tiež stimulujú produkciu hepcidínu spoluprácou medzi homologmi TfR1 a TfR2. Afinita TfR2 k holotransferínu je

nižšia v porovnaní s TfR1 a v rámci metabolizmu železa je jeho funkcia skôr signalizačná. Pri normálnych hladinách železa TfR1 asociuje s HFE, ale pri zvýšenej TSAT je TfR1 vytiesnený jeho homológom TfR2. Komplex HFE/TfR2 ďalej interaguje s HJV a spúšťa BMP/SMAD dráhu (Gao a kol., 2009) (Obr. 6B).

K zvýšeniu hladiny hepcidínu dochádza aj v reakcii na zápal a infekciu (Obr. 5), čím je zabezpečená ochrana organizmu hostiteľa pred patogénmi obmedzením dostupnosti železa potrebného pre ich rast. Na molekulárnej úrovni expresiu *HAMP* stimulujú zápalové cytokíny IL-6 alebo aktivín-B (Lee a kol., 2006; Verga Falzacappa a kol., 2007; Canali a kol., 2016). Kým aktivín-B podporuje expresiu hepcidínu cez BMP/SMAD signalizáciu, tak IL-6 ju stimuluje najmä prostredníctvom JAK/STAT3 signálnej dráhy (Obr. 6C). Pravdepodobne však funguje isté prepojenie oboch uvedených dráh. Dôkazom toho sú SMAD4 *knock-out* myši, ktoré vykazujú zníženú hepcidínovú odozvu po stimulácii s cytokínom IL-6 (Wang a kol., 2005). Rovnako to potvrdzujú aj iné štúdie, u ktorých bola pri absencii BMP6, BMPR a HJV proteínov indukcia expresie hepcidínu na zápalovú signalizáciu oslabená (Latour a kol., 2017; Fillebein a kol., 2018). Okrem toho aj ďalšie zápalové molekuly napr. lipopolysacharid (LPS), či IL-1 β môžu stimulovať expresiu hepcidínu cez c-Jun N-terminal kinázovú (JNK) a/alebo NF- κ B (nuclear factor kappa-light-chain-enhancer of activated B cell) signálnu dráhu (Kanamori a kol., 2017; Kanamori a kol., 2018; Lee a kol., 2017). To naznačuje, že regulácia expresie hepcidínu je veľmi komplexná a zahŕňa interakciu rôznych pozitívne a negatívne pôsobiacich signálov.



Obr. 6: Kontrola produkcie hepcidínu kódovaného génon *HAMP* spočíva v jeho transkripcnej regulácii. Pozitívna regulácia BMP (bone morphogenetic proteins)/BMPR (bone morphogenetic proteins receptor) /SMAD (small and mothers against decapentaplegic protein) signálou dráhou (A) vyžaduje pre jej

plnohodnotnú aktiváciu zostavenie HJV (hemojuvelin) a HFE (hemochromatosis protein)/TfR2 (transferin receptor 2) proteínového komplexu (B). Ďalším pozitívnym regulátorom *HAMP* expresie je IL-6 (interleukin-6)/JAK (Janus kinase)/STAT3 (signal transducer and activator of transcription 3) signalizácia (C). Pravdepodobná kooperácia týchto dráh je naznačená prerušovanou čiarou. Matriptáza štiepiaca HJV (D) spolu s dominantným efektom ERFE (E), ktorý vychytáva BMP ligandy, tlmí BMP/BMPR/SMAD signalizáciu a negatívne ovplyvňuje *HAMP* expresiu.

Pri nízkych hladinách železa v cirkulácii membránová proteáza matriptáza-2 štiepi HJV a pôsobí ako negatívny regulátor BMP/SMAD signalizácie a produkcie hepcidínu (Silvestri a kol., 2008) (Obr. 6D). Rozhodujúcim a kritickým **negatívnym regulátorom** hepcidínu je erytroidný regulačný signál sprostredkovaný hormónom ERFE. Úloha ERFE počas ustálenej erytropoézy je zanedbateľná (Kautz a kol., 2014), ale počas indukovej/stresovej erytropoézy erytroidné prekurzory prostredníctvom JAK2/STAT5 signálnej dráhy zvyšujú produkciu ERFE, ktorý sa vylučuje do obehu a pôsobí priamo na hepatocyty, kde dochádza k zníženiu transkripcie hepcidínu (Obr. 5). Mechanizmus pôsobenia ERFE pravdepodobne spočíva v naviazaní a vychytávaní BMP6 a BMP2 ligandov, čím dochádza k útlmu aktivity BMP/SMAD signálnej dráhy a produkcie hepcidínu (Arezes a kol., 2018; Wang a kol., 2020) (Obr. 6E). Erytroidné regulačné signály sa považovali za hlavného regulátora hepcidínu, pretože dominujú nad signálmi analyzujúcimi stav cirkujúceho/zásobného železa. Najlepšie to dokumentujú patologické stavy, akými sú β -talasémia, vrozená dyserytropoetická anémia alebo MDS, počas ktorých je neefektívna erytropoéza sprevádzaná preťažením železom súbežne s veľmi nízkymi alebo takmer nedetektovateľnými hladinami hepcidínu (Papanikolaou a kol., 2005). Ďalšie štúdie však spochybňujú jednoznačnú pozíciu ERFE ako dominantného faktora a poukazujú na dôležité postavenie zápalu v regulačnej sieti hepcidínu. Napríklad ERFE *knock-out* myší model ukázal, že anémia zápalového ochorenia má závažnejší charakter ako u kontrolných zvierat a je spojená s vyššími hladinami hepcidínu (Kautz a kol., 2014). Navyše sa zdá, že ERFE nie je schopný potlačiť zápalom stimulovanú produkciu hepcidínu. Anémia zápalu počas aktívnej tuberkulóznej infekcie indukuje prostredníctvom IL-6 vysoké hladiny hepcidínu potláčajúc supresívny účinok ERFE, ktorý je produkovaný erytroblastmi ako odpoveď na anémiu a EPO signalizáciu (Cercamondi a kol., 2021). Okrem toho sa ukazuje, že pohlavný hormón testosterón je tiež zapojený do regulácie hepcidínu. Podporuje sekréciu EPO a erytropoetickú aktivitu, avšak EPO a erytropoéza nie sú priamo zodpovedné za testosterónom sprostredkovanú supresiu *HAMP* expresie (Bachman a kol., 2014). Boli popísané mechanizmy spájajúce testosterónom indukovanú Egf (epidermal growth factor)/EgfR (epidermal growth factor receptor) signalizáciu so supresiou hepcidínu, no ich

priebeh *in vivo* nie je ešte známy (Latour a kol., 2014). Inhibícia hepcidínu závislá od rastového faktora môže vysvetliť jeho nízku produkciu v období rastu a vývoja mladých myší, počas ktorého sú zvýšené požiadavky na železo (Girelli a kol., 2009).

Regulácia hepcidínu u primárnych erytrocytív je čiastočne popísaná u PV s mutáciami JAK2 v exóne 12, ktorá je typická izolovanou erytrocytívou. Bolo ukázané, že vyššia expresia génov kódujúcich TfR1 a ERFE je sprevádzaná s nižšími sérovými hladinami hepcidínu, naznačujúc také zmeny v metabolizme železa, ktoré zvyšujú dostupnosť železa pre akcelerovanú produkciu erytrocytov (Grisouard a kol., 2016). Podobne, znížené hladiny hepcidínu a/alebo známky deficitu železa boli popísané u pacientov so sekundárnou (Ang a kol., 2002; Gordeuk a kol., 2011; Sable a kol., 2012) a idiopatickou (Pavic a kol., 2003) erytrocytívou. Avšak u dedičných primárnych erytrocytív mechanizmus regulácie metabolizmu železa v spojení s nadmernou erythropoetickou aktivitou neboli doposiaľ študované.

2. CIELE DIZERTAČNEJ PRÁCE

Predložená práca je zameraná na molekulárnu a patofyziologickú charakterizáciu vybraných hematologických porúch na rôznych biologických modeloch a primárnych vzorkách pacientov.

Špecifické ciele tejto práce sú:

- 2.1 Analýza dôsledkov *gain-of-function EPOR* mutácie na erytropoézu a metabolizmus železa na myšom modeli.**
- 2.2 Štúdium vybraných hereditárnych *JAK2* mutácií**
- 2.3 Kritické zhodnotenie literatúry týkajúcej sa nových poznatkov patofyziológie Ph-negatívnych MPN**

3. METODICKÉ POSTUPY

Táto časť obsahuje podrobnejší popis metód týkajúcich sa mojej experimentálnej práce, ktoré som vykonávala sama a ktoré boli realizované na Ústave biologie Lékařské fakulty Univerzity Palackého v Olomouci – LF UPOL.

3.1 Postupy s použitím PFCP myšieho modelu

3.1.1 PFCP myší model

Inbredný kmeň myší C57BL/6 bol použitý na vytvorenie geneticky modifikovaných *knock-in* myší s ľudským *gain-of-function* EPOR (zámena c.1278C>G; podľa databázy LOVD, www.lovd.nl) (Divoky a kol., 2001). Heterozygotné *knock-in* potomstvo bolo krížené za vzniku všetkých experimentálnych myší t.j.: homozygotné *mtHEPOR/mtHEPOR*, heterozygotné *mtHEPOR/mEpoR* ako aj kontrolné *mEpoR/mEpoR* myši. Myši boli chované a udržiavané v Centre pro práci s laboratorními zvířaty LF UPOL podľa predpisov Výboru pro ochranu zvířat používaných pro vedecké účely. Samce myší boli odstavené po 4 týždňoch, udržovali sa na štandardnej strave a boli utratené v uvedených časových bodoch.

3.1.2 Genotypizácia PFCP myšieho modelu

Na genotypizáciu bola použitá DNA izolovaná z venóznej krvi retro-orbitálnej dutiny odoberaná do skúmavky s obsahom K₃EDTA. DNA bola izolovaná pomocou kitu DNeasy Blood & Tissue Kit (QIAGEN) podľa pokynov výrobcu. Genotypizácia bola realizovaná pomocou PCR analýzy, ktorej výstupom bolo odlišenie jedincov nesúcich myší *EpoR* alebo ľudský *EPOR*. PCR reakcia bola realizovaná s použitím kitu HotStarTaq Master Mix Kit (QIAGEN) podľa pokynov výrobcu v MJ Mini Thermal Cycler (Bio-Rad), jej podmienky a sekvencie primerov sú uvedené nižšie. Výsledné PCR produkty boli analyzované gélovou elektroforézou.

Krok		Teplota	Dĺžka
Úvodná denaturácia		95°C	15 min.
Denaturácia	33 opakovanie	95°C	10 sek.
Anelácia	33 opakovanie	60°C	30 sek.
Polymerizácia	33 opakovanie	72°C	30 sek.
Záverečná polymerizácia		72°C	2 min.

EPOR primer	sekvencia 5‘- 3‘	dĺžka ľudského produktu	dĺžka myšieho produktu
mouse forward	GGAGTTCCCTTGACCTTAGCG	331 bp	548 bp
human forward	ACTGGGATTATAGTGTGGTGTAAA		
human/mouse reverse	GATGCCAGGCCAGATCTTC		

3.1.3 Stanovenie expozície fosfatidylserínu

Expozícia fosfatidylserínu na membráne erytrocytov bola stanovená pomocou AnnexinV/FITC (BD Bioscence) podľa protokolu výrobcu. Po inkubácii sa erytrocyty premyli 1 x Annexin Binding Buffer a farbili s Annexin V počas 15 minút v tme pri izbovej teplote. Intenzita fluorescencie erytrocytov sa merala pomocou FACS Calibur (BD Bioscience, Franklin Lakes, NJ, USA) na FL1.

3.1.4 Stanovenie parametrov železa a detekcia železa v tkanive

Myšie sérum bolo získané po centrifugácii (2000 ot./min., 20 min. pri 4°C) koagulovanej krvi odobratej po punkcii srdca. Saturácia transferínu bola vypočítaná na základe hodnôt hladín železa a väzbovej kapacity železa nameraných pomocou analyzátoru Cobas 8000 (Roche/Hitachi) z myšieho séra. Hodnoty boli namerané na Oddelení klinické biochemie FN Olomouc.

Koncentrácia nehémového železa v pečeni, slezine, obličkách a srdci bola meraná pomocou chromogénnej kolorimetrickej analýzy podľa Horvathova a kol. (2012). Päťdesiat mg tkaniva bolo narezaných a rozpustených v 0,5 ml roztoku kyseliny trichlórooctovej (Sigma-Aldrich) a kyseliny chlorovodíkovej (LachNer) počas 24 hodín pri 65°C v laboratórnej trepačke. Päťdesiat μ l extraktu bolo pridaných k 1,5 ml chromogénu [octan sodný (Sigma-Aldrich), bathofenantrolín a kyselina thioglykolová (Erba Lachema) v deionizovanej vode]. Po 15 minútach bola meraná absorbancia roztoku pri 540 nm pomocou NanoQuant infinite M200 (TECAN). Ako štandardná krivka bola použitá zvyšujúca koncentrácia (0; 2,5; 5; 10; 25; 50 μ g/ml) vodného roztoku hexohydrtátu síranu železnato-amónneho (Sigma-Aldrich). Deparafinované tkanivové rezy boli zafarbené Perlsovou pruskou modrou špecificky viažucou nehémové Fe^{3+} železo podľa Horvathova a kol. (2012). Z rezov tkaniva bol odstránený parafín pomocou zostupnej alkoholovej rady. Preparáty boli premyté v destilovanej vode a vložené do roztoku ferokyanidu draselného (2%) a kyseliny chlorovodíkovej (2%) v pomere 1:1 počas 40 min. Preparáty boli premyté v destilovanej

vode a dofarbené Jadrovou červeňou počas 7 min. Preparáty boli odvodnené vzostupnou alkoholovou radou, následne bol zmontovaný trvalý preparát. Sklíčka boli analyzované svetelným mikroskopom Olympus BX 51 (Olympus, Hamburg, Nemecko).

3.1.5 Izolácia RNA z tkaniva

RNA z buniek myšej kostnej drene bola izolovaná s použitím činidla TRIreagent (Sigma-Aldrich). Na 1 ml TRIreagentu bolo pridaných 200 µl vychladeného chloroformu. Po 3 minútach inkubácie pri izbovej teplote sa zmes centrifugovala pri 12 000 ot./min. počas 15 minút pri 4°C. Horná vodná fáza (obsahujúca RNA) sa opatrne preniesla do novej skúmavky; do ktorej bolo pridaných 500 µl vychladeného izopropylalkoholu, RNA bola precipitovaná v tejto zmesi počas 10 minút pri izbovej teplote. Následne bola vzorka centrifugovaná pri 12 000 ot./min. počas 10 minút pri 4°C. Supernatant bol odstránený a pelet bol premytý 1 ml vychladeného 75% etanolu (zriedeneho vo vode ošetrenej s činidlom DEPC; Sigma Aldrich). Po 5 minútach centrifugácie pri 7500 ot./min. pri 4°C bol pelet vysušený, rozsuspendovaný v 15 – 25 µl vody ošetrenej DEPC a rozpustený v termobloku pri 65°C počas 10 minút.

Na izoláciu RNA z myších sleziny a pečene boli použité QIAshredder a RNeasy Mini Kit (QIAGEN) podľa pokynov výrobcu. RNA bola rozpustená v 15 – 30 µl vody (bez RNázy).

3.1.6 Stanovenie hladín hepcidínu, ferritínu, EPO

Sérové hladiny Hepcidínu, Ferritínu a EPO sa kvantifikovali pomocou ELISA kitov: Hepcidin-Murine Compete ELISA (Intrinsic LifeSciences), ab157713 Ferritin (FTL) Mouse ELISA kit (Abcam), Mouse Erythropoietin Quantikine ELISA Kit (R&D Systems) podľa pokynov výrobcu. Patričné absorbancie boli stanovené na spektrofotometri Infinite 200 NanoQuant, (Tecan).

3.1.7 Kvantitatívna *real time* PCR

Celková RNA izolovaná z tkanív bola ošetrená pomocou DNázy DNA-free DNase I (Ambion). Koncentrácia RNA bola meraná na spektrofotometri Infinite 200 NanoQuant (Tecan) a 1 µg RNA bol reverzne transkribovaný pomocou súpravy SuperScript® VILO™ cDNA Synthesis Kit (Invitrogen) podľa pokynov výrobcu. Komplementárna cDNA bola kvantifikovaná na Light Cycler 480 (Roche Applied Science) pomocou FastStart TaqMan Probe Master (Roche Applied Science; gény Il6, Epo, Actb), LightCycler 480 SYBR Green

I Master (gény Hamp, Bmp6, Actb) alebo s využitím analýzy TaqMan® Gene Expression (gény Fam232b, GypA, Actb). Primery pre gény Il6 a bActin boli navrhnuté pomocou Assay Design Centrum for systémy UPL (Roche Applied Science). Primery pre gény Hamp, Bmp6 a bActin boli skonštruované podľa Horvathova a kol. (2012). Primery pre gény Fam132b, GypA a bActin boli skonštruované podľa Grisouard a kol. (2016). Expresia špecifických génov stanovená pomocou kvantitatívnej – qPCR (quantitative PCR) bola normalizovaná proti *housekeeping* génu pre beta-aktín alebo proti erytroidne-špecifickému génu pre glykoforín A a k stanoveným hladinám mRNA u kontrolných myší mEpoR.

Gén	Mechanizmus kvantifikácie	Próby/ Sekvencie primerov 5'- 3'
Fam132b	TaqMan Gene Expression Master Mix	Mm00557748_m1
Gypa	TaqMan Gene Expression Master Mix	Mm00494848_m1
Epo	TaqMan Gene Expression Master Mix	Mm01202755_m1
Actb	TaqMan Gene Expression Master Mix	Mm00607939_s1
Hamp	LightCycler 480 SYBR Green I Master	F: CCTGAGCAGCACCACTATCT R: TCAGGATGTGGCTCTAGGCTATGT
Bmp6	LightCycler 480 SYBR Green I Master	F: AACAGCTTGAAGAACATGAG R: TGGACCAAGGTCTGTACAATGG
Actb	LightCycler 480 SYBR Green I Master	F: TCAACACCCAGCCATGTA R: GTGGTACGACCAGAGGCATAC
Il6 probe #6(cat. no. 04685032001)	FastStart TaqMan Probe Master	F: GATGGATGCTACCAAACGGAT R: CCAGGTAGCTATGGTACTCCAGA
bActb probe #56 (cat. no. 04688538001)	FastStart TaqMan Probe Master	F: AAGGCCAACCGTGAAAAGAT R: GTGGTACGACCAGAGGCATAC

3.1.8 Analýza erytroidnej diferenciácie a maturácie pomocou prietokovej cytometrie

Analýza erytroidnej diferenciácie a maturácie bola realizovaná podľa Horváthová a kol. 2012 a Socolovsky a kol. 1999. Bunky kostnej drene a sleziny sa izolovali pomocou prefiltrovania cez MASH filter, potom boli centrifugované (1800 ot./min, 5 min. pri 4°C), následne boli premyté s 0,5 % BSA v PBS a centrifugované (1800 ot./min, 5 min. pri 4°C). Následne sa bunky spoločne farbili v s 0,1 % BSA v PBS s FITC-konjugovanými CD71 a Ter119 protilátkami konjugovanými s fykoerytrínom (BD Biosciences) počas 1 hodiny v tme na ľade. Nasledovala séria dvoch premytí s 0,1 % BSA v PBS (2000 ot./min, 5 min. pri 4°C). Intenzita fluorescencie sa merala pomocou FACS Calibur (BD Bioscience, Franklin Lakes, NJ, USA).

3.1.9 Meranie hladiny reaktívnych foriem kyslíka

Hladiny ROS v myšom sére boli stanovené pomocou kitu OxiSelect In Vitro ROS/RNS Assay podľa pokynov výrobcu. Intenzita fluorescencie sa merala v FACS Calibur (BD Bioscience, Franklin Lakes, NJ, USA).

3.1.10 Prežívanie erytrocytov

Prežívanie erytrocytov bolo realizované podľa Akel a kol. (2007). Erytrocyty sa izolovali z celkovej krvi, potom boli centrifugované (2000 ot./min, 10 min.), následne boli premyté s 1xPBS a spočítané. Celkový počet erytrocytov 2×10^9 bol inkubovaný s $10 \mu\text{M}$ CFSE (karboxyfluoresceín diacetát sukcínimidylester; Molecular Probes, Invitrogen) v PBS po dobu 30 minút pri 37°C v tme. Nasledovala séria dvoch premytí 1% FBS v PBS (predhriaty na 37°C) a centrifugácií pri 2000 ot./min. 5 minút. Výsledný pelet bol rozsuspendovaný v $100 \mu\text{l}$ 0,9% NaCl (predhriaty na 37°C). Fluorescenčne označené erytrocyty sa injikovali do chvostových žíl recipientných myší. Intenzita fluorescencie erytrocytov sa merala pomocou FACS Calibur (BD Bioscience, Franklin Lakes, NJ, USA) na FL1 z krvi odoberanej z chvostovej žily (zriedenej v pomere 1:1300 s PBS) vo vybraných časových intervaloch nasledujúcich po injekcii (2 hodiny, 24 hodín, 2 dni, 7, 14, 21, 28 a 35 dní). Percento CFSE-pozitívnych erytrocytov stanovené po dvoch hodinách od injekcie fluorescenčne označených erytrocytov bolo považované za 100%.

3.2 Postupy s použitím bunkového modelu

3.2.1 Konštrukcia vektora a mutagenéza

Podľa inštrukcií výrobcu bol použitý kit QuickChange II XL pre cielenú mutagenézu (Agilent Technologies) s použitím PfuUltra DNA polymerázy (Agilent Technologies) na vytvorenie JAK2 c.1849G>T (JAK2_V617F), JAK2 c.2538G>C (JAK2_E846D) a JAK2 c.3188G>A (JAK2_R1063H) a JAK2 c.1849G>T.3188G>A (JAK2_V617F_R1063H) ľudskej ORF cDNA JAK2, ktorá bola následne klonovaná do pCMV6-AC-IRES-GFP-Puro cicavčieho expresného vektora (OriGene). Produkt mutagenézy PCR bol štiepený DpnI (Agilent Technologies) a transformovaný do ultrakompetentných buniek XL10-Gold (Agilent Technologies) alebo SIG10 5-alpha (Sigma-Aldrich) podľa protokolu výrobcov. Bakteriálne kolónie sa preniesli do 3ml bakteriálneho kvapalného média (LB Broth, Sigma-Aldrich) obsahujúceho $50 \mu\text{g}/\text{ml}$ ampicilínu (Sigma-Aldrich) a nechali sa rásť 8 až 12 hodín

pri 37°C v laboratórnej trepačke Lab Companion SI-600 (GMI). Plazmidová DNA bola izolovaná pomocou kitu QIAGEN® Plasmid Minii (QIAGEN). Plazmidová DNA sa najskôr overila štiepením pomocou nasledujúcich reštrikčných enzýmov: EcoRV, XbaI, EcoRI, BamHI, BsiWI a NaeI (New England Biolabs). Úplná sekvencia JAK2 finálnych klonov bola overená sekvenovaním firmou SEQme. Kit QIAGEN® Plasmid Maxi (QIAGEN) bol použitý na izoláciu väčšieho množstva plazmidu. Tri mutantné plazmidy pCMV6-AC-IRES-GFP-Puro_JAK2_E846D, pCMV6-AC-IRES-GFP-Puro_JAK2_R1063H, pCMV6-AC-IRES-GFP-Puro_JAK2_V617F, dvojity mutant pCMV6-AC-IRES-GFP-Puro_JAK2_V617F_R1063H a plazmid s JAK2 WT boli použité na elektroporáciu do Ba/F3 buniek.

Primery použité na mutagenézu	
JAK2 V617F sense	5'-agcattggtttaaattatggaggatgtttctgtggagacgaga-3'
JAK2 V617F antisense	5'-tctcgctccacagaaaacatactccataattaaaaaccaaatgct-3'
JAK2 E846D sense	5'-cgggatccacacagttaaagacacatgttgaatttc-3'
JAK2 E846D antisense	5'-gaaattcaatgtctgtttcaacttgttaggatccg-3'
JAK2 R1063H sense	5'-tttgcatggcaatcatatgcataaaattccgcgtgg-3'
JAK2 R1063H antisense	5'-ccaccagcggaaatttatgcataatgatggcaatgaca-3'

3.2.2 Transfekcia plazmidovej DNA do buniek Ba/F3

Na transfekciu plazmidovej DNA do buniek bunkovej línie Ba/F3 bola zvolená metóda elektroporácie. Bunková línia Ba/F3 je myšia pro-B bunková línia závislá od IL-3, exprimujúca EPOR wt a bola darom od Roberta Kralovicsa (CeMM, Viedeň, Rakúsko) (D'Andrea a kol., 1991). Bunky Ba/F3-EPOR boli kultivované v médiu IMDM (Life Technologies) obsahujúcim 10% FBS (Life Technologies) a 1U/ml EPO (Janssen Pharmaceuticals) alebo 2 ng/ml IL-3 (Prospec).

Na transfekciu bolo použité celkové množstvo 5×10^6 buniek Ba/F3-EPOR. Dvadsať μg plazmidovej DNA: pCMV6-AC-IRES-GFP-Puro_JAK2E846D, pCMV6-AC-IRES-GFP-Puro_JAK2R1063H, pCMV6-AC-IRES-GFP-Puro_JAK2V617F, pCMV6-AC-IRES-GFP-Puro_JAK2_V617F_R1063H, pCMV6-AC-IRES-GFP-Puro_JAK2WT bolo elektroporovaných do buniek Ba/F3-EPOR pri podmienkach 420V a $250\mu\text{F}$ pomocou sterilnej elektroporačnej kyvety v Gene-Pulser (obidve od Bio-Rad). Stabilné transfektanty boli selektované s 1 $\mu\text{g}/\text{ml}$ puromycínu (Life Technologies) počas 2 týždňov.

3.2.3 Test senzitivitu k inhibitorom

Test senzitivitu k JAK2 inhibitorom bol vykonávaný pomocou kolorimetrického MTT testu podľa Koledova a kol. (2010). Stabilne transfekované bunky Ba/F3-EPOR rastúce v IMDM s 10% FBS a 2 ng/ml IL-3 boli trikrát premyté s PBS a nanesené na 96-jamkové kultivačné doštičky v koncentrácií 4×10^4 buniek/ml v troch opakovaniach so znižujúcimi koncentráciami inhibítora – Ruxolitinib (Jakavi, Novartis)/AZ-960 (Santa Cruz Biotechnology) (1; 0,5; 0,25; 0,1; 0,05; 0,01; 0,001; 0 μM). Taktiež boli pripravené tri kontrolné jamky čistého média bez buniek, ktoré slúžili ako tzv. blank pri meraní absorbancie. Bunky boli kultivované počas 72 hodín a následne bol vykonaný MTT test pridaním MTT (3-(4,5-dimethylthiazol-2-yl)-2,5-difenyltetrazolium bromid; Sigma-Aldrich) s výslednou koncentráciou 0,5 mg/ml. Bunky boli kultivované ďalšie 2,5 hodiny. Po centrifugácii doštičky (1500 ot./min) bolo odsaté médium a bolo pridaných 200 μl 10% dodecylsulfátu sodného (SDS, Sigma-Aldrich), doštička bola inkubovaná v tme na orbitálnej trepačke min. 8 hodín. Následne bola odčítaná absorbancia pri 570 nm v spektrofotometri Infinite 200 NanoQuant (Tecan). Hodnota IC₅₀ bola definovaná ako koncentrácia inhibítora potrebná na inhibíciu bunkového rastu o 50%.

3.2.4 Imunoblot

Stabilne transfekované bunky Ba/F3-EPOR rastúce v IMDM s 10% FBS a 2 ng/ml IL-3, boli štyrikrát premyté s PBS a následne boli v koncentrácií 5×10^6 buniek/ml kultivované bez akéhokoľvek rastového faktora po dobu 12 hodín. Potom boli kultivované s rozdielnou koncentráciou EPO (0; 0,1; 1) počas 15 min. Bunky boli centrifugované pri 1700 ot./3min. a ich pelet bol rozpustený v RIPA lyzačnom pufri (Sigma-Aldrich) so zmesou proteázových a fosfatázových inhibítordov (Sigma-Aldrich). Sedemdesiat μg vzorky proteínu bolo denaturovaných počas 5 minút, boli prenesené na nitrocelulózovú membránu pomocou Semi-Dry Transfer Cell Trans-Blot SD (Bio-Rad) počas 1 h blotovania pri 20 V. Membrána bola blokovaná počas 1 h v 5% mlieku v PBST (PBS s 0,1% Tween 20, Sigma-Aldrich). Na detekciu proteínu boli použité nasledujúce primárne protilátky (Cell Signaling) zriedené v 5% mlieku v PBS: fosfo-Jak2 (Y1007/1008, 1:250), Jak2 (1:500), fosfo-Stat5 (Y694, 1:250), Stat5 (1:500), fosfo-Stat1 (Y701, 1:250), Stat1 (1:500), a tubulín (1:1000). Väzba protilátky bol realizovaná cez noc pri 4°C. Po 3 premytiach v PBST bola membrána inkubovaná s králičou alebo myšou sekundárnu protilátkou (Sigma-Aldrich, 1:1000) po dobu 1,5 hodín pri izbovej teplote. Proteíny boli vizualizované chemiluminiscenčným spôsobom pomocou

substrátu SuperSignal® West Dura Extended Duration (Thermo Fisher Scientific), Následne bol vyvolávaný pomocou fixačného roztoku (AGFA, G354) s vývojky (AGFA, G150) svetlocitlivý film, ktorý bol analyzovaný denzitometrickou kvantifikáciou pomocou programu ImageJ.

3.3 Postupy s použitím ľudských vzoriek

3.3.1 Vzorky pacientov

Všetky vzorky pacientov boli získané s informovaným súhlasom schváleným Etickou komisiou LF UPOL a Fakultnej nemocnice – FN Olomouc. Informovaný súhlas bol získaný podľa Helsinskej deklarácie. Vzorky periférnej krvi boli zbierané do skúmaviek s obsahom EDTA alebo heparínu a následne boli použité na separáciu krviniek a/alebo izoláciu DNA.

3.3.2 Izolácia DNA z periférnej krvi

Izolácia genómovej DNA zo vzorky periférnej krvi bola realizovaná pomocou kitu Gentra Puregene (Qiagen) podľa odporúčaní výrobcu s niektorými modifikáciami: studený 1x lyzačný pufor (150 mM NH₄Cl, 10 mM NH₄ HCO₃, 1 mM Na₂ EDTA; všetky činidlá boli od spoločnosti Sigma-Aldrich) bol zmiešaný so vzorkou celej krvi v 50 ml skúmavke a inkubovaný na ľade počas 30 – 40 minút za občasného premiešania obrátením skúmavky. Vzorka bola následne centrifugovaná 10 minút pri 2000 otáčkach/minúta pri 4°C a pelet bol resuspendovaný v ďalších 15 ml studeného lyzačného pufra a znova centrifugovaný. Pelet bielych krviniek bol resuspendovaný v 600 µl roztoku Cell Lysis Solution (roztok súpravy), prenesený do 1,5 ml skúmavky Eppendorf a inkubovaný pri teplote 37°C počas 20 minút. Vzorka bola udržiavaná pri izbovej teplote počas 2 dní. Následná izolácia DNA bola realizovaná podľa protokolu výrobcu s použitím činidiel kitu Gentra Puregene. Čistota a koncentrácia DNA sa stanovila spektrofotometrickým meraním absorbancie (pri 260 nm a 280 nm) pomocou spektrofotometru Infinite 200 NanoQuant (Tecan).

3.3.3 Skríning mutácie JAK2 R1063H pomocou T-ARMS PCR

Špecifická PCR (polymerase chain reaction) – T-ARMS PCR (tetra-primer amplification refractory mutation system PCR) je jednoduchá a ekonomická metóda na genotypizáciu jednonukleotidových zámen. Pomocou Primer1 (Collins a Ke, 2012) bola vytvorená štvorica primerov, ktoré sa použili na skríning mutácie JAK2 c.3188G>A (p.R1063H) u pacientov

s myeloidnou neopláziou a kontrol. Reakcia bola realizovaná s použitím kitu HotStarTaq Master Mix Kit (QIAGEN) podľa odporúčania výrobcu. Podmienky PCR, sekvencie primerov a ich konečná koncentrácia v reakcii sú uvedené nižšie (tučným je zvýraznený *mismatch* a podčiarknutie zvýrazňuje zámennu G>A). Výsledné PCR produkty boli analyzované gélovou elektroforézou.

Krok		Teplota	Dĺžka
Úvodná denaturácia		95°C	15 min.
Denaturácia	30 opakovanie	95°C	10 sek.
Anelácia	30 opakovanie	60°C	30 sek.
Polymerizácia	30 opakovanie	72°C	30 sek.
Záverečná polymerizácia		72°C	5 min.

JAK2 R1063H primer	sekvencia 5'- 3'	Výsledná konc.	dĺžka vonkajšieho produkту	dĺžka produktu s alelou G (WT)	dĺžka produktu s alelou A (MUT)
outer forward	TTGTGTTGAGTTTATTACAGCTATGGA	0.4µM			
outer reverse	AAATGAACACTAAGGGCCATCTT		542 bp	341 bp	254 bp
inner forward	AAAGTGGGTTGTTTAGGAATTATTTCG	0.2µM			
inner reverse	CCTTGTTGTCATTGCCAATCAGAT				

3.3.4 Stanovenie *cis/trans* konfigurácie mutácií JAK2 V617F a R1063H

Vzorka RNA pacientov bola izolovaná našim spolupracujúcim laboratóriom, následne bola reverzne transkribovaná pomocou súpravy SuperScript® VILO™ cDNA Synthesis Kit (Invitrogen) podľa pokynov výrobcu. Pomocou semi-nested PCR s použitím nižšie uvedených primerov bol amplifikovaný PCR produkt zahŕňajúci exóny 14 – 24 génu *JAK2*, ktorý bol následne purifikovaný pomocou NucleoSpin® Gel and PCR Clean-up (MACHEREY-NAGEL) a klonovaný do pGEM-T easy vektora (Promega) podľa pokynov výrobcu. Izolácia plazmidovej DNA z kolónií obsahujúcich plazmid a sekvenovanie PCR inzertu boli realizované spoluautormi.

Primery použité pri semi-nested PCR	
1. Kolo forward	5'-ACGGTCAACTGCATGAAACA -3'
1. Kolo reverse	5'-AGGAGGGCGTTGATTACA -3'
2. Kolo reverse	5'-ATCTCATCTGGGCATCCATC -3'

3.4 Štatistické analýzy

Všetky údaje sú predstavené ako priemer najmenej troch nezávislých experimentov, \pm označuje stredná chybu priemera. Pri analýze korelácie medzi *Hamp* a *Erfe* mRNA expresiou bola použitá Pearsonova korelačná analýza. Na výpočet polčasu prežívania erytrocytov bola využitá exponenciálna regresná rovnica. Štatistické analýzy boli realizované v programe Microsoft Excel (Microsoft) alebo Prism6 (GraphPad), testovacími štatistickými hypotézami boli Studentov t-test, Welchov t-test a Chí-kvadrát test. Hodnoty P menšie ako 0,05 boli považované za štatisticky významné: označenie *#/ pre $P < 0,05$, **/## pre $P < 0,01$ a ***/### pre $P < 0,001$.

4. KOMENTÁR K PREDLOŽENÉMU SÚBORU PUBLIKÁCIÍ

Moja dizertačná práca je písaná ako komentár k zbierke publikovaných článkov. V tejto kapitole uvádzam štyri pôvodné výskumné práce (publikované jedenkrát v American Journal of Hematology, jedenkrát Journal of Molecular Medicine a dvakrát v Blood Journal) a zároveň jeden súhrnný článok (publikovaný v Transfuze a Hematologie Dnes).

Pôvodné výskumné práce:

Divoky V, Song J, Horvathova M, **Kralova B**, Votavova H, Prchal JT, Yoon D. Delayed hemoglobin switching and perinatal neocytolysis in mice with gain-of-function erythropoietin receptor. *J Mol Med (Berl)*. 2016;94(5):597-608.

Kralova B, Sochorcova L, Song J, Jahoda O, Hlusickova Kapralova K, Prchal JT, Divoky V, Horvathova M. Developmental changes in iron metabolism and erythropoiesis in mice with human gain-of-function erythropoietin receptor. *Am J Hematol*. 2022;97(10):1286-1299.

Kapralova K, Horvathova M, Pecquet C, Fialova Kucerova J, Pospisilova D, Leroy E, **Kralova B**, Milosevic Feenstra JD, Schischlik F, Kralovics R, Constantinescu SN, Divoky V. Cooperation of germ line JAK2 mutations E846D and R1063H in hereditary erythrocytosis with megakaryocytic atypia. *Blood*. 2016;128(10):1418-23.

Mambet C, Babosova O, Defour JP, Leroy E, Necula L, Stanca O, Tatic A, Berbec N, Coriu D, Belickova M, **Kralova B**, Lanikova L, Vesela J, Pecquet C, Saussoy P, Havelange V, Diaconu CC, Divoky V, Constantinescu SN. Cooccurring JAK2 V617F and R1063H mutations increase JAK2 signaling and neutrophilia in myeloproliferative neoplasms. *Blood*. 2018;132(25):2695-2699.

Súhrnný článok:

B. Kráľová; K. Hlušičková Kapraľová; V. Divoký; M. Horváthová. Nové poznatky v patofyziológii Ph-negatívnych myeloproliferatívnych neoplázií. *Transfuze Hematol. Dnes*. 2021;27(3): 208-217.

4.1 Analýza dôsledkov *gain-of-function EPOR* mutácie na erytropoézu a metabolizmus železa na myšom modeli.

Mutácie vedúce k skráteniu cytoplazmatickej domény ľudského EPOR vedú k zosilneniu JAK2 signalizácie a k dominantne dedičnej erytrocytóze označovanej ako PFCP. V štúdii Divoky a kol. (2001) bol nahradený myší *Epor* gén (*mEpoR*) ľudským *wild-type EPOR* génom (*wtHEPOR*) a jeho mutovanou verziou (c.1278C>G) (*mtHEPOR*), ktorá viedie k skráteniu receptora po prvom tyrozínovom zvyšku v jeho intracelulárnej doméne. Myši heterozygotné pre mutovanú alelu – *mtHEPOR/mEpoR* resp. *mtHEPOR/wtHEPOR* mimikovali ľudské ochorenie PFCP. Fenotyp erytrocytózy sa u nich prejavil najskôr 3 až 6 týždňov po narodení zvýšením počtu červených krviniek, Hct a *in vitro* hypersenzitivou erytroidných progenitorov k EPO. Homozygotné mutantné myši – *mtHEPOR/mtHEPOR* vykazovali v porovnaní s heterozygotmi ďažší stupeň erytrocytózy, ktorá ale bola zlučiteľná so životom. Naopak, myši s *wild-type* ľudským *EPOR* génom, homozygotné (*wtHEPOR/wtHEPOR*) ako aj heterozygotné (*wtHEPOR/mEpoR*), boli v porovnaní s *mEpoR/mEpoR* kontrolami anemické (Divoky a kol., 2001).

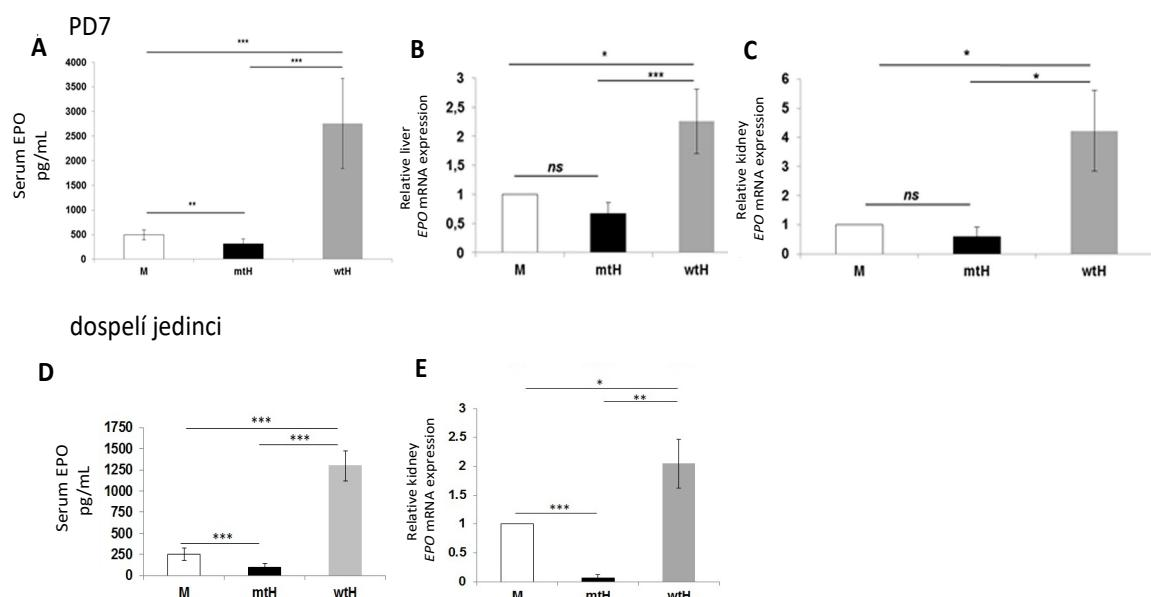
4.1.1 Štúdium primitívnej erytropoézy a ranej definitívnej erytropoézy u myší s *gain-of-function EPOR* mutáciou

Cieľom predloženého článku bolo a) vysvetlenie rozdielnych fenotypov zaznamenaných u *mtHEPOR* a *wtHEPOR* myší, b) analýza časovej osi rozvoja erytrocytózy u *mtHEPOR* myší a anémie u *wtHEPOR* myší. Pre určené analýzy boli použité jedince s homozygotným *wild-type EPOR* génom (*wtHEPOR/wtHEPOR*, označené ako wtH) a homozygotným mutantným *EPOR* génom (*mtHEPOR/mtHEPOR*, označené ako mtH). Kontrolnou skupinou boli myši nesúce myší *EpoR* gén (*mEpoR/mEpoR*, označené ako M).

Analýzy realizované spoluautormi ukazujú, že počas **strednej až neskorej gestácie mtH myši majú zvýšené hladiny Hct** v porovnaní s kontrolami. Naopak, **wtH myši**, podobne ako dospelí jedinci, sú značnú časť tohto obdobia **anemické**. Predpokladáme, že anemický fenotyp wtH myší môže byť zapríčinený nižšou úrovňou signalizácie ľudského EPOR v porovnaní s myším EpoR. Paralelne s tým ďalšie experimenty potvrdzujú, že kým skrátený ľudský EPOR spôsobuje po stimulácii s EPO zvýšenú a predĺženú fosforyláciu Stat5 vo FL bunkách mtH myší, tak u wtH myší je fosforylácia Stat5 takmer nedetektovateľná. V rovnakom období embryonálneho vývinu u mtH myší zaznamenávame zmnoženú

populáciu primitívnych nezrelých erytroidných buniek v porovnaní s wtH a kontrolnými myšami. Ďalšie výsledky, ktoré popisujú pomalšiu mieru enukleácie a diferenciácie erytroidných progenitorov a oneskorenie prepínania globínovej expresie u mtH myší naznačujú, že **u mtH myší je predĺžené obdobie primitívnej erytropoézy**.

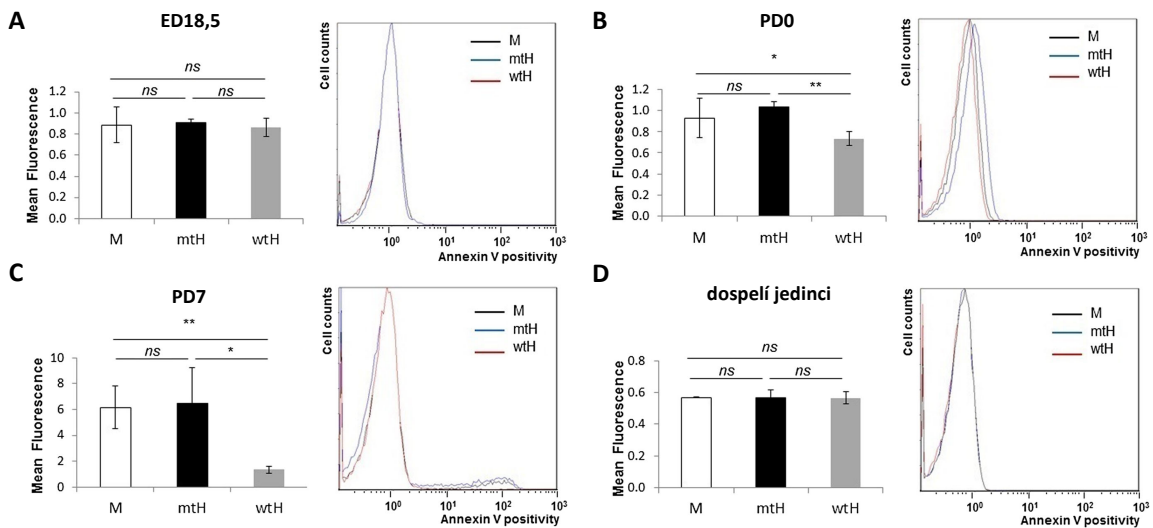
Krátko po narodení Hct všetkých analyzovaných myší klesá, pričom najrapídnejší pokles zaznamenávame práve u polycytemických mtH myší; najmenší rozdiel Hct u wtH myší. V tomto období majú anemické wtH myši signifikantne vyššiu perinatálnu produkciu Epo v porovnaní s mtH a kontrolnými myšami (Obr. 7A, B, C); a významne vyššie hladiny Epo u týchto myší pretrvávajú až do dospelosti (Obr. 7D, E). Naopak, mtH myši znížením produkcie Epo si už v perinatálnom období (Obr. 7A, B, C) v dôsledku erytrocytózy začínajú budovať kompenzačný efekt, ktorý sa v dospelosti prehlubuje signifikantne zníženou produkciu Epo (Obr. 7D, E). To naznačuje, že **regulácia tvorby Epo je adekvátna k rozdielom Hct**.



Obr. 7: Produkcia EPO v perinatálnom období a v dospelosti. Hladiny EPO analyzované ELISA testom zo séra (A) a relatívnu expresiou v pečeni (B) a obličkách (C) u kontrolných *EpoR* - M, *mtHEPOR/mtHEPOR* - mtH a *wtHEPOR/wtHEPOR* myší - wtH myši starých 7 dní (postnatal day – PD7). Hladiny EPO analyzované ELISA testom zo séra (D) a relatívnu expresiou v obličkách (E) kontrolných *EpoR* – M, *mtHEPOR/mtHEPOR* – mtH a *wtHEPOR/wtHEPOR* – wtH dospelých myší *P < .05, **P < .01, ***P < 0.001 vs. *mEpOR* (M) (Prevzaté a upravené z Divoky a kol., 2016)

Ďalšie rozdiely medzi fenotypmi študovaných zvierat sú spojené s rôznymi hladinami PS exponovaného na extracelulárnu stranu erytrocytov. V prenatálnom období (Obr. 8A) aj v dospelosti (Obr. 8D) je expozícia PS u myší všetkých genotypov porovnateľná. Avšak v deň narodenia – PD0 (postnatal day 0) a týždeň po ňom – PD7 (postnatal day 7) sú hladiny

exponovaného PS významne nižšie u wtH myší v porovnaní s hladinami exponovaného PS u kontrol a aj mtH myší (Obr. 8B, C), čo naznačuje zvýšené vychytávanie mtH a kontrolných erytrocytov makrofágmi RES v porovnaní s erytrocytmi wtH myší.



Obr. 8: Expozícia membránového PS v prenatálnom a perinatálnom období a v dospelosti. Schopnosť Annexinu V viazať sa na exponovaný PS (phosphatidylserine) bola analyzovaná pomocou prietokovej cytometrie z izolovaných erytrocytov embryí v embryonálny deň 18,5 – ED 18,5 (embryonic day 18,5) a myší v postnatálny deň 0 a 7 – PD0, PD7 (posnatal day 0, 7) a v dospelosti. Originálny histogram meraní je zobrazený vpravo vedľa grafu. *P < .05, **P < .01 vs. mEpoR (M) (Prevzaté a upravené z Divoky a kol., 2016)

U wtH myší, ktoré podstupujú len mierne perinatálne zmeny Hct predpokladáme, že výrazne vyššie hladiny Epo, obzvlášť v tomto období, môžu mať protektívny účinok na destrukciu erytrocytov (Risso a kol., 2014). Nakoľko pri pôrode jedinec prechádza z hypoxického prostredia do prostredia s vyšším atmosférickým obsahom kyslíka, domnievame sa, že za perinatálny pokles Hct a dočasnú korekciu erytrocytózy u mtH myší môže byť zodpovedná neocytolýza.

Touto prácou (príloha 1), na ktorej som sa priamo podielala analýzou hladín exponovaného PS a produkcie Epo, demonštrujeme, že **myši s *gain-of-function* EPOR (mtH) majú a) fetálnu erytrocytózu spojenú s predĺženou primitívnu erytropoézou a oneskoreným prechodom primitívnej na definitívnu erytropoézu; b) dočasné korekcie erytrocytózy v perinatálnom období, ktorá sa znova objavuje v postnatálnom období; c) nízke hladiny Epo pretrvávajúce od narodenia až do dospelosti.** Naopak, **wtH myši sú a) od fetálneho obdobia anemické; b) od narodenia majú stabilne vyššie hladiny Epo; c) v perinatálnom období u nich nedochádza k takým dramatickým zmenám Hct, aké sú popísané u mtH myší.**

4.1.2 Štúdium vzťahu erytropoézy a metabolizmu železa u myší s *gain-of-function EPOR* mutáciou

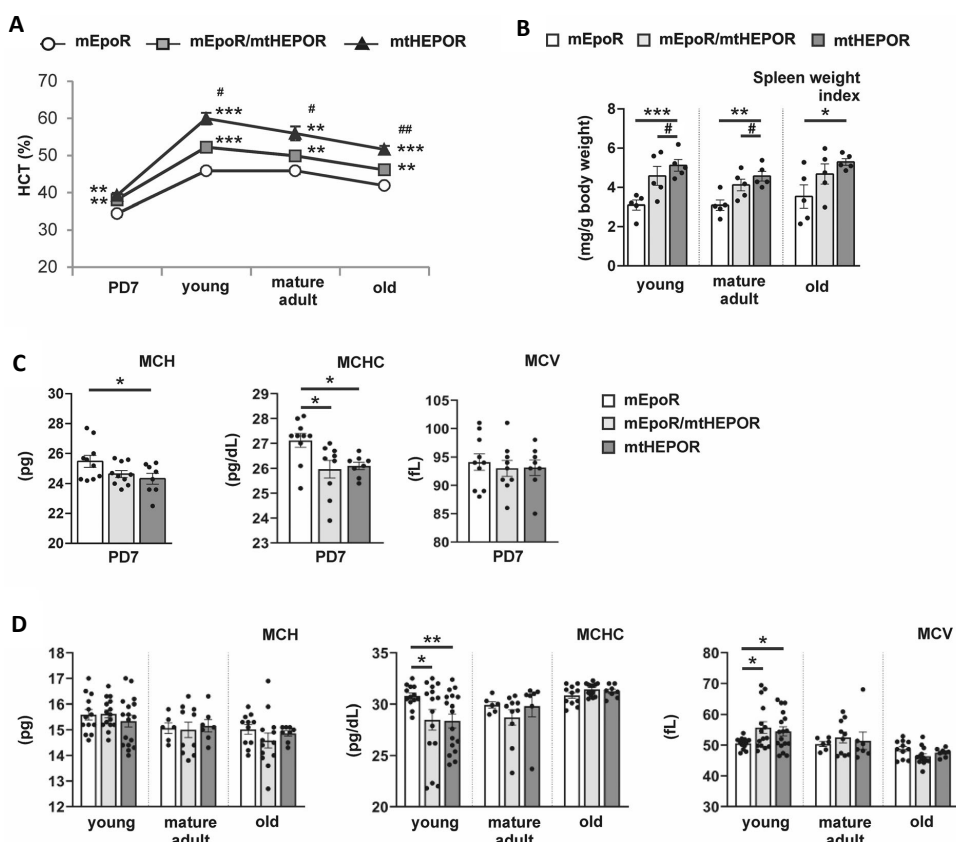
Koregulácia erytropoézy a metabolizmu železa je pomerne dobre popísaná u chorobných stavov charakteristických neefektívnej erytropoézou akými sú napr. β -talasémie, kongenitálne dyserytropoetické anémie, alebo MDS, u ktorých dochádza v dôsledku nízkych hladín hepcidínu k preťaženiu železom. Naopak, u pacientov s rôznymi typmi erytrocytóz je dostupných relatívne málo štúdií. Je známe, že u pacientov s Čuvašskou erytrocytózou (spôsobenou VHL mutáciou; Ang a kol., 2002) alebo PV (Ginzburg a kol., 2018) sú znížené koncentrácie cirkulujúceho hepcidínu súčasne pozorované s nedostatkom železa. Málo sa však vie o metabolizme železa pri vrodenej chronickej erytrocytéze s nízkymi hladinami EPO, akou je PFCP.

Cieľom predloženého článku bolo štúdium zmien metabolizmu železa v spojení so zmenami erytronu v rôznych vývinových štádiách vyššie popísaného PFCP myšieho modelu. V práci boli použité myši s mutovaným ľudským *EPOR* génom v homozygotnom (*mtHEPOR/mtHEPOR*) a heterozygotnom (*mtHEPOR/mEpoR*) stave, ktoré sa líšia intenzitou erytrocytózy (Divoky a kol., 2001), spoločne s kontrolnými jedincami s myším *mEpoR* génom (*mEpoR/mEpoR*). Analýzy boli realizované v rôznych vývinových obdobiach: prenatálne v embryonálny deň – ED17,5, postnatálne 7. deň po narodení – PD7 a u dospelých jedincov starých ~2.5 mesiaca (označených ako „young“), ~6.5 mesiaca („mature adult“) a ~16 mesiacov („old“). Jedná sa o nosný projekt mojej dizertačnej práce. Experimenty realizované spoluautormi sú explicitne uvedené.

Erytropoéza so znakmi nedostatku železa u *mtHEPOR* myší krátko po narodení

Najskôr sme hodnotili vývoj erytrocytózy u *mtHEPOR* myší v priebehu postnatálneho obdobia, od narodenia po vek 16 mesiacov. Aj napriek čiastočnej korekcií erytrocytózy u *mtHEPOR* myší, ktoré nastáva hned po narodení (PD7), je **Hct signifikantne zvýšený ako u heterozygotných, tak aj homozygotných *mtHEPOR* myší** v porovnaní s *mEpoR* kontrolnými myšami. Hladiny Hct ostávajú permanentne zvýšené vo všetkých nasledujúcich analyzovaných štádiách (Obr. 9A). Najvyššie hladiny Hct, zistené u *mtHEPOR* homozygotov, sú sprevádzané miernou splenomegáliou (Obr. 9B). Zároveň sme zistili, že v priebehu **starnutia zvierat** všetkých genotypov dochádza k **postupnému znižovaniu hladín Hct** (Obr. 9A).

Detailná analýza parametrov červených krviniek, konkrétnie znížené hodnoty priemerného korpuskulárneho hemoglobínu – MCH (mean corpuscular hemoglobin) a strednej koncentrácie korpuskulárneho hemoglobínu – MCHC (mean corpuscular hemoglobin concentration) naznačujú **obmedzený prísun železa** pre erytropoézu u ***mtHEPOR* heterozygotov aj homozygotov v perinatálnom období** (PD7) (Obr. 9C), ale nie u dospelých myší (Obr. 9D). Neprítomnosť mikrocytózy v PD7 (Obr. 9C), typická pre deficit železa, je u *mtHEPOR* novorodencov pravdepodobne maskovaná zvýšeným podielom makrocytických červených krviniek generovaných v prenatálnom období (Lucarelli a kol., 1964) v dôsledku oneskoreného prechodu z primitívnej erytropoézy na erytropoézu definitívnu, ktorú sme predtým naznamenali u *mtHEPOR* myší (Divoky a kol., 2016). Znížené hladiny MCH, MCHC a MCV (mean corpuscular volume); anizocytóza a retikulocytóza pozorované aj u štvortýždňových *mtHEPOR* heterozygotov a homozygotov sa čiastočne alebo úplne normalizujú u starších jedincov (Obr. 9D). Tieto dátu naznačujú, že **stav nedostatku železa pre erytropoézu je u *mtHEPOR* myší dočasné**.

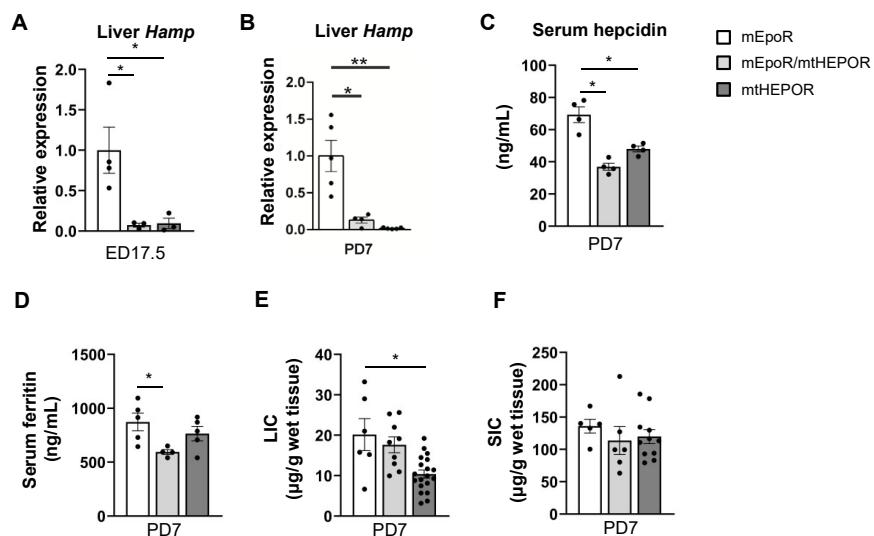


Obr. 9: Hematologické parametre a veľkosť sleziny. hladiny hematokritu – Hct (Hematocrit) u myší vo veku: postnatálny deň 7 (PD7), ~2,5 mesiaca staré (young), ~6,5 mesiaca staré (mature adult) a ~16 mesiacov staré (old) myší. Pokles hladín Hct medzi mladými a starými zvieratami: 14 % u *mtHEPOR* myší ($P < 0,001$), 12 % u *mEpoR/mtHEPOR* myší ($P < 0,001$) a 9 % u *mEpoR* kontrol ($P < 0,01$) (A). Hmotnosť sleziny v pomere k celkovej hmotnosti jedinca (B) u mladých, dospelých a starých myší. (C a D) parametre červených krviniek; stredný korpuskulárny hemoglobín – MCH (mean corpuscular hemoglobin), stredná koncentrácia

korpuskulárneho hemoglobínu – MCHC (mean corpuscular hemoglobin concentration) a stredný korpuskulárny objem – MCV (mean corpuscular volume) v PD7 (C) a u mladých, dospelých a starých myší (D). **P < 0,05, **P < 0,01, ***P < 0,001 vs. *mEpoR*; #P < 0,05 a ##P < 0,01, *mtHEPOR* vs. *mtHEPOR/mEpoR* (Prevzaté a upravené z Kralova a kol., 2022)

Prechod od nedostatku železa k zvýšenému ukladaniu železa u *mtHEPOR* myší

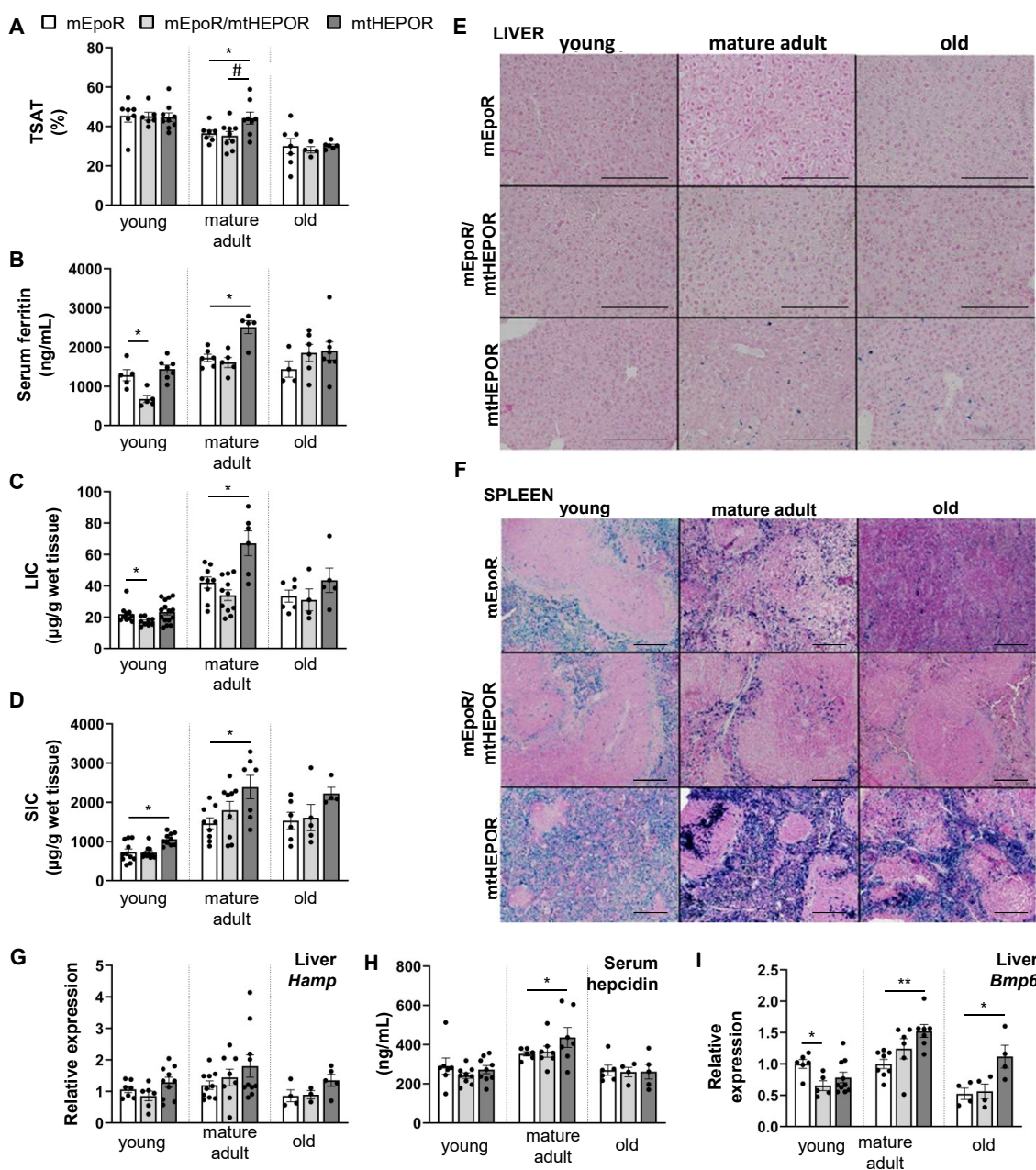
S cieľom korelovať uvedené zmeny erytropoézy so stavom železa, sme následne hodnotili vybrané parametre železa. V čase prenatálneho rozvoja erytrocytózy (ED17,5) (Divoky a kol., 2016), pozorujeme silné potlačenie expresie *Hamp* mRNA vo FL u *mtHEPOR* heterozygotných aj homozygotných myší (Obr. 10A). Krátko po narodení v PD7, je výrazne znížená expresia *Hamp* mRNA v pečeni (Obr. 10B) potvrdená aj zníženými hladinami hepcidínu v sére (Obr. 10C). To je v súlade so zníženými hladinami feritínu a zníženou koncentráciou nehémového železa v pečeni – LIC (liver iron content) detekovanými u mutantných myší oboch genotypov (Obr. 10D, E). Obsah železa v slezine – SIC (spleen iron content) je porovnatelný medzi všetkými genotypmi (Obr. 10F), čo môže byť dôsledkom intenzívnejšej destrukcie červených krviniek u *mtHEPOR* novorodencov (Divoky a kol., 2016).



Obr. 10: Analýza hepcidínu, parametrov železa počas prenatálneho a perinatálneho obdobia. Expresia *Hamp* mRNA v embryonálny deň 17,5 (ED17,5, A) a postnatálny deň 7 (PD7, B) bola stanovená pomocou qPCR (expresia mRNA cieľového génu bola normalizovaná k expresii génu pre b-aktín a vztiahnutá k expresii cieľového génu u kontrolných *mEpoR* myší). Hladiny hepcidínu (C) a feritínu (D) v PD7 boli merané pomocou ELISA testu. Obsah železa v PD7 v tkanive pečene (LIC, E) a sleziny (SIC, F) bol kvantifikovaný kolorimetrickým testom. *P < 0,05, **P < 0,01 vs. *mEpoR*. (Prevzaté a upravené z Kralova a kol., 2022)

V neskoršom postnatálnom období, predovšetkým u 2,5 a 6,5 mesačných *mtHEPOR* homozygotných myší, je normálna až zvýšená TSAT sprevádzaná vyššími hladinami feritínu, LIC a SIC (Obr. 11A – F), spoločne s miernou stimuláciou hepcidínu (Obr. 11G,

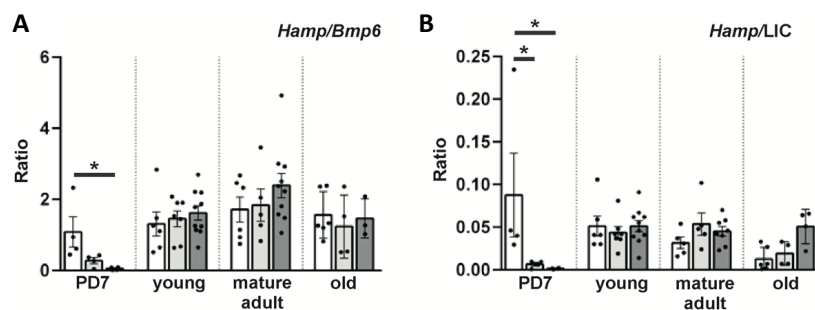
H) a zvýšenou expresiou *Bmp6* (Obr. 11I). Na rozdiel od *mtHEPOR* homozygotov, majú mladé 2,5 mesačné *mtHEPOR* heterozygotné myši signifikantne znížené hladiny sérového feritínu, LIC a *Bmp6* transkriptov (Obr. 11B, C, I). Tieto parametre sa v neskoršom veku upravujú a sú porovnateľné s hodnotami *mEpoR* kontrol (Obr. 11A – I). Tieto výsledky ukazujú, že **so starnutím u oboch genotypov *mtHEPOR* myší dochádza k postupnému zvyšovaniu parametrov metabolizmu železa; ktoré kulminujú vo veku 6,5 mesiaca najmä u *mtHEPOR* homozygotov, v dôsledku čoho tieto myši vykazujú známky mierneho pret'aženia železom.**



Obr. 11: Analýza parametrov železa počas postnatálneho obdobia. Transferínová saturácia (TSAT, A) bola stanovená z myšieho séra rovnako ako hladiny feritínu (B), ktoré boli stanovené pomocou ELISA testu. Obsah železa v tkanive pečene (C, E) a sleziny (D, F) bol kvantifikovaný kolorimetrickým testom (C, D) a Perlsovým

farbením tkanivových rezov (E, F). Expresia *Hamp* (G) bola stanovená pomocou qPCR (expresia mRNA cielového génu bola normalizovaná k expresii génu pre b-aktín a vztiahnutá k expresii cielového génu u kontrolných *mEpoR* myší). Hladiny hepcidínu (H) boli merané pomocou ELISA testu. Expresia *Bmp6* (I) bola stanovená pomocou qPCR (expresia mRNA cielového génu bola normalizovaná k expresii génu pre b-aktín a vztiahnutá k expresii cielového génu u kontrolných *mEpoR* myší). * $P < 0.05$, ** $P < 0.01$ vs. *mEpoR*; # $P < 0.05$ *mtHEPOR* vs. *mtHEPOR/mEpoR* (Prevzaté a upravené z Kralova a kol., 2022)

Analýza pomeru medzi mRNA *Hamp* a *Bmp6* (Obr. 12A), ako aj medzi mRNA *Hamp* a LIC (Obr. 12B) ukazuje jeho zníženú hodnotu u *mtHEPOR* heterozygotov a homozygotov v porovnaní s *mEpoR* kontrolami v štádiu PD7, čo indikuje **neadekvátne potlačenie produkcie hepcidínu** vzhľadom na stav železa v organizme. V neskorších štádiach postnatálneho života sa tieto pomery normalizujú a sú porovnateľné medzi všetkými genotypmi. Tým dokazujeme, že **hladiny hepcidínu u dospelých *mtHEPOR* myší odrážajú skutočný stav železa v organizme a zároveň vylučujeme, že by sa relatívne znížená produkcia hepcidínu podieľala na akumulácii železa.**

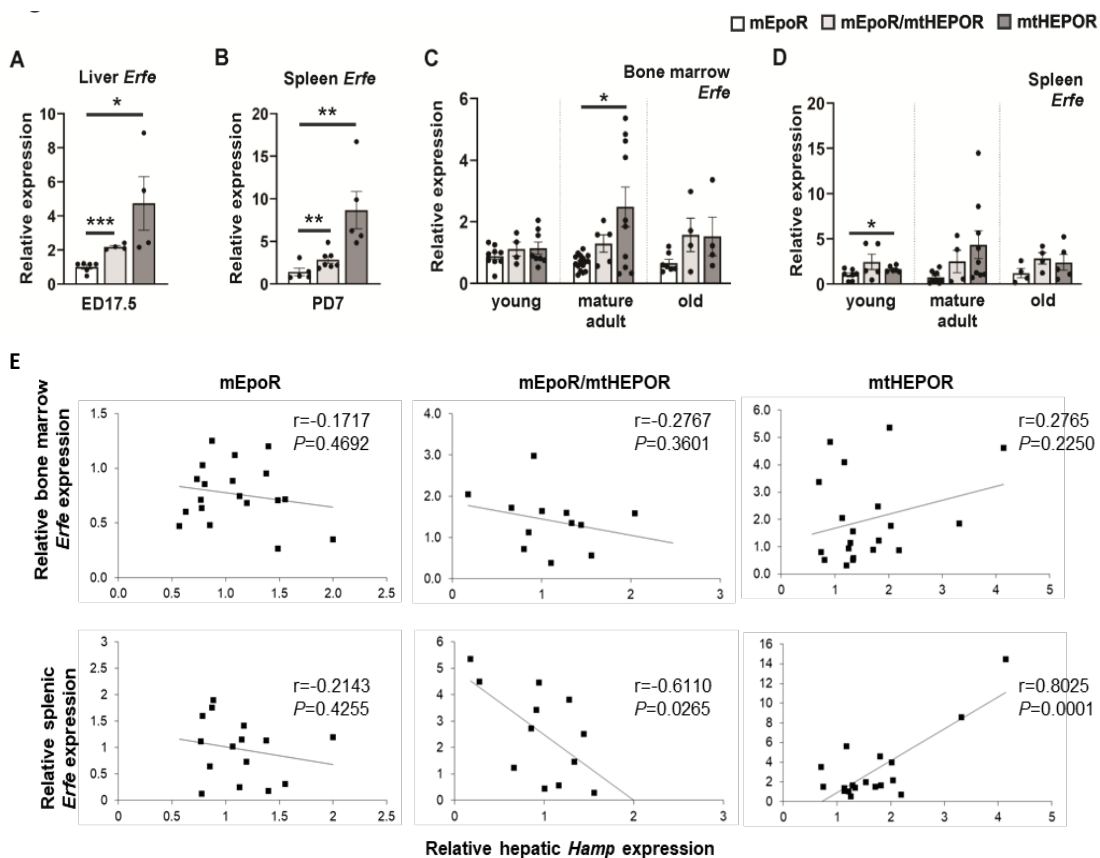


Obr. 12: Analýza expresie hepcidínu v porovnaní s expresiou *Bmp6* mRNA (A) a v pomere k LIC (B). (Prevzaté a upravené z Kralova a kol., 2022)

Inverzný vzťah Erfe/hepcidín a akumulácia nezrelých erytroblastov sú u *mtHEPOR* myší pozorované len v prenatálnom a perinatálnom období

V súlade s už publikovaným zmnožením **nezrelých erytroblastov u *mtHEPOR* homozygotných myší v prenatálnom a perinatálnom období** (Divoky, 2016) a známou negatívnou reguláciou hepcidínu prostredníctvom ERFE, v ED17,5 a PD7 zaznamenávame zvýšenú expresiu *Erfe* mRNA v pečeni a slezine u *mtHEPOR* heterozygotov aj homozygotov (Obr. 13A – B). V neskorších štádiach postnatálneho života sú však *Erfe* transkripty v kostnej dreni a slezine *mtHEPOR* myší zvýšené len nepatrne (Obr. 13C – D). Navyše, negatívna korelácia medzi expresiou *Hamp* a *Erfe* je čiastočne zachovaná iba u *mtHEPOR* heterozygotov (Obr. 13E). Naopak, u *mtHEPOR* homozygotov je medzi expresiami oboch génov zistená pozitívna korelácia (Obr. 13E). Napriek miernej transkripčnej stimulácii *Erfe*, sú jeho hladiny v sére *mtHEPOR* myší pod prahom detekcie

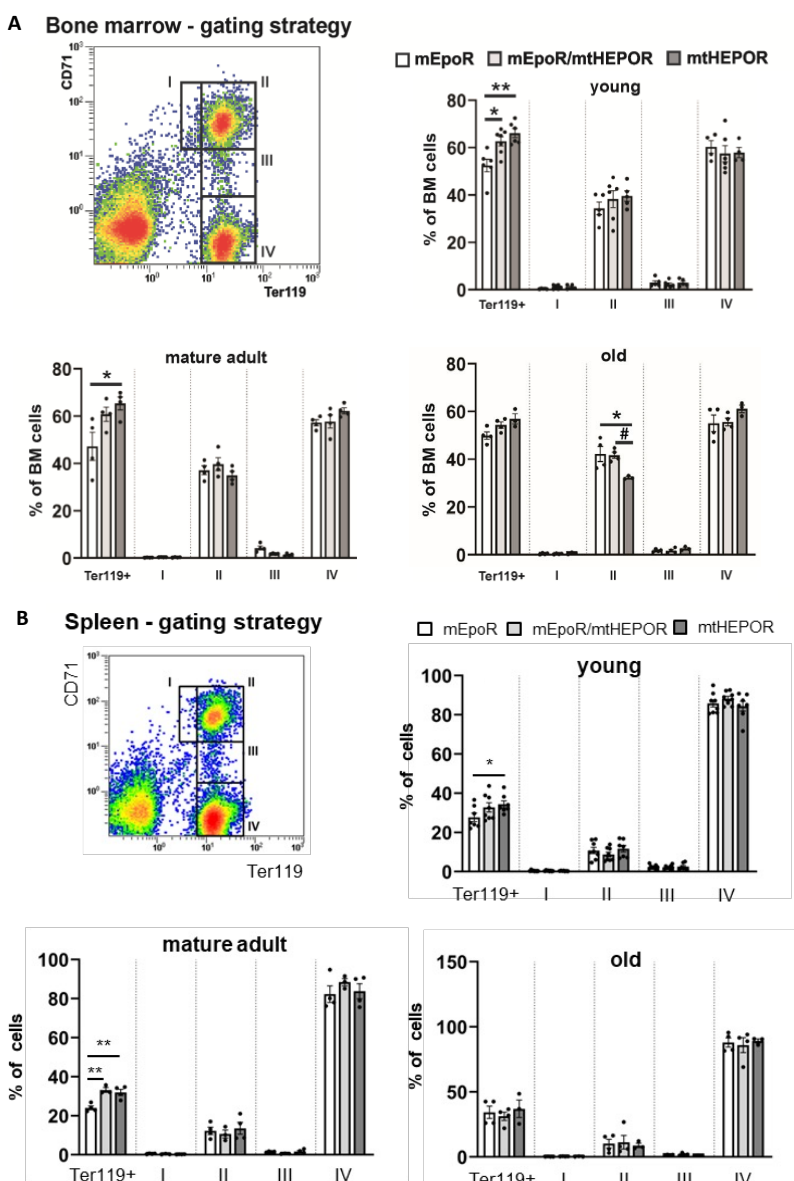
ELISA testu s výnimkou troch mutantných *mtHEPOR* myší (jeden heterozygot a dva homozygoti); hladina Erfe u kontrolných myší je takisto pod detekčným limitom (experiment bol realizovaný spoluautormi). Týmto ukazujeme, že **stupeň indukcie Erfe je v postnatálnom období života *mtHEPOR* myší oveľa nižší** v porovnaní s inými modelmi stimulovanej erytropoézy s nadmernou produkciou Erfe napr.: u β -talasémie intermedia (myši Th3/+) (Garcia-Santos a kol., 2018) alebo u kontrolných myší po podaní EPO (experiment bol realizovaný spoluautormi).



Obr. 13: Analýza Erfe expresie v korelácii s Hamp expresiou. Erfe mRNA expresia stanovená pomocou qPCR (expresia mRNA cielového génu bola normalizovaná k expresii génu pre b-aktín a vztiahnutá k expresii cielového génu u kontrolných *mEpoR* myší) vo fetálnej pečeni (FL – fetal liver) v ED 17,5 (A), postnatálne v slezine v PD7 (B) a u mladých, dospelých a starých myší v kostnej dreni (C) a slezine (D). Korelačná analýza bola stanovená Pearsonovou koreláciou medzi postnatálnou *Hamp*/ β -*Actin* mRNA expresiou v pečeni a *Erfe*/ β -*Actin* mRNA expresiou v kostnej dreni (vrchný rad) a v slezine (spodný rad) (E). *P < 0.05, **P < 0.01, ***P < 0.001 vs. *mEpoR* (Prevzaté a upravené z Kralova a kol., 2022)

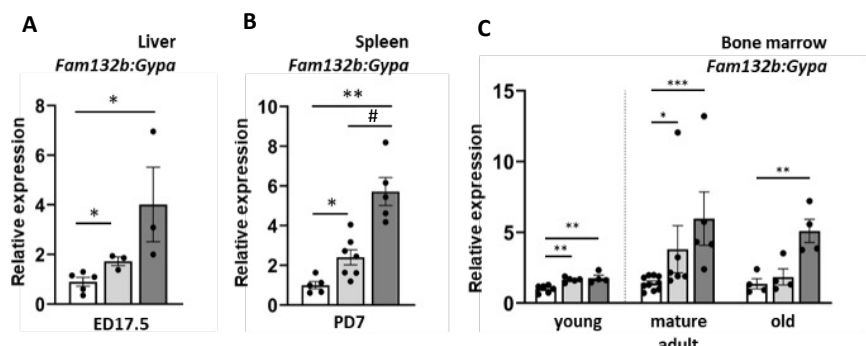
Ked'že hlavným zdrojom Erfe sú nezrelé erytroblasty, v následných analýzach sme sa zamerali na hodnotenie erytroidnej diferenciácie. Zvýšené percento erytroidných buniek exprimujúcich Ter119 v kostnej dreni a v slezine (Obr. 14A, B) pozorujeme u *mtHEPOR* heterozygotov aj homozygotov v porovnaní s *mEpoR* kontrolami takmer vo všetkých vývinových štadiách. V kostnej dreni s vekom u všetkých jedincov dochádza k poklesu

Ter119 pozitívnych buniek, najmä u *mtHEPOR* homozygotných myší, konkrétnie o 7,34 % (u *mEpoR* myší o 5,82 %, u *mtHEPOR* heterozygotných myší o 6,37 %). Rozdelenie erytroidných buniek do jednotlivých diferenciačných štadií sa však u *mtHEPOR* myší v porovnaní s kontrolami nelísi, s výnimkou podielu nezrelých erytroblastov (identifikovaných ako Ter119highCD71high) v kostnej dreni, ktorý je výrazne nižší u starých (vek 16 mesiacov) *mtHEPOR* homozygotných myší v porovnaní s mladými (vek 2,5 mesiaca) jedincami toho istého genotypu a tiež s jedincami ostatných genotypov rovnakého veku (Obr. 14A). Tieto výsledky ukazujú, že na rozdiel od prenatálneho a perinatálneho obdobia nedochádza **u *mtHEPOR* myší v neskoršom období postnatálneho života** k akumulácii nezrelých erytroblastov, ale naopak **dochádza k predčasnemu útlmu erytropoézy**.



Obr. 14: Analýza erytroidnej diferenciácie stanovená pomocou prietokovej cytometrie, ktorá hodnotila percento buniek kostnej dreny (A) a sleziny (B) exprimujúcich markery CD71 a Ter119. Relatívny počet buniek v oblastiach I až IV je vyjadrený ako percento všetkých erytroidných buniek. * $P < 0.05$, ** $P < 0.01$ vs. *mEpoR*; # $P < 0.05$ *mtHEPOR* vs. *mtHEPOR/mEpoR* (Prevzaté a upravené z Kralova a kol., 2022)

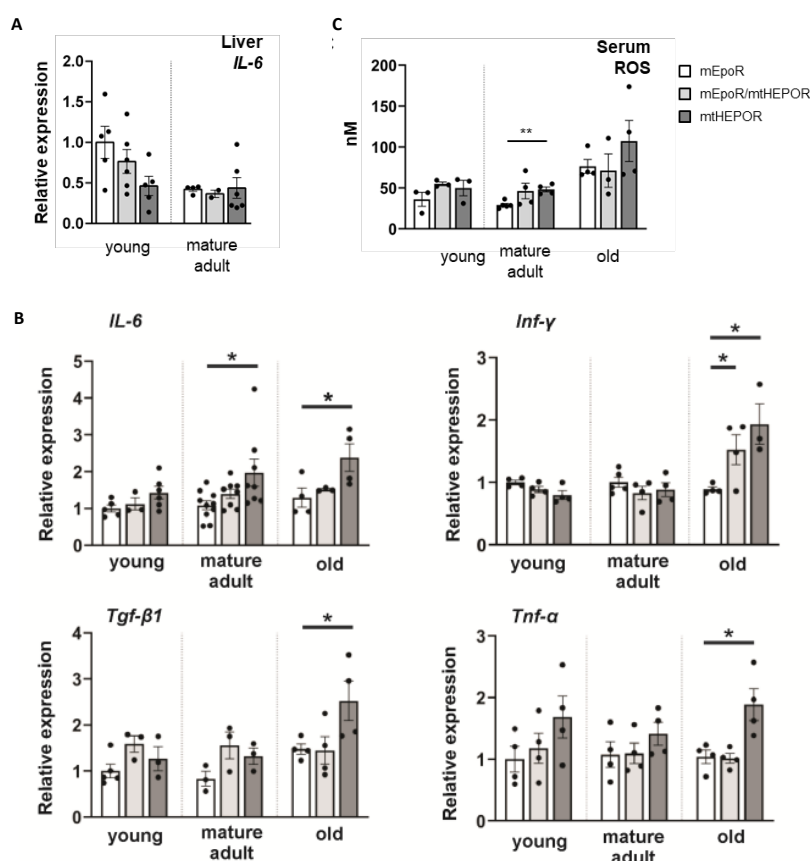
S cieľom zistiť, či za relatívnym poklesom erytropoézy v neskoršom veku *mtHEPOR* myší stojí utlmenie EPOR/JAK2 signalizácie sme normalizovali expresiu *Erfe*, priameho ciela STAT5, k špecifickému génu erytroidných buniek glykoforínu A – *Gypa*. Táto normalizácia nám umožnila posúdiť mieru transkripcnej aktivácie *Erfe* v jednom erytroidnom prekurzore. Porovnatelná miera indukcie *Erfe* transkriptov v prenatálnom, perinatálnom a neskoršom postnatálnom období (Obr. 15A – C) **nenačasuje dramatickú zmenu aktivácie EPOR/JAK2/STAT5 u *mtHEPOR* myší v priebehu života**. Druhým nepriamym ukazovateľom aktivácie tejto dráhy je hypersenzitivita erytroidných progenitorov k EPO, ktorá je charakteristickým znakom PFCP (Arcasoy a kol., 1999). Experimenty realizované spoluautormi ukazujú, že táto hypersenzitivita je zachovaná aj u starých *mtHEPOR* myší a to v podobnej miere ako bolo publikované u mladých myší (Divoky a kol., 2001). Tieto údaje spoločne ukazujú **trvalú aktiváciu EPOR/JAK2/STAT5 signálnej kaskády u *mtHEPOR* myší**. Pokles Hct počas starnutia teda nie je zapríčinený významnými modifikáciami aktivácie tejto signálnej dráhy. Rovnako, v priebehu postnatálneho vývinu *mtHEPOR* myší nepozorujeme ani zmeny v expresii *Epo* alebo iných cielov hypoxickej signálnej dráhy (experimenty realizované spoluautormi).



Obr. 15: Analýza *Erfe* expresie. *Erfe* mRNA expresia stanovená pomocou qPCR (expresia mRNA cielového génu bola normalizovaná k expresii génu pre GypA a vzťahnutá k expresii cielového génu u kontrolných *mEpoR* myší) vo FL v ED 17,5 (A), postnatálne v slezine v PD7 (B) a u mladých, dospelých a starých myší v kostnej dreni (C). * $P < 0.05$, ** $P < 0.01$, *** $P < 0.001$ vs. *mEpoR*; # $P < 0.05$ *mtHEPOR* vs. *mtHEPOR/mEpoR* (Prevzaté a upravené z Kralova a kol., 2022)

Starnutie erytropoézy spojené s dominanciou myelopoézy je výraznejšie u *mtHEPOR* myší

Ked'že systémový zápal pôsobí ako priamy induktor produkcie hepcidínu, v ďalších experimentoch sme stanovovali sérové hladiny vybraných zápalových cytokínov: **IL-6, Tnf- α , Ifn- γ a Tgf- β 1**. Táto analýza však neukazuje žiadne známky systémového zápalu alebo lokálnej indukcie transkripcie *IL-6* v pečeni (Obr. 16A). Avšak qPCR analýza (experiment čiastočne realizovaný aj spoluautormi) zodpovedajúcich génov kódujúcich zápalové cytokíny odhaluje ich **lokálnu transkripčnú stimuláciu v kostnej dreni *mtHEPOR* homozygotov** (Obr. 16B) spoločne s badateľným trendom k zvýšenej produkcii ROS (Obr. 16C), čo naznačuje progresívne, s vekom súvisiace, zmeny v mikroprostredí kostnej drene.

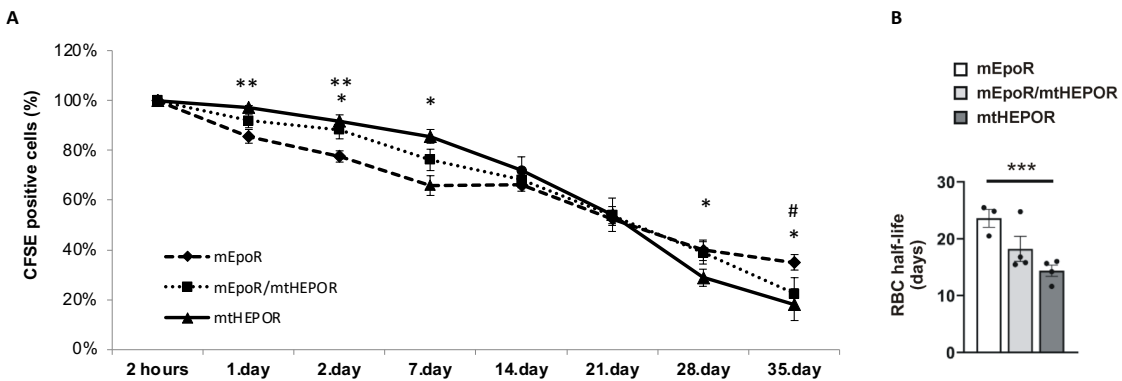


Obr. 16: Hodnotenie transkripčnej úrovne zápalových génov a sérových hladín ROS. *IL-6* mRNA expresia stanovená pomocou qPCR (expresia mRNA cielového génu bola normalizovaná k expresii génu pre b-aktín a vzťahnutá k expresii cielového génu u kontrolných *mEpoR* myší) u mladých, dospelých a starých myší v pečeni (A); *IL-6*, *Tnf- α* , *Ifn- γ* a *Tgf- β 1* mRNA expresia stanovená pomocou qPCR (expresia mRNA cielového génu bola normalizovaná k expresii génu pre b-aktín a vzťahnutá k expresii cielového génu u kontrolných *mEpoR* myší u mladých, dospelých a starých myší v kostnej dreni (B); hladiny ROS boli merané pomocou OxiSelect In Vitro ROS/RNS testu a kvantifikované stanovením fluorescencie (C). * $P < 0.05$, ** $P < 0.01$ vs. *mEpoR* (Prevzaté a upravené z Kralova a kol., 2022)

Nakoľko je známe, že zápalové prostredie kostnej drene, na podklade parakrinného a/alebo autokrinného signálisu, podporuje predčasné starnutie hematopoézy typické dominanciou myelopoézy a útlom erytropoézy (Pang a kol., 2011), rozhodli sme sa analyzovať jednotlivé subpopulácie HSC a primitívnych progenitorov kostnej dreny prietokovou cytometriou a zároveň testom klonálnej proliferácie zhodnotiť zastúpenie viac diferencovaných štadií erytroidných a myeloidných progenitorov (prvý experiment bol realizovaný na zákazku a vyhodnotený spoluautormi článku – detaily sú uvedené v Supplement Kralova a kol., 2022; druhý experiment bol realizovaný spoluautormi článku). Tieto experimenty odhalujú: a) signifikantne zvýšený počet erytroidných kolónií derivovaných z BFU-E a/alebo CFU-E progenitorov len u mladých *mtHEPOR* heterozygotných aj homozygotných myší v porovnaní s *mEpoR* kontrolnými myšami; b) signifikantný nárast celkového počtu kolónií derivovaných z neerytroidných progenitorov typu CFU-GM (granulocyte-macrophage colony-forming unit), CFU-G (granulocyte colony-forming unit), a predovšetkým CFU-M (macrophage colony-forming unit) u starých *mtHEPOR* heterozygotov aj homozygotov v porovnaní s *mEpoR* kontrolami; c) signifikantný nárast počtu LSKs ($\text{Lin}^- \text{Sca}-1^+ \text{c-Kit}^+$) kmeňových buniek u starých *mtHEPOR* homozygotných myší v porovnaní s mladými jedincami; d) signifikantný nárast počtu granulocytovo-monocytových progenitorov – GMP (granulocyte-monocyte progenitor) u starých *mtHEPOR* homozygotných myší v porovnaní s mladými jedincami. Tieto výsledky naznačujú, že progresívne utlmenie erytropoetickej aktivity a **indukcia myelopoézy** sú v priebehu starnutia výraznejšie **u starých *mtHEPOR* homozygotných myší** v porovnaní s kontrolnými myšami. V súlade s týmto výsledkom staré *mtHEPOR* homozygotné myši, na rozdiel od mladých jedincov, majú v kostnej dreni dominantnú expresiu myeloidného transkripčného faktora *PU.1*.

Znížené prežívanie erytrocytov u *mtHEPOR* myší

Okrem starnutia erytropoézy v kostnej dreni tiež pozorujeme **skrátené prežívanie cirkulujúcich červených krviniek u *mtHEPOR* homozygotných myší** (Obr. 17), ktoré je sprevádzané zniženou expresiou CD47 na ich povrchu (experiment realizovaný spoluautormi). CD47 inhibuje fagocytózu erytrocytov makrofágmi RES (Oldenborg a kol., 2000). Tento výsledok naznačuje, že **zvýšené odstraňovanie erytrocytov** spolu so zniženým dopytom po železe erytropoézou v dôsledku jej vekom podmienenému utlmeniu môže vysvetlovať postupné **zvyšovanie zásob železa** v pečeni a následné zvýšenie expresie *Bmp6* a syntézy hepcidínu u *mtHEPOR* homozygotných myší (Obr. 11).



Obr. 17: Hodnotenie prežívania erytrocytov. Fluorescencia červených krviniek značených s CFSE, injikovaných do chvostových žíl *mEpoR* myší sa sledovala po 2 hod. od aplikácie – deň 0 (100%) a následne po dobu 35 dní (v deň 1, 2, 7, 14, 21, 28 a 35). Hodnoty kriky prežívania boli vztiahnuté proti dňu 0 (A). Pre každú analyzovanú myš sa určila exponenciálna regresná rovnica, ktorá sa použila na výpočet polčasu erytrocytov (B). * $P < 0.05$, ** $P < 0.01$, *** $P < 0.001$ vs. *mEpoR*, # $P < 0.05$ *mtHEPOR* vs. *mtHEPOR/mEpoR*. (Prevzaté a upravené z Kralova a kol., 2022)

Na záver tejto štúdie (príloha 2) môžeme zhrnúť, že erytrocytóza u PFCP myší, ako aj expresia hepcidínu, Erfe a hladina železa podliehajú počas ontogenézy dynamickým zmenám. Pozorované zmeny metabolizmu železa v prenatálnom/perinatálnom a postnatálnom období odrážajú dynamiku a silu protichodných signálov, konkrétnie erythropoetickej aktivity a zásob železa, regulujúcich produkciu hepcidínu. **Regulácia expresie hepcidínu u *mtHEPOR* homozygotných plodov a novorodencov je pod vplyvom nadradeného faktora – erytropoézy**, ktorého dominancia je neskôr potlačená a **hlavným regulátorom expresie hepcidínu sa v postnatálnom období stávajú zvýšené zásoby železa v pečeni**. Ďalej predpokladáme, že parakrinné zápalové signály ovplyvňujúce remodeláciu kostnej drene spoločne s celoživotnou predĺženou aktiváciou EPOR/JAK2/STAT5 signalizácie vedú k progresívному poklesu erytroidných progenitorov a predčasnemu starnutiu hematopoézy u *mtHEPOR* myšieho modelu. Rozdiely pozorované medzi *mtHEPOR* heterozygotmi a homozygotmi naznačujú, že zmeny stimulácie EPOR/JAK2 signalizácie sú závislé od alelovej zátaze resp. dávky *EPOR* mutácie.

4.2 Štúdium vybraných hereditárnych JAK2 mutácií

Ústav biológie LF UPOL je v spolupráci s Hemato-onkologickou – HOK a Detskou klinikou FN Olomouc centrom pre diagnostiku a liečbu pacientov s erytrocytózou. V rámci molekulárnej diagnostiky sme u jedného pediatrickeho pacienta so známkami primárnej erytrocytózy našli **dve dedičné heterozygotné mutácie v géne kódujúcom JAK2 – E846D a R1063H**. JAK2 dedičné mutácie boli už predtým popísané u pacientov s MPN alebo s hereditárной trombocytózou v niektorých prípadoch pripomínajúcou MPN fenotyp

(Lanikova a kol., 2016; Mead a kol., 2013; Marty a kol., 2014; Etheridge a kol., 2014; Rumi a kol., 2014) a u prípadov s tzv. *triple* negatívou MPN (Milosevics Feenstra a kol., 2016), ktorá sa vyznačuje neprítomnosťou žiadnej *driver* mutácie v JAK2, CALR alebo MPL. Nájdené mutácie sú lokalizované v kinázovej (R1063H) a pseudokinázovej (E846D) doméne JAK2, preto sa predpokladal ich možný funkčný efekt na JAK2 kinázu. Funkčné štúdie identifikovaných variant boli nutné na potvrdenie ich kauzality. Za týmto účelom bol vytvorený bunkový model, na ktorého tvorbe som sa priamo podieľala a predovšetkým som potom participovala na štúdiu signálnej transdukcie JAK2, tak ako je uvedené v kapitole 4.2.1.

V rámci realizácie tohto cieľa som sa podieľala aj na práci analyzujúcej kooperáciu somatickej JAK2 V617F mutácie so zárodočnou mutáciou JAK2 R1063H u pacientov s MPN a na bunkovom modeli. Hlavnou náplňou mojej práce, tak ako je uvedené v kapitole 4.2.2, bolo vytvorenie bunkového modelu nesúceho obe mutácie a štúdium jeho senzitivity k JAK2 inhibítorm.

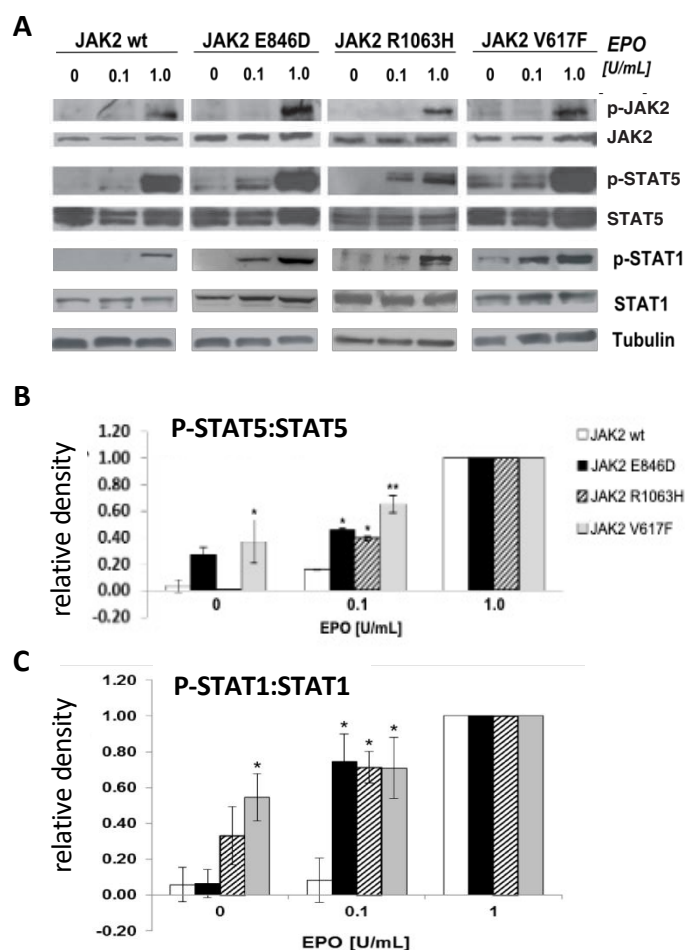
Súčasťou tohto cieľa sú aj zatiaľ nepublikované výsledky uvedené v kapitole 4.2.3, ktoré predbežne hodnotia frekvenciu výskytu R1063H mutácie v zdravej populácii a u pacientov s myeloidnou neopláziou.

4.2.1 Štúdium kooperácie dedičných JAK2 E846D a R1063H mutácií

V tejto práci sme študovali pacienta s erytrocytózou a abnormálnou megakaryopoézou v kostnej dreni pripomínajúc tak prípady PV s mutáciami exónu 12. Pri diagnostickej DNA analýze jeho a následne jeho rodinných príslušníkov sme zistili, že proband je dvojitý heterozygot pre mutácie JAK2 E846D a R1063H a zdedil po jednej mutácii od každého rodiča. Hladiny Hb a Hct rodičov spadali do referenčných hodnôt, ale *in vitro* test erytropoetínej senzitivity erytroidných progenitorov u nich preukázal mierne zvýšenú citlivosť v porovnaní s kontrolami, ktorá však nebola tak výrazná ako u pacienta. Za účelom analýzy funkčného efektu týchto mutácií bol, s mojím priamym prispením, vytvorený bunkový model s použitím Ba/F3 bunkovej línie závislej od IL-3 a exprimujúcej ľudský EPOR wt gén (Ba/F3-EPOR). Do týchto buniek sme elektroporáciou vniesli expresný vektor nesúci ľudský JAK2 wt gén (negatívna kontrola) alebo jeho mutované verzie: JAK2 E846D, JAK2 R1063H a JAK2 V617F (pozitívna kontrola).

Analýza signálnej transdukčnej dráhy JAK2, po 12 hodinovej starváciu buniek v médiu bez IL-3 a následnej stimulácií rôznymi koncentráciami EPO ukazuje významne zvýšenú

fosforyláciu STAT5 a STAT1 v bunkách exprimujúcich JAK2 E846D a JAK2 R1063H mutácie pri koncentrácií 0,1 U/mL EPO v porovnaní s kontrolnými bunkami nesúcimi JAK2 wt. Bunky exprimujúce onkogénnu verziu JAK2 V617F vykazujú konštitutívnu aktiváciu STAT5 a STAT1 (Obr. 18). **Účinok mutácií E846D a R1063H má na JAK2 signálnu dráhu slabší dopad** v porovnaní s účinkom mutácie V617F, čo sa prejavuje len v miernej aktivácii tejto dráhy v podmienkach bez prítomnosti EPO, kým mutácia JAK2 E846D má v týchto podmienkach tendenciu preferenčnej fosforylácie STAT5 molekúl (Obr. 18B), tak mutácia JAK2 R1063H fosforylácie STAT1 molekúl (Obr. 18C). Obe **JAK2 mutácie majú miernejší efekt na proliferáčnu kapacitu buniek** v porovnaní s onkogénnou mutáciou V617F (experimenty realizované spoluautormi), čo je v súlade s ich hereditárny prenosom.



Obr. 18: Aktivita JAK2 signalizačnej dráhy analyzovaná pomocou immunoblotu. Stabilné transfektanty Ba/F3-EPOR závislé od IL-3 boli po dočasnej absencii IL-3 stimulované indikovanými koncentráciami EPO počas 15 minút (A). Relatívna kvantifikácia p-STAT5 (B) a p-STAT1 (C) bola vykonaná softvérom ImageJ. Každý stĺpček predstavuje pomer medzi množstvom fosforylovaného proteínu k celkovému množstvu jeho nefosforylovej formy v pomere k výsledku vypočítanému pre koncentráciu 1,0 U/ml EPO. Výsledky sú uvedené ako priemer troch nezávislých experimentov. *P < 0,05, **P < 0,01 vs. JAK2 wt (Prevzaté z Kapralova a kol., 2016)

Diferenciálna signalizácia JAK2 dráhy spočíva v kvalitatívnych rozdieloch aktivity proteínov STAT rodiny a v rámci skupiny MPN vedie k rôznym klinickým fenotypovým prejavom. Bolo preukázané, že ET progenitory s JAK2 V617F mutáciou vykazujú vyššiu mieru fosforylácie STAT1 a STAT3 molekúl, kým v PV progenitoroch boli prednostne fosforylované molekuly STAT5 (Chen a kol., 2010). Preukázaná zvýšená aktivita STAT5 a STAT1 v bunkovom modeli s JAK2 E846D a R1063H substitúciami (Tab. 17) je preto v súlade s erytrocytózou pacienta a rovnako aj vysvetľuje atypickú megakaryopoézu v kostnej dreni. Ďalšie analýzy realizované spoluautormi odhalujú, že **JAK2 E846D a R1063H aktivujú transkripčnú aktivitu STAT5 špecificky prostredníctvom EPOR** a nie cez MPL či G-CSFR. *In silico* analýzy ukazujú, že kým mutácia JAK2 E846D zodpovedá za predĺženú aktivitu JAK2 signalizácie, JAK2 R1063H mutácia podporuje aktívnu konformáciu JAK2 enzymu. Navyše, aktivita JAK2 E846D/R1063H signálnej dráhy je efektívne utlmená použitím JAK2 inhibítarov, akými sú ruxolitinib a AZ-960.

Záver tejto štúdie (príloha 3) je, že **JAK2 E846D a R1063H sú slabo aktivujúce mutácie, ktorých vzájomná kooperácia je potrebná k indukcii polyklonálnej erytrocytózy s megakaryocytovou atypiou.**

4.2.2 Štúdium interakcie získanej JAK2 V617F a dedičnej JAK2 R1063H mutácie

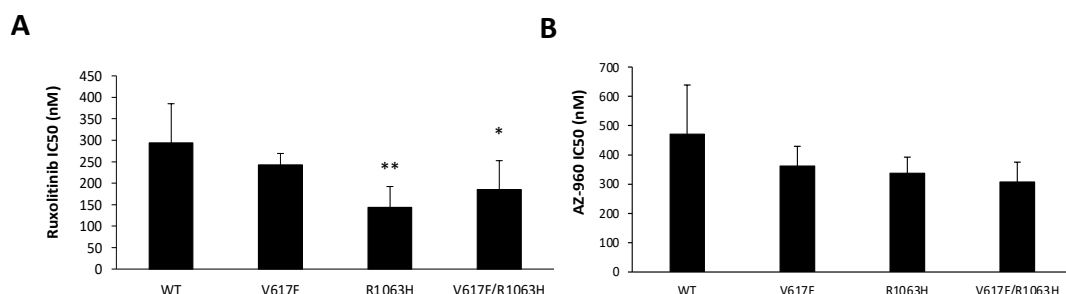
Frekvencia JAK2 R1063H variantu bola pri jeho identifikácii v súbore JAK2 V617F pozitívnych PV pacientov vyššia ako je uvedená v databáze (Levine a kol., 2005). Preto nás zaujímalo, či variant JAK2 R1063H má okrem kooperácie s JAK2 E846D mutáciou funkčné dôsledky na JAK2 signalizáciu (Kapralova a kol., 2016) aj v kooexistencii so silnou onkogénnou JAK2 V617F mutáciou.

Najskôr spoluautori predloženého článku detegovali prítomnosť JAK2 R1063H mutácie až u 14 z 390 JAK2 V617F pozitívnych pacientov s MPN.

U týchto pacientov sme sa, aj s mojím parciálnym prispätím, zamerali na charakterizáciu genotypovej konštitúcie a konfigurácie JAK2 mutácií. Výsledky ddPCR (digital droplet PCR) popisujú, že alelická frekvencia JAK2 R1063H mutácie je vo väčšine prípadov blízka 50% naznačujúc, že JAK2 R1063H mutácia má dedičný charakter. Ďalej sme prostredníctvom sekvenovania subklonovaných RT-PCR (real time PCR) produktov zahrňajúcich exóny 14 – 24 génu JAK2 zistili, že z 10 analyzovaných pacientov má 6 pacientov konfiguráciu mutácií v pozícii *cis* a len 4 pacienti v pozícii *trans*. S použitím

bunkového modelu bol spoluautormi hodnotený funkčný dopad oboch JAK2 mutácií v *cis* aj *trans* konfigurácii. Táto analýza odhaluje, že po stimulácii cytokínmi EPO, TPO a G-CSF **JAK2 signálna dráha vykazuje signifikantne vyššiu konštitutívnu aktivitu u dvojitych mutantov v konfigurácii *cis*** v porovnaní s bunkami exprimujúcimi samostatne mutáciu JAK2 V617F alebo bunkami nesúcimi obe mutácie v *trans* konfigurácii.

Okrem toho, sme pomocou Ba/F3-EPOR bunkového modelu exprimujúceho JAK2 wt, JAK2 V617F, JAK2 R1063H a JAK2 V617F/R1063H verzie testovali citlivosť buniek k dvom JAK2 inhibítorm - ruxolitinib a AZ-960. Ruxolitinib je silný a selektívny inhibítorka JAK1 a JAK2 kináz, schválený k liečbe MPN. Ďalší inhibítorka AZ-960 je charakterizovaný ako selektívny ATP kompetitívny inhibítorka špecifický k JAK2 kináze. Stabilne transfekované bunky boli kultivované 72 hodín so znižujúcou sa koncentráciou inhibítorm. Výsledky naznačujú, že **bunky s JAK2 R1063H a JAK2 V617F/R1063H mutáciami sú signifikantne citlivejšie k Ruxolitinibu** ako bunky exprimujúce JAK2 wt (Obr. 19A), čo môže mať terapeutické využitie. Rozdiely citlivosti buniek k AZ-960 nie sú štatisticky významné, ale podobne ako s použitím Ruxolitinibu, bunky s JAK2 R1063H mutáciou majú tendenciu k zvýšenej senzitivite (Obr. 19B). Dáta s použitím AZ-960 inhibítora nie sú uvedené v predloženom článku.



Obr. 19: *In vitro* test senzitivity k inhibítorm. Hodnota IC50 bola definovaná ako koncentrácia inhibítora potrebná na 50% inhibíciu bunkového rastu s použitím inhibítorm: Ruxolitinib (A) a AZ-960 (B). *P < 0.05, **P < 0.01 vs. JAK2 wt (prevzaté a upravené z Mambet a kol., 2018)

Na záver tejto štúdie (príloha 4) môžeme uviesť, že **v súbore 390 MPN JAK2 V617F pozitívnych pacientov, je frekvencia pravdepodobne dedičnej JAK2 R1063H mutácie vyššia ako v bežnej populácii. Komutácia JAK2 V617F/R1063H vedie k a) zvýšenej väzbovej afinité JAK2 enzymu k G-CSFR; b) kumulatívnomu zvýšeniu aktivity JAK2 signalizácie; c) zvýšenej senzitivite k inhibítoru Ruxolitinibu.**

4.2.3 Skríning JAK2 R1063H mutácie v zdravej populácii a u pacientov s myeloidnými neopláziami

Technologický pokrok v podobe celogenómového/celoexómového sekvenovania je spojený s prínosom veľkého množstva genetických dát, no jednou z prekážok ich klinickej implementácie je prítomnosť vysokého počtu variantov neznámeho významu. Problémy pri interpretácii klinickej relevancie variantov pramenia z toho, že a) väčšina z nich je definovaná ako veľmi zriedkavé polymorfizmy; b) sú zaznamenané zo špecifických populácií tvorených pacientmi s určitým ochorením alebo jedincami s rodinnou anamnézou a preto tieto poznatky nie sú reprezentatívne. Varianty môžu vznikať *de novo* alebo majú dedičný charakter a väčšina poznatkov práve o týchto variantoch pochádza od jednotlivcov, ktorí už majú určitý klinický prejav. Ďalšiu komplikáciu môžu predstavovať demografické rozdiely v alelických frekvenciach variantov a rovnako aj to, že niektoré varianty majú nízku penetranciu alebo ich patologický efekt sa prejaví až v kombinácii účinkov viacerých variantov s nízkym až stredným rizikom penetrancie.

Variant JAK2 R1063H bližšie popísaný v predchádzajúcich kapitolách je označovaný ako polymorfizmus rs41316003. Ide o *missense* variant (c.3188G>A), ktorý má podľa viacerých programovacích nástrojov (Tab. 4) zohľadňujúcich konzervatívne homologické sekvencie a fyzikálno-chemické komparácie negatívny vplyv na štruktúru a funkciu ľudského JAK2 proteínu. V súlade s tým sú vyššie uvedené *in silico* a funkčné analýzy, ktoré ukazujú, že táto mutácia má buď synergickým (v kombinácii s dedičnou JAK2 E846D mutáciou) alebo aditívnym (v kooperácii so získanou JAK2 V617F mutáciou) spôsobom patologický efekt na JAK2 signalizáciu.

Tab. 4: Funkčný dopad JAK2 R1063H na funkciu JAK2 kinázy

Nástroj	Funkčný dopad
SIFT	Deleterious
PolyPhen	Possibly damaging
CADD	Likely benign
REVEL	Likely disease causing
MetaLR	Tolerated

Pozn.: použité dáta sú uvedené z nasledujúceho zdroja:

https://uswest.ensembl.org/Homo_sapiens/Variation/Mappings?db=core;r=9:5125843-5126843;v=rs41316003;vdb=variation;vf=733418198

Polymorfizmus rs41316003 je pomerne zriedkavý a globálna alelická frekvencia uvádzaná v normálnej populácii je podľa databázy 1000 Genomes Project Phase 3 0,0018 (Tab. 5). Výnimku tvoria populácie Estónska, Fínska a Holandska, u ktorých je frekvencia

v porovnaní s bežnou populáciou z iných štúdií viac ako dvojnásobná (Tab. 5). Naopak kórejská populácia má najnižšiu frekvenciu zastúpenia tejto alely (Tab. 5). Pri analýze súboru JAK2 V617F pozitívnych MPN pacientov s diagnózou PV bol pôvodne JAK2 R1063H variant zaznamenaný u 3 z 93 pacientov (Levine a kol., 2005), čo zodpovedá alelickej frekvencii rovnej 0,01613. Podobná frekvencia (0,01795) bola zaznamenaná aj vo vyššie uvedenej štúdii (Mambet a kol., 2018), v ktorej bola potvrdená prítomnosť tejto mutácie u 14 z 390 JAK2 V617F pozitívnych MPN pacientov.

Tab. 5: JAK2 R1063H frekvencie podľa rôznych databáz

	databáza	MAF
1000 Genomes Project Phase 3		0,0018
1000 Genomes Project Phase 3 (European)		0,00398
1000 Genomes Project Phase 3 (Finnish)		0,00507
gnomAD 3.0 (Non-Finnish European)		0,00657
gnomAD 3.0 (Finnish European)		0,01077
NCBI ALFA (European)		0,00584
NHLBI Exome Sequencing Project (European American)		0,00558
TOPMED		0,00382
UK10K		0,00493
Estonian Biobank		0,02033
GoNL		0,01189
Korea1K		0,00055
Northern Sweden		0,00662

Pozn.: použité dátá sú uvedené z nasledujúcich zdrojov:

https://www.ensembl.org/Homo_sapiens/Variation/Population?db=core;r=9:5125843-5126843;v=rs41316003;vdb=variation;vf=733418198;

[https://www.nlgenome.nl/menu/main/dataexplorer?entity=gonl_chr9&hideselect=true&mod=data&filter=\(POS=ge=5126341;POS=le=5126343\);](https://www.nlgenome.nl/menu/main/dataexplorer?entity=gonl_chr9&hideselect=true&mod=data&filter=(POS=ge=5126341;POS=le=5126343);)

https://www.ncbi.nlm.nih.gov/snp/rs41316003#frequency_tab

<https://bravo.sph.umich.edu/freeze8/hg38/variant/snv/9-5126343-G-A>

https://gnomad.broadinstitute.org/variant/9-5126343-G-A?dataset=gnomad_r2_1

Nakoľko je frekvencia variantu JAK2 R1063H podstatne vyššia v kohorte MPN pacientov ako v bežnej populácii, zaujímalo nás, či frekvencia závisí od demografických rozdielov alebo je jej prítomnosť v korelácii s patológiou myeloidnej línie. Preto sme analyzovali distribúciu variantu v súbore pacientov s AML a sAML (vzorky poskytnuté HOK FN Olomouc s láskavým zvolením prof. MUDr. Tomáša Papajíka, CSc. a doc. MUDr. Tomáša Szotkowského, Ph.D.). Zo 78 pacientov s AML, 9 jednotlivci nesú JAK2 R1063H mutáciu v heterozygotnom stave, tzn. frekvencia uvedenej alely sa rovná 0,05769 (Tab. 6). Pomocou NGS (next generation sequencing) sa u týchto pacientov odhalila prítomnosť somatických *driver* mutácií a iných mutácií (napr. v génoch kódujúcich proteíny Ras, receptor c-kit, izocitrátdehydrogenázu – IDH2 (isocitratedehydrogenase), nukleofosmin – NPM (nucleophosmin) a i.), ktoré sa často nachádzajú u potvrdených prípadov AML alebo asociujú s preleukemickým stavom označovaným ako klonálna hematopoéza s neurčitým

potenciálom – CHIP (clonal hematopoiesis of indeterminate potential) (Stengel a kol., 2021). Aj u pacientov so sAML sme zaznamenali porovnatelne vyššiu alelickú frekvenciu JAK2 R1063H (0,0417).

Ďalej sme hodnotili lokálnu frekvenciu tohto variantu v kontrolnej populácii 283 darcov kostnej drene (zo spádovej oblasti HOK FN Olomouc). Analýza odhalila 7 heterozygotných nositeľov JAK2 R1063H mutácie (Tab. 6). Hodnota frekvencie (0,01237) v kontrolnej skupine je vyššia ako je uvedené v dostupných databázach: 1000 Genomes Project Phase 3 (European) 0,00398 a gnomAD 3.0 (Non-Finnish European) 0,00657 (Tab. 5). Alelická frekvencia variantu v tejto skupine môže byť do istej miery skreslená a nadhodnotená, nakoľko istú časť darcov kostnej drene tvoria príbuzní pacientov s hematologickými malignitami. Ďalším dôvodom môže byť celkovo vyššia frekvencia tohto variantu v českej populácii, podobne ako v estónskej, fínskej, či holandskej populácii (Tab. 5). Aj napriek tomu, je frekvencia JAK2 R1063H mutácie v skupine pacientov s AML v porovnaní s kontrolným súborom približne 5x vyššia, na rozdiel od skupiny CML (0,0198) a akútnej lymfoidnej leukémie – ALL (0,015) pacientov (Tab. 6), u ktorých je frekvencia variantu blízka frekvencii zaznamenanej u kontrol. Preto sme ako ďalšiu kontrolnú skupinu testovali kohortu pacientov s hemoglobinopatiou (s potvrdenou/suspektnou talasémiou alebo hemoglobínovým variantom). Z 270 pacientov nesie 6 pacientov JAK2 R1063H mutáciu v heterozygotnom stave (z toho dvaja nositelia sú súrodenci s diagnózou alfa talasémia). Frekvencia variantu v kohorte s hemoglobinopatiou je 0,01111 (Tab. 6).

Tab. 6: Alelické frekvencie JAK2 R1063H mutácie v rámci rôznych kohort.

Diagnóza	MAF
Kontroly	0,0124
AML	0,0577
sAML	0,0417
CML	0,0198
ALL	0,0150
Hemoglobinopatie	0,0111

Uvedené, zatiaľ nepublikované dátá naznačujú **zvýšený výskyt JAK2 R1063H mutácie v českej populácii a jej asociáciu s rozvojom/transformáciou do AML** (odds ratio – OD = 4,95; 95% confidence interval – CI = 2,1 – 11,64; p = 6,02437E-05). V súčasnosti naše pracovisko spolupracuje s ďalšími centrami v ČR na podrobnejšej populačnej analýze mutácie JAK2 R1063H mutácie u kontrolných skupín ako aj u myeloidných malignít.

Na základe uvedeného sa domnievame, že frekvencia variantov JAK2 sa mení v závislosti od populácie a môže tým ovplyvňovať rozvoj nielen AML, ale aj iných hematologických ochorení napr. MPN. Predpokladáme, že prítomnosť variantu môžeme prirovnáť k určitému premalígnemu stavu (ako napr. CHIP). JAK2 R1063H mutácia môže predisponovať k zisku iných kauzálnych mutácií a rozvoju myeloidnej malignity. Alebo môže pôsobiť ako koonkogén v prítomnosti leukemického *driver* onkogénu, ktorý vznikol bez ohľadu na prítomnosť tohto variantu. Uvedené vzájomne nevylučujúce sa hypotézy podporuje aj pomerne vysoká frekvencia (8,3%) tohto variantu v nami študovanej skupine pacientov s diagnózou sAML. Podobne, aj v inej štúdii z MD Anderson v USA (Benton a kol., 2019) zahŕňajúcej 2154 MPN pacientov, sa potvrdil zvýšený výskyt (15,3%) JAK2 variantov v subpopulácii pacientov so sAML transformovaných z MPN. Pričom spomedzi 35 identifikovaných JAK2 variantov práve R1063H variant spolu s L393V a N1108S variantami patril medzi najčastejšie sa vyskytujúce a alelická záťaž týchto variantov sa podobne ako v našej štúdii (Mambet a kol., 2018) blíži k 50%, čo naznačuje, že ide o dedičné mutácie. Na základe uvedeného sa domnievame, že **súbor dedičných samostatne sa vyskytujúcich slabo aktivujúcich variantov predstavuje pre jedinca nízke riziko.** Avšak kooperácia takýchto dedičných mutácií môže a) spoločne so získanými mutáciami vytvoriť alebo zosilniť onkogénnu aktivitu, a viest' tak k rozvoju a progresii ochorenia; b) prispievať k fenotypovej heterogenite ochorenia.

Uvedené experimentálne dátá sú súčasťou zatial' pripravovanej publikácie, ktorej ďalšie analýzy spočívajú v a) rozšírení kontrolnej rovnako exponovanej skupiny o vzorky pochádzajúce aj z iných regiónov ČR a tiež iných krajín pre potvrdenie asociácie JAK2 R1063H mutácie s myeloidnou malignitou, prípadne lokálne zvýšenej frekvencie JAK2 R1063H mutácie v českej populácii; b) realizácie funkčných štúdií približujúcich vzťah tejto mutácie aj s inými onkogénmi. Nakol'ko kooperujúci efekt onkomutácie JAK2 V617F s mutáciou JAK2 R1063H bol už popísaný (Mambet a kol., 2018), je potrebné definovať vzťah tejto mutácie s ďalšími onkogénmi, ktorých prítomnosť bola zaznamenaná spoločne s JAK2 R1063H mutáciou.

4.3 Kritické zhodnotenie literatúry týkajúcej sa nových poznatkov patofyziológie Ph-negatívnych MPN

Poslednou časťou mojej dizertačnej práce je súhrnný článok (príloha 5), ktorý popisuje najnovšie poznatky komplexného pozadia biológie MPN. Okrem klasickej somatickej

genetiky Ph-negatívnych MPN, je v článku diskutovaná aj otázka **genetickej predispozície**, ktorá **pravdepodobne v súčinnosti s ďalšími aj negenetickými činiteľmi** (napr. faktor prostredia, životného štýlu, komorbidity alebo veku) **ovplyvňuje riziko rozvoja a/alebo určuje fenotypový smer Ph-negatívnych MPN.**

5. SÚHRN

Poruchy hematopoézy prípadne erytropoézy, vrodené aj získané, ovplyvňujú zásadným spôsobom štruktúru a funkciu kostnej drene, čo sa môže prejaviť v závažných zmenách počtu a aktivity krvných elementov. Nakoľko erytropoéza je úzko spätá s metabolizmom železa, jej poruchy sú spojené s narušenou homeostázou železa. Cieľom mojej dizertačnej práce bolo študovať a) vývinové zmeny erytropoézy a ich prepojenie s metabolizmom železa u myšieho modelu PFCP; b) vplyv dedičných *JAK2* mutácií na krvotvorbu.

Na myšom modeli vrodenej primárnej erytrocytózy sme analyzovali dopad *gain-of-function EPOR* mutácie na prenatálne, perinatálne a postnatálne štadium erytropoézy a metabolizmus železa. Ukázali sme, že ľudský *gain-of-function EPOR* vedie k rozvoju erytrocytózy už prenatálne, potom nasleduje krátke perinatálne obdobie korekcie Hct, po ktorom sa erytrocytóza opäť vyvíja v rozmedzí 3 – 6 týždňov života. Oscilácia hladín Hct u *gain-of-function EPOR* mutantných myší v perinatálnom období pravdepodobne odzrkadľuje zvýšenú deštrukciu prenatálne vytvorených červených krviniek, ktorá súvisí s prechodom z hypoxického prostredia do prostredia normoxie. Prenatálne a perinatálne, *gain-of-function EPOR* myši majú zvýšené transkripty *Erfe*, znížený hepcidín a nedostatok železa. Postnatálne sa hepcidín u týchto myší zvyšuje, čo je sprevádzané nízkou indukciami *Erfe* a akumuláciou železa, ku ktorému pravdepodobne prispieva železo pochádzajúce z predčasne starnúcich erytrocytov. Starnutím jedincov, najmä u *gain-of-function EPOR* homozygotov, dochádza k poklesu erytropoézy, myeloidnej expanzii a lokálnemu zápalu kostnej drene. Znížený dopyt po železe erytropoézou, v dôsledku jej útlmu súvisiaceho s vekom, môže rovnako prispievať k zvýšenému ukladaniu železa u starých *gain-of-function EPOR* myší. Záverom môžeme zhrnúť, že erytrocytóza u *gain-of-function EPOR* mutantných myší, ako aj expresia hepcidínu, erytroferónu a hladina železa podliehajú počas ontogenézy dynamickým zmenám; a že krvotvorba týchto myší vykazuje známky predčasného starnutia.

V druhej časti práce sme sa venovali otázke úlohe dedičných *JAK2* mutácií v signalizácii, ktorú tento enzým sprostredkúva. Zistili sme, že dedičné varianty *JAK2* E846D a R1063H majú samostatne slabý dopad na aktivitu enzýmu, ale ich vzájomná súčinnosť alebo kooperácia s inou mutáciou vedie k patologicky zvýšenej intenzite *JAK2* signalizácie. Popísali sme tak fenotyp primárnej erytrocytózy s abnormálnou megakaryopoézou u zloženého *JAK2* E846D/R1063H heterozygota, aj zosilnenie fenotypu MPN účinkom zárodočnej *JAK2* R1063H mutácie. Naše predbežné výsledky zároveň ukazujú vyššiu

frekvenciu výskytu zárodočného JAK2 R1063H variantu u pacientov s MPN a obzvlášť s AML; táto alela by tak mohla predstavovať isté predispozičné riziko. Naše zistenia sú tak v súlade v súčasnosti diskutovanou úlohou genetickej predispozície v patofyziológii MPN. V predloženom súhrnnom článku sme sa zamerali na popis heterogenity klasických Ph negatívnych MPN a zhodnotili sme aj donedávna podcenené postavenie dedičného rizika v rámci ich rozvoja a komplexnej patobiológie.

SUMMARY

Disorders of hematopoiesis or erythropoiesis, inherited and acquired, fundamentally affect the structure and function of the bone marrow, and can be manifested in severe changes in the number and activity of blood elements. Since erythropoiesis is linked to iron metabolism, its disorders are associated with disturbed iron homeostasis. My Ph.D. thesis aimed to study a) the relationship between developmental changes in erythropoiesis and iron metabolism in the PFCP mouse model; b) the impact of hereditary *JAK2* mutations on hematopoiesis.

In a mouse model of congenital primary erythrocytosis, we analyzed the impact of gain-of-function *EPOR* mutation of erythropoiesis and iron metabolism at prenatal, perinatal, and postnatal stages. We have shown that human gain-of-function *EPOR* leads to the development erythrocytosis prenatally, followed by a short period of perinatal Hct correction, after which erythrocytosis develops again between 3 – 6 weeks of life. The perinatal oscillation of Hct levels in the *EPOR* mutant mice probably reflects the increased destruction of red blood cells created prenatally, which is related to the transition from a hypoxic environment to normoxia. Prenatally and perinatally, *EPOR* mutant mice have increased *Erfe* transcripts, reduced hepcidin, and iron deficiency. Postnatally, hepcidin increases in these mice, accompanied by low Erfe induction and iron accumulation, likely contributed by iron derived from prematurely senescent erythrocytes. With aging, the old, especially *EPOR* mutant homozygotes exhibit a decline of erythropoiesis, myeloid expansion, and local bone marrow inflammatory stress. Reduced iron demand for erythropoiesis, due to its age-related attenuation, also is another contributing factor to increased iron deposition in the aged *EPOR* mutant mice. We conclude, that erythrocytosis as well as the expression of hepcidin, erythroferrone and iron levels undergo dynamic changes during the ontogenesis of the *EPOR* mutant mice which also exhibit features of premature aging of hematopoiesis.

In the second part of the thesis, we addressed the question the role of hereditary *JAK2* mutations in the signaling mediated by this kinase. We found that the inherited variants *JAK2* E846D and R1063H separately have a weak impact on kinase activity. However, their interaction or cooperation with another mutation leads to a pathologically increased intensity of *JAK2* signaling. We described the phenotype of primary erythrocytosis with abnormal megakaryopoiesis in a compound *JAK2* E846D/R1063H heterozygote and the exacerbation of the MPN phenotype by the germline *JAK2* R1063H mutation. Simultaneously, our preliminary results show a higher frequency of germline *JAK2* R1063H variant in patients

with MPN, and especially with AML. We propose that JAK2 R1063H may represent a predisposing factor towards the development of myeloid malignancies, which is in agreement with recently proposed genetic predisposition to be an important factor in the pathophysiology of MPN. In the presented review article, we focused on the description of the heterogeneity of classical Ph negative MPN and evaluated the role of hereditary risk in the development and complex pathobiology of MPN.

6. POUŽITÁ LITERATÚRA

- Abboud S, Haile DJ. A novel mammalian iron-regulated protein involved in intracellular iron metabolism. *J Biol Chem.* 2000; 275:19906-12.
- Afreen S, Bohler S, Müller A, a kol. BCL-XL expression is essential for human erythropoiesis and engraftment of hematopoietic stem cells. *Cell Death Dis.* 2020;11(1):8.
- Akel A, Wagner CA, Kovacikova J, a kol. Enhanced suicidal death of erythrocytes from gene-targeted mice lacking the Cl-/HCO₃(-) exchanger AE1. *m J Physiol Cell Physiol.* 2007;292(5):C1759-67.
- Albadari N, Deng S, Li W. The transcriptional factors HIF-1 and HIF-2 and their novel inhibitors in cancer therapy. *Expert Opin Drug Discov.* 2019;14(7):667-682.
- Andriopoulos B Jr, Corradini E, Xia Y, a kol. BMP6 is a key endogenous regulator of hepcidin expression and iron metabolism. *Nat Genet.* 2009;41(4):482–487.
- Ang SO, Chen H, Hirota K, a kol. Disruption of oxygen homeostasis underlies congenital Chuvash polycythemia. *Nat Genet.* 2002;32(4):614-621.
- Antoniani C, Romano O, Miccio A. Concise Review: Epigenetic Regulation of Hematopoiesis: Biological Insights and Therapeutic Applications. *Stem Cells Transl Med.* 2017;6(12):2106-2114.
- Arber DA, Orazi A, Hasserjian R, a kol. The 2016 revision to the World Health Organization classification of myeloid neoplasms and acute leukemia. *Blood.* 2016;127:2391-2405.
- Arcasoy MO, Harris KW, Forget BG. A human erythropoietin receptor gene mutant causing familial erythrocytosis is associated with deregulation of the rates of Jak2 and Stat5 inactivation. *Exp Hematol.* 1999;27(1):63-74.
- Arezes J, Foy N, McHugh K, a kol. Erythroferrone inhibits the induction of hepcidin by BMP6. *Blood.* 2018;132(14):1473-1477.
- Artuso I, Pettinato M, Nai A, a kol. Transient decrease of serum iron after acute erythropoietin treatment contributes to hepcidin inhibition by ERFE in mice. *Haematologica.* 2019;104(3):e87-e90.
- Aschemeyer S, Qiao B, Stefanova D, a kol. Structure-function analysis of ferroportin defines the binding site and an alternative mechanism of action of hepcidin. *Blood.* 2018;131(8):899-910.
- Bachman E, Travison TG, Basaria S, a kol. Testosterone induces erythrocytosis via increased erythropoietin and suppressed hepcidin: evidence for a new erythropoietin/hemoglobin set point. *J Gerontol A Biol Sci Med Sci.* 2014;69(6):725-35.
- Baker SJ, Rane SG, Reddy EP. Hematopoietic cytokine receptor signaling. *Oncogene.* 2007;26(47):6724-37.
- Bento C, Almeida H, Maia TM, a kol. Molecular study of congenital erythrocytosis in 70 unrelated patients revealed a potential causal mutation in less than half of the cases (Where is/are the missing gene(s)?). *Eur J Haematol.* 2013 Oct;91(4):361-8.
- Benton CB, Prajwal CB, DiNardo CD, a kol. Janus Kinase 2 variants associated with the transformation of myeloproliferative neoplasms into acute myeloid leukemia. *Cancer.* 2019;125:1855-1866.
- Bernaudin M, Bellail A, Marti HH, a kol. Neurons and astrocytes express EPO mRNA: oxygen-sensing mechanisms that involve the redox-state of the brain. *Glia.* 2000;30(3):271-8.
- Bhoopalan SV, Huang LJ, Weiss MJ. Erythropoietin regulation of red blood cell production: from bench to bedside and back. *F1000Res.* 2020;9:F1000 Faculty Rev-1153.

Biagetti G, Catherwood M, Robson N, a kol. HFE mutations in idiopathic erythrocytosis. *Br. J. Haematol.* 2018;181:270-272.

Billesbølle CB, Azumaya CM, Kretsch RC, a kol. Structure of hepcidin-bound ferroportin reveals iron homeostatic mechanisms. *Nature*. 2020;586(7831):807-811.

Blobel GA, Bodine D, Brand M, a kol. An international effort to cure a global health problem: A report on the 19 th Hemoglobin Switching Conference. *Exp Hematol*. 2015;43(10):821837.

Bonaud A, Lemos JP, Espéli M, Balabanian K. Hematopoietic Multipotent Progenitors and Plasma Cells: Neighbors or Roommates in the Mouse Bone Marrow Ecosystem? *Front Immunol*. 2021;12:658535.

Bourdeau A, Dubé N, Tremblay ML. Cytoplasmic protein tyrosine phosphatases, regulation and function: the roles of PTP1B and TC-PTP. *Curr Opin Cell Biol*. 2005;17:203-9.

Brand KA, Hermfisse U. Aerobic glycolysis by proliferating cells: a protective strategy against reactive oxygen species. *FASEB J*. 1997;11(5):388-95.

Bunn HF. Erythropoietin. *Cold Spring Harb Perspect Med*. 2013;3(3):a011619.

Burda P, Laslo P, Stopka T. The role of PU.1 and GATA-1 transcription factors during normal and leukemogenic hematopoiesis. *Leukemia*. 2010; 24:1249-57.

Burlet B, Bourgeois V, Buriller C, a kol. High HFE mutation incidence in idiopathic erythrocytosis. *Br. J. Haematol*. 2019;185:794-95.

Byrne SL, Krishnamurthy D, Wessling-Resnick M. Pharmacology of Iron Transport. *Annu Rev Pharmacol Toxicol*. 2013;53:17-36.

Camps C, Petousi N, Bento C, a kol. Gene panel sequencing improves the diagnostic work-up of patients with idiopathic erythrocytosis and identifies new mutations. *Haematologica*. 2016;101(11):1306-1318.

Canali S, Core AB, Zumbrennen-Bullough KB, Merkulova M, a kol. Activin B Induces Noncanonical SMAD1/5/8 Signaling via BMP Type I Receptors in Hepatocytes: Evidence for a Role in Hepcidin Induction by Inflammation in Male Mice. *Endocrinology*. 2016;157(3):1146-1162.

Carmona U, Li L, Zhang L, Knez M. Ferritin light-chain subunits: key elements for the electron transfer across the protein cage. *Chem Commun (Camb)* 2014;50:15358-15361.

Cercamondi CI, Stoffel NU, Moretti D, a kol. Iron homeostasis during anemia of inflammation: a prospective study of patients with tuberculosis. *Blood*. 2021;138(15):1293-1303.

Chandrasekhar C, Pasupuleti SK, Sarma PVGK. Novel mutations in the EPO-R, VHL and EPAS1 genes in the Congenital Erythrocytosis patients. *Blood Cells Mol Dis*. 2020;85:102479.

Chapelle A, Sistonen P, Lehväslaiho H, Ikkala E, Juvonen E. Familial erythrocytosis genetically linked to erythropoietin receptor gene. *Lancet*. 199;341(8837):82-4.

Chauveau A, Luque Paz D, Lecucy L, a kol. A new point mutation in EPOR inducin a short deletion in congenital erythrocytosis. *Br J Haematol*. 2016; 172(3):475-477.

Chen E, Beer PA, Godfrey AL, a kol. Distinct clinical phenotypes associated with JAKV617F reflect differential STAT1 signaling. *Cancer cell*.2010;18:524-535.

Cheng H, Zheng Z, Cheng T. New paradigms on hematopoietic stem cell differentiation. *Protein Cell*. 2020; 11(1): 34-44.

Chen X, Li J, Kang R, Klionsky DJ, Tang D. Ferroptosis: machinery and regulation. *Autophagy*. 2021;17(9):2054-2081.

Collins A a Ke X. Primer1: Primer design Web service for Tetra-Primer ARMS-PCR. The Open Bioinformatics Journal. 2012;6:55-58.

Collins JF, Wessling-Resnick M, Knutson MD. Hepcidin regulation of iron transport. *J Nutr*. 2008;138(11):2284-8.

Le Couedic JP, Mitjavila MT, Villevial JL, a kol. Missense mutation of the erythropoietin receptor is a rare event in human erythroid malignancies. *Blood*. 1996;87(4):1502-11.

Crispino JD. GATA1 in normal and malignant hematopoiesis. *Semin Cell Dev Biol*. 2005;16(1):137-147.

Dahl R, Iyer SR, Owens KS, Cuylear DD, Simon MC. The transcriptional repressor GFI-1 antagonizes PU.1 activity through protein-protein interaction. *J Biol Chem*. 2007;282(9):6473-83.

Dame C, Fahnenstich H, Freitag P, a kol.. Erythropoietin mRNA expression in human fetal and neonatal tissue. *Blood*. 1998; 92(9):3218-25.

D'Andrea AD, Yoshimura A, Youssoufian H, a kol. The cytoplasmic region of the erythropoietin receptor contains nonoverlapping positive and negative growth-regulatory domains. *Mol Cell Biol*. 1991;11(4):1980-1987.

Dausinas Ni P, Basile C, Junge C, Hartman M, O'Leary HA. Hypoxia and hematopoiesis. *Current Stem Cell Reports*. 2022; 8:24-34.

De Bruijn MF, Speck NA, Peeters MC, Dzierzak E. Definitive hematopoietic stem cells first develop within the major arterial regions of the mouse embryo. *EMBO J*. 2000;19:2465-2474.

De Maria R, Testa U, Luchetti L, a kol. Apoptotic role of Fas/Fas ligand system in the regulation of erythropoiesis. *Blood*. 1999; 93(3):796-803.

Diaz V, Gammella E, Recalcati S, a kol. Liver iron modulates hepcidin expression duritn chronically elevated erythropoiesis in mice. *Hepatology*. 2013; 58:2122-2132.

Di Lorenzo VR, Margraf, R, Swierczek S, Hickman K, Voelkerding K, Prchal J. A Novel EPO Gene Mutation In a Family With Autosomal Dominant Polycythemia. *Blood*. 2013;122 (21):950.

Divoky V, Liu Z, Ryan TM, Prchal JF, Townes TM, Prchal JT. Mouse model of congenital polycythemia: homologous replacement of murine gene by mutant human erythropoietin receptor gene. *Proc Natl Acad Sci USA*. 2001;98:986-991.

Divoky V, Song J, Horvathova M, a kol. Delayed hemoglobin switching and perinatal neocytolysis in mice with gain-of-function erythropoietin receptor. *J Mol Med (Berl)*. 2016; 94:597-608.

Donovan A, Brownlie A, Zhou V, a kol. Positional cloning of zebrafish ferroportin1 identifies a conserved vertebrate iron exporter. *Nature*. 2000; 403:776-81.

Duan C. Hypoxia-inducible factor 3 biology: complexities and emerging themes. *Am J Physiol Cell Physiol*. 2016;310(4):260-269.

Dzierzak E, Philipsen S. Erythropoiesis: development and differentiation. *Cold Spring Harb Perspect Med*. 2013;3(4):a011601.

Eisele AS, Cosgrove J, Magniez A, a kol. Erythropoietin directly remodels the clonal composition of murine hematopoietic multipotent progenitor cells. *Elife*. 2022;11:e66922.

Etheridge SL, Cosgrove ME, Sangkhae V, a kol. A novel activating, germline JAK2 mutation, JAK2R564Q, causes familial essential thrombocytosis. *Blood*. 2014;123(7):1059-1068.

Ferkowicz MJ, Yoder MC. Blood island formation: longstanding ob- servations and modern interpretations. *Exp Hematol*. 2005;33:1041-1047.

- Fillebeen C, Wilkinson N, Charlebois E, Katsarou A, Wagner J, Pantopoulos K. Hepcidin-mediated hypoferremic response to acute inflammation requires a threshold of Bmp6/Hjv/Smad signaling. *Blood*. 2018;132(17):1829-1841.
- Filser M, Giansily-Blaizot M, Grenier M, et al. Increased incidence of germline PIEZO1 mutations in individuals with idiopathic erythrocytosis. *Blood*. 2021;137(13):1828-1832.
- Fleming MD, Trenor CC, 3rd, Su MA, et al. Microcytic anaemia mice have a mutation in Nramp2, a candidate iron transporter gene. *Nat Genet*. 1997;16:383-386.
- Föller M, Huber SM, Lang F. Erythrocyte programmed cell death. *IUBMB Life*. 2008;60(10):661-668.
- Föller M, Lang F. Ion Transport in Eryptosis, the Suicidal Death of Erythrocytes. *Front Cell Dev Biol*. 2020; 8:597.
- Forejtníková H, Vieillevoye M, Zermati Y, et al. Transferrin receptor 2 is a component of the erythropoietin receptor complex and is required for efficient erythropoiesis. *Blood*. 2010;116(24):5357-5367.
- Fu J, Zuber J, Martinez M, et al. Human Intestinal Allografts Contain Functional Hematopoietic Stem and Progenitor Cells that Are Maintained by a Circulating Pool. *Cell Stem Cell*. 2019; 24(2):227-239.e8.
- Ganz T, Nemeth E. Hepcidin and iron homeostasis. *Biochim Biophys Acta*. 2012; 1823:1434-43.
- Gao J, Chen J, Kramer M, Tsukamoto H, Zhang AS, Enns CA. Interaction of the hereditary hemochromatosis protein HFE with transferrin receptor 2 is required for transferrin-induced hepcidin expression. *Cell Metab*. 2009;9(3):217-227.
- Garcia-Santos D, Hamdi A, Saxova Z, et al. Inhibition of heme oxygenase ameliorates anemia and reduces iron overload in a β-thalassemia mouse model. *Blood*. 2018;131(2):236-246.
- Gekas C, Dieterlen-Lievre F, Orkin SH, Mikkola HK. The placenta is a niche for hematopoietic stem cells. *Dev Cell*. 2005;8:365-375.
- Ginzburg Y. Hepcidin-ferroportin axis in health and disease. *Vitam Horm*. 2019;110:17-45.
- Ginzburg YZ, Feola M, Zimran E, Varkonyi J, Ganz T, Hoffman R. Dysregulated iron metabolism in polycythemia vera: etiology and consequences. *Leukemia*. 2018;32(10):2105-2116.
- Girelli D, Pasino M, Goodnough JB, et al. Reduced serum hepcidin levels in patients with chronic hepatitis C. *J Hepatol* 2009;51:845-52.
- Girodon F, Airaud F, Garrec C, Bézieau S, Gardie B. Gene panel sequencing in idiopathic erythrocytosis. *Haematologica*. 2017;102(1):e30-e30.
- Gomme PT, McCann KB, Bertolini J. Transferrin: structure, function and potential therapeutic actions. *Drug Discov Today*. 2005;10(4):267-73.
- Gordeuk VR, Miasnikova GY, Sergueeva AI, et al. Chuvash polycythemia VHLR200W mutation is associated with down-regulation of hepcidin expression. *Blood*. 2011 Nov 10;118(19):5278-82.
- Gottlieb Y, Topaz O, Cohen LA, et al. Physiologically aged red blood cells undergo erythrophagocytosis in vivo but not in vitro. *Haematologica*. 2012; 97(7): 994-1002.
- Grabek J, Straube J, Bywater M, Lane SW. MPN: The Molecular drivers of disease initiation, progression and transformation and their effect on treatment. *Cells*. 2020;9(8):1901.
- Grebien F, Kerényi MA, Kovacic B, et al. Stat5 activation enables erythropoiesis in the absence of EpoR and Jak2. *Blood* 2008; 111(9):4511-4522.

Grisouard J, Li S, Kubovcakova L, a kol. JAK2 exon 12 mutant mice display isolated erythrocytosis and changes in iron metabolism favoring increased erythropoiesis. *Blood*. 2016;128 (6): 839-851.

Gross M, Ben-Califa N, McMullin MF, a kol. Polycythaemia-inducing mutations in the erythropoietin receptor (EPOR): mechanism and function as elucidated by epidermal growth factor receptor-EPOR chimeras. *Br J Haematol*. 2014;165(4):519-28.

Grover A, Mancini E, Moore S, a kol. Erythropoietin guides multipotent hematopoietic progenitor cells toward an erythroid fate. *J Exp Med*. 2014;211(2):181-8.

Gunshin H, Fujiwara Y, Custodio AO, Direnzo C, Robine S, Andrews NC. Slc11a2 is required for intestinal iron absorption and erythropoiesis but dispensable in placenta and liver. *J Clin Invest* 2005; 115: 1258-66.

Haan M, Is'harc H, Hermanns HM, a kol. Mapping of a region within the N terminus of Jak1 involved in cytokine receptor interaction. *J. Biol. Chem.* 2001; 276(40):37451-8.

Hamdi A, Roshan TM, Kahawita TM, Mason AB, Sheftel AD, Ponka P. Erythroid cell mitochondria receive endosomal iron by a "kiss-and-run" mechanism. *Biochim Biophys Acta*. 2016;1863(12):2859-2867.

Harrison CN, Mead AJ, Panchal A, a kol. Ruxolitinib vs best available therapy for ET intolerant or resistant to hydroxycarbamide. *Blood*. 2017;130:1889-1897.

Hariharan P, Nadkarni A. Insight of fetal to adult hemoglobin switch: Genetic modulators and therapeutic targets. *Blood Rev*. 2021; 49:100823.

Heir P, Srikumar T, Bikopoulos G, a kol. Oxygen-dependent Regulation of Erythropoietin Receptor Turnover and Signaling. *J Biol Chem*. 2016; 291(14):7357-72.

Hentze MW, Muckenthaler MU, Andrews NC. Balancing acts: molecular control of mammalian iron metabolism. *Cell*. 2004;117(3):285-297.

Higgs DR, Wood WG, Jarman AP, a kol. A major positive regulatory region located far upstream of the human alpha-globin gene locus. *Genes Dey*. 1990;4(9):1588-1601.

Horvathova M, Kapralova K, Zidova Z, Dolezal D, Pospisilova D, Divoky V. Erythropoietin-driven signaling ameliorates the survival defect of DMT1-mutant erythroid progenitors and erythroblasts. *Haematologica*. 2012; 97(10):1480-8.

Huang P, Zhao Y, Zhong J, a kol. Putative regulators for the continuum of erythroid differentiation revealed by single-cell transcriptome of human BM and UCB cells. *Proc Natl Acad Sci USA*. 2020; 117(23):12868-12876.

Hu X, Li J, Fu M, Zhao X, Wang W. The JAK/STAT signaling pathway: from bench to clinic. *Signal Transduct Target Ther*. 2021;6(1):402.

Ihle JN. Cytokine receptor signalling. *Nature*. 1995; 377:591-4.

Ingle E, Klinken SP. Cross-regulation of JAK and Src kinases. *Growth Factors*. 2006;24(1):89-95.

Jafari M, Ghadami E, Dadkhah T, Akhavan-Niaki H. PI3k/AKT signaling pathway: Erythropoiesis and beyond. *J Cell Physiol*. 2019;234(3):2373-2385.

Jegalian AG, Wu H. Differential roles of SOCS family members in EpoR signal transduction. *J. Interferon Cytokine Res*. 2002;22:853-860.

Jiang L, Wang J, Wang K, a kol. RNF217 regulates iron homeostasis through its E3 ubiquitin ligase activity by modulating ferroportin degradation. *Blood*. 2021; 138:689-705.

Juvonen E, Ikkala E, Fyhrquist F, Ruutu T. Autosomal dominant erythrocytosis caused by increased sensitivity to erythropoietin. *Blood*. 1991;78: 3066-3069.

Kanamori Y, Murakami M, Matsui T, Funaba M. JNK facilitates IL-beta-induced hepcidin transcription via JunB activation. *Cytokina*. 2018; 111:295-302.

Kanamori Y, Murakami M, Sugiyama M, Hashimoto O, Matsui T, Funaba M. Interleukin-1beta (IL-1beta) transcriptionally activates hepcidin by inducing CCAAT enhancer-binding protein delta (C/EBP δ) expression in hepatocytes. *J.Biol.Chem.* 2017; 292(24):10275-10287.

Kapralova K, Horvathova M, Pecquet C, et al. Cooperation of germline JAK2 mutations E846D and R1063H in hereditary erythrocytosis with megakaryocytic atypia. *Blood*. 2016;128(10):1418-1423.

Kautz L, Jung G, Valore EV, Rivella S, Nemeth E, Ganz T. Identification of erythroferrone as an erythroid regulator of iron metabolism. *Nat Genet* 2014; 46:678-84.

Kautz L, Nemeth E. Molecular liaisons between erythropoiesis and iron metabolism. *Blood*. 2014;124(4):479-482.

Kerenyi MA, Grebien F, Gehart H, et al. Stat5 regulates cellular iron uptake of erythroid cells via IRP-2 and TfR-1. *Blood*. 2008; 112(9): 3878-3888.

Khalil S, Delehanty L, Grado S, et al. Iron modulation of erythropoiesis is associated with Scribble-mediated control of the erythropoietin receptor. *J. Exp. Med.* 2018;215:661-679.

Kim MY, Yan B, Huang S, Qiu Y. Regulating the Regulators: The Role of Histone Deacetylase 1 (HDAC1) in Erythropoiesis. *Int J Mol Sci.* 2020;21(22):8460.

Kirito K, Nakajima K, Watanabe T, et al. Identification of the human erythropoietin receptor region required for Stat1 and Stat3 activation. *Blood*. 2002;99(1):102-110.

Knight T, Zaidi AU, Wu S, Gadgeel M, Buck S, Ravindranath Y. Mild erythrocytosis as a presenting manifestation of PIEZO1 associated erythrocyte volume disorders. *Pediatr Hematol Oncol*. 2019;36(5):317-326.

Knutson M, Wessling-Resnick M. Iron metabolism in the reticuloendothelial system. *Crit Rev Biochem Mol Biol*. 2003;38(1):61-88.

Koledova Z, Raskova Kafkova L, Calabkova L, Krystof V, Dolezal P, Divoky V. Cdk2 inhibition prolongs G1 phase progression in mouse embryonic stem cells. *Stem cells and development*. 2010; 19(2):181-194.

Kralova B, Sochorcova L, Song J, et al. Developmental changes in iron metabolism and erythropoiesis in mice with human gain-of-function erythropoietin receptor. *American Journal of Hematology*. 2022; 97(10):1286-1299.

Kralovics R, Indrak K, Stopka T, Berman BW, Prchal JT, Prchal JT. Two new EPO receptor mutations: truncated EPO receptors are most frequently associated with primary familial and congenital polycythemias. *Blood*. 1997;90(5):2057-2061. a)

Kralovics R, Sokol L, Broxson Jr EH, Prchal JT. The erythropoietin receptor gene is not linked with the polycythemia phenotype in a family with autosomal dominant primary polycythemia. *Proc Assoc Am Physicians*. 1997;109(6):580-5. b)

Kralovics R, Prchal JT. Genetic heterogeneity of primary familial and congenital polycythemia. *Am J Hematol*. 2001; 68(2):115-121.

Kumkhaek C, Aerbajinai W, Liu W, et al. MASL1 induces erythroid differentiation in human erythropoietin-dependent CD34+ cells through the Raf/MEK/ERK pathway. *Blood*. 2013;121(16):3216-27.

Landgren O, Goldin LR, Kristinsson SY, Helgadottir EA, Samuelsson J, Bjorkholm M. Increased risks of polycythemia vera, essential thrombocythemia, and myelofibrosis among 24,577 first-degree relatives of 11,039 patients with myeloproliferative neoplasms in Sweden. *Blood*. 2008;112:2199-2204.

Lanikova L, Babosova O, Swierczek S, a kol. Coexistence of gain-of-function JAK2 germ line mutations with JAK2V617F in polycythemia vera. *Blood*. 2016;128(18):2266-2270.

Latour C, Besson-Fournier C, Gourbeyre O, Meynard D, Roth MP, Coppin H. Deletion of BMP6 worsens the phenotype of HJV-deficient mice and attenuates hepcidin levels reached after LPD challenge. *Blood*. 2017;130(21):2339-2343.

Latour C, Kautz L, Besson-Fournier C, a kol. Testosterone perturbs systemic iron balance through activation of epidermal growth factor receptor signaling in the liver and repression of hepcidin. *Hepatology*. 2014;59(2):683-94.

Lee C, Lim HK, Sakong J, a kol. Janus kinase signal transducer and activator of transcription mediates phosphatidic acid-induced interleukin (IL)-1 β and IL-6 production. *Molecular Pharmacology*. 2006;69:1041-1047.

Lee YS, Kim YH, Jung YS, a kol. Hepatocyte toll-like receptor 4 mediates lipopolysaccharide-induced hepcidin expression. *Exp Mol Med*. 2017; 46(12):e408.

Lefrançais E, Ortiz-Muñoz G, Caudrillier A, a kol. The lung is a site of platelet biogenesis and a reservoir for haematopoietic progenitors. *Nature*. 2017;544(7648):105-109.

Lenglet M, Robiquet F, Schwarz K, a kol. Identification of a new VHL exon and complex splicing alterations in familial erythrocytosis or von Hippel-Lindau disease. *Blood*. 2018;132(5):469-483.

Levine RL, Wadleigh M, Cools J, a kol. Activating mutation in the tyrosine kinase JAK2 in polycythemia vera, essential thrombocythemia, and myeloid metaplasia with myelofibrosis. *Cancer Cell*. 2005;7(4):387-397.

Li H, Natarajan A, Ezike J, a kol. Rate of progression through a continuum of transit-amplifying progenitor cell states regulates blood cell production. *Dev Cell*. 2019; 49(1):118-129.e7.

Li Q, Peterson KR, Fang X, Stamatoyannopoulos G. Locus control regions. *Blood*. 2002;100(9):3077-3086.

Li W, Guo R, Song Y, Jiang Z. Erythroblastic Island Macrophages Shape Normal Erythropoiesis and Drive Associated Disorders in Erythroid Hematopoietic Diseases. *Front Cell Dev Biol*. 2021;8:613885.

Liang R, Campreciós G, Kou Y, a kol. A Systems Approach Identifies Essential FOXO3 Functions at Key Steps of Terminal Erythropoiesis. *PLoS Genet*. 2015;11(10):e1005526.

Libregts SF, Gutiérrez L, de Bruin AM, a kol. Chronic IFN- γ production in mice induces anemia by reducing erythrocyte life span and inhibiting erythropoiesis through an IRF-1/PU.1 axis. *Blood*. 2011;118(9):2578-88.

Lin CS, Lim SK, D'Agati V, Costantini F. Differential effects of an erythropoietin receptor gene disruption on primitive and definitive erythropoiesis. *Genes Dev*. 1996; 10(2):154-64.

Liu B, Liao, J, Rao, X, a kol. Inhibition of Stat1-mediated gene activation by PIAS1. *Proceedings of the National Academy of Sciences U.S.A.* 1998;95:10626-10631.

Liu N, Hargreaves VV, Zhu Q, a kol. Direct Promoter Repression by BCL11A Controls the Fetal to Adult Hemoglobin Switch. *Cell*. 2018;173(2):430-442.e17.

Lodish H, Flygare J, Chou S. From stem cell to erythroblast: regulation of red cell production at multiple levels by multiple hormones. *IUBMB Life*. 2010;62(7):492-6.

Lucarelli G, Howard D, Stohlman F Jr. Regulation of Erythropoiesis. XV. Neonatal Erythropoiesis and the Effect of Nephrectomy. *J Clin Invest*. 1964;43(11):2195-2203.

Lutz HU, Bogdanova A, Mechanisms tagging senescent red blood cells for clearance in healthy humans. *Front Physiol*. 2013;4:387.

Lux CT, Yoshimoto M, McGrath K, Conway SJ, Palis J, Yoder MC. All primitive and definitive hematopoietic progenitor cells emerging before E10 in the mouse embryo are products of the yolk sac. *Blood*. 2008;111:3435-3438.

Mambet C, Babosova O, Defour JP, a kol. Co-Occurring JAK2 V617F and R1063H Mutations Increase JAK2 Signaling and Neutrophilia in MPN Patients. *Blood*. 2018;132(25):2695-2699.

Mancias JD, Wang X, Gygi SP, Harper JW, Kimmelman AC. Quantitative proteomics identifies NCOA4 as the cargo receptor mediating ferritinophagy. *Nature*. 2014;509(7498):105-109.

Mann Z, Sengar M, Verma YK, Rajalingam R, Raghav PK. Hematopoietic Stem Cell Factors: Their Functional Role in Self-Renewal and Clinical Aspects. *Front Cell Dev Biol*. 2022;10:664261.

Marinkovic D, Zhang X, Yalcin S, a kol. Foxo3 is required for the regulation of oxidative stress in erythropoiesis. *J Clin Invest*. 2007;117(8):2133-44.

Marty C, Saint-Martin C, Pecquet C, a kol. Germ-line JAK2 mutations in the kinase domain are responsible for hereditary thrombocytosis and are resistant to JAK2 and HSP90 inhibitors. *Blood*. 2014;123(9):1372-1383.

Maxwell PH, Osmond MK, Pugh CW, a kol. Identification of the renal erythropoietin-producing cells using transgenic mice. *Kidney Int*. 1993; 44:1149-62.

McGrath K, Palis J. Ontogeny of Erythropoiesis in the Mammalian Embryo. *Curr Top Dev Biol*. 2008;82:1-22.

McGrath KE, Frame JM, Fegan KH, a kol. Distinct sources of hematopoietic progenitors emerge before HSCs and provide functional blood cells in the mammalian embryo. *Cell Rep*. 2015;11:1892-1904.

McKie AT. The role of Dcytb in iron metabolism: an update. *Biochem Soc Trans*. 2008;36(Pt 6):1239-41.

McMullin MF, Cario H. LNK mutations and myeloproliferative disorders. *Am. J. Hematol*. 2016;91(2):248-251.

Mead AJ, Chowdhury O, Pecquet C, a kol. Impact of isolated germline JAK2V617I mutation on human hematopoiesis. *Blood*. 2013;121(20):4156-4165.

Mead PE, Deconinck AE, Huber TL, Orkin SH, Zon LI. Primitive erythropoiesis in the Xenopus embryo: the synergistic role of LMO-2, SCL and GATA-binding proteins. *Development*. 2001;128(12):2301-8.

Medvinsky A, Dzierzak E. Definitive hematopoiesis is autonomously initiated by the AGM region. *Cell*. 1996;86:897-906.

Mei Y, Liu Y, Ji P. Understanding terminal erythropoiesis: An update on chromatin condensation, enucleation, and reticulocyte maturation. *Blood Rev*. 2021;46:100740.

Menon V, Ghaffari S. Transcription factors FOXO in the regulation of homeostatic hematopoiesis. *Current Opinion in Hematology*. 2018;25(4):290-298.

Meynard D, Kautz L, Darnaud V, Canonne-Hergaux F, Coppin H, Roth MP. Lack of the bone morphogenetic protein BMP6 induces massive iron overload. *Nat Genet*. 2009;41(4):478-481.

Milosevic Feenstra JD, Nivarthi H, Gisslinger H, a kol. Whole-exome sequencing identifies novel MPL and JAK2 mutations in triple-negative myeloproliferative neoplasms. *Blood*. 2016;127(3):325-32.

Mochizuki-Kashio M, Mishima Y, Miyagi S, a kol. Dependency on the polycomb gene Ezh2 distinguishes fetal from adult hematopoietic stem cells. *Blood*. 2011;118(25):6553-61.

Mole DR. Iron homeostasis and its interaction with prolyl hydroxylases. *Antioxid Redox Signal*. 2010;12(4):445-58.

Nai A, Pellegrino RM, Rausa M, a kol. The erythroid function of transferrin receptor 2 revealed by Tmprss6 inactivation in different models of transferrin receptor 2 knockout mice. *Haematologica*. 2014;99(6): 1016-1021.

Nandakumar SK, Ulirsch JC, Sankaran VG. Advances in understanding erythropoiesis: evolving perspectives. *Br J Haematol*. 2016;173(2):206-218.

Nielsen MJ, Moler HJ, Moestrup SK. Hemoglobin and heme scavenger receptors. *Antioxid Redox Signal*. 2010;12(2):261-73.

Notta F, Zandi S, Takayama N, a kol. Distinct routes of lineage development reshape the human blood hierarchy across ontogeny. *Science*. 2016; 351(6269):aab2116.

Oldenborg PA, Zheleznyak A, Fang YF, Lagenaar CF, Gresham HD, Lindberg FP. Role of CD47 as a marker of self on red blood cells. *Science*. 2000;288(5473):2051-2054.

Orkin SH, Zon LI. Hematopoiesis and stem cells: plasticity versus developmental heterogeneity. *Nat Immunol*. 2002; 3:323-28.

Oskarsson G, Oddsson A, Magnusson MK, a kol. Predicted loss and gain of function mutations in ACO1 are associated with erythropoiesis. *Commun Biol*. 2020;3(1):189.

O'Sullivan J, Mead AJ. Heterogeneity in myeloproliferative neoplasms: Causes and consequences. *Adv Biol Regul*. 2019;71:55-68.

Oskarsson GR, Kristjansson RP, Lee AL, a kol. A truncating mutation in EPOR leads to hypo-responsiveness to erythropoietin with normal haemoglobin. *Commun Biol*. 2018;1:49.

Palis J. Primitive and definitive erythropoiesis in mammals. *Front Physiol*. 2014;5:3.

Palis J, Robertson S, Kennedy M, Wall C, Keller G. Development of erythroid and myeloid progenitors in the yolk sac and embryo proper of the mouse. *Development*. 1999;126:5073-5084.

Palvimo JJ. PIAS proteins as regulators of small ubiquitin-related modifier (SUMO) modification and transcription. *Biochem Soc Trans*. 2007;35:1405-1408.

Pang WW, Price EA, Sahoo D. Human bone marrow hematopoietic stem cells are increased in frequency and myeloid-biased with age. *Proc Natl Acad Sci USA*. 2011; 108(50):20012-20017.

Park CH, Valore EV, Waring AJ, Ganz T. Hepcidin, a urinary antimicrobial peptide synthesized in the liver. *J Biol Chem*. 2001;276(11):7806-7810.

Papanikolaou G, Tzilianos M, Christakis J, a kol. Hepcidin in iron overload disorders. *Blood* 2005;105(10):4103-5.

Pasquier F, Marty C, Balligand T, a kol. New pathogenic mechanisms induced by germline erythropoietin receptor mutations in primary erythrocytosis. *Haematologica*. 2018; 103(4): 575-586.

Paulson RF, Hariharan S, Little JA. Stress erythropoiesis: definitions and models for its study. *Exp Hematol*. 2020;89:43-54.e2.

Pavic M, Francina A, Durand DV, Rousset H. Polycythaemia and iron deficiency. *Lancet*. 2003;362(9396):1624.

Perkins AC, Gaensler KM, Orkin SH. Silencing of human fetal globin expression is impaired in the absence of the adult beta-globin gene activator protein EKLF. *Proc Natl Acad Sci U S A*. 1996; 93:12267-71.

Peroni E, Bertozzi I, Gherlinzoni F, a kol. Two novel missense mutations in EPOR gene causes erythrocytosis in two unrelated patients. *Br J Haematol*. 2018;180(6):908-911.

Petersen KB, Hokland P, Petersen GB, Nyvold CG. Erythropoietin receptor defect: a cause of primary polycythaemia. *Br J Haematol.* 2004;125(4):537-438.

Prchal JT. Primary and Secondary Polycythemias (Erythrocytosis). In: Kaushansky K, Lichtman MA, Beutler E, Kipps TJ, Seligsohn U, Prchal JT, eds. *Williams Hematology*, Eighth Edition. New York, NY: McGraw Hill; 2010:823-38.

Rabidan Moraes G, Pasquier F, Marzac C, et al. An inherited gain-of-function risk allele in EPOR predisposes to familial JAK2V617F myeloproliferative neoplasms. *Br J Haematol.* 2022;198(1):131-136.

Rawlings JS, Rosler KM, Harrison DA. The JAK/STAT signaling pathway. *J Cell Sci.* 2004;117(Pt 8):1281-1283.

Repsold L, Joubert AM. Eryptosis: An Erythrocyte's Suicidal Type of Cell Death. *Biomed Res Int.* 2018;2018:9405617.

Rice L, Alfrey CP. The negative regulation of red cell mass by neocytolysis: physiologic and pathophysiologic manifestations. *Cell Physiol Biochem.* 2005;15(6):245-250.

Risso A, Ciana A, Achilli C, Minetti G. Survival and senescence of human young red cells in vitro. *Cell Physiol Biochem.* 2014; 34: 1038-1049.

Risso A, Turello M, Biffoni F, Antonutto G. Red blood cell senescence and neocytolysis in humans after high altitude acclimatization. *Blood Cells Mol Dis.* 2007;38(2):83-92.

Rodrigues NP, Janzen V, Forkert R, et al. Haploinsufficiency of GATA-2 perturbs adult hematopoietic stem-cell homeostasis. *Blood.* 2005;106(2):477484.

Rumi E, Harutyunyan AS, Casetti I, et al. A novel germline JAK2 mutation in familial myeloproliferative neoplasms. *Am J Hematology.* 2014;89(1):117-118.

Sable CA, Aliyu ZY, Dham N, et al. Pulmonary artery pressure and iron deficiency in patients with upregulation of hypoxia sensing due to homozygous VHL(R200W) mutation (Chuvash polycythemia). *Haematologica.* 2012;97(2):193-200.

Saharinen P, Silvennoinen O. The pseudokinase domains is required for suppression of basal activity of Jak2 and Jak3 tyrosine kinases and for cytokine-inducible activation of signal transduction. *J. Biol.Chem.* 2002; 277(49):47954-63.

Sankaran VG, Xu J, Orkin SH. Advances in the understanding of hemoglobin switching. *Br J Haematol.* 2010;149(2):181-194.

Sasaki A, Yasukawa H, Shouda T, Kitamura T, Dikic I, Yoshimura A. CIS3/SOCS-3 suppresses erythropoietin (EPO) signaling by binding the EPO receptor and JAK2. *J Biol Chem.* 2000;275(38):29338-29347.

Semenza GL, Wang GL. A nuclear factor induced by hypoxia via de novo protein synthesis binds to the human erythropoietin gene enhancer at a site required for transcriptional activation. *Mol Cell Biol.* 1992;12(12):54475454.

Shah YM, Matsubara T, Ito S, et al. Intestinal hypoxia-inducible transcription factors are essential for iron absorption following iron deficiency. *2009;9(2):152-64.*

Shah YM, Xie L. Hypoxia-inducible factors link iron homeostasis and erythropoiesis. *Gastroenterology.* 2014;146(3):630-42.

Shivdasani RA, Orkin SH. Erythropoiesis and globin gene expression in mice lacking the transcription factor NF-E2. *Proc Natl Acad Sci U S A.* 1995;92:8690-94.

Silvestri L, Pagani A, Nai A, De Domenico I, Kaplan J, Camaschella C. The serine protease matriptase-2 (TMPRSS6) inhibits hepcidin activation by cleaving membrane hemojuvelin. *Cell Metab.* 2008;8(6):502511.

- Socolovsky M, Fallon AE, Wang S, Brugnara C, Lodish HF. Fetal anemia and apoptosis of red cell progenitors in Stat5a-/-5b-- mice: a direct role for Stat5 in Bcl-X(L) induction. *Cell*. 1999;98:181-91.
- Sokol L, Luhovy M, Guan Y, Prchal JF, Semenza GL, Prchal JT. Primary familial polycythemia: a frameshift mutation in the erythropoietin receptor gene and increased sensitivity of erythroid progenitors to erythropoietin. *Blood*. 1995;86:15-22.
- Sokol L, Prchal JF, D'Andrea A, Rado TA, Prchal JT. Mutation in the negative regulatory element of the erythropoietin receptor gene in a case of sporadic primary polycythemia. *Exp Hematol*. 1994;22(5):447-53.
- Song J, Yoon D, Christensen RD, Horvathova M, Thiagarajan P, Prchal JT. HIF-mediated increased ROS from reduced mitophagy and decreased catalase causes neocytolysis. *J Mol Med (Berl)*. 2015;93:857-66.
- Stengel A, Baer C, Walter W, a kol. Mutational patterns and their correlation to CHIP-related mutations and age in hematological malignancies. *Blood Adv*. 2021;5(21):4426-4434.
- Stopka T, Zivny JH, Stopkova P, Prchal JF, Prchal JT. Human hematopoietic progenitors express erythropoietin. *Blood*. 1998;91:3766-3772.
- Sulahian R, Cleaver O, Huang LJ. Ligand-induced EpoR internalization is mediated by JAK2 and p85 and is impaired by mutations responsible for primary familial and congenital polycythemia. *Blood*. 2009;113(21):5287-97.
- Tashi T, Swierczek S, Prchal JT. Familial MPN Predisposition. *Curr Hematol Malig Rep*. 2017;12(5):442-447.
- Tefferi A, Pardanani A. Myeloproliferative Neoplasms: A Contemporary Review. *JAMA Oncol*. 2015;1(1):97-105.
- Tober J, Koniski A, McGrath KE, a kol. The megakaryocyte lineage originates from hemangioblast precursors and is an integral component both of primitive and of definitive hematopoiesis. *Blood*. 2007;109:1433-1441.
- Tong W, Zhang J, Lodish HF. Lnk inhibits erythropoiesis and Epo-dependent JAK2 activation and downstream signaling pathways. *Blood*. 2005; 105:4604-12.
- Tóthová Z, Šemeláková M, Solárová Z, Tomc J, Debeljak N, Solár P. The Role of PI3K/AKT and MAPK Signaling Pathways in Erythropoietin Signalization. *Int J Mol Sci*. 2021;22(14):7682.
- Tsang AP, Fujiwara Y, Hom DB, Orkin SH. Failure of megakaryopoiesis and arrested erythropoiesis in mice lacking the GATA-1 transcriptional cofactor FOG. *Genes Dev*. 1998;12(8):1176-1188.
- Turnis ME, Kaminska E, Smith KH, a kol. Requirement for antiapoptotic MCL-1 during early erythropoiesis. *Blood*. 2021;137(14):1945-1958.
- Vassen L, Beauchemin H, Lemsaddek W, Krongold J, Trudel M, Möröy T. Growth factor independence 1b (gf1b) is important for the maturation of erythroid cells and the regulation of embryonic globin expression. *PLoS One*. 2014;9(5):e96636.
- Velten L, Haas SF, Raffel S, a kol. Human haematopoietic stem cell lineage commitment is a continuous process. *Nat Cell Biol* 2017;19: 271-281.
- Verga Falzacappa MV, Vujic SM, Kessler R, Stolte J, Hentze MW, Muckenthaler MU. STAT3 mediates hepatic hepcidin expression and its inflammatory stimulation. *Blood*. 2007;109(1):353-358.
- Vulpe CD, Kuo YM, Murphy TL, a kol. Hephaestin, a ceruloplasmin homologue implicated in intestinal iron transport, is defective in the *sla* mouse. *Nat Genet*. 1999; 21:195-99.
- Wang CY, Xu Y, Traeger L, a kol. Erythroferrone lowers hepcidin by sequestering BMP2/6 heterodimer from binding to the BMP type I receptor ALK3. *Blood*. 2020;135(6):453-456.

Wang RH, Li C, Xu X, a kol. A role of SMAD4 in iron metabolism through the positive regulation of hepcidin expression. *Cell Metab.* 2005;2(6):399-409.

Wang S, Dale GL, Song P, Viollet B, Zou MH. AMPKalpha1 deletion shortens erythrocyte life span in mice: role of oxidative stress. *J Biol Chem.* 2010;285(26):19976-85.

Walrafen P, Verdier F, Kadri Z, Chrétien S, Lacombe C, Mayeux P. Both proteasomes and lysosomes degrade the activated erythropoietin receptor. *Blood.* 2005;105(2):600-8.

Warnecke C, Zaborowska Z, Kurreck J, a kol. Differentiating the functional role of hypoxia-inducible factor (HIF)-1alpha and HIF-2alpha (EPAS-1) by the use of RNA interference: erythropoietin is a HIF-2alpha target gene in Hep3B and Kelly cells. *FASEB J.* 2004; 18:1462-4.

Weidemann A, Johnson RS. Nonrenal regulation of EPO synthesis. *Kidney Int.* 2009;75(7):682-8.

Wu H, Liu X, Jaenisch R, Lodish HF. Generation of committed erythroid BFU-E and CFU-E progenitors does not require erythropoietin or the erythropoietin receptor. *Cell.* 1995;83:59-67.

Yang L, Bryder D, Adolfsson J, a kol. Identification of Lin(-)Sca1(+)kit(+)CD34(+)Flt3- short-term hematopoietic stem cells capable of rapidly reconstituting and rescuing myeloablated transplant recipients. *Blood.* 2005; 105(7):2717-23.

Yokota T. "Hierarchy" and "Holacracy"; A Paradigm of the Hematopoietic System. *Cells.* 2019;8(10):1138.

Yoshimoto M, Montecino-Rodriguez E, Ferkowicz MJ, a kol. Embry- onic day 9 yolk sac and intra-embryonic hemogenic endothelium independently generate a B-1 and marginal zone progenitor lacking B-2 potential. *Proc Natl Acad Sci U S A.* 2011;108:1468-1473.

Yoshimoto M, Porayette P, Glosson NL, a kol. Autonomous murine T- cell progenitor production in the extra-embryonic yolk sac before HSC emergence. *Blood.* 2012;119:5706-5714.

Zang H, Sato K, Nakajima H, McKay C, Ney PA, Ihle JN. The distal region and receptor tyrosines of the Epo receptor are non-essential for in vivo erythropoiesis. *EMBO J.* 2001;20(12):3156-66.

Zhang H, Wang S, Liu D, a kol. EpoR-tdTomato-Cre mice enable identification of EpoR expression in subsets of tissue macrophages and hematopoietic cells. *Blood.* 2021;138(20):1986-1997.

Zhu T, Goh EL, Lobie PE. Growth hormone stimulates the tyrosine phosphorylation and association of p125 focal adhesion kinase (FAK) with JAK2. Fak is not required for stat-mediated transcription. *J Biol Chem.* 1998;273(17):10682-9.

Zmajkovic J, Lundberg P, Nienhold,R, a kol. A gain-of-function mutation in EPO in familial erythrocytosis. *New Eng. J. Med.* 2018; 378: 924-930.

7. ZOZNAM SKRATIEK

aCML	atypical CML
AGM	aorta-gonad-mesonefros
ALL	acute lymphoid leukemia
AML	acute myeloid leukemia
ARNT	aryl hydrocarbon receptor nuclear translocator
ATP	adenosine triphosphate
Bcl-XL	B-cell lymphoma-extra large
BCL11A	B cell lymphoma/leukemia 11A
BFU-E	burst forming unit-erythroid
CALR	calreticulin
CFU-E	colony forming unit-erythroid
CFU-G	granulocyte colony-forming unit
CFU-GM	granulocyte-macrophage colony-forming unit
CFU-M	macrophage colony-forming unit
CHIP	clonal hematopoiesis of indeterminate potential
CI	confidence interval
CLP	common lymphoid progenitor
CMP	common myeloid progenitor
BMP	bone morphogenic protein
BMPR	bone morphogenic protein receptor
DCYTB	duodenal cytochrome B ferrireductase
DNMT3A	DNA methyltransferase 3A
DMT1	divalent metal transporter 1
ED	embryonic day
EEC	endogenous erythroid colonies
Egf	epidermal growth factor
Egfr	epidermal growth factor receptor
EKLF	erythroid Krüppel-like factor
EMP	erytromyeloid progenitors
EPC	erytrophagocytosis
EPO	erythropoietin
EPOR	erythropoietin receptor
ERFE	erythroferrone
ERK1/2	extracellular signal-regulated kinase 1/2
EryP	primitive erythrocyt
ET	esencial thrombocytosis
EZH2	enhancer of zeste 2
FAK	focal adhesion kinase
FERM	band 4.1, ezrin, radixin, moesin domain
FL	fetal liver
FOG-1	friend of GATA protein 1
FOXO3	forkhead box O-3
FPN	ferroportin
GATA	GATA-binding factor
G-CSF	granulocyte colony-stimulating factor
GFI1B	growth factor independence 1b
GLUT-1	glucose trasporter-1
GM-CSF	granulocyte macrophage colony-stimulating factor
GMP	granulocyte-monocyte progenitor
Hb	hemoglobin
HbF	fetal hemoglobin

HbA	adult hemoglobin
Hct	hematocrit
HDAC	histone deacetylase
HFE	hemochromatosis protein
HIF	hypoxia inducible factor
HJV	hemojuvelin
HRE	hypoxia responsive element
HSC	hematopoietic stem cell
HS40	hypersensitivity site 40
ID1	inhibitor of DNA binding 1
IDH	isocitrate dehydrogenase
IE	idiopathic erythrocytosis
IFN- γ	interferon γ
IGF-1	insulin-like growth factor 1
IgG	immunoglobulin G
IL	interleukin
IRP	iron regulatory protein
JAK	Janus kinase
JH	JAK homology
JNK	c-Jun N-terminal kinase
LCR	locus control region
LIC	liver iron content
LIP	labile iron pool
LMO2/LDB1	LIM domain only 2/LIM Domain Binding 1
LNK	lymphocyte adaptor protein
LSK	Lin-Sca-1+c-Kit+
LT-HSC	long term hematopoietic stem cell
MAPK	mitogen activated protein kinase
Mcl-1	myeloid cell leukemia 1
MCH	mean corpuscular hemoglobin
MCHC	mean corpuscular hemoglobin concentration
M-CSF	macrophage colony-stimulating factor
MCV	mean corpuscular volume
MDS	myelodysplastic syndrome
MPL	myeloproliferative leukemia virus oncogene
MPN	myeloproliferative neoplasm
MPP	multipotent progenitor
NCOA4	nuclear receptor coactivator 4
NF-E2	nuclear factor erythroid-2
NF- κ B	nuclear factor kappa-light-chain-enhancer of activated B cell
NGS	next generation sequencing
NTBI	non-transferrin-bound-iron
OR	odds ratio
PD	postnatal day
PFCP	primary familial and congenital polycythemia
Ph	Philadelphia chromosome
PHD	prolyl hydroxylase domain
PIAS	proteins inhibiting activated STATs
PI3K	phosphatidylinositol 3-kinase
PMF	primary myelofibrosis
PS	phosphatidylserine
PTP	protein tyrosine phosphatase
PU.1	hematopoietic transcription factor putative oncogene Spi-1

PV	polycythemia vera
RES	reticuloendothelial system
RNF17	ring finger protein 17
ROS	reactive oxygen species
sAML	secondary AML
SCF	stem cell factor
SCL/TAL1	stem cell leukemia/T-cell acute leukemia
SH	Src homology domain
SHP-1	SH2 domain-containing protein phosphatase-1
SH2B3	SH2B adaptor protein 3
SIC	spleen iron content
SMAD	small and mothers against decapentaplegic protein
SOCS	suppressors of cytokine signaling
SPI2A	serine protease inhibitor 2A
STAT	signal transducer and activator of transcription
Tf	transferin
TfR	transferrin receptor
TFRC	transferrin receptor
TGF- β	transforming growth factor- β
TNF- α	tumor necrosis factor- α
TPO	thrombopoietin
TRIB3	tribbles pseudokinase 3
TSAT	transferin saturation
TYK	tyrosine kinase
VEGF	vascular endothelial growth factor
VHL	von Hippel Lindau
WHO	world health organisation

8. PRÍLOHY

Príloha 1

Divoky V, Song J, Horvathova M, **Kralova B**, Votavova H, Prchal JT, Yoon D.

Delayed hemoglobin switching and perinatal neocytolysis in mice with gain-of-function erythropoietin receptor.

Journal of Molecular Medicine. 2016; 94(5):597-608.

ORIGINAL ARTICLE

Delayed hemoglobin switching and perinatal neocytolysis in mice with gain-of-function erythropoietin receptor

Vladimir Divoky¹ · Jihyun Song² · Monika Horvathova¹ · Barbora Kralova¹ · Hana Votavova³ · Josef T. Prchal² · Donghoon Yoon^{2,4}

Received: 17 April 2015 / Revised: 18 November 2015 / Accepted: 24 November 2015
© Springer-Verlag Berlin Heidelberg 2015

Abstract

Mutations of the truncated cytoplasmic domain of human erythropoietin receptor (EPOR) result in gain-of-function of erythropoietin (EPO) signaling and a dominantly inherited polycythemia, primary familial and congenital polycythemia (PFCP). We interrogated the unexplained transient absence of perinatal polycythemia observed in PFCP patients using an animal model of PFCP to examine its erythropoiesis during embryonic, perinatal, and early postnatal periods. In this model, we replaced the murine *EpoR* gene (*mEpoR*) with the wild-type human *EPOR* (wtHEPOR) or mutant human *EPOR* gene (mtHEPOR) and previously reported that the gain-of-function mtHEPOR mice become polycythemic at 3–6 weeks of age, but not at birth, similar to the phenotype of PFCP patients. In contrast, wtHEPOR mice had sustained anemia. We report that the mtHEPOR fetuses are polycythemic, but their polycythemia is abrogated in the perinatal period and reappears

again at 3 weeks after birth. mtHEPOR fetuses have a delayed switch from primitive to definitive erythropoiesis, augmented erythropoietin signaling, and prolonged Stat5 phosphorylation while the wtHEPOR fetuses are anemic. Our study demonstrates the in vivo effect of excessive EPO/EPOR signaling on developmental erythropoiesis switch and describes that fetal polycythemia in this PFCP model is followed by transient correction of polycythemia in perinatal life associated with low Epo levels and increased exposure of erythrocytes' phosphatidylserine. We suggest that neocytolysis contributes to the observed perinatal correction of polycythemia in mtHEPOR newborns as embryos leaving the hypoxic uterus are exposed to normoxia at birth.

Key message

- Human gain-of-function EPOR (mtHEPOR) causes fetal polycythemia in knock-in mice.
- Wild-type human EPOR causes fetal anemia in knock-in mouse model.
- mtHEPOR mice have delayed switch from primitive to definitive erythropoiesis.
- Polycythemia of mtHEPOR mice is transiently corrected in perinatal life.
- mtHEPOR newborns have low Epo and increased exposure of erythrocytes' phosphatidylserine.

Electronic supplementary material The online version of this article (doi:10.1007/s00109-015-1375-y) contains supplementary material, which is available to authorized users.

✉ Josef T. Prchal
josef.prchal@hsc.utah.edu

¹ Department of Biology, Faculty of Medicine and Dentistry, Palacky University, 775 15 Olomouc, Czech Republic

² Hematology Division, Department of Medicine, University of Utah and VAH, Salt Lake City, UT 84132, USA

³ Institute of Hematology and Blood Transfusion, 12820 Prague, Czech Republic

⁴ Myeloma Institute University of Arkansas for Medical Science, Little Rock, AR, USA

Keywords Human EPOR mutation · Fetal polycythemia · Prolonged primitive erythropoiesis · Augmented Stat5 signaling · Neocytolysis

Introduction

Erythropoietin (EPO)/EPO receptor (EPOR) signaling plays a central role in survival, proliferation, and differentiation of

committed erythroid progenitors in definitive erythropoiesis. *Epo*- and *EpoR*-null mutant mice die at ~E13.5 due to severe anemia [1]. These loss-of-function mutations of *Epo* and *EpoR* genes permit production of primitive erythroblasts during E10~E11, albeit at low levels, but definitive fetal liver (FL) erythropoiesis is blocked at the more differentiated erythropoiesis stage (CFU-E) [1]. The gain-of-function of *EPOR* mutations resulting from truncation mutations of the cytoplasmic domain of *EPOR* are associated with primary familial and congenital polycythemia (PFCP) characterized by augmented EPO/EPOR signaling and hypersensitivity of erythroid progenitors to EPO [2].

The yolk sac is the first site of erythropoiesis during mouse and human ontogeny, followed by FL erythropoiesis in developing fetuses. In the mouse, the first blood cells arise in the yolk sac around embryonic days (E)7~8. These are unipotential progenitors giving rise to nucleated primitive erythroblasts, which synthesize embryonic hemoglobins. After E8, these primitive erythroblasts enter the circulation [3]. The definitive hematopoietic progenitor cells emerging before E10 in the mouse embryo are also the products of the yolk sac [3, 4]. Definitive hematopoiesis is then established in the FL and produces enucleated erythrocytes from E11.5, when these cells first enter the bloodstream. Definitive erythroid cells predominate in the circulation from E14 [4]. There is a temporal overlap of the appearance of primitive and definitive erythrocytes in the circulation, as primitive erythroid cells undergo progressive enucleation between E12.5 and E16.5 and form mature primitive erythrocytes in the circulation [5]. Around birth, the mouse spleen and bone marrow become the principal sites of adult erythropoiesis, producing definitive erythroid cells; however, primitive erythrocytes circulate as late as 5 days after birth [5].

The switch from embryonic to adult erythropoiesis coincides with the differential use of globin genes; in the mouse, the β -globin cluster is composed of four functional β -globin genes ($\epsilon\gamma$ -, β H1-, β 1-, and β 2-globins). The $\epsilon\gamma$ - and β H1-globins are expressed in the primitive erythroid lineage, and the β 1- and β 2-globins are expressed in definitive erythroid cells. A transient wave of early definitive erythroid lineage in murine FL that originates from yolk sac-derived erythromyeloid progenitors expresses adult β -globins along with embryonic β H1-globin [4]. In contrast, in the human β -globin cluster, ϵ gene expression is followed by expression of γ -globin genes in fetal life ($A\gamma$ and $G\gamma$), while adult δ - and β -globins are expressed after birth. The α -globin cluster is characterized by the expression of the ζ -globin gene in primitive erythropoiesis in both humans and mice, while fetal and adult erythropoiesis is characterized by the expression of α 1- and α 2-globin genes [5].

We have previously shown that an animal model of PFCP—the mice having gain-of-function *EPOR* mutation (mtHEPOR)—become polycythemic at 3~6 weeks of age,

but not at birth similar to the polycythemic phenotype of affected humans, and that the mice with wild-type human EPOR (wtHEPOR) are anemic [6]. Here, we report that PFCP mouse embryos have fetal polycythemia associated with a delayed switch from embryonic to adult erythropoiesis. This fetal polycythemia is transiently overcorrected in the perinatal period and reappears again at 3 weeks of postnatal life. The observed perinatal fall of hematocrit in the mtHEPOR mice could be parallel to transient anemia in normal human newborns associated with neocytolysis; i.e., a selective destruction (hemolysis) of young (hypoxia-made) erythrocytes [7].

Material and methods

Mice

The mice (wtHEPOR—homozygous wild-type human *EPOR* knock-in, mtHEPOR—homozygous gain-of-function human *EPOR* knock-in (substitution c.1278C>G; designation of the mutation according to the LOVD database, www.lovd.nl), and the murine *EpoR* (m*EpoR*)—wild-type mouse control) were bred and maintained in an IACUC-approved CCM facility at the University of Utah and in the Center for Laboratory Animals, Palacky University (PU), in accordance with the regulations of PU Institutional Animal Care and Use Committee, Olomouc, Czech Republic.

The wtHEPOR or mtHEPOR knock-in mice were generated by gene targeting [6] and then backcrossed onto the C57BL/6 strain at least 6 times. Thereafter, the heterozygous knock-in offspring were intercrossed to produce all experimental mice, i.e., the model homozygous wtHEPOR and homozygous mtHEPOR as well as the control m*EpoR* mice.

Hematocrit assessment and isolation of fetal liver cells from fetuses

Mice aged 10 weeks or older were used for timed mating. When the vaginal plug was detected, noon of that day was considered E0.5. Fetuses were removed from the uterus at the indicated time points. Fetal blood was immediately drawn from carotid arteries by a *Drummond* 2 lambda microcap (Fisher Scientific; Pittsburgh, PA) for hematocrit measurement and by hand-drawn pipette for other analyses. Hematocrits were recorded with a hematocrit reader (International Equipment Company; Needham Heights, MA). FLs were dissected and dispersed by repeated pipetting in cold phosphate-buffered saline (PBS). Red blood cells (RBCs) were lysed by RBC lysis buffer (0.15 M NH₄Cl, 1 mM KHCO₃, 0.1 mM EDTA).

Immunostaining and flow cytometry analysis of erythroid progenitors and erythroblasts

Fetal liver cells (FLCs) or peripheral blood (PB) were stained with phycoerythrin (PE)-conjugated anti-CD71 and fluorescein isothiocyanate (FITC)-conjugated anti-TER119 (BD Biosciences; San Diego, CA) antibodies as described [8], followed by 1 % formaldehyde fixation. The cells were analyzed by flow cytometry on a Coulter Epics Profile instrument (Beckman/Coulter; Miami, FL); five different regions were analyzed based on the expression levels of CD71/TER119 [8]. Each region represented differentiation cell stage as previously described [8].

Real-time PCR analysis of globin genes

For details of quantifications including specific primer sequences, see [Supplementary Material](#).

Assessment of enucleation

PB cells were washed twice with cold PBS, then stained with 10 µM DRAQ5 (Biostatus, Leicestershire, UK) for 15 min at ambient temperature, followed by FACS analysis.

Stat5 phosphorylation analysis

Antibodies specific to phospho-Stat5 and total Stat5 were purchased from Cell Signaling Technology (Beverly, MA) and Santa Cruz Biotechnology, respectively. After 2 h of starvation in RPMI with 10 % fetal calf serum (FCS), FLCs were treated with recombinant human (rh) EPO (Amgen Co., Thousand Oaks, CA), and cell lysates were prepared as described [9]. Proteins were separated on 7.5 % SDS-PAGE and transferred to PVDF membranes (Bio-Rad; Hercules, CA).

Hypoxia treatment

Mice of all genotypes (8 to 12 weeks old) were placed in a hypobaric chamber (BioSpherix, Lacona, NY) for 10 days at 12 % O₂. Mice were then returned to ambient condition for 29 days, and hematocrits (using 10 µl of blood) were measured at selected time points. The consecutive blood samplings did not materially influence hematocrits (data not shown).

Quantification of Epo

The serum levels of Epo in neonatal (7 days old) and adult (8 to 12 weeks old) mice were quantified according to the manufacturer's instructions for the Mouse Erythropoietin Quantikine ELISA Kit (R&D Systems). The expression of *Epo* messenger RNA (mRNA) was determined in the liver and kidney by quantitative real-time (qRT)-PCR (see

[Supplementary Material](#) for details). The statistical significance of relative expression changes in target mRNA levels was analyzed using the REST© 2009 software [10].

Erythrocyte Annexin V binding

PB erythrocytes were labeled using Annexin V/FITC kit (BD Biosciences) as described [11]. Fluorescence intensity was measured by FACS Calibur (BD Biosciences).

Statistical analysis

Student's test and ANOVA test were used for the statistical analyses. Significant differences were assumed when *P*<0.05. The software GraphPad Prism 4 (GraphPad Software Inc., San Diego, CA) or Origin 6.1 (OriginLab Corporation, Northampton, MA) was used for the statistical calculations.

Results

Truncated human EPOR causes polycythemia, while wild-type human EPOR causes anemia at mid- to late-gestation mouse embryonic stages

Our previous studies demonstrated that polycythemia in the mtHEPOR mice was not apparent until 3 to 6 weeks after birth [6]; thus, the effect of the gain-of-function of *EPOR* mutation in mtHEPOR fetuses was not clear. We examined wtHEPOR, mtHEPOR, and mEpoR fetuses at various time points of mouse development: E12.5, E14.5, E16.5, and E18.5, and mice at the following postnatal (PN) time points: 0 day, 1 week, 2 weeks, 3 weeks, and 5 weeks. Unexpectedly, as shown in Fig. 1 and similarly to what we reported in adult mice [6, 12], mtHEPOR fetuses were polycythemic and wtHEPOR were anemic from E12.5 to E16.5 as compared to mEpoR fetuses. However, all genotypes had significantly reduced hematocrits at perinatal time, mEpoR from E18.5 to PN 2 weeks and mtHEPOR and wtHEPOR from PN 0 day to PN 2 weeks. In wtHEPOR and mtHEPOR, the peaks of hematocrit levels were reached at E18.5 in contrast to E16.5 of mEpoR. From 3 weeks of PN, hematocrits from mtHEPOR (polycythemic) and wtHEPOR (anemic) were comparable to those at the mid gestation. At these examined developmental stages, there were no apparent size differences of the fetuses and volumes of FLs among the studied genotypes (not shown).

wtHEPOR and mtHEPOR have a greater proportion of immature circulating erythroid progenitors than mEpoR

We hypothesized that polycythemia of mtHEPOR and anemia of wtHEPOR in embryos could be influenced by an aberrant

erythroid differentiation. Therefore, PB erythroid progenitors were analyzed at various time points of mouse development using two differentially regulated erythroid specific surface markers, CD71 and TER119 by FACS [8]. The relative proportion of the erythroid R2 region (proerythroblasts and early basophilic erythroblasts) in mtHEPOR rapidly decreased (51 % at E12.5 versus 14 % at E16.5), while wtHEPOR had only a small reduction of this population until E16.5 (28 % at E12.5 versus 21 % at E16.5) (Fig. 2). At E18.5, immature erythroid cells (R2 region) from PB of all genotypes were no longer detectable. At birth, all genotypes had circulated erythroid cells of a comparable differentiation stage.

All genotypes had immature circulating erythroid progenitors and underwent their ongoing differentiation from E12.5 to PN 3 weeks (Fig. 2). However, PB from wtHEPOR and mtHEPOR at late gestation and the perinatal period contained significantly higher proportions of immature erythroid progenitors compared to mEpoR until PN 3 weeks, suggesting delayed ongoing differentiation. Erythroid FLCs had no significant differences of their maturation pattern at any time point (not shown).

PB of mid- to late-gestation mtHEPOR embryos contain more primitive erythroid cells in circulation

Lux et al. showed that primitive and definitive hematopoietic progenitor cells co-exist and emerge in the mouse embryo before E10 [3]. Progressive maturation of immature primitive erythroid cells occurs in the circulation, as evaluated by changes of globin isotypes [5]. We postulated that the higher proportion of circulating immature erythroid cells from mtHEPOR embryos during mid- to late-gestation embryogenesis may be due to the presence of a greater proportion of

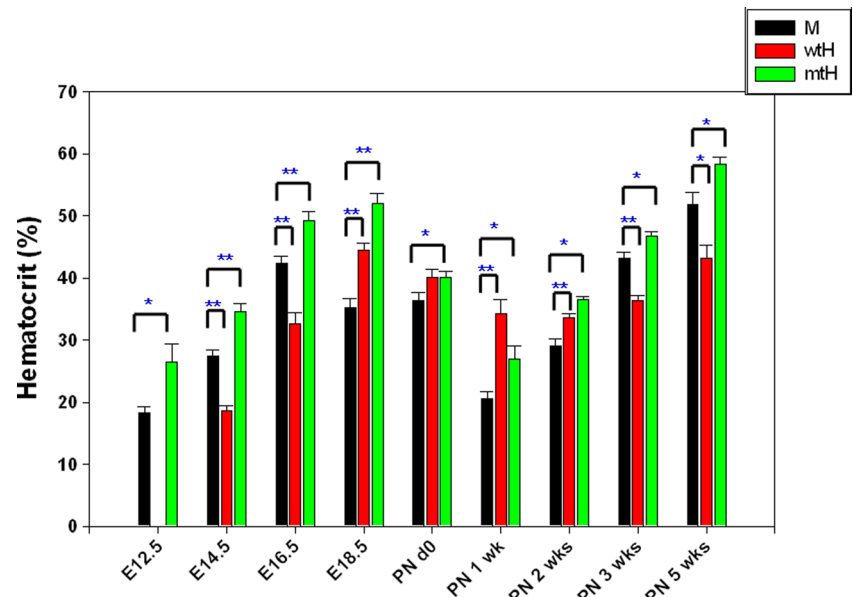
Fig. 1 The mtHEPOR fetuses are polycythemic and wtHEPOR fetuses are anemic compared to mEpoR fetuses at mid to late gestation (E12.5–E16.5). These phenotypes transiently disappear around perinatal period and then reappear at 3 weeks (wks) after birth. M, wtH, and mtH denote mEpoR, wtHEPOR, and mtHEPOR genotypes, respectively. * and ** denote $P < 0.05$ and $P < 0.001$ for mEpoR versus wtHEPOR, and mtHEPOR, respectively; PN denotes postnatal. The mean and standard error of hematocrit levels from at least 10 embryos/neonatal pups for each time point are shown

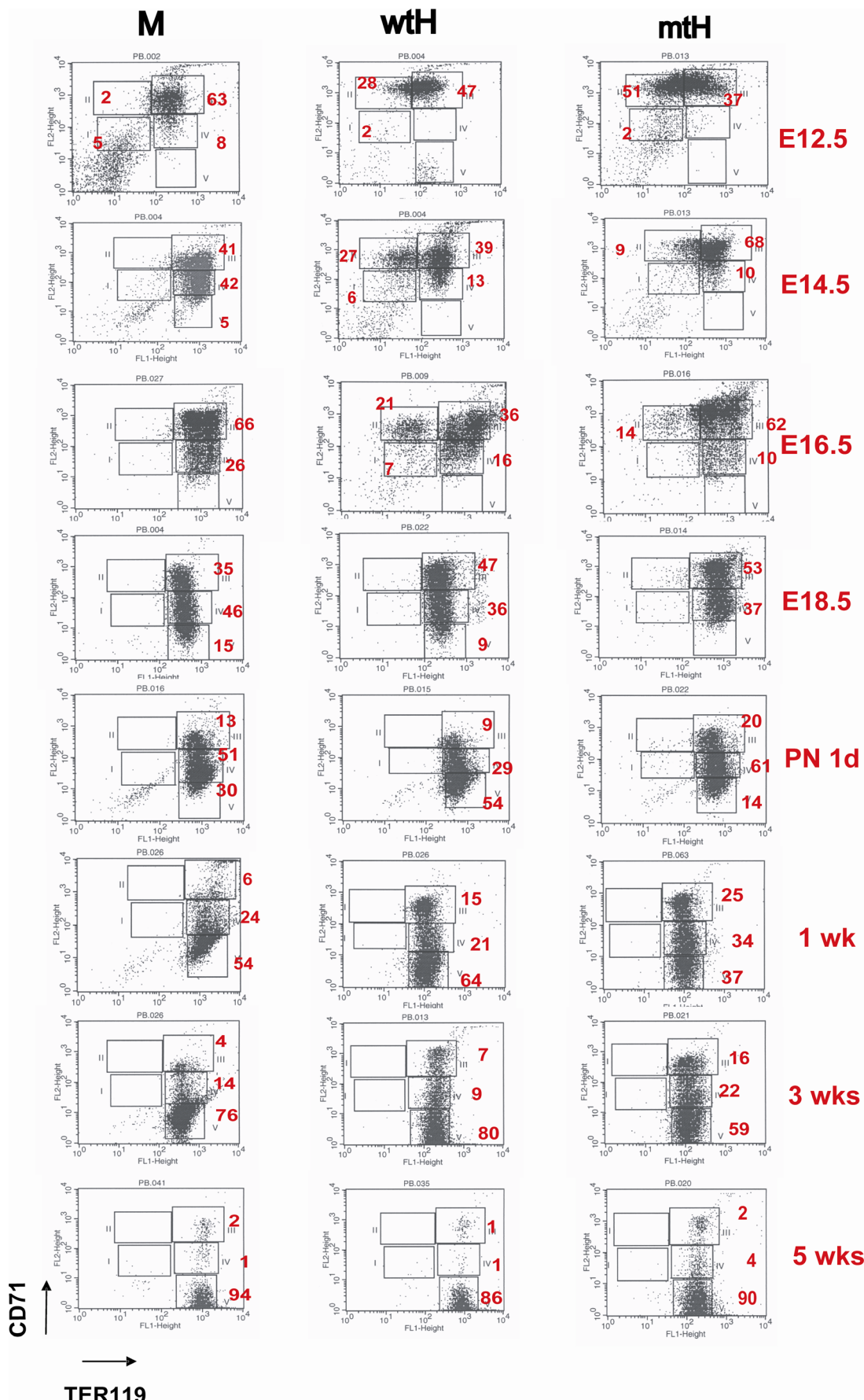
Fig. 2 Peripheral blood (PB) from all genotypes contains early erythroid cells while wtHEPOR and mtHEPOR mice have delayed maturation. PB was obtained from all homozygous fetuses/neonatal pups at the indicated time points, stained with CD71/TER119 antibodies and analyzed by FACS. Each differentiation stage (R1–R5) was gated as previously described [8]; R1 (CD71mid/TER119negative)-primitive progenitor cells and proerythroblasts, R2 (CD71high/TER119negative)-proerythroblasts and early basophilic erythroblasts, R3 (CD71high/TER119positive)-early and late basophilic erythroblasts, R4 (CD71mid/TER119positive)-chromatophilic and orthochromatophilic erythroblasts, and R5 (CD71low/TER119positive)-late orthochromatophilic erythroblasts and reticulocytes. Numbers are the averages of each differentiation stage in mice derived from multiple litters. M, wtH, and mtH denote mEpoR, wtHEPOR, and mtHEPOR genotypes, respectively. * indicates $P < 0.05$

primitive erythroid cells. As shown in Fig. 3a, fetal PB from mtHEPOR embryos had higher levels of embryonic globin transcripts ($\epsilon\gamma/\beta H1$ and ζ) than mEpoR, while fetal PB from wtHEPOR embryos had comparable levels of embryonic globin transcripts to mEpoR controls. We also evaluated the enucleation status of fetal PB using a DNA dye, DRAQ5. In agreement with globin analysis, mtHEPOR fetuses from E13.5 and E14.5 had higher proportion of nucleated erythroblasts than other genotypes (Fig. 3b). These data indicate that the mtHEPOR mice have prolonged primitive erythropoiesis, i.e., delayed switch from primitive to definitive erythropoiesis.

Stat5 phosphorylation is increased and sustained upon EPO stimulation in mtHEPOR FLCs

To evaluate the EPO signal transduction, we tested the EPO dose-response and kinetics of Stat5 phosphorylation in FLCs. FLCs were obtained from all genotypes at E14.5 and E18.5, starved for 2 h in RMPI+10 % FCS, and stimulated with





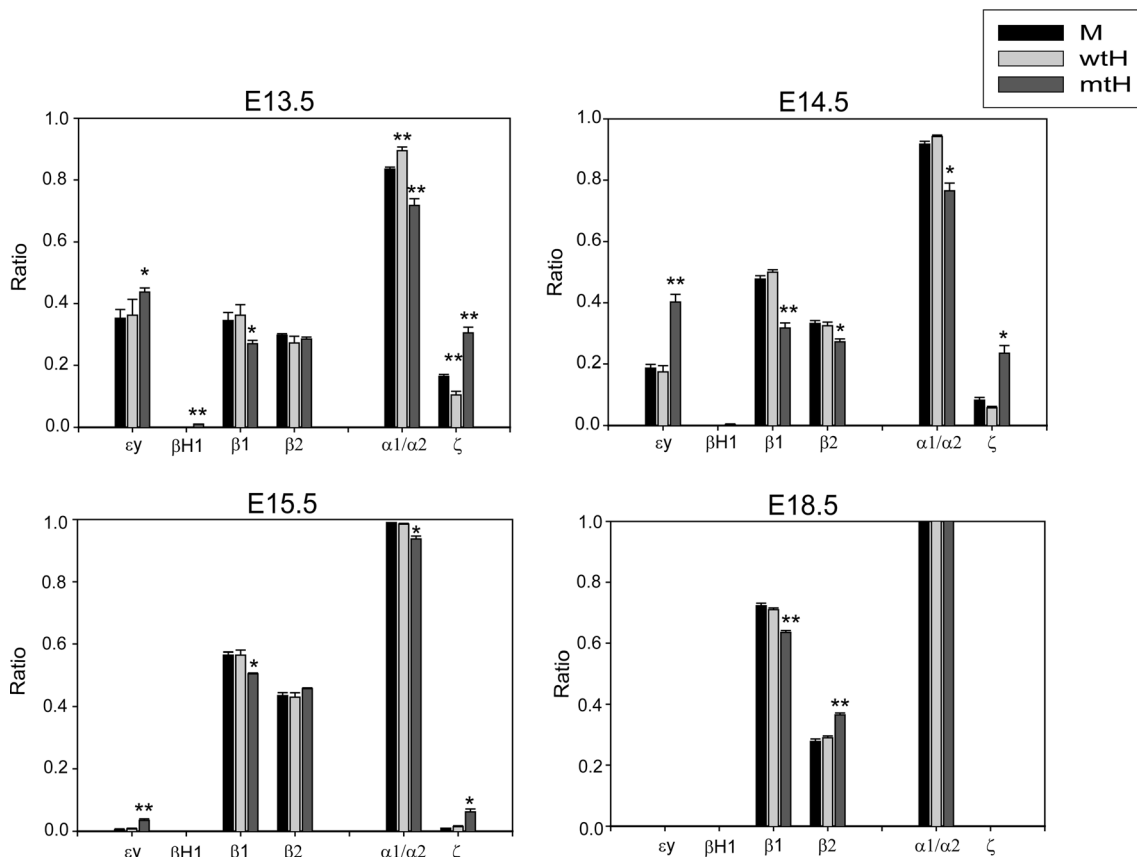


Fig. 3 mtHEPOR fetuses have more embryonic globin transcripts than the other two genotypes. **a** Peripheral blood (PB) was obtained from carotid arteries of fetuses at indicated time points, and total RNA was extracted using manufacturer's protocol. Embryonic and adult globin transcripts were analyzed by real-time PCR using SYBR green dye with primer sets as described in the Supplementary Material. M, wtH, and mtH

denote *mEpoR*, *wtHEPOR*, and *mtHEPOR* genotypes, respectively. **b** PB was obtained and stained by DRAQ5 dye. Nucleated and enucleated cells in PB were analyzed by FACS. Average numbers were calculated from multiple embryos (at least 10 for each genotype). M, wtH, and mtH denote *mEpoR*, *wtHEPOR*, and *mtHEPOR* genotypes, respectively

recombinant human EPO (rhEPO) at ambient temperature. The results were identical for E14.5 and E18.5. As shown in Fig. 4a, mtHEPOR FLCs at 0.01 U/ml of EPO had detectable phosphorylation of Stat5, whereas *mEpoR* FLCs had detectable phosphorylation of Stat5 only at 1 and 10 U/ml of EPO. The *wtHEPOR* FLCs had only a barely detectable level of Stat5 phosphorylation at 10 U/ml of rhEPO (Fig. 4a). As shown in Fig. 4b and Supplementary Fig. 1, phosphorylation of Stat5 in *mEpoR* was seen after 15 min of stimulation and almost disappeared after 60 min, whereas in mtHEPOR FLCs, Stat5 was comparably phosphorylated after 15 min of stimulation but only minor decline in Stat5 phosphorylation was detected during the 120-min observation time period.

mtHEPOR mice have greater decrease of hematocrit upon normoxic return from hypoxia

We interrogated the observed fall of hematocrit in the mtHEPOR neonates. Since mouse pups underwent significant

change of oxygen tension at delivery (from the uterus to ambient atmosphere), we tested whether it may account for the decrease in perinatal hematocrit levels (Fig. 1). Mice exposed to hypoxia at hypobaric chamber for 10 days had their hematocrit level followed for 29 days after returning to normoxia. As shown in Fig. 5a, hypoxia increased the hematocrit levels by a similar degree in individual genotypes, i.e., *mEpoR*=60.0 (1.2 times); *wtHEPOR*=53.9 (1.13 times); *mtHEPOR*=65.0 (1.12 times). However, upon normoxic return, the reduction of hematocrits differ among individual genotypes. The hematocrits reached the lowest levels between days 10 and 14 and decreased to *mEpoR*=45.2 (drop of 14.8 %), *wtHEPOR*=40.1 (drop of 13.8 %), and *mtHEPOR*=48.1 (drop of 16.9 %). The most pronounced relative hematocrit drop was observed for mtHEPOR mice and showed statistical significance compared to *wtHEPOR* ($P=0.0071$) and *mEpoR* ($P=0.0291$) mice, respectively. Thus, the mtHEPOR mice undergo greater changes of hematocrit than other genotypes in response to changes in oxygen tension.

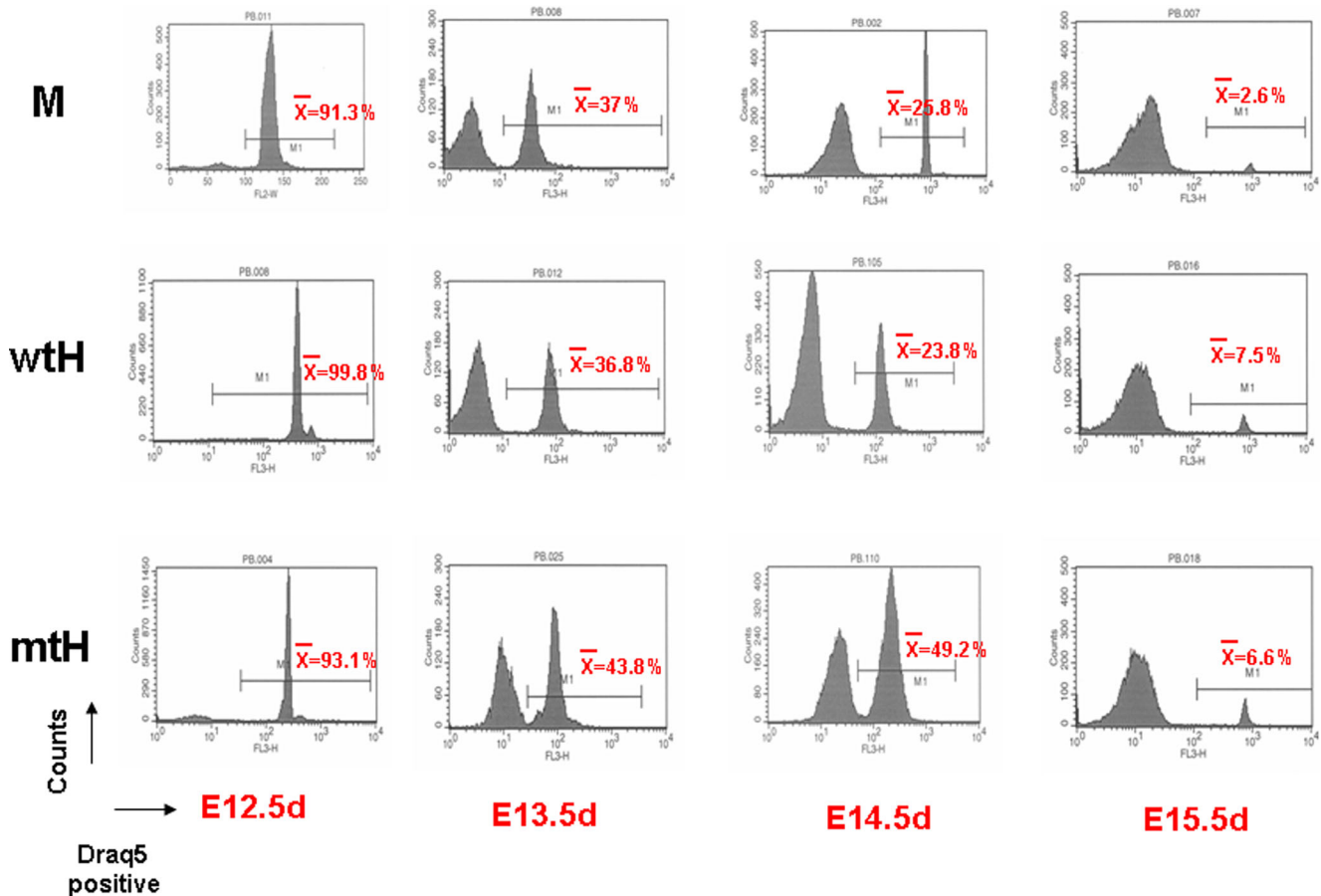


Fig. 3 (continued)

Neonatal and adult mice of individual mouse genotypes differ in Epo production

We reasoned that possible differences in Epo concentrations might reflect mtHEPOR and wtHEPOR perinatal phenotypes. As Epo levels of mtHEPOR and wtHEPOR mice have not been previously reported, we measured their Epo concentrations. wtHEPOR newborns had higher Epo levels in relation to those of mtHEPOR and their wild-type mEpoR counterparts (Fig. 5b). Serum Epo levels correlated with changes of *Epo* mRNA expression in the liver and kidney as determined by qRT-PCR (Fig. 5c). We also assessed the serum Epo levels and *Epo* mRNA expression in adult animals in normoxia and during exposure to hypoxia. We observed that serum Epo levels are highest in wtHEPOR mice and lowest in mtHEPOR mice in both normoxic and hypoxic conditions (Supplementary Fig. 2A). The differences in serum Epo levels between the individual genotypes were paralleled by differences in *Epo* mRNA expression in the kidney; the highest was detected for wtHEPOR mice and the lowest for mtHEPOR mice, again in both normoxic and hypoxic conditions (Supplementary Fig. 2B), suggesting that the regulation of Epo levels is appropriate and commensurate to differences of hematocrit.

mtHEPOR erythrocytes have increased surface exposure of phosphatidylserine in perinatal period

We next measured the exposure of phosphatidylserine on the erythrocytes' membranes at E18.5, PN 0 day, PN 7 days and in adult mice using Annexin V staining and flow cytometry. The exposure of phosphatidylserines (determined by mean fluorescence values) at E18.5 was comparable among the different genotypes (mean fluorescence around 0.8) (Fig. 6). In contrast, there was a gradual increase in phosphatidylserine exposure on the mtHEPOR erythrocytes after birth and, to a lower extent, also on mEpoR erythrocytes between PN 0 and PN 7. The maximum increase of surface exposure of phosphatidylserines on erythrocytes was PN 7 (mean fluorescence of 6.5 ± 2.8 and 6.2 ± 1.7 , respectively). This corresponded to a maximal drop of hematocrit and lowest Epo levels at PN 7 in polycythemic mtHEPOR, in contrast to a milder reduction of hematocrit and slightly higher Epo levels in non-polycythemic mEpoR mice. While there was a trend to a higher level of surface exposure of phosphatidylserines on the mtHEPOR erythrocytes compared to mEpoR erythrocytes, it did not achieve statistical significance. The anemic wtHEPOR's erythrocytes had the lowest

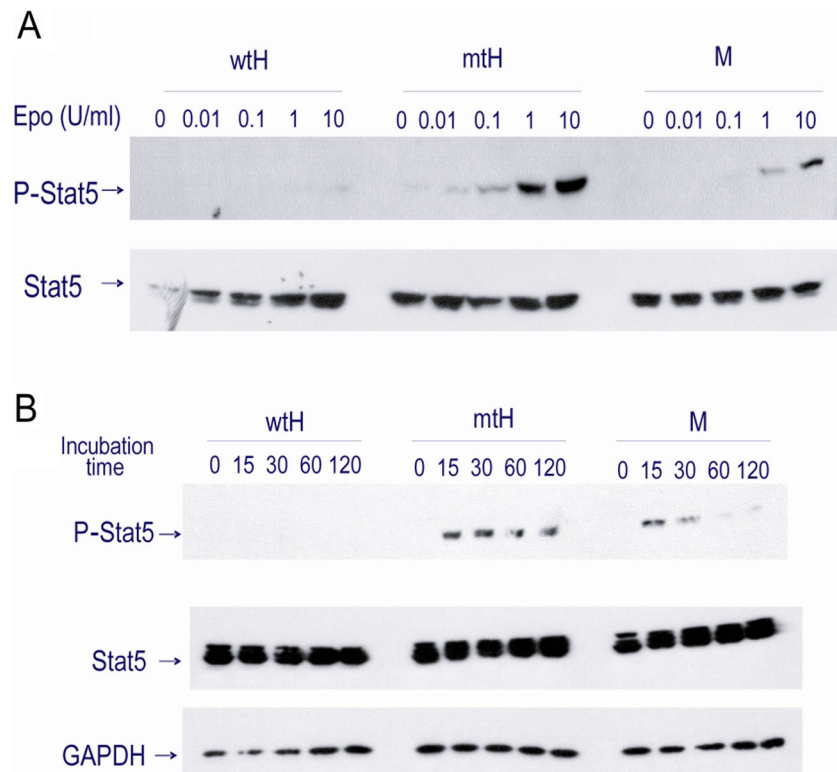


Fig. 4 EPO-induced Stat5 phosphorylation in mtHEPOR fetal liver erythroid progenitors is augmented and sustained. FLCs were obtained from mEpoR (M), wtHEPOR (wtH), and mtHEPOR (mtH) E14.5 fetuses and starved for 2 h in RPMI+10 % FCS prior to stimulation with recombinant human (rh) EPO. The cell lysates (equivalent to 10^6 cells) were immunoblotted with a phospho-Stat5 (P-Stat5) antibody, followed by re-probing with antibodies specific for total Stat5 and GAPDH. **a** EPO

dose-response test of Stat5 activation. FLCs were stimulated with indicated concentrations of EPO for 15 min. **b** Stat5 phosphorylation kinetic study. Analysis of P-Stat5 in FLCs stimulated with 1 U/ml of EPO for indicated periods of time. The relative quantification of P-Stat5 for mtHEPOR and mEpoR FLCs is presented graphically in Supplementary Fig. 1

exposure of phosphatidylserines at all analyzed time points, and the increase between PN 0 and PN 7 was only subtle (from 0.7 ± 0.1 to 1.3 ± 0.3) consistent with the lowest reduction in perinatal hematocrit and highest Epo levels (Fig. 6). The exposure of phosphatidylserines on erythrocytes' membranes then declined, and comparable levels were detected in adult mice of all three genotypes (mean fluorescence around 0.6). Thus, the increased exposure of phosphatidylserines in the perinatal period likely contributes to enhanced recognition and destruction of mtHEPOR erythrocytes by reticuloendothelial macrophages paralleling the dramatic drop of hematocrit in the neonatal period [13].

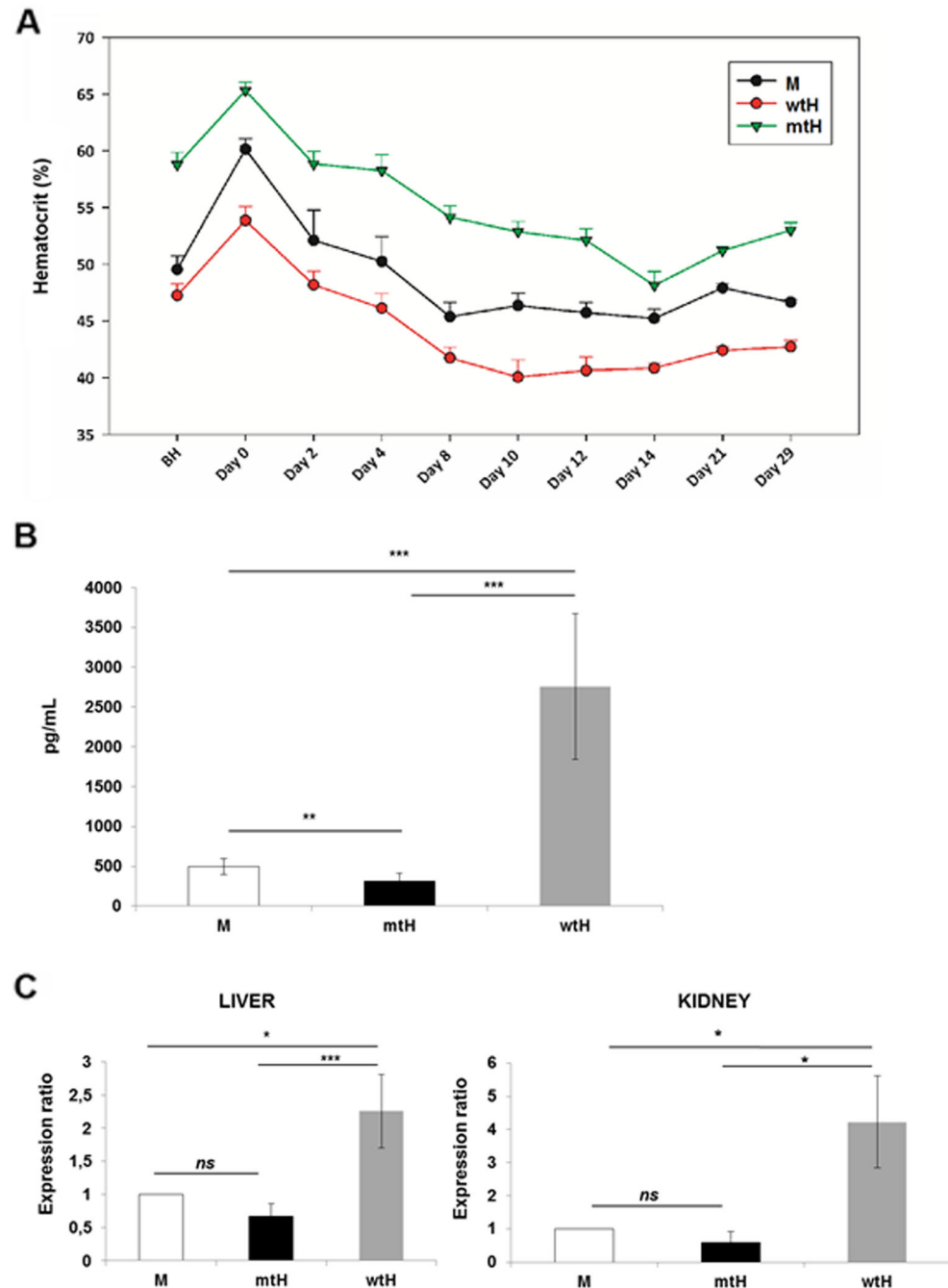
Discussion

We previously reported the PFCP phenotype of gain-of-function EPOR gene (mtHEPOR) resulting from the EPOR truncation and the loss of negative regulatory domain [2] and showed that mtHEPOR mouse mimics human disease [6]. At 3–6 weeks after birth, both heterozygous wtHEPOR/mtHEPOR and homozygous gain-of-function

mtHEPOR animals develop polycythemia while homozygous wtHEPOR become anemic [6, 12]. The lack of perinatal polycythemic phenotype in this mouse model eluded an obvious explanation and suggested that polycythemia may be only confined to adult hematopoiesis. However, we now show that at the mid- and late-gestation stages of erythropoiesis (E12.4–E16.5), mtHEPOR fetuses are polycythemic while the wtHEPOR fetuses are anemic, similar to what we observed in adult mice (Fig. 1). These phenotypes temporarily disappear during the perinatal period (E16.5–PN 2 weeks) and then reappear at the adult stage (>PN 3 weeks).

To better understand how these phenotypes occur during mid- to late-gestation (E12.5–E16.5) and in the perinatal and neonatal periods, we analyzed distribution of maturation stages of erythroid precursors, proportion of nucleated/enucleated erythroid cells, and expression of globin genes in fetuses and neonates. It has been previously demonstrated that immature primitive erythroid cells enter the embryonic circulation and progressively mature in the circulation during embryogenesis [14]. It was also shown that EPO/EPOR signaling promotes survival and delays maturation of primitive

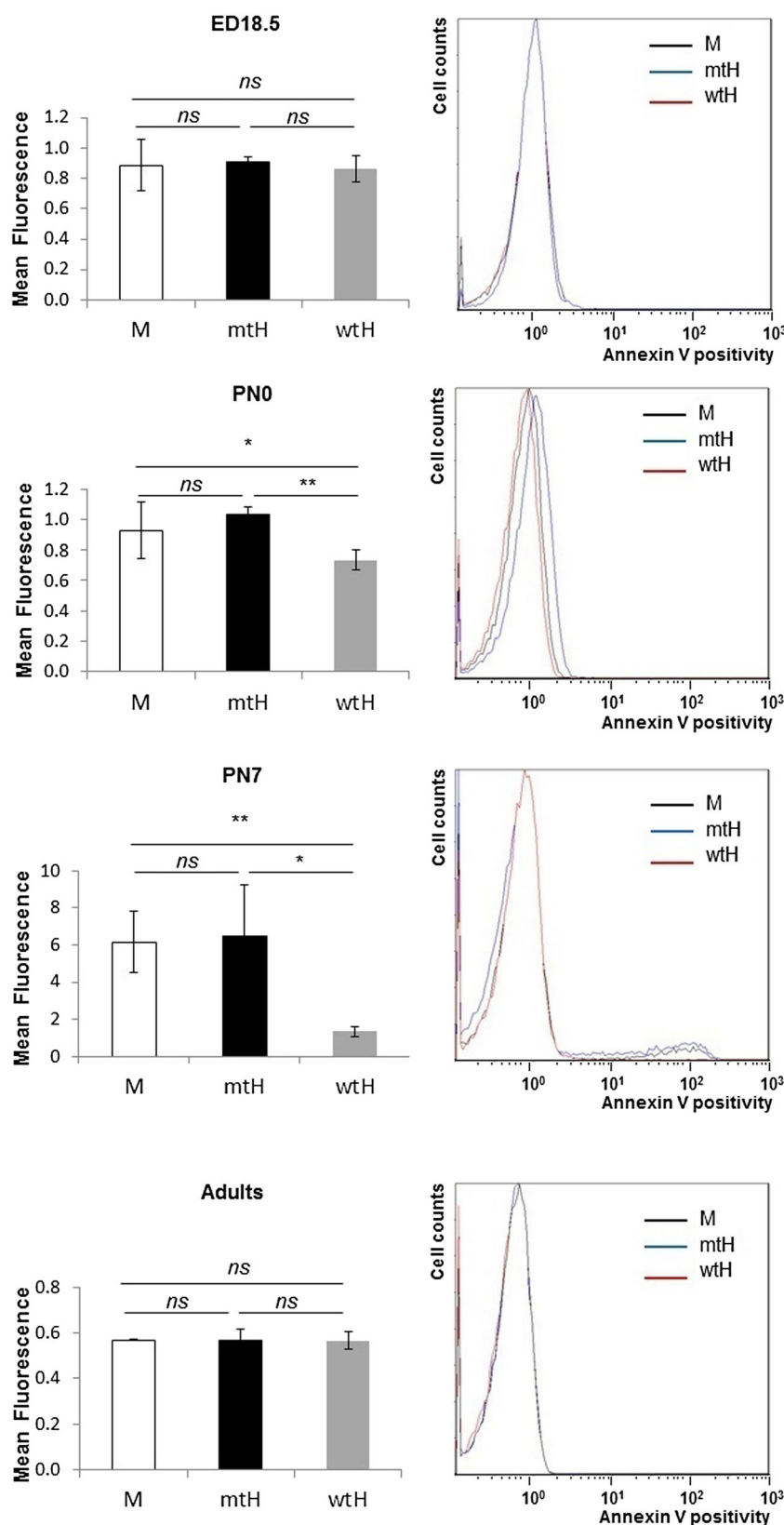
Fig. 5 Upon return from hypoxia to normoxia, mtHEPOR mice undergo greater changes of hematocrit than other genotypes. Neonatal mice of individual genotypes have different Epo levels. **a** Mice (*mEpoR* (M), *wtHEPOR* (wtH), and *mtHEPOR* (mtH)) were treated in a hypobaric chamber for 10 days at 12 % O₂, and their hematocrit were measured at indicated time points for 29 days after returning to normoxia. The mean and standard error of hematocrit levels ($n \geq 4$) are shown. BH denotes before hypoxia. **b** ELISA measurements of Epo levels in neonatal mice (7 days old) of the indicated genotypes. Epo levels (pg/ml) in individual mouse genotypes are expressed as the mean value \pm SD of measurements for seven *mEpoR* mice (M), six *mtHEPOR* (mtH), and four *wtHEPOR* (wtH) mice. **c** qRT-PCR analysis of Epo expression in the liver and kidney of day 7 neonates using *Epo* Taqman probe. The results were normalized to the expression of beta-actin and to mRNA levels of wild-type mouse control (M) using REST[©] 2009 software. $n = 6$ for *mEpoR* mice (M) and $n = 4$ for *mtHEPOR* (mtH), and *wtHEPOR* (wtH) mice. *** $P < 0.001$, ** $P < 0.01$, * $P < 0.05$, ns not significant



erythroblasts [15]. In agreement, our data show the presence of immature erythroid cells in the circulation of mouse fetuses as well as newborns until 3 weeks after birth; the mtHEPOR mouse with augmented EPOR signaling has a larger proportion of immature erythroblasts than wtHEPOR and *mEpoR* mice, predominantly in the mid- and late-gestation period (Fig. 2). Since most of the progeny of primitive erythropoiesis in wild-type mouse disappear around E15.5 [14, 16], the circulating immature erythroid cells from E15.5 and thereafter were expected to be the progeny of definitive erythropoiesis.

The globin gene expression analysis suggested that this applies only to the *mEpoR* and *wtHEPOR* genotypes. Interestingly, in the mtHEPOR mice, the observed delayed maturation paralleled with delayed hemoglobin switching (Fig. 3). This delayed switch from embryonic to fetal/adult globins could be attributed to a slower clearance of primitive erythroid cells from the circulation in mtHEPOR fetuses and/or to a delayed “maturational” switch in the mtHEPOR primitive erythroblasts, as supported by data in Fig. 2. This conclusion is also supported by assessment of the enucleation status of erythroid

Fig. 6 mtHEPOR erythrocytes show increased phosphatidylserine exposure on erythrocytes membrane. Annexin V binding to exposed phosphatidylserines on the membrane of erythrocytes isolated from embryos at day 18.5 (ED18.5), neonatal mice at postnatal day 0 (PN 0) and 7 (PN 7), and adult mice (8–12 weeks old) was determined by flow cytometry. The mean intensity of fluorescence gradually increased for mtHEPOR mice (mtH, $n=9$ for PN 7, $n=3$ for E18.5, PN 0, and adults) and mEpoR mice (M, $n=5$ for PN 7, $n=3$ for E18.5, PN 0, and adults). The lowest phosphatidylserine exposure was detected for wtHEPOR mice; with subtle changes in perinatal period (wtH, $n=4$ for PN 7, $n=3$ for E18.5, PN 0, and adults). The overlays of the original histograms of representative measurements are also shown (right). The results are expressed as the mean value \pm SD. *** $P<0.001$, ** $P<0.01$, ns not significant



cells in PB using DRAQ5. In aggregate, our results suggest that at mid to late gestation, a significantly higher proportion

of primitive erythroid cells was present in mtHEPOR mouse PB compared to wtHEPOR and mEpoR embryos.

EPO signaling has a unique role in primitive erythropoiesis. Primitive erythropoiesis in *EpoR*-deficient mouse and zebra fish models is impaired, but not completely abolished [1, 17, 18]. The proliferative maturation of primitive erythroblasts is highly dependent on EPO/EPOR-mediated signaling [15]. These combined results demonstrate that EPO signaling does not fully affect primitive erythroid cell differentiation and formation but plays a role in the proliferation of primitive erythroid progenitors and modulates primitive erythroblast maturation which, in turn, influences the abundance of primitive erythroid cells in embryonic circulation. Our data support the following concept—gain-of-function EPOR mutation causes enhanced EPO/EPOR signaling and results in delayed terminal maturation of primitive erythroid cells.

We have previously investigated the effects of recombinant mouse (rm) Epo on adult bone marrow-derived mtHEPOR and wtHEPOR erythroid progenitors in vitro and showed that while mtHEPOR BFU-Es were hypersensitive to rmEpo, the wtHEPOR were hyposensitive to rmEpo in these culture conditions [6]. Because these findings could be influenced by interaction differences between mouse Epo with human EPOR, we examined in this study of mtHEPOR and wtHEPOR FLCs the effects of rhEPO on EPOR signal transduction pathway. The data shown here are consistent with our previous studies. Here, we demonstrate augmented and sustained activation of Stat5 in mtHEPOR FLCs and significantly reduced Stat5 activation in wtHEPOR FLCs (Fig. 4a, b). Collectively, these data are in agreement with the observed polycythemia of mtHEPOR and yet not fully explained anemia of wtHEPOR adult mice [6, 12] and fetuses (this study). We show here that the Epo production in wtHEPOR neonatal mice (day 7) was significantly elevated (Fig. 5b, c). These data likely reflect weaker signaling downstream human EPOR when compared to murine EpoR [19] leading to anemia and chronic hypoxia resulting in increased Epo production in wtHEPOR mice.

The causes of observed perinatal fall of hematocrit in the mtHEPOR neonates could be associated with transient anemia in normal human newborns [20]. We reported that neocytolysis, a selective destruction (hemolysis) of young (hypoxia-made) erythrocytes, first described in astronauts [13] but also observed in people acclimatized to hypoxic high altitude upon their return to normoxic sea levels [7, 21], can account for the perinatal fall of hematocrit in mice [7]. We propose that the same phenomenon contributes to the observed perinatal correction of polycythemia in mtHEPOR newborns as embryos leaving the hypoxic uterus are exposed to normoxia at birth. We report here differential decrease of hematocrits in perinatal period in studied genotypes but to a greater degree in mtHEPOR mice (Fig. 1). We could then demonstrate that hypoxic exposure of adult mice bearing these three different genotypes when followed by rapid normoxic change was also accompanied by similar changes of

hematocrits mimicking those we observed in the perinatal life of these mice (Fig. 5a). We can only speculate that the relatively moderate hematocrit decrease in the wtHEPOR neonates could be a result of a protective effect of Epo on neocytolytic process of young erythrocytes [21]—and we show here that anemic wtHEPOR newborns have greatly increased Epo levels (Fig. 5b). In contrast, mtHEPOR mice have low Epo levels and exhibit greater decrease of hematocrit following their birth. Increased phosphatidylserine exposure on the membrane of mtHEPOR erythrocytes (Fig. 6) in the perinatal period is congruent with accelerated destruction of these cells by macrophages [22, 23], thus contributing to the fall of hematocrit in these neonatal mice. However, because the hematocrit in perinatal period is significantly lower in mEpoR mice compared to mtHEPOR mice notwithstanding a comparable degree of phosphatidylserine exposure on their RBCs, it is likely that other biochemical features besides phosphatidylserine exposure are involved in the clearance of hypoxia-born RBCs [24].

In conclusion, we demonstrate that the human gain-of-function *EPOR* causes fetal polycythemia associated with prolonged primitive erythropoiesis and delayed switch from primitive to definitive erythropoiesis and transient lack of polycythemia in perinatal life. In addition, we demonstrate that wtHEPOR embryos are anemic, and that this anemia is a consequence of decreased STAT5 activation in wtHEPOR FLCs. A transient correction of polycythemia in mtHEPOR newborns may result from neocytolysis.

Acknowledgments The study was supported by the VAH Merit Review Award (DY and JTP). VD and MH were supported by the Czech Science Foundation (project P301-12-1503) and by the European Commission (project CZ.1.07/2.3.00/20.0164). We thank Merav Socolovsky (University of Massachusetts), Paul Kingsley, and James Palis (Rochester University) for the helpful advice and Zuzana Korbasova (Palacky University) for the mouse genotyping.

Compliance with ethical standards

Conflict of interest The authors declare that they have no competing interests.

References

- Wu H, Liu X, Jaenisch R, Lodish HF (1995) Generation of committed erythroid BFU-E and CFU-E progenitors does not require erythropoietin or the erythropoietin receptor. *Cell* 83:59–67
- Kralovics R, Prchal JT (2000) Congenital and inherited polycythemia. *Curr Opin Pediatr* 12:29–34
- Lux CT, Yoshimoto M, McGrath K, Conway SJ, Palis J, Yoder MC (2008) All primitive and definitive hematopoietic progenitor cells emerging before E10 in the mouse embryo are products of the yolk sac. *Blood* 111:3435–3438

4. McGrath KE, Frame JM, Fromm GJ, Koniski AD, Kingsley PD, Little J, Bulger M, Palis J (2011) A transient definitive erythroid lineage with unique regulation of the β -globin locus in the mammalian embryo. *Blood* 117:4600–4608
5. Kingsley PD, Malik J, Emerson RL, Bushnell TP, McGrath KE, Bloedorn LA, Bulger M, Palis J (2006) “Maturational” globin switching in primary primitive erythroid cells. *Blood* 107: 1665–1672
6. Divoky V, Liu Z, Ryan TM, Prchal JT, Townes TM, Prchal JT (2001) Mouse model of congenital polycythemia: homologous replacement of murine gene by mutant human erythropoietin receptor gene. *Proc Natl Acad Sci U S A* 98:986–991
7. Song J, Yoon D, Christensen RD, Horvathova M, Thiagarajan P, Prchal JT (2015) HIF-mediated increased ROS from reduced mitophagy and decreased catalase causes neocytolysis. *J Mol Med (Berl)* 93:857–866
8. Zhang J, Socolovsky M, Gross AW, Lodish HF (2003) Role of Ras signaling in erythroid differentiation of mouse fetal liver cells: functional analysis by a flow cytometry-based novel culture system. *Blood* 102:3938–3946
9. Yoon D, Watowich SS (2003) Hematopoietic cell survival signals are elicited through non-tyrosine-containing sequences in the membrane-proximal region of the erythropoietin receptor (EPOR) by a Stat5-dependent pathway. *Exp Hematol* 31:1310–1316
10. Pfaffl MW, Horgan GW, Dempfle L (2002) Relative expression software tool (REST) for group-wise comparison and statistical analysis of relative expression results in real-time PCR. *Nucleic Acids Res* 30:36
11. Lang KS, Roll B, Myssina S, Schittenhelm M, Scheel-Walter HG, Kanz L, Fritz J, Lang F, Huber SM, Wieder T (2002) Enhanced erythrocyte apoptosis in sickle cell anemia, thalassemia and glucose-6-phosphate dehydrogenase deficiency. *Cell Physiol Biochem* 12:365–372
12. Divoky V, Prchal JT (2002) Mouse surviving solely on human erythropoietin receptor (EpoR): model of human EpoR-linked disease. *Blood* 99:3873–3874
13. Rice L, Alfrey CP (2005) The negative regulation of red cell mass by neocytolysis: physiologic and pathophysiological manifestations. *Cell Physiol Biochem* 15:245–250
14. Kingsley PD, Malik J, Fantauzzo KA, Palis J (2004) Yolk sac-derived primitive erythroblasts enucleate during mammalian embryogenesis. *Blood* 104:19–25
15. Malik J, Kim AR, Tyre KA, Cherukuri AR, Palis J (2013) Erythropoietin critically regulates murine and human primitive erythroblast survival and terminal maturation. *Haematologica* 98: 1778–1787
16. Fraser ST, Isern J, Baron MH (2007) Maturation and enucleation of primitive erythroblasts during mouse embryogenesis is accompanied by changes in cell-surface antigen expression. *Blood* 109:343–352
17. Lin CS, Lim SK, D'Agati V, Costantini F (1996) Differential effects of an erythropoietin receptor gene disruption on primitive and definitive erythropoiesis. *Genes Dev* 10:154–164
18. Paffett-Lugassy N, Hsia N, Fraenkel PG, Paw B, Leshinsky I, Barut B, Bahary N, Caro J, Handin R, Zon LI (2007) Functional conservation of erythropoietin signaling in zebrafish. *Blood* 110:2718–2726
19. Ebie AZ, Fleming KG (2007) Dimerization of the erythropoietin receptor transmembrane domain in micelles. *J Mol Biol* 366:517–524
20. Halvorsen S, Bechensteen AG (2002) Physiology of erythropoietin during mammalian development. *Acta Paediatr Suppl* 91:17–26
21. Risso A, Ciana A, Achilli C, Minetti G (2014) Survival and senescence of human young red cells in vitro. *Cell Physiol Biochem* 34: 1038–1049
22. Kuypers FA, de Jong K (2004) The role of phosphatidylserine in recognition and removal of erythrocytes. *Cell Mol Biol (Noisy-le-Grand)* 50:147–158
23. Risso A, Turello M, Biffoni F, Antonutto G (2007) Red blood cell senescence and neocytolysis in humans after high altitude acclimatization. *Blood Cells Mol Dis* 38:83–92
24. Risso A, Ciana A, Achilli C, Antonutto G, Minetti G (2014) Neocytolysis: none, one or many? A reappraisal and future perspectives. *Front Physiol* 14:54, eCollection

**Delayed Hemoglobin Switching and Perinatal Neocytolysis in Mice with
Gain-of-Function Erythropoietin Receptor.**

**Vladimir Divoky¹, Jihyun Song², Monika Horvathova¹, Barbora Kralova¹, Hana
Votavova³, Josef T Prchal^{2*}, and Donghoon Yoon^{2,4}**

¹Department of Biology, Faculty of Medicine and Dentistry, Palacky University, 775 15 Olomouc, Czech Republic.

²Hematology Division, Department of Medicine, University of Utah and VAH, Salt Lake City, Utah, USA 84132.

³ Institute of Hematology and Blood Transfusion, 12820 Prague, Czech Republic.

⁴ Myeloma Institute University of Arkansas for Medical Science Little Rock, AR, USA

Supplementary Material

Real-time PCR analysis of globin genes

PB was washed with cold PBS once and then lysed by Trizol (Molecular Research Center Inc; Cincinnati, OH). Total RNA was isolated and cDNA was synthesized using SuperScript II kit (Invitrogen; Carlsbad, CA). Expression of embryonic and adult globin genes was measured by real-time PCR (qRT-PCR) using SYBR green dye. Specific primer sets for each globin gene and for control 18S rRNA gene were as follows:

ϵ y 5'-CTC TAG CTG TCC AGC AAT CCT G-3' and 5'-GCT TTC AAG GAA CAG TCC AGT ATT C-3';

β H1 5'-AGT TTG GAA ACC TCT CTT CTG CCC TG-3' and 5'-TGT TCT TAA CCC CCA AGC CCA AG-3';

β 1 5'-GCT CTT GCC TGT GAA CAA TG -3' and 5'-GTC AGA AGA CAG ATT TTC AAA TG-3';

β 2 5'-GCC CCT TTT CTG CTA TTG TCT A-3' and 5'-GAT AAA AGC TAG ATG CCC AAA GG-3';

α 1/ α 2 5'-TGC TCT CTG GGG AAG ACA AAA G-3' and 5'-GGC TTC AGC TCC ATA TTC AGC AC-3';

ζ 5'-CCG CCA CGA CCC CCA TGA CC-3' and 5'-AAA GAC CTG AGG GAG GGT TCA AT-3';

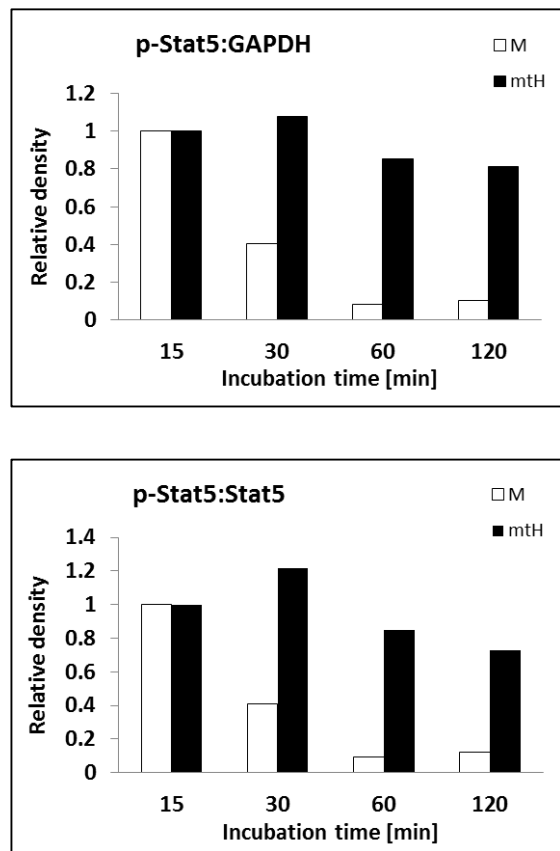
18S 5'-TTG ACG GAA GGG CAC CAC CAG-3' and 5'-GCA CCA CCA CCC ACG GAA TCG-3'.

Real-time PCR analysis of Epo transcripts

Total RNA from liver and kidney was isolated using RNeasy Mini Kit (QIAGEN, Valencia, CA) and reverse-transcribed by SuperScript® VILO™ cDNA Synthesis Kit (Invitrogen), according to manufacturer's instructions. Transcript levels of Epo were measured by qRT-

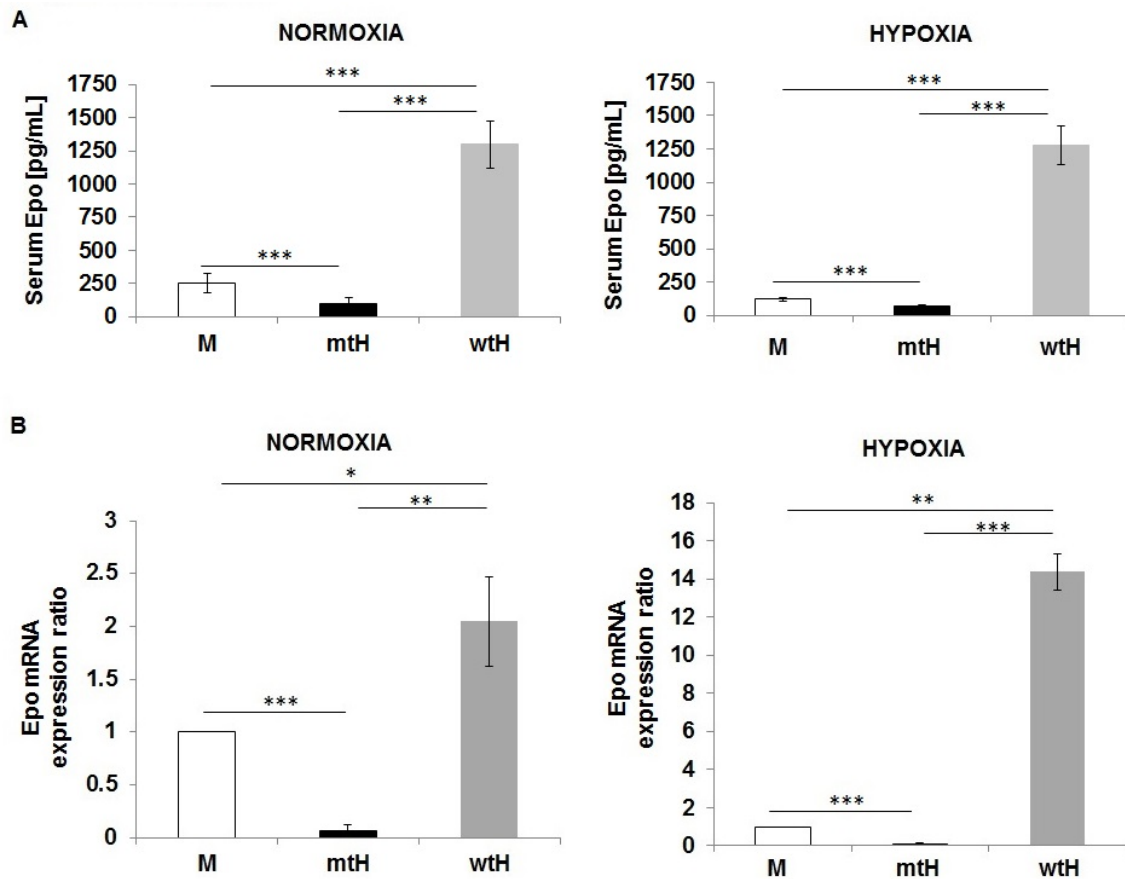
PCR using Epo specific Taqman probe, Mm01202755_m1. The data were normalized to the expression of beta-actin (Actb; 4352341E) and to mRNA levels of wild-type mouse control (mEpoR).

Supplementary Figure 1.



Supplementary Figure 1. Relative quantification of Stat5 phosphorylation for mtHEPOR (mtH) and mEpoR (M) FLCs. The relative quantification of gel bands from immunoblot analyses shown on Figure 4B was performed by ImageJ software (<http://imagej.nih.gov/ij/>). Each bar represents the ratio of the density of phosphorylated Stat5 (p-Stat5) to the density of loading control (GAPDH, top graph or total Stat5, bottom graph) and is presented as fold change against the 15 min time-point.

Supplementary Figure 2.



Supplementary Figure 2. The trends in the differences in the Epo levels between individual genotypes are consistent in normoxia and hypoxia. A) Serum Epo levels are highest in wtHEPOR (wtH) mice and lowest in mtHEPOR (mtH) mice in both normoxic and hypoxic conditions. Epo level increase in wtHEPOR mice compared to control mEpoR mice (M) is higher in hypoxic conditions (10x) than in normoxia (5x). On the other hand the reduction in serum Epo in mtHEPOR mice compared to mEpoR mice (M) is greater in normoxia (2.6-times) than in hypoxia (1.7-times). B) The differences in serum Epo levels were paralleled by differences in *Epo* mRNA expression in the kidney; the highest in wtH mice and the lowest in mtH mice in both normoxic and hypoxic conditions. The results were normalized to the expression of beta-actin and to mRNA levels of wild-type mouse control (M) using REST© 2009 software. M mice, n = 6 for normoxia and hypoxia; mtH mice, n = 3 for normoxia and n = 7 for hypoxia; wtH mice, n = 4 for normoxia and n = 6 for hypoxia. ***P<0.001, **P<0.01, *P<0.05.

Note: the analyses were separately performed using mice housed in two different institutions

- Olomouc, Czech Republic (the “normoxia” measurements, left panels of the figure) and in SLC, USA (the “hypoxia” measurements, right panels). Because the measured parameters could be influenced by the differences in the altitude of the two laboratories (Olomouc 230 m versus SLC 1300 m elevation above sea level), the graphs compare serum Epo levels and *Epo* mRNA expression between individual genotypes in normoxia and hypoxia separately.

Príloha 2

Kralova B, Sochorcova L, Song J, Jahoda O, Hlusickova Kapralova K, Prchal JT,

Divoky V, Horvathova M.

Developmental changes in iron metabolism and erythropoiesis in mice with human gain-of-function erythropoietin receptor.

American Journal of Hematology. 2022; 97(10):1286-1299.

Developmental changes in iron metabolism and erythropoiesis in mice with human gain-of-function erythropoietin receptor

Barbora Kralova¹ | Lucie Sochorcova¹ | Jihyun Song² | Ondrej Jahoda¹  |
 Katarina Hlusickova Kapralova¹  | Josef T. Prchal² | Vladimir Divoky¹  |
 Monika Horvathova¹ 

¹Department of Biology, Faculty of Medicine and Dentistry, Palacky University, Olomouc, Czech Republic

²Division of Hematology & Hematologic Malignancies, The University of Utah School of Medicine, Salt Lake City, Utah, USA

Correspondence

Monika Horvathova, Department of Biology, Faculty of Medicine and Dentistry, Palacky University, Hnevotinska 3, Olomouc 775 15, Czech Republic.
 Email: monika.horvathova@upol.cz

Funding information

Ministry of Health of the Czech Republic, Grant/Award Number: NV19-07-00412; European Union - Next Generation EU, Program EXCELES, Grant/Award Number: LX22NPO5102; Internal grant of Palacky University, Grant/Award Number: IGA_LF_2022_003; Ministry of Education, Youth and Sports (to animal facility BIOCEV), Grant/Award Numbers: LM2018126, CZ.02.1.01/0.0/0.0/18_046/0015861

Abstract

Iron availability for erythropoiesis is controlled by the iron-regulatory hormone hepcidin. Increased erythropoiesis negatively regulates hepcidin synthesis by erythroferrone (ERFE), a hormone produced by erythroid precursors in response to erythropoietin (EPO). The mechanisms coordinating erythropoietic activity with iron homeostasis in erythrocytosis with low EPO are not well defined as exemplified by dominantly inherited (heterozygous) gain-of-function mutation of human EPO receptor (*mtHEPOR*) with low EPO characterized by postnatal erythrocytosis. We previously created a mouse model of this *mtHEPOR* that develops fetal erythrocytosis with a transient perinatal amelioration of erythrocytosis and its reappearance at 3–6 weeks of age. Prenatally and perinatally, *mtHEPOR* heterozygous and homozygous mice (differing in erythrocytosis severity) had increased *Erfe* transcripts, reduced hepcidin, and iron deficiency. *Epo* was transiently normal in the prenatal life; then decreased at postnatal day 7, and remained reduced in adulthood. Postnatally, hepcidin increased in *mtHEPOR* heterozygotes and homozygotes, accompanied by low *Erfe* induction and iron accumulation. With aging, the old, especially *mtHEPOR* homozygotes had a decline of erythropoiesis, myeloid expansion, and local bone marrow inflammatory stress. In addition, *mtHEPOR* erythrocytes had a reduced lifespan. This, together with reduced iron demand for erythropoiesis, due to its age-related attenuation, likely contributes to increased iron deposition in the aged *mtHEPOR* mice. In conclusion, the erythroid drive-mediated inhibition of hepcidin production in *mtHEPOR* mice in the prenatal/perinatal period is postnatally abrogated by increasing iron stores promoting hepcidin synthesis. The differences observed in studied characteristics between *mtHEPOR* heterozygotes and homozygotes suggest dose-dependent alterations of downstream EPOR stimulation.

1 | INTRODUCTION

Iron is essential for erythropoiesis and its levels are controlled by the iron-regulatory hormone hepcidin.¹ Hepcidin (encoded by *HAMP* gene) expression is regulated by a complex interplay of signals, predominantly by inflammation, iron status, hypoxia, and erythropoietic

drive.^{1–4} Increased erythropoietic activity negatively regulates hepcidin synthesis by erythroferrone (ERFE), a hormone produced by erythroid precursors in response to erythropoietin (EPO).⁴ A tight control of iron balance is essential to sustain iron demand and avoid iron deficiency or iron overload. Augmented erythropoiesis whether productive or ineffective, via EPO-induced ERFE expression, attenuates

hepcidin production to increase iron availability for hemoglobin synthesis.⁴ In disease states characterized by ineffective erythropoiesis such as thalassemia, dyserythropoietic congenital anemias, and myelodysplastic syndrome, the erythropoiesis is hyperproliferative and the affected anemic subjects develop secondary iron overload caused by inappropriately suppressed hepcidin, resulting from excessive accumulation of immature erythroblasts and exaggerated ERFE production.^{5,6} The transgenic mice with graded erythroid overexpression of Erfe develop dose-dependent iron overload and relative hepcidin deficiency.⁷

The co-regulation of erythropoiesis and iron metabolism as exemplified by ERFE is less clear in congenital diseases characterized by chronically elevated effective erythropoiesis.⁸ Decreased circulating hepcidin concentrations and iron deficiency were reported among individuals with Chuvash polycythemia,⁹ the congenital erythrocytosis characterized by augmented hypoxia-induced transcription factors (HIFs) due to a hypomorphic mutation of negative HIFs regulator von Hippel Lindau gene (*VHL*^{R200W}).¹⁰ Similarly, erythrocytic mice overexpressing human EPO (named Tg6)¹¹ displayed iron deficiency and hepcidin suppression.¹² Patients with polycythemia vera (PV), an acquired erythrocytosis with constitutively active JAK2¹³ and subnormal EPO levels,^{14,15} have slightly elevated ERFE and normal/insufficiently suppressed hepcidin given the degree of expanded erythropoiesis and iron deficiency.¹⁶

However, little is known about iron metabolism in congenital erythrocytosis characterized by low EPO levels; originally named primary familial and congenital polycythemia (PFCP)^{8,14} which is due to heterozygous gain-of-function EPO receptor (EPOR) mutations. These EPOR mutations have typically truncated the cytoplasmic part of EPOR with loss of its negative regulatory domain leading to augmented EPOR-JAK2-STAT5 signaling, resulting in excessive proliferation, survival, and differentiation of erythroid progenitors.^{8,17-20}

We previously created a mouse model of PFCP bearing the gain-of-function erythrocytosis-causing human EPOR gene mutation (*mtHEPOR*). We generated not only the heterozygous mouse model analogous to human disease but also the homozygous mice.^{21,22} We have shown that *mtHEPOR* embryos develop erythrocytosis around embryonic day (ED)17.5, followed by transient amelioration of erythrocytosis in perinatal life and its reappearance at 3–6 weeks of age.²² Similarly, erythrocytosis is absent in patients with PFCP in the perinatal period and develops within a few weeks of neonatal life.⁸ The *mtHEPOR* homozygous mice have even greater erythrocytosis than their heterozygous counterparts.^{21,22}

Here, we investigated how the developmental and age-related changes of erythron in *mtHEPOR* heterozygotes and homozygotes are interconnected with changes in iron homeostasis.

2 | MATERIALS AND METHODS

2.1 | Animals

The gain-of-function human EPOR knock-in mice (substitution c.1278C > G; designation of the mutation according to LOVD

database, www.lovd.nl) were produced on a C57BL/6 background.²¹ Detailed information about mouse breeding and assessment of hematological and iron status parameters²³ and detection of megakaryocytes²⁴ can be found in supplemental Methods. All analyses were performed according to the regulations of Palacky University (PU) Institutional Animal Care and Use Committee.

2.2 | Real-time PCR analysis

Quantitative reverse transcriptase-polymerase chain reaction (q-PCR) was performed as described in supplemental Methods. Relative gene expression was normalized against β -Actin.

2.3 | Enzyme-linked immunosorbent assay (ELISA)

Commercially available ELISA kits, specified in supplemental Methods, were used for the measurements of serum levels of hepcidin, ferritin, erythroferrone, Epo, and selected inflammatory cytokines.

2.4 | Flow cytometry

Bone marrow (BM) and spleen cells were isolated and co-stained with FITC-conjugated CD71 and phycoerythrin-conjugated Ter119 antibodies (BD Biosciences).^{23,25} The surface expression of CD47 on red blood cells (RBCs) was determined using FITC-conjugated anti-mouse CD47 antibody (BD Biosciences).²⁶ The intensity of fluorescence was measured by FC500 (Beckman-Coulter). Multi-parameter flow cytometry analysis of hematopoietic stem and progenitor cell (HSPC) populations was performed as a custom service, as specified in supplemental Methods.

2.5 | Hematopoietic colony assay

Freshly isolated BM cells were plated in methylcellulose media (StemCell Technologies) according to the manufacturer's instructions as we previously described^{21,27} and further specified in supplemental Methods. Colonies were scored by standard morphologic criteria under an inverted microscope (Olympus).

2.6 | RBC lifespan

Red blood cells were isolated from total blood and stained in vitro with carboxyfluorescein diacetate succinimidyl ester (CFSE, Thermo-Fisher Scientific).^{28,29} CFSE labeled RBCs were injected into the tail veins of control mice expressing mouse *EpoR* (*mEpoR*) and their fluorescence was tracked for 35 days using FC500.

2.7 | Human subjects

The Ethics Committee of PU Hospital approved the collection and analysis of human subjects' samples according to an informed consent obtained as per the Declaration of Helsinki. Hematocrit (Hct) was measured using a Sysmex XE-500 analyzer (Sysmex Corp). Iron parameters were determined with standard biochemical methods. Hepcidin and ERFE serum concentrations were measured with commercial ELISA kits according to the manufacturers' instructions (DRG Instruments GmbH and Intrinsic LifeSciences, respectively); serum EPO was measured by radioimmunoassay.³⁰

2.8 | Statistics

All data are presented as mean \pm standard error of the mean (SEM). An unpaired *t*-test with Welch's correction or linear regression analysis was used to determine the statistical significance of the results and calculated by GraphPad Prism 8 Software (GraphPad Software Inc.). Correlation analyses were performed using the same software. *p*<.05 were considered statistically significant.

3 | RESULTS

3.1 | Iron-restricted erythropoiesis in mtHEPOR mice shortly after birth

We first evaluated the evolution of erythrocytosis in mtHEPOR mice at different postnatal ages: at postnatal day (PD)7, ~2.5 months (referred to as young mice), ~6.5 months (mature adult), and ~16 months (old). Despite partial amelioration of erythrocytosis in mtHEPOR mice, we previously reported at PD7,²² Hct was significantly increased in both mtHEPOR heterozygotes and homozygotes compared to *mEpoR* controls and remained elevated at all subsequent analyzed stages (Figure 1A). The highest Hct levels, detected in mtHEPOR homozygotes, were accompanied by mild splenomegaly (Figure 1B). A progressive reduction in Hct levels was observed with aging in animals of all genotypes (Figure 1A). RBC count and hemoglobin were also consistently higher in mtHEPOR heterozygotes and homozygotes than in *mEpoR* littermates; both parameters decline with postnatal aging (Figure S1A).

RBC indices, mean corpuscular hemoglobin (MCH), and mean corpuscular hemoglobin concentration (MCHC), indicated limited iron supply for erythropoiesis in both mtHEPOR heterozygotes and homozygotes in the perinatal period (Figure 1C) but not in mature adult and old mice (Figure 1D). The absence of microcytosis at PD7 (Figure 1C), typical for iron deficiency states, was likely masked in mtHEPOR heterozygous and homozygous neonates by an increased proportion of macrocytic RBCs generated in the prenatal period,³¹ as a result of delayed switch from primitive to definitive erythropoiesis we previously reported in mtHEPOR mice.²² Reduced RBC indices, anisocytosis, and reticulocytosis observed in four-weeks-old mtHEPOR

heterozygotes and homozygotes (Figure S1B-D) partially or completely normalized in their older counterparts (Figure 1D,E), including normalization of red cell distribution width (RDW, Figure 1F). This indicated the existence of a transient iron deficiency not sufficient for productive erythropoiesis in an early life.

Consistently with the finding that low iron potentiates the commitment of megakaryocytic (Mk)-erythroid progenitors (MEP) toward the Mk lineage,³² platelet (PLT) counts were elevated in both mtHEPOR heterozygotes and homozygotes compared to *mEpoR* controls at PD7 (Figure 1G). On the other hand, low PLT observed in mtHEPOR homozygotes later in life (Figure 1G) resembled the human phenotype wherein affected patients had slightly decreased PLT counts likely due to a marked increase in RBC and total blood volumes, suggesting that their normal PLT mass was diluted by increased blood volume.^{8,14}

3.2 | Developmental transition from iron deficiency to increased tissue iron deposition in mtHEPOR mice

To correlate the temporal changes in RBC indices with iron status, selected iron parameters were assessed. At the time of prenatal development of erythrocytosis at ED17.5,²² strong downregulation of *Hamp* mRNA expression was observed in both heterozygous and homozygous mtHEPOR fetal livers (FL, Figure 2A). At PD7, significantly decreased *Hamp* mRNA expression was also found in the liver (Figure 2B) along with decreased serum hepcidin levels (Figure 2C). This was consistent with lower ferritin levels, reduced non-heme liver iron concentration (LIC), and diminished expression of the iron-store regulator of hepcidin, *Bmp6*² in these mice (Figure 2D-F). The measurements of serum iron concentration and transferrin saturation (TSAT) were precluded at ED17.5 and PD7 due to a limited volume of samples. The activation of Bmp/Smad pathway, responsible for iron-induced hepcidin production, was partly blunted in both heterozygous and homozygous mtHEPOR newborns, as documented by diminished expression of two Bmp/Smad target genes,⁷ *Smad7* and *Id1* (Figure S2A). Thus, available iron status data, together with reduced RBC indices (MCH and MCHC), as a whole support the conclusion about transient iron deficiency. Spleen iron content (SIC) was comparable between mice of all genotypes at PD7 (Figure 2G), but this may be influenced by reported accelerated destruction of RBCs in mtHEPOR neonates compared to *mEpoR* littermates.²²

Normal to increased TSAT, ferritin levels, LIC, and SIC were detected in mtHEPOR homozygotes at later postnatal age (Figure 2H-K, Figure S2B,C). This was accompanied by the induction of hepcidin (Figure 2L,M) and upregulation of hepatic *Bmp6* transcripts, primarily in the mature adult and old mtHEPOR homozygotes (Figure 2N). Young mtHEPOR heterozygotes had slightly diminished iron stores (Figure 2I-N), but all analyzed iron status parameters, including hepcidin, became comparable to *mEpoR* controls with aging. The increase in hepatic *Smad7* and *Id1* expression reflected postnatal restoration of Bmp/Smad pathway activation (Figure S2D) in both mtHEPOR heterozygotes and homozygotes.

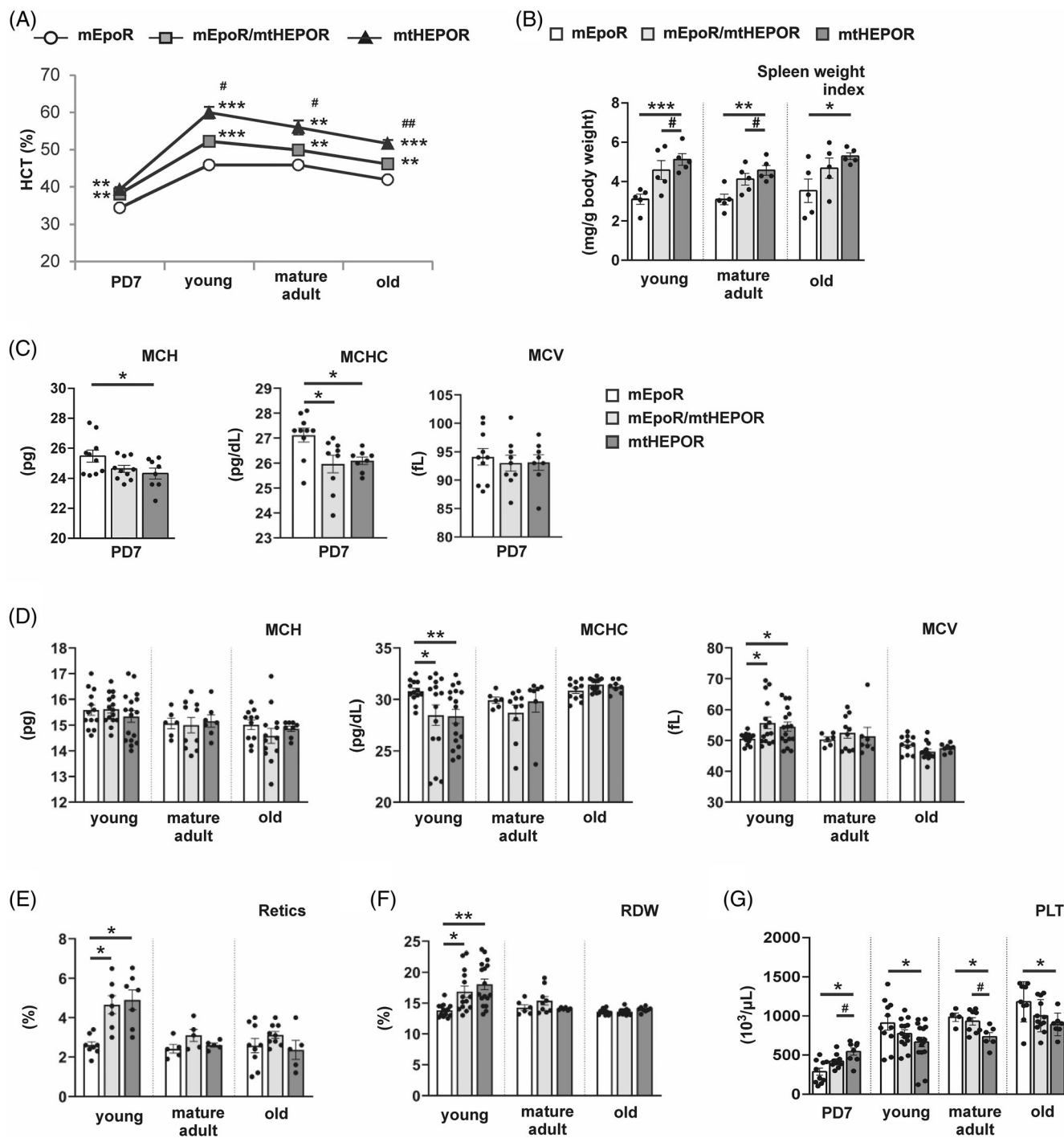
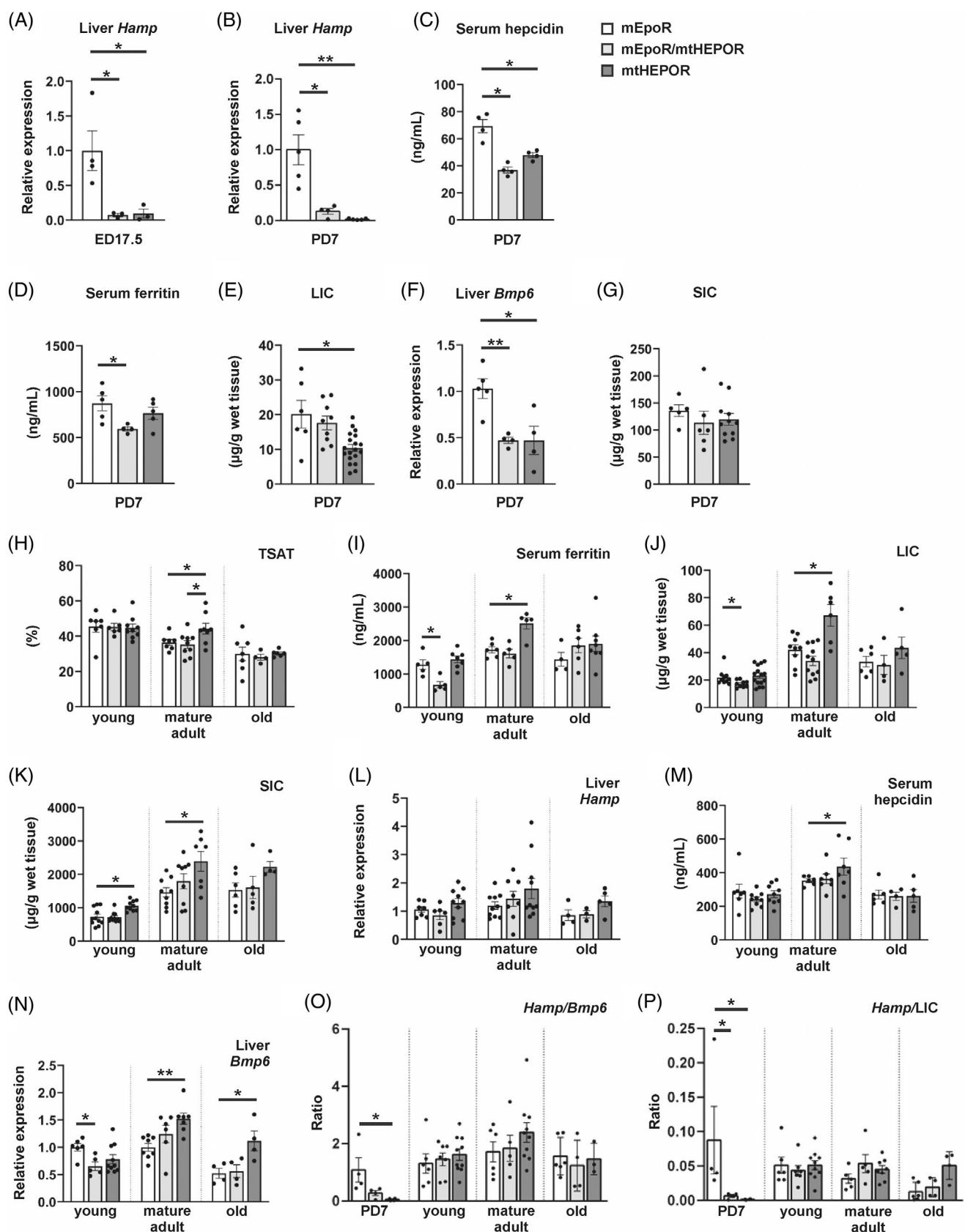


FIGURE 1 Evaluation of hematological parameters and spleen size in mice of all studied genotypes. (A) Hematocrit (Hct) levels in mice of different postnatal ages: postnatal day 7 (PD7), ~2.5 months old (young), ~6.5 months old (mature adult), and ~16 months old (old) mice. The decline in Hct levels between young and old animals: 14% in mtHEPOR mice ($p < .001$), 12% in mEpoR/mtHEPOR mice ($p < .001$), and 9% in mEpoR controls ($p < .01$). (B) Spleen weight index (the ratio of spleen weight to gross bodyweight) in young, mature adult, and old mice. (C and D) RBC indices: mean corpuscular hemoglobin (MCH), mean corpuscular hemoglobin concentration (MCHC), and mean corpuscular volume (MCV) at PD7 (C) and in young, mature adult, and old mice (D). (E) Percentage of reticulocytes (Retics) in young, mature adult, and old mice. (F) Red cell distribution width (RDW) in young, mature adult, and old mice. (G) Platelet (PLT) counts at PD7 and in young, mature adult, and old mice. All parameters were measured in at least 5 mice per each group and genotype at all indicated time points. Values indicate mean \pm SEM; * $p < .05$, ** $p < .01$, *** $p < .001$ versus mEpoR; # $p < .05$ and ## $p < .01$, mtHEPOR versus mEpoR/mtHEPOR calculated by unpaired t-test with Welch's correction

**FIGURE 2** Legend on next page.

Importantly, the ratio between *Hamp* mRNA and *Bmp6* mRNA (Figure 2O) as well as between *Hamp* mRNA and LIC (Figure 2P) was lower in *mtHEPOR* heterozygotes and homozygotes than in *mEpoR* controls only at PD7 and indicated inappropriate hepcidin suppression at this stage. At later stages of postnatal life, normal ratios of *Hamp* mRNA to *Bmp6* mRNA (Figure 2O) and *Hamp* mRNA to LIC (Figure 2P) excluded the contribution of relatively decreased hepcidin to iron loading.

3.3 | Inverse relationship between ERFE and hepcidin in *mtHEPOR* mice at embryonic and perinatal periods but not in postnatal life

In agreement with the known inhibition of hepcidin by ERFE,⁴ relative hepatic and splenic *Erfe* mRNA expression was stimulated in both *mtHEPOR* heterozygotes and homozygotes at ED17.5 and PD7 (Figure 3A,B). This corresponded to a significantly higher proportion of immature erythroid progenitors in fetal hepatic and perinatal peripheral blood circulation, which we previously reported in *mtHEPOR* homozygotes.²²

Erfe transcripts were only modestly increased in the BM and spleen of both *mtHEPOR* heterozygotes and homozygotes at later stages of postnatal life (Figures 3C,D). Moreover, a negative correlation between *Hamp* and *Erfe* expression was only partly retained in *mtHEPOR* heterozygotes, but not in *mtHEPOR* homozygotes, wherein a positive correlation was detected (Figure S3A). Despite transcriptional *Erfe* stimulation, serum *Erfe* levels were below the ELISA detection threshold in all but three analyzed *mtHEPOR* mice (one heterozygote and two homozygotes) (Figure S3B), as were in all *mEpoR* control samples. This showed that the degree of *Erfe* induction in *mtHEPOR* mice is much lower compared to previously reported *Erfe* up-regulation in a mouse model of β-thalassemia intermedia (Th3/+ mice)²⁷ or in control mice after EPO administration²³ (Figure S3B,C).

3.4 | Modest expression of ERFE and absence of excessive accumulation of immature erythroblasts in the postnatal *mtHEPOR* BM and spleen

The assessment of erythroid differentiation and maturation²⁵ revealed an increased percentage of BM erythroid cells expressing Ter119 in

young and mature adult *mtHEPOR* heterozygotes and homozygotes compared to *mEpoR* controls (Figure 3E) and their progressive decline with age (old vs. young mice: *mEpoR* by 5.82%; *mtHEPOR* heterozygotes by 6.37%, and *mtHEPOR* homozygotes by 7.34%). No major differences in the distribution of BM erythroid cells into individual maturation stages were detected in young and mature adult mice. However, the percentage of immature Ter119^{high}CD71^{high} BM erythroblasts (region II,²⁵ Figure 3E) was lower in old *mtHEPOR* homozygotes in comparison to their young counterparts and also to the age-matched *mEpoR* controls and *mtHEPOR* heterozygotes. Analyses of splenic erythropoiesis showed higher percentage of total Ter119-positive cells in young and mature adult *mtHEPOR* heterozygotes and homozygotes than in controls, normal maturation pattern, and no decline with age (Figure S4). These data showed an absence of excessive accumulation of immature erythroblasts (known to drive substantial overproduction of ERFE)^{5,6} in *mtHEPOR* mice during later postnatal life and also indicated aging-related relative suppression of BM erythropoiesis in *mtHEPOR* homozygotes.

We questioned whether a possible attenuation of the EPOR signaling cascade during aging contributes to a relative decrease of BM erythropoiesis in *mtHEPOR* mice. We, therefore, tested whether the hypersensitive EPO dose-response phenotype of erythroid progenitors,³³ we previously published in young *mtHEPOR* homozygotes,²¹ is maintained in aged *mtHEPOR* animals. Analysis of erythroid progenitors' responses to various EPO doses in serum-containing cultures from old mice revealed EPO hypersensitivity of *mtHEPOR* colony forming unit-erythroid (CFU-E) and burst forming unit-erythroid (BFU-E) progenitors (Figure 3F), identical to that published for three-months-old animals.²¹ Therefore, the EPO hypersensitivity phenotype, caused by EPO-induced EPOR signaling overactivation,³⁴ is preserved in BM erythroid progenitors during the aging of *mtHEPOR* animals. In addition, normalization of *Erfe* expression (a direct Stat5 target) to an erythroid marker glycoporphin A (*Gypa*), revealed that *Erfe* mRNA expression is increased in individual erythroid precursors in *mtHEPOR* heterozygotes and homozygotes compared to control mice and that the degree of induction is comparable at all analyzed stages, that is, ED17.5, PD7, young, mature adult, and old mice (Figure S5). Additional analyses comparing Stat5 activation in young versus aged erythroid progenitors, such as immunohistochemical staining of Stat5 phosphorylation and analysis of other downstream targets were not conclusive.

FIGURE 2 Assessment of hepcidin, iron status parameters, and tissue iron content during prenatal, perinatal, and postnatal period. (A-G) Parameters analyzed during prenatal and perinatal period: Hepatic hepcidin (*Hamp*) mRNA expression at embryonic day (ED)17.5 (A) and postnatal day 7 (PD7) (B); serum hepcidin (C) and ferritin (D) levels at PD7; liver iron content (LIC) (E), hepatic *Bmp6* mRNA expression (F), and spleen iron content (SIC) (G) at PD7. (H-N) Parameters analyzed during postnatal life (in young, mature adult, and old mice): Transferrin saturation (TSAT) (H), serum ferritin levels (I), LIC (J), SIC (K), hepatic *Hamp* mRNA expression (L), serum hepcidin (M), and hepatic *Bmp6* mRNA expression (N). (O and P) *Hamp* mRNA expression relative to *Bmp6* mRNA expression (O) and the ratio of *Hamp* mRNA to LIC (P) at different stages of ontogenesis. In Panels A, B, and F, the target gene mRNA expression determined by q-PCR was normalized to *b*-Actin and to the mRNA expression levels of the *mEpoR* controls. Serum levels of hepcidin (C and M) and ferritin (D and I) were measured by ELISA. LIC (E and J) and SIC (G and K) were quantified by colorimetric assay. In Panels L and N, the target gene expression analyzed by q-PCR and normalized to *b*-Actin, is presented as fold change relative to young *mEpoR* control group. Values indicate mean ± SEM. **p* < .05, ***p* < .01 versus *mEpoR* by unpaired t-test with Welch's correction; *n* ≥ 3 mice per analysis and genotype

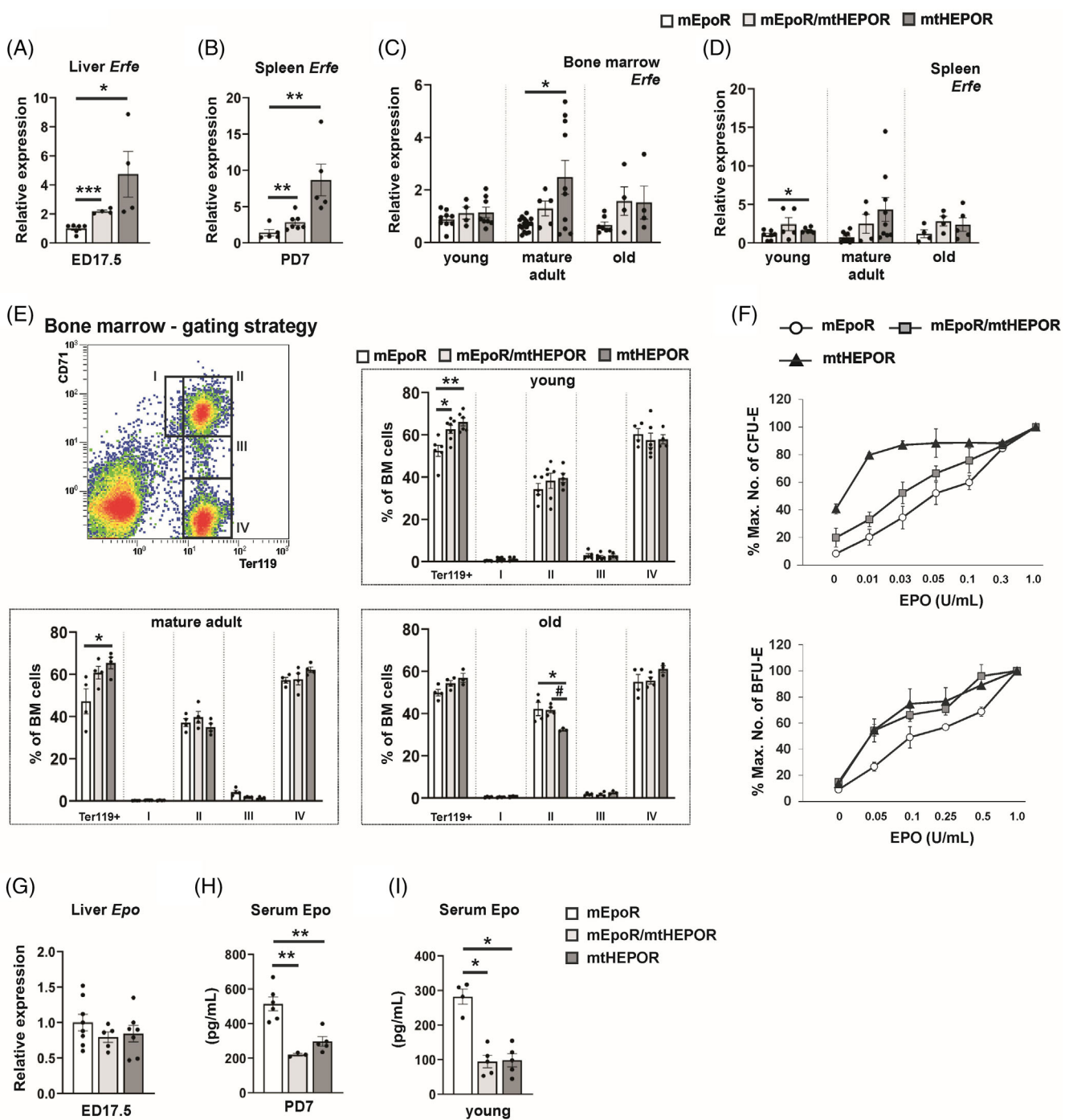


FIGURE 3 Analysis of erythroferrone (*Erfe*) expression, bone marrow (BM) erythropoietic activity, sensitivity of erythroid progenitors to erythropoietin (EPO), and Epo production. (A-D) *Erfe* mRNA expression (normalized to *b*-Actin) measured in the liver at embryonic day (ED)17.5 (A), in the spleen at postnatal day 7 (PD7, B), and in the BM (C) and spleen (D) of young, mature adult, and old mice by q-PCR. In panels C and D, the expression is presented as fold change relative to young *mEpoR* control samples. (E) Flow cytometry analysis of CD71 and Ter119 expression on BM cells in young, mature adult, and old mice of *mEpoR*, *mEpoR/mtHEPOR*, and *mtHEPOR* genotype. The relative number of cells in regions I to IV²⁵ is expressed as a percentage of all viable erythroid cells. (F) EPO dose-response curves of colony forming-unit erythroid (CFU-E) and burst forming-unit erythroid (BFU-E) progenitors; plots of the number of erythroid colonies as a percent maximum versus the concentration of recombinant human (rh) EPO. Each point indicates mean ± SEM of three independent experiments (performed each in duplicates), n = 3 mice per each genotype. (G-I) Assessment of Epo production. Hepatic *Epo* mRNA expression (normalized to *b*-Actin) at ED17.5 (G) and Epo levels (pg/mL) in the serum at PD7 (H) and in young mice (I) were determined by q-PCR and ELISA, respectively. Values indicate mean ± SEM; *p < .05, **p < .01, versus age-matched *mEpoR* controls; #p < .05 *mtHEPOR* versus *mEpoR/mtHEPOR* calculated by unpaired t-test with Welch's correction; n ≥ 3 mice per group and genotype at all indicated time points

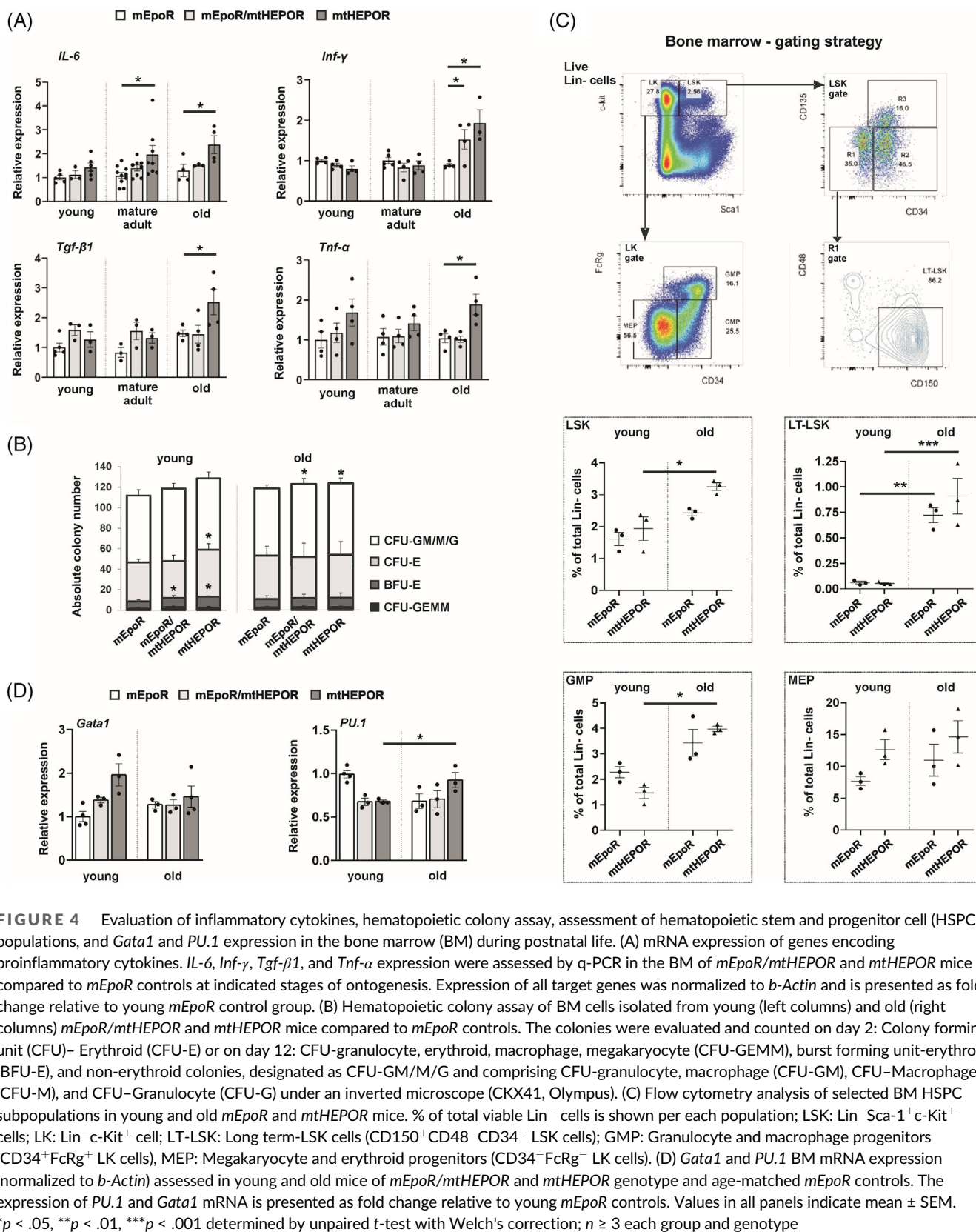


FIGURE 4 Evaluation of inflammatory cytokines, hematopoietic colony assay, assessment of hematopoietic stem and progenitor cell (HSPC) populations, and *Gata1* and *PU.1* expression in the bone marrow (BM) during postnatal life. (A) mRNA expression of genes encoding proinflammatory cytokines. *IL-6*, *Inf-γ*, *Tgf-β1*, and *Tnf-α* expression were assessed by q-PCR in the BM of *mEpoR/mtHEPOR* and *mtHEPOR* mice compared to *mEpoR* controls at indicated stages of ontogenesis. Expression of all target genes was normalized to *b*-Actin and is presented as fold change relative to young *mEpoR* control group. (B) Hematopoietic colony assay of BM cells isolated from young (left columns) and old (right columns) *mEpoR/mtHEPOR* and *mtHEPOR* mice compared to *mEpoR* controls. The colonies were evaluated and counted on day 2: Colony forming unit (CFU)- Erythroid (CFU-E) or on day 12: CFU-granulocyte, erythroid, macrophage, megakaryocyte (CFU-GEMM), burst forming unit-erythroid (BFU-E), and non-erythroid colonies, designated as CFU-GM/M/G and comprising CFU-granulocyte, macrophage (CFU-GM), CFU-Macrophage (CFU-M), and CFU-Granulocyte (CFU-G) under an inverted microscope (CKX41, Olympus). (C) Flow cytometry analysis of selected BM HSPC subpopulations in young and old *mEpoR* and *mtHEPOR* mice. % of total viable Lin⁻ cells is shown per each population; LSK: Lin⁻Sca1⁺c-Kit⁺ cells; LK: Lin⁻c-Kit⁺ cell; LT-LSK: Long term-LSK cells (CD150⁺CD48⁻CD34⁻ LSK cells); GMP: Granulocyte and macrophage progenitors (CD34⁺FcRg⁺ LK cells), MEP: Megakaryocyte and erythroid progenitors (CD34⁺FcRg⁻ LK cells). (D) *Gata1* and *PU.1* BM mRNA expression (normalized to *b*-Actin) assessed in young and old mice of *mEpoR/mtHEPOR* and *mtHEPOR* genotype and age-matched *mEpoR* controls. The expression of *PU.1* and *Gata1* mRNA is presented as fold change relative to young *mEpoR* controls. Values in all panels indicate mean ± SEM. **p* < .05, ***p* < .01, ****p* < .001 determined by unpaired *t*-test with Welch's correction; *n* ≥ 3 each group and genotype

Nevertheless, the presented data suggest there is no dramatic modification of EPOR/Stat5 activation in *mtHEPOR* animals during aging.

Since EPO is the primary driver of erythropoiesis and ERFE production,^{4,5} we measured its expression during ontogenesis in our model. *Epo* expression was prenatally normal in both *mtHEPOR*

heterozygotes and homozygotes (Figure 3G), decreased at PD7 (Figure 3H), and remained low in early and late adulthood (Figure 3I and Figure S6A), in agreement with our previously published data²² and in accordance with the aforementioned hypersensitive EPO dose-response phenotype of BM progenitors demonstrated in young²¹ as well as old *mtHEPOR* animals. This indicates no clear-cut positive correlation of Epo with Erfe or stimulated erythropoiesis in *mtHEPOR* mice. Changes in *Epo* expression in *mtHEPOR* mice during ontogenesis, not seen in control mice, did not seem to be significantly modulated by differences in hypoxia signaling because of unaltered expression of several other target genes of HIFs (Figure S6B-D). In agreement, we previously reported unaltered expression of HIF target genes in *EPOR*-mutated patients.³⁵ The only exception, significantly increased *Slc2a1* transcripts (encoding glucose transporter 1-Glut1) in ED17.5 FL of *mtHEPOR* heterozygotes and homozygotes (Figure S6B), likely reflects increased glucose uptake and metabolism³⁶ during the period of the highest erythroid expansion.

3.5 | Progressive augmentation of inflammatory cytokines and age-related myeloid dominance in the BM of *mtHEPOR* homozygotes

In order to evaluate the possible contribution of inflammation to the regulation of hepcidin production^{1,3} in *mtHEPOR* mice, serum levels of selected inflammatory cytokines: IL-6, tumor necrosis factor- α (Tnf- α), interferon- γ (Ifn- γ), and transforming growth factor- β (Tgf- β 1) were measured. No indications for systemic inflammation or local *IL-6* mRNA induction in the liver were observed in *mtHEPOR* heterozygotes and homozygotes (Figure S7A,B). However, q-PCR analysis of corresponding inflammatory genes revealed their local stimulation mainly in the BM of *mtHEPOR* homozygotes (Figure 4A), together with moderate, but detectable trend toward increased ROS production (Figure S7C), suggesting progressive aging-related alterations in their BM microenvironment. These data indicate activation of inflammatory signaling mechanisms in aged *mtHEPOR* mice, known to promote BM remodeling, premature aging, and myelopoiesis in a paracrine or an autocrine fashion.^{37–40}

We, therefore, evaluated the numbers of individual hematopoietic progenitors in the BM of young and old animals by clonogenic assays. While the numbers of colonies derived from a multilineage colony forming unit – granulocyte, erythroid, macrophage, megakaryocyte (CFU-GEMM) progenitor did not differ, significantly increased numbers of BFU-E-derived and/or CFU-E-derived colonies were found in both young heterozygous and homozygous *mtHEPOR* mice, compared to *mEpoR* controls (Figure 4B). In old *mtHEPOR* heterozygotes and homozygotes, however, we observed significant increase in the total number of non-erythroid colonies derived from granulocyte and/or macrophage progenitor cells compared to *mEpoR* controls (Figure 4B). This was predominantly due to the elevation of CFU-macrophage (CFU-M) and less so of CFU-granulocyte, macrophage (CFU-GM) colonies (Figure S8A), and suggested myeloid lineage bias of hematopoiesis.^{38,41}

Subsequent flow cytometry of subpopulations of hematopoietic stem cells (HSCs) and primitive progenitors from *mtHEPOR* homozygotes and *mEpoR* controls revealed a significant increase in the numbers of lineage (Lin) $^-$ Sca-1 $^+$ c-Kit $^+$ (LSK) stem cells in old *mtHEPOR* homozygotes compared to young counterparts, while this increase was less prominent in *mEpoR* controls (Figure 4C). From the major subsets within Lin $^-$ c-Kit $^+$ (LK) cells in *mtHEPOR* homozygotes, granulocyte-monocyte progenitors (GMPs) were significantly increased in old animals compared to young animals (Figure 4C). Since megakaryocyte-erythroid progenitors (MEPs) dominated the GMPs in young *mtHEPOR* mice (Figure 4C), the myeloid expansion in old *mtHEPOR* homozygotes reflects the restoration of myelopoiesis, attenuated in young *mtHEPOR* counterparts, when compared to controls, indicating a progressive reduction of erythropoietic drive and augmentation of myelopoiesis during aging in *mtHEPOR* mice; to a far greater extent than in control mice. In agreement, relatively increased transcripts of the myeloid master regulator *PU.1* and decreased transcripts of erythroid regulator *Gata1*⁴² can be seen in the BM of old *mtHEPOR* heterozygotes and homozygotes, but not in *mEpoR* controls (Figure 4D). It is known that pro-inflammatory cytokines and elevated megakaryocytes in BM microenvironment are drivers of excessive myelopoiesis in aged hematopoiesis.³⁸ Indeed, in addition to the aforementioned local inflammation, a significant induction in the number of BM megakaryocytes (~1.4-times) between young and old mice was observed in *mtHEPOR* homozygotes (Figure S8B,C).

3.6 | Impaired survival of *mtHEPOR* RBCs

The recycling of iron through erytrophagocytosis by macrophages is a major contributor to systemic iron homeostasis.⁴³ We previously showed that the dramatic decrease of Hct in *mtHEPOR* homozygotes at PD7 was paralleled by induced exposure of phosphatidylserine (PS) on the membrane of *mtHEPOR* homozygous RBCs,²² which likely contributed to their enhanced recognition and destruction by reticuloendothelial macrophages.⁴⁴ Because PS exposure was comparable in *mtHEPOR* homozygotes and *mEpoR* controls during adult life,²² we analyzed the surface expression of CD47, also known as “don’t eat me” signal, another marker priming RBCs for clearance.⁴⁵ The CD47 surface expression was reduced on young *mtHEPOR* heterozygous and more significantly homozygous RBCs compared to *mEpoR* RBCs (Figure S9A). In addition, the *in vivo* lifespan of *mtHEPOR* homozygous RBCs was reduced to almost half compared to *mEpoR* controls (Figure S9B) and less so in *mtHEPOR* heterozygotes. These data indicate that induced RBC recycling in *mtHEPOR* mice may contribute to increased iron deposition.

3.7 | Undetectable ERFE in PFCP patients

To investigate whether the results from the mouse model reflect characteristics of human disease, we measured hematological and iron status parameters of four PFCP, *EPOR*-mutant patients (Table S1). Two

of them were available for ERFE and hepcidin levels assessment (Table S1 and Figure S10). In parallel, patients with congenital erythrocytosis caused by augmented hypoxia signaling due to a gain-of-function mutation of HIF 2-alpha (encoded by EPAS1 gene)³⁵ were evaluated. Hereditary hemolytic anemias with ineffective erythropoiesis (pyruvate kinase deficiency or hereditary spherocytosis)^{46,47} served as positive controls for elevated ERFE and low/inappropriately normal hepcidin (Figure S10). All pediatric patients with both types of erythrocytoses had elevated Hct and normal RBC indices (MCV, MCH, and MCHC), serum iron and ferritin levels, and reduced TSAT (Table S1). While slightly elevated ERFE and undetectable hepcidin levels were observed in EPAS1-mutant patients, EPOR-mutant patients had normal hepcidin and ERFE levels below the detection threshold (Table S1 and Figure S10). Thus, EPOR-mutant patients with moderate iron deficiency and normal hepcidin levels resemble young *mtHEPOR* murine heterozygotes.

4 | DISCUSSION

In this study, we evaluated developmentally-related changes in erythropoietic activity and iron metabolism in a mouse model of congenital erythrocytosis with human gain-of-function EPOR.^{21,22} We observed that in the prenatal/perinatal period *mtHEPOR* heterozygotes and homozygotes presented with significantly down-regulated hepcidin, up-regulated Erfe, and iron deficient erythropoiesis (Figures 1C, 2A-F, and 3A,B). This corresponded to significantly higher proportions of immature erythroid progenitors in the fetal hepatic circulation and neonatal peripheral blood²² and reflected an inverse correlation between Erfe and hepcidin^{4,6} and high iron demand by EPOR mutation-directed augmented erythropoiesis⁵ at these stages. In contrast, normal to elevated iron parameters and hepcidin levels were seen in young, mature adult, and old *mtHEPOR* homozygous mice (Figure 2H-N). Though young *mtHEPOR* heterozygotes had slightly reduced iron stores, adult and old mice with this genotype were iron-replete with physiological hepcidin levels (Figure 2H-N). Mild Erfe induction (Figure S3B) was consistent with the absence of excessive accumulation of immature erythroblasts^{5,6} in the BM or spleen of *mtHEPOR* heterozygotes and homozygotes during adult life (Figure 3E and Figure S4). These changes in iron metabolism in the prenatal/perinatal stage and postnatal life likely reflect the dynamics and strength of opposed signals, that is, erythropoietic drive and iron stores, regulating hepcidin production.⁴⁸ A dominant factor affecting hepcidin expression in *mtHEPOR* fetuses/newborns, the erythropoietic drive, is later overridden by hepatic iron accumulation (Figure 2O,P).

Low Epo levels in *mtHEPOR* mice (Figure 3I and Figure S6A), as a physiological response to erythroid progenitors' Epo hypersensitivity²¹ (Figure 3F), were only observed after birth. During the prenatal development, Epo production in *mtHEPOR* mice was normal (Figure 3G). We suggest that this could be related to the proposed role of EPO in non-erythroid tissue/organ development.⁴⁹ Since heterodimeric EPOR complexes, found in non-erythroid cells,⁵⁰ require

higher concentrations of EPO for signaling than homodimeric EPOR,^{51,52} the attenuation of EPO synthesis might be blunted during the prenatal life of *mtHEPOR* mice. Also, fetal hypoxia and augmented glucose metabolism, indicated by significantly increased Glut1 transcripts in *mtHEPOR* FL (Figure S6B), likely linked to increased energy expenditure associated with the erythroid lineage expansion at murine FL stage,³⁶ was reported to require high EPO.⁵³

We next interrogated the changes in erythron and progenitor cell populations during the aging of *mtHEPOR* mice. We observed a progressive decline in the percentage of Ter119-positive BM cells and immature Ter119^{high}CD71^{high} erythroblasts in *mtHEPOR* heterozygotes and homozygotes with age (Figure 3E). Concomitantly, suppression of early and late erythroid progenitors' numbers and induction of non-erythroid progenitors were detected (Figure 4B) and paralleled by the upregulation of PU.1 expression (Figure 4D). Assessment of HSPCs revealed a higher increase of LSK cells in aged *mtHEPOR* mice than in *mEpoR* mice (Figure 4C), hematopoietic progenitor cell type known to increase during aging.⁵⁴ Significant increase in GMPs (Figure 4C) in aged *mtHEPOR* animals was consistent with progressive myeloid cell expansion during aging. This, together with significant induction in the number of BM megakaryocytes in old *mtHEPOR* homozygotes (Figure S8B,C), represents signs of premature hematopoietic aging.³⁸ These effects are likely due to a combination of cell-autonomous as well as microenvironmental regulations. Our earlier transplantation studies using *mtHEPOR* mice suggested BM progenitor cell-intrinsic, EPOR-driven regulation of megakaryopoiesis.⁵⁵ The megakaryocytes may then contribute to hematopoietic aging through secretion of pro-inflammatory cytokines, as do JAK2^{V617F}-positive PV megakaryocytes.⁵⁶ In agreement, age-related induction of pro-inflammatory cytokine mRNA expression was observed in the BM of mainly *mtHEPOR* homozygotes (Figure 4A), suggesting alterations in the BM microenvironment.^{38,41,54,56} Increased levels of IL-6, TGF- β , TNF- α , and/or INF- γ are known to suppress erythropoiesis.⁵⁷⁻⁶⁰ Overall, these data suggest progressive attenuation of BM erythroid drive in *mtHEPOR* homozygotes and, to a lesser extent, also in *mtHEPOR* heterozygotes when compared to *mEpoR* controls, further supported by a more profound decline in Hct levels between young and old animals of both *mtHEPOR* heterozygotes and homozygotes compared to *mEpoR* controls (Figure 1A).

The above-mentioned observations have raised the question of a possible attenuation of the EPOR signaling cascade in our model during aging. Nevertheless, our data do not favor such mechanism, since prolonged EPO-induced Jak2 and Stat5 activation appears to be maintained in *mtHEPOR* BM erythroid progenitors during aging, as demonstrated by the preserved EPO-hypersensitivity dose-response phenotype (Figure 3F) and comparable extent of Erfe induction (a Stat5 target) in individual erythroid precursors during all studied stages of postnatal development (Figure S5). Other subtle in vivo modifications of signaling downstream mutant EPOR during aging, e.g., in MAPK and Akt kinase pathways, cannot be excluded but have not been analyzed. Another intriguing possibility is that the erythroid expression of transferrin receptor 2 (TfR2) could be altered in our *mtHEPOR* model over time which could eventually affect the

presentation of EPOR/TfR2 complexes⁶¹ at the cell membrane. Indeed, dynamic changes in TfR2 mRNA expression in the erythroid cells were observed in *mtHEPOR* mice during ontogenesis (data not shown), suggesting that TfR2 may modulate EPOR surface presentation in our model. However, with respect to the complex and different regulation of the presentation of truncated EPOR on the cell membrane compared to murine EpoR,⁶² together with the fact that also Epo-dependent EpoR internalization is impaired for truncated EPOR,⁶³ only a comprehensive genetic study involving breeding of *mtHEPOR* mice with the BM-specific TfR2 knock-out mice would help to address this question.

Instead, our data suggest that *mtHEPOR* HSCs in the late adult BM may have an increased proliferative history, contributing to the relative exhaustion of progenitors with erythroid lineage-priming program in the aged marrow. In this regard, we have previously documented⁶⁴ a higher proportion of LSKs (Flt3⁺ Rh123^{low} subset of cKit⁺Sca1⁺ cells) to total BM cells in *mtHEPOR* mice than in knock-in mice expressing wild-type human EPOR gene (*wtHEPOR*) that has hypoactive EPOR signaling.^{21,65} In addition, a reduced reconstitution capacity of *mtHEPOR* HSCs compared to *wtHEPOR* HSCs was observed.^{64,66} In the current study, we revealed a significant increase in the numbers of LSKs (i.e., Lin⁻Sca-1⁺c-Kit⁺) in old *mtHEPOR* homozygotes compared to young counterparts, while this increase was less prominent in aged *mEpoR* controls. These data collectively suggest that life-lasting prolonged activation of EPOR-Jak2-Stat5 signaling promotes the proliferation of LSKs. Increased HSCs activation then presumably results in their increased proliferative history and aging that potentially leads to increased myeloid bias.⁶⁷ This could be due to a non-cell-autonomous effect of mild local BM inflammation (Figure 4A) and moderate, but detectable increase in ROS production (Figure S7C). This likely leads to paracrine signaling between HSCs and other cell types in the *mtHEPOR* BM, facilitating HSC entry into the cell cycle.⁶⁸ In addition, cell-autonomous proliferative stimuli could also play a role, as suggested by recent studies demonstrating physiological EpoR expression in a subset of HSCs and their immediate progeny.⁶⁹

In addition to age-related decline of BM erythropoiesis, we also observed a reduced lifespan of *mtHEPOR* RBCs (Figure S9B) accompanied by diminished surface expression of CD47 (Figure S9A), which inhibits phagocytosis of erythrocytes by macrophages of the reticuloendothelial system.⁴⁵ Diminished surface expression of CD47, related to enhanced erythrophagocytosis, was previously reported in other erythrocytic mouse models including Tg6 transgenic mice overexpressing Epo²⁶ and in JAK2^{V617F} PV mouse model.⁷⁰ We, therefore, propose that the enhanced clearance of RBCs together with reduced iron demand for erythropoiesis due to its age-related decline in the BM causes elevation in liver iron stores and consequent increase in *Bmp6* expression and hepcidin synthesis (Figure 2I,J,L-N).^{1,2}

We show here that in contrast to so far analyzed other mouse models of erythrocytoses,^{12,71,72} *mtHEPOR* mice neither present with postnatal iron deficiency nor with hepcidin suppression (Figure 2H-N). The absence of expansion of immature erythroblasts in the BM and spleen of *mtHEPOR* mice (Figure 3E and Figure S4) is another

distinguishing characteristic. The discrepant phenotypic manifestations between erythrocytoses with high EPO levels and our model likely result from differences in the cell-autonomous and non-cell-autonomous consequences of signaling present in erythrocytosis disorders having high EPO compared to low EPO, which is characteristic of truncated gain-of-function EPOR of affected PFCP individuals as well as observed in this mouse model. Studies using BM chimeras generated from Tg6 EPO transgenics⁷³ or *mtHEPOR* mice⁵⁵ and C57BL/6 mice as donors to C57BL/6 recipients revealed dissimilarities between erythropoiesis driven by BM HSPCs after exposure to excessive EPO versus those bearing gain-of-function EPOR. Besides the cell-intrinsic mechanisms responsible for transient (Tg6) versus sustained (*mtHEPOR*) differentiation potential of BM HSPCs toward erythroid lineage, chronic exposure to EPO⁷³ versus prolonged EPOR signaling due to EPOR gain-of-function,³⁴ may have different impacts on BM niche. In this regard, EPOR expression in non-erythroid tissues, including erythroblastic island macrophages, adipocytes, or osteoblasts^{74,75} should be taken into consideration. Moreover, a comparison of two mouse models of PV, with either V617F- or exon 12-mutant JAK2, showed that changes in iron metabolism (including Erfe and hepcidin) were more pronounced in exon 12-mutant mice relative to V617F-mutant mice.⁷¹ This fits with more prominent erythrocytosis observed in JAK2 exon 12 compared with JAK2^{V617F}-mutant mice, hypothetically related to exon 12-mutant JAK2 favoring interaction with EPOR.⁷⁶ This further indicates that qualitative differences in disordered EPOR/JAK2 signaling variously modulate iron metabolism and/or erythropoiesis itself. Moreover, the differences in the severity of phenotype between *mtHEPOR* heterozygotes and homozygotes observed in our study suggest dose-dependent alterations related to different degrees of downstream EPOR stimulation. Additional factors, absent in *mtHEPOR* mice, including systemic inflammation^{10,77} (Figure S7A) and/or HIF-mediated mechanisms^{35,78} (Figure S6B-D), may further impact iron homeostasis and erythroid drive in PV and erythrocytoses with augmented hypoxia signaling.

The absence of augmented hypoxia signaling and systemic inflammation may also prevent clonal evolution and malignant transformation of hematopoiesis with gain-of-function EPOR mutation. PFCP patients are known to carry polyclonal hematopoiesis³⁴ and do not seem to accumulate additional somatic mutations known in PV,^{79,80} although a predisposing potential of one of the activating EPOR germline variants (EPOR^{P488S}) for myeloproliferative neoplasms has recently been documented.⁸¹ The above-mentioned changes associated with *mtHEPOR* BM microenvironment are mild and do not necessarily represent permanent challenges that would contribute to an increased incidence of hematological malignancies in PFCP. Some of the observed changes we describe in *mtHEPOR* homozygous mice may not apply to individuals affected by PFCP as these patients are always heterozygotes.^{8,14} Nevertheless, a comprehensive understanding of the predisposing potential of activating EPOR germline variants for malignant transformation will require long-term monitoring of the patients and further studies.

We conclude that the erythrocytic phenotype, as well as hepcidin, Erfe, and Epo expression undergoes dynamic changes during

ontogenesis in a mouse model of congenital erythrocytosis bearing human gain-of-function EPOR. We propose that even in the absence of systemic inflammation, albeit with possible paracrine inflammatory signals, known to affect BM remodeling and hematopoietic aging, life-lasting prolonged activation of EPOR-Jak2-Stat5 signaling promoted a progressive decrease of committed erythroid progenitors and resulted in an age-related decline of accelerated erythropoiesis in *mtHEPOR* mice. Overall, our data demonstrate that in *mtHEPOR* mice with augmented effective erythropoiesis, hepcidin production is to a greater extent regulated by liver iron content which in turn reflects iron consumption by erythroid cells. Consistently with the mouse model, patients' analyses supported that ERFE is not the main regulator of hepcidin in pediatric/young adult EPOR-mutated erythrocytosis with low EPO levels (Table S1 and Figure S10).

AUTHOR CONTRIBUTIONS

Barbora Kralova: Performed most experiments, analyzed results, and contributed to manuscript writing; **Lucie Sochorcova, Jihyun Song, Ondrej Jahoda, and Katarina Hlusickova Kapralova:** Performed some experiments and analyzed results. **Vladimir Divoky:** Contributed to study design, results interpretation, and wrote the manuscript; **Josef T. Prchal:** Contributed to study design, results interpretation, and revised the manuscript. **Monika Horvathova:** Designed the research, interpreted results, and wrote the manuscript. All authors have read and agreed to the published version of the manuscript.

ACKNOWLEDGEMENTS

This work was supported by the Ministry of Health of the Czech Republic (NV19-07-00412), the project National Institute for Cancer Research (Programme EXCELES, ID Project No. LX22NPO5102) - Funded by the European Union - Next Generation EU, and the Internal grant of Palacky University (IGA_LF_2022_003). Further support (to animal facility BIO-CEV) was provided from these projects: LM 2018126 Czech Center for Phenogenomics by the Ministry of Education, Youth and Sports (MEYS) OP RDE and CZ.02.1.01/0.0/0.0/18_046/0015861 CCP Infrastructure Upgrade II by MEYS and ESIF. We thank prof. D. Pospisilova, Faculty Hospital Olomouc and Palacky University Olomouc, Czech Republic, and Dr. D. Prochazkova, J. E. Purkyne University, Usti nad Labem, Czech Republic for providing patients' clinical data and patients' sampling.

CONFLICT OF INTEREST

The authors declare no conflict of interest.

DATA AVAILABILITY STATEMENT

The data are available from the corresponding author upon reasonable request.

ORCID

Ondrej Jahoda  <https://orcid.org/0000-0001-7246-6449>

Katarina Hlusickova Kapralova  <https://orcid.org/0000-0001-6235-2915>

Vladimir Divoky  <https://orcid.org/0000-0003-0202-245X>

Monika Horvathova  <https://orcid.org/0000-0003-3857-8986>

REFERENCES

- Ganz T, Nemeth E. Hepcidin and iron homeostasis. *Biochim Biophys Acta*. 2012;1823(9):1434-1443.
- Andriopoulos B Jr, Corradini E, Xia Y, et al. BMP6 is a key endogenous regulator of hepcidin expression and iron metabolism. *Nat Genet*. 2009;41(4):482-487.
- Ganz T, Nemeth E. Iron homeostasis in host defense and inflammation. *Nat Rev Immunol*. 2015;15(8):500-510.
- Kautz L, Jung G, Valore EV, Rivella S, Nemeth E, Ganz T. Identification of erythroferrone as an erythroid regulator of iron metabolism. *Nat Genet*. 2014;46(7):678-684.
- Ganz T. Erythropoietic regulators of iron metabolism. *Free Rad Biol Med*. 2019;133:69-74.
- Kautz L, Jung G, Du X, et al. Erythroferrone contributes to hepcidin suppression and iron overload in a mouse model of β-thalassemia. *Blood*. 2015;126(17):2031-2037.
- Coffey R, Jung G, Olivera JD, et al. Erythroid overproduction of erythroferrone causes iron overload and developmental abnormalities in mice. *Blood*. 2022;139(3):439-451.
- Prchal JT. Primary and secondary Erythrocytoses/polycythemias. In Kaushansky K, Lichtman MA, Prchal JT, Levi M, Burns LJ, Linch DC, eds. *Williams Hematology*, 10th ed. McGraw Hill; 2021: 941-960.
- Ang SO, Chen H, Hirota K, et al. Disruption of oxygen homeostasis underlies congenital Chuvash polycythemia. *Nat Genet*. 2002;32: 614-621.
- Gordeuk VR, Miasnikova GY, Sergueeva AI, et al. Chuvash polycythemia VHLR200W mutation is associated with down-regulation of hepcidin expression. *Blood*. 2011;118(19):5278-5282.
- Ruschitzka FT, Wenger RH, Stallmach T, et al. Nitric oxide prevents cardiovascular disease and determines survival in polyglobulic mice overexpressing erythropoietin. *Proc Natl Acad Sci USA*. 2000;97(21): 11609-11613.
- Díaz V, Gammella E, Recalcati S, et al. Liver iron modulates hepcidin expression during chronically elevated erythropoiesis in mice. *Hepatology*. 2013;58(6):2122-2132.
- James C, Ugo V, Le Couédic JP, et al. A unique clonal JAK2 mutation leading to constitutive signalling causes polycythaemia vera. *Nature*. 2005;434(7037):1144-1148.
- Prchal JT, Crist WM, Goldwasser E, Perrine G, Prchal JF. Autosomal dominant polycythemia. *Blood*. 1985;66(5):1208-1214.
- Arber DA, Orazi A, Hasserjian R, et al. The 2016 revision to the World Health Organization classification of myeloid neoplasms and acute leukemia. *Blood*. 2016;127(20):2391-2405.
- Ginzburg YZ, Feola M, Zimran E, Varkonyi J, Ganz T, Hoffman R. Dysregulated iron metabolism in polycythemia vera: etiology and consequences. *Leukemia*. 2018;32(10):2105-2116.
- de la Chapelle A, Träskelin AL, Juvonen E. Truncated erythropoietin receptor causes dominantly inherited benign human erythrocytosis. *Proc Natl Acad Sci USA*. 1993;90(10):4495-4499.
- Sokol L, Luhovy M, Guan Y, Prchal JF, Semenza GL, Prchal JT. Primary familial polycythemia: a frameshift mutation in the erythropoietin receptor gene and increased sensitivity of erythroid progenitors to erythropoietin. *Blood*. 1995;86(1):15-22.
- Arcasoy MO, Harris KW, Forget BG. A human erythropoietin receptor gene mutant causing familial erythrocytosis is associated with deregulation of the rates of Jak2 and Stat5 inactivation. *Exp Hematol*. 1999; 27(1):63-74.
- Huang LJ, Shen YM, Bulut GB. Advances in understanding the pathogenesis of primary familial and congenital polycythemia. *Br J Haematol*. 2010;148(6):844-852.
- Divoky V, Liu Z, Ryan TM, Townes TM, Prchal JT. Mouse model of congenital polycythemia: homologous replacement of murine gene by mutant human erythropoietin receptor gene. *Proc Natl Acad Sci USA*. 2001;98(3):986-991.

22. Divoky V, Song J, Horvathova M, et al. Delayed hemoglobin switching and perinatal neocytolysis in mice with gain-of-function erythropoietin receptor. *J Mol Med (Berl)*. 2016;94(5):597-608.
23. Horvathova M, Kapralova K, Zidova Z, Dolezal D, Pospisilova D, Divoky V. Erythropoietin-driven signaling ameliorates the survival defect of DMT1-mutant erythroid progenitors and erythroblasts. *Haematologica*. 2012;97(10):1480-1488.
24. Shammas FV, Engeset A. Glycogen content and PAS staining pattern of human megakaryocytes. *Scand J Haematol*. 1986;37(3):237-242.
25. Socolovsky M, Nam H, Fleming MD, Haase VH, Brugnara C, Lodish HF. Ineffective erythropoiesis in Stat5a^{-/-}/Stat5b^{-/-} mice due to decreased survival of early erythroblasts. *Blood*. 2001;98(12):3261-3273.
26. Bogdanova A, Mihov D, Lutz H, Saam B, Gassmann M, Vogel J. Enhanced erythro-phagocytosis in polycythemic mice overexpressing erythropoietin. *Blood*. 2007;110(2):762-769.
27. Garcia-Santos D, Hamdi A, Saxova Z, et al. Inhibition of heme oxygenase ameliorates anemia and reduces iron overload in a β-thalassemia mouse model. *Blood*. 2018;131(2):236-246.
28. Akel A, Wagner CA, Kovacikova J, et al. Enhanced suicidal death of erythrocytes from gene-targeted mice lacking the cl-HCO(3)(-) exchanger AE1. *M J Physiol Cell Physiol*. 2007;292(5):C1759-C1767.
29. Zidova Z, Kapralova K, Koralkova P, et al. DMT1-mutant erythrocytes have shortened life span, accelerated glycolysis and increased oxidative stress. *Cell Physiol Biochem*. 2014;34(6):2221-2231.
30. Zadrazil J, Horak P, Horcicka V, Zahalkova J, Strebl P, Hruba M. Endogenous erythropoietin levels and anemia in long-term renal transplant recipients. *Kidney Blood Press Res*. 2007;30(2):108-116.
31. Lucarelli G, Howard D, Stohlman F Jr. Regulation of erythropoiesis. XV. Neonatal erythropoiesis and the effect of nephrectomy. *J Clin Invest*. 1964;43(11):2195-2203.
32. Xavier-Ferrucio J, Scanlon V, Li X, et al. Low iron promotes megakaryocytic commitment of megakaryocytic-erythroid progenitors in humans and mice. *Blood*. 2019;134(18):1547-1557.
33. Watowich SS, Xie X, Klingmuller U, et al. Erythropoietin receptor mutations associated with familial erythrocytosis cause hypersensitivity to erythropoietin in the heterozygous state. *Blood*. 1999;94(7):2530-2532.
34. Pasquier F, Marty C, Balligand T, et al. New pathogenic mechanisms induced by germline erythropoietin receptor mutations in primary erythrocytosis. *Haematologica*. 2018;103(4):575-586.
35. Kapralova K, Lanikova L, Lorenzo F, et al. RUNX1 and NF-E2 upregulation is not specific for MPNs, but is seen in polycythemic disorders with augmented HIF signaling. *Blood*. 2014;123(3):391-394.
36. Montel-Hagen A, Blanc L, Boyer-Clavel M, et al. The Glut1 and Glut4 glucose transporters are differentially expressed during perinatal and postnatal erythropoiesis. *Blood*. 2008;112(12):4729-4738.
37. Pietras EM. Inflammation: a key regulator of hematopoietic stem cell fate in health and disease. *Blood*. 2017;130(15):1693-1698.
38. Ho YH, Del Toro R, Rivera-Torres J, et al. Remodeling of bone marrow hematopoietic stem cell niches promotes myeloid cell expansion during premature or physiological aging. *Cell Stem Cell*. 2019;25(3):407-418.e6.
39. Roy A, Wang G, Iskander D, et al. Transitions in lineage specification and gene regulatory networks in hematopoietic stem/progenitor cells over human development. *Cell Rep*. 2021;36(11):109698.
40. Zhao JL, Ma C, O'Connell RM, et al. Conversion of danger signals into cytokine signals by hematopoietic stem and progenitor cells for regulation of stress-induced hematopoiesis. *Cell Stem Cell*. 2014;14(4):445-459.
41. Cho RH, Sieburg HB, Muller-Sieburg CE. A new mechanism for the aging of hematopoietic stem cells: aging changes the clonal composition of the stem cell compartment but not individual stem cells. *Blood*. 2008;111(12):5553-5561.
42. Rekhtman N, Choe KS, Matushansky I, Murray S, Stopka T, Skoultschi AI. PU.1 and pRB interact and cooperate to repress GATA-1 and block erythroid differentiation. *Mol Cell Biol*. 2003;23(21):7460-7474.
43. Ganz T. Macrophages and systemic iron homeostasis. *J Innate Immun*. 2012;4(5-6):446-453.
44. Lee SJ, Park SY, Jung MY, Bae SM, Kim IS. Mechanism for phosphatidylserine-dependent erythrophagocytosis in mouse liver. *Blood*. 2011;117(19):5215-5223.
45. Oldenborg PA, Zheleznyak A, Fang YF, Lagenaar CF, Gresham HD, Lindberg FP. Role of CD47 as a marker of self on red blood cells. *Science*. 2000;288(5473):2051-2054.
46. Mojzikova R, Koralkova P, Holub D, et al. Iron status in patients with pyruvate kinase deficiency: neonatal hyperferritinemia associated with a novel frameshift deletion in the PKLR gene (p.Arg518fs), and low hepcidin to ferritin ratios. *Br J Haematol*. 2014;165(4):556-563.
47. Sulovska L, Holub D, Zidova Z, et al. Characterization of iron metabolism and erythropoiesis in erythrocyte membrane defects and thalassemia traits. *Biomed Pap Med Fac Univ Palacky Olomouc Czech Repub*. 2016;160(2):231-237.
48. Huang H, Constante M, Layoun A, Santos MM. Contribution of STAT3 and SMAD4 pathways to the regulation of hepcidin by opposing stimuli. *Blood*. 2009;113(15):3593-3599.
49. Suresh S, Rajvanshi PK, Noguchi CT. The many facets of erythropoietin physiologic and metabolic response. *Front Physiol*. 2020;10:1534.
50. Brines M, Grasso G, Fiordaliso F, et al. Erythropoietin mediates tissue protection through an erythropoietin and common beta-subunit heteroreceptor. *Proc Natl Acad Sci USA*. 2004;101(41):14907-14912.
51. Broxmeyer HE. Erythropoietin: multiple targets, actions, and modifying influences for biological and clinical consideration. *J Exp Med*. 2013;210(2):205-208.
52. Zhang YL, Radhakrishnan ML, Lu X, Gross AW, Tidor B, Lodish HF. Symmetric signaling by an asymmetric 1 erythropoietin: 2 erythropoietin receptor complex. *Mol Cell*. 2009;33(2):266-274.
53. Teng R, Gavrilova O, Suzuki N, et al. Disrupted erythropoietin signaling promotes obesity and alters hypothalamus proopiomelanocortin production. *Nat Commun*. 2011;2:520.
54. Valletta S, Thomas A, Meng Y, et al. Micro-environmental sensing by bone marrow stroma identifies IL-6 and TGFβ1 as regulators of hematopoietic ageing. *Nat Commun*. 2020;11(1):4075.
55. Huang X, Pierce LJ, Chen GL, Chang KT, Spangrude GJ, Prchal JT. Erythropoietin receptor signaling regulates both erythropoiesis and megakaryopoiesis in vivo. *Blood Cells Mol Dis*. 2010;44(1):1-6.
56. Lee S, Wong H, Castiglione M, Murphy M, Kaushansky K, Zhan H. JAK2V617F mutant megakaryocytes contribute to hematopoietic aging in a murine model of myeloproliferative neoplasm. *Stem Cells*. 2022;40(4):359-370.
57. McCranor BJ, Kim MJ, Cruz NM, et al. Interleukin-6 directly impairs the erythroid development of human TF-1 erythroleukemic cells. *Blood Cells Mol Dis*. 2014;52(2-3):126-133.
58. Zermati Y, Fichelson S, Valensi F, et al. Transforming growth factor inhibits erythropoiesis by blocking proliferation and accelerating differentiation of erythroid progenitors. *Exp Hematol*. 2000;28(8):885-894.
59. Johnson RA, Waddelow TA, Caro J, Oliff A, Roodman GD. Chronic exposure to tumor necrosis factor in vivo preferentially inhibits erythropoiesis in nude mice. *Blood*. 1989;74(1):130-138.
60. Wang CQ, Udupa KB, Lipschitz DA. Interferon-gamma exerts its negative regulatory effect primarily on the earliest stages of murine erythroid progenitor cell development. *J Cell Physiol*. 1995;162(1):134-138.
61. Forejtniková H, Vieillevoye M, Zermati Y, et al. Transferrin receptor 2 is a component of the erythropoietin receptor complex and is required for efficient erythropoiesis. *Blood*. 2010;116(24):5357-5367.

62. Watowich SS. The erythropoietin receptor: molecular structure and hematopoietic signaling pathways. *J Invest Med.* 2011;59(7):1067-1072.
63. Sulahian R, Cleaver O, Huang LJ. Ligand-induced EpoR internalization is mediated by JAK2 and p85 and is impaired by mutations responsible for primary familial and congenital polycythemia. *Blood.* 2009; 113(21):5287-5297.
64. Chen GL, Chang K, Huang X, Spangrude GJ, Prchal JT. Erythropoietin signaling inhibits long term marrow reconstitution. *Blood.* 2006; 108(11):912a Abstract 3194.
65. Divoky V, Prchal JT. Mouse surviving solely on human erythropoietin receptor (EpoR): model of human EpoR-linked disease. *Blood.* 2002; 99(10):3873-3874.
66. Chang K, Pastore YD, Nussenzveig RH, Prchal JT. Erythropoietin signaling inhibits the short-term marrow reconstitution. *Blood.* 2005; 106(11):848a Abstract 3028.
67. Orford KW, Scadden DT. Deconstructing stem cell self-renewal: genetic insights into cell-cycle regulation. *Nat Rev Genet.* 2008;9: 115-128.
68. Haas S, Trumpp A, Milsom MD. Causes and consequences of hematopoietic stem cell heterogeneity. *Cell Stem Cell.* 2018;22(5):627-638.
69. Zhang H, Wang S, Liu D, et al. EpoR-tdTomato-Cre mice enable identification of EpoR expression in subsets of tissue macrophages and hematopoietic cells. *Blood.* 2021;138(20):1986-1997.
70. Wang W, Liu W, Fidler T, et al. Macrophage inflammation, Erythrophagocytosis, and accelerated atherosclerosis in Jak2^{V617F} mice. *Circ Res.* 2018;123(11):e35-e47.
71. Grisouard J, Li S, Kubovcakova L, et al. JAK2 exon 12 mutant mice display isolated erythrocytosis and changes in iron metabolism favoring increased erythropoiesis. *Blood.* 2016;128(6):839-851.
72. Wilkinson N, Pantopoulos K. IRP1 regulates erythropoiesis and systemic iron homeostasis by controlling HIF2α mRNA translation. *Blood.* 2013;122(9):1658-1668.
73. Singh RP, Grinenko T, Ramasz B, et al. Hematopoietic stem cells but not multipotent progenitors drive erythropoiesis during chronic erythroid stress in EPO transgenic mice. *Stem Cell Reports.* 2018;10(6): 1908-1919.
74. Noguchi CT, Wang L, Rogers HM, Teng R, Jia Y. Survival and proliferative roles of erythropoietin beyond the erythroid lineage. *Expert Rev Mol Med.* 2008;10:e36.
75. Li W, Wang Y, Zhao H, et al. Identification and transcriptome analysis of erythroblastic Island macrophages. *Blood.* 2019;134(5):480-491.
76. Kota J, Caceres N, Constantinescu SN. Aberrant signal transduction pathways in myeloproliferative neoplasms. *Leukemia.* 2008;22(10): 1828-1840.
77. Spivak JL. Polycythemia Vera. *Curr Treat Options Oncol.* 2018; 19(2):12.
78. Gangaraju R, Song J, Kim SJ, et al. Thrombotic, inflammatory, and HIF-regulated genes and thrombosis risk in polycythemia vera and essential thrombocythemia. *Blood Adv.* 2020;4(6):1115-1130.
79. Rives S, Pahl HL, Florena L. Molecular genetic analyses in familial and sporadic congenital primary erythrocytosis. *Haematologica.* 2007; 92(5):674-677.
80. Al-Sheikh M, Mazurier E, Gardie B. A study of 36 unrelated cases with pure erythrocytosis revealed three new mutations in the erythropoietin receptor gene. *Haematologica.* 2008;93(7):1072-1075.
81. Rabadan Moraes G, Pasquier F, Marzac C, et al. An inherited gain-of-function risk allele in EPOR predisposes to familial JAK2V617F myeloproliferative neoplasms. *Br J Haematol.* 2022;198(1):131-136.

SUPPORTING INFORMATION

Additional supporting information can be found online in the Supporting Information section at the end of this article.

How to cite this article: Kralova B, Sochorcova L, Song J, et al. Developmental changes in iron metabolism and erythropoiesis in mice with human gain-of-function erythropoietin receptor. *Am J Hematol.* 2022;1-14. doi:10.1002/ajh.26658

Supplemental data for Kralova et al.

Supplemental Methods

Housing and breeding of mice

Heterozygous males and females were intercrossed to produce experimental mice of all studied genotypes (*mEpoR/mtHEPOR* and *mtHEPOR* mutants and *mEpoR* controls). Male mice were weaned at 4 weeks, maintained on a standard diet (iron content 176 mg/kg, Ssniff), and sacrificed at indicated time-points. Mice were bred and maintained in the pathogen-free barrier facility of the Center for Laboratory Animals, Palacky University or of the Institute of Molecular Genetics of the Academy of Sciences and Charles University (BIOCEV) in Vestec, Czech Republic.

Assessment of hematological parameters, spleen size, and detection of megakaryocytes

Hematological parameters were determined using Hematology Analyzer MEK-6550 (Nihon Kohden). Blood smears were stained by standard procedure using May Grunwald-Giemsa (MGG) stain for assessment of red blood cell (RBC) morphology or new methylene blue (Merck) for detection of reticulocytes. Spleen weight index was calculated as the ratio of spleen weight to gross bodyweight. Periodic acid-Schiff (PAS) method was used to detect megakaryocytes in the BM,¹ the slides were counterstained with hematoxylin. The slides were analyzed by light microscopy.

Iron status parameters

Tissue non-heme iron concentration was measured by modified colorimetric assay.² Briefly, 50 mg of tissue samples were cut and digested in 0,5mL acid solution for 24 hours at 65°C. The extract was added to 1.5 mL of chromogen and the solution absorbance was measured at 540nm after 15 min using NanoQuant infinite M200 (TECAN). A standard curve was plotted using ammonium iron (II) sulfate hexahydrate diluted - chromogen solution in increasing concentrations.

Transferrin saturation was calculated based on the values of serum iron levels and unsaturated iron binding capacity measured by Modular Analytics SWA Evo (Roche, Hitachi) using the commercial kits from Roche (#1876996 and #2146398) (F. Hoffmann-La Roche Ltd).

Deparaffinized tissue sections were stained with the Perls' Prussian blue stain for non-heme iron and counterstained with nuclear fast red.²

RNA isolation and real-time PCR analysis

RNA from liver or spleen tissue and flushed bone marrow (BM) cells was extracted using QIAshredder and Rneasy Mini Kit (Qiagen) or using TRI Reagent (Merck), respectively. One µg of RNA was reverse transcribed with SuperScript VILO Master Mix (ThermoFisher Scientific) or Transcriptor First Strand cDNA Synthesis Kit (Roche) where the RNA was pretreated with TURBO DNA-free Kit (ThermoFisher Scientific). q-PCR was performed using TaqMan Gene Expression Master Mix (Applied Biosystems), LightCycler 480 Probes Master Mix or LightCycler 480 SYBR Green I Master (both from Roche) depending on used primers and/or probes as specified below. Relative gene expression was normalized against housekeeping gene β -Actin and calculated in LightCycler 480 Software (Roche) using advanced relative quantification method. The primers and/or probes used for reactions are specified below.

The list of TaqMan® Gene Expression probes:

Epo - Mm01202755_m1; *Erfe* (*Fam132b*) - Mm00557748_m1; *Id1* - Mm00775963_g1; *Smad7* - Mm00484742_m1; *Ifn-gamma* - Mm01168134_m1; *PU.1* - Mm00488140_m1, *Gata1* - Mm01352636; *Cited2* - Mm00516121_m1; *Hk1* - Mm00439344_m1; *Ldha* - Mm01612132_g1; *Pgk1* - Mm00435617_m1; *Serpine1* - Mm00435858_m1; *Slc2a1* - Mm00441480_m1; *Vegfa* - Mm00437306_m1; *Gypa* - Mm00494848_m1; and β -Actin -Mm00607939_s1.

The list of UPL probes and primers:

IL-6: probe #6 (cat. no. 04685032001)
F: 5' GATGGATGCTACCAAACTGGAT 3'
R: 5' CCAGGTAGCTATGGTACTCCAGA 3'

Tnf-alpha: probe #49 (cat. no. 04688104001)
F: 5' TGC CTA TGT CTC AGC CTC TTC - 3'
R: 5' GAG GCC ATT TGG GAA CTT CT - 3'

β -*Actin*: probe #56 (cat. no. 04688538001)
F: 5' AAGGCCAACCGTGAAAAGAT 3'
R: 5' GTGGTACGACCAGAGGCATAC 3'

The list of primers for SYBR Green:

Hamp (*Hepc1*) F: 5' CCTGAGCAGCACCCACCTATCT 3'
R: 5' TCAGGATGTGGCTCTAGGCTATGT 3'

Bmp6 F: 5' AACAGCTTGCAAGAACATGAG 3'
R: 5' TGGACCAAGGTCTGTACAATGG 3'

Tgf-beta1 F: 5' TCGACAACAAAATAGAGCAAGC 3'

R: 5' CTTTGATCTGCTCCTTCAGAACT 3'

β -Actin F: 5' TCAACACCCCAGCCATGTA 3'
 R: 5' GTGGTACGACCAGAGGCATAC 3'

Enzyme-linked immunosorbent assay (ELISA)

Serum hepcidin and ferritin levels were quantified using the Hepcidin-Murine Compete ELISA (Intrinsic LifeSciences) and Ferritin (FTL) Mouse Elisa kit (Abcam), respectively according to the manufacturer's instructions. Mouse cytokine array (micro-elisa quantification) for determination of serum concentrations of IL-6, tumor necrosis factor- α (Tnf- α), and interferon- γ (Ifn- γ) was performed as a custom service by RayBiotech. Transforming growth factor- β (TGF- β) was measured using TGF beta-1 Mouse ELISA Kit (Thermo Fisher Scientific) as per manufacturer's instructions. The serum levels of Epo in neonatal (7 days old) and young adult (8 to 12 weeks old) mice were quantified according to the manufacturer's instructions for the Mouse Erythropoietin Quantikine ELISA Kit (R&D Systems).

Flow cytometry analysis of hematopoietic stem and progenitor cells

Multi-parameter flow cytometry analysis of hematopoietic stem and progenitor cell (HSPC) populations was performed as a custom service by the Czech Centre for Phenogenomics (BIOCEV/IMG). The EasySep™ Mouse Hematopoietic Cell Isolation Kit was used to isolate stem and progenitor cells from single-cell suspension of BM cells by negative selection with biotinylated antibodies directed against CD5, CD11b, CD19, CD45R/B220, Ly6G/C(Gr-1), TER119, 7-4 and streptavidin-coated magnetic particles (RapidSpheres™). The following primary conjugated antibodies and stains were used for subsequent staining:

Antigen	Fluorochrome	Manufacturer
Lineage Cocktail: CD3, Ly-6G/Ly-6C, CD11b, CD45R/B220, TER-119	PB	BioLegend
CD48	BV510	BioLegend
CD34	FITC	Thermo Fisher Scientific
Sca-1	PerCP-Cy5.5	BioLegend
CD135	PE	Thermo Fisher Scientific
CD150	PE-Cy7	BioLegend
c-kit	APC	BioLegend
FcRg	APC-Cy7	BioLegend
viability	Hoechst 33258	Sigma-Aldrich

The results were analyzed by BD LSRFortessa SORP (BD Biosciences).

Hematopoietic colony assay and EPO sensitivity testing

M3334 media and 1×10^5 BM cells were used for the detection of colony forming unit-erythroid (CFU-E) colonies as we described.³ M3534 media, with the addition of 1 U of recombinant human EPO (rh, Janssen Pharmaceuticals) per mL of media and 5×10^4 BM cells were used for the detection of colonies derived from colony forming unit (CFU) – granulocyte, erythroid, macrophage, megakaryocyte (CFU-GEMM) progenitor, burst forming unit-erythroid (BFU-E) progenitor and additional types of non-erythroid progenitors: CFU-granulocyte, macrophage (CFU-GM), CFU-granulocyte (CFU-G), and CFU-macrophage (CFU-M). In parallel experiments, rh EPO (Janssen Pharmaceuticals) dose–responses of BM-derived cells were tested. MethoCult medium M3236 with addition of 20% (vol/vol) fetal bovine serum (Thermo Fisher Scientific) and M3534 medium, both supplemented with appropriate doses of rh EPO, were used for CFU-E and BFU-E sensitivity assay, respectively. The cells were incubated at 37°C, 5% CO₂ and 21% O₂. CFU-E colonies were scored by standard morphologic criteria on day 3; CFU-GEMM, BFU-E, and non-erythroid colonies at day 10, under an inverted microscope (Olympus).

Reactive oxygen species (ROS) measurements

ROS levels in murine serum were determined using OxiSelect *In Vitro* ROS/RNS Assay kit (Thermo Fisher Scientific) according to the manufacturer's instructions. Fluorescence was measured on a FACS Calibur (BD Bioscience).

References:

1. Shammas FV, Engeset A. Glycogen content and PAS staining pattern of human megakaryocytes. *Scand J Haematol.* 1986;37(3):237-242.
2. Horvathova M, Kapralova K, Zidova Z, Dolezal D, Pospisilova D, Divoky V. Erythropoietin-driven signaling ameliorates the survival defect of DMT1-mutant erythroid progenitors and erythroblasts. *Haematologica.* 2012;97(10):1480-1488.
3. Garcia-Santos D, Hamdi A, Saxova Z, Fillebeen C, Pantopoulos K, Horvathova M, Ponka P. Inhibition of heme oxygenase ameliorates anemia and reduces iron overload in a β-thalassemia mouse model. *Blood.* 2018;131(2):236-246.
4. Socolovsky M, Nam H, Fleming MD, Haase VH, Brugnara C, Lodish HF. Ineffective erythropoiesis in Stat5a-/-5b-/- mice due to decreased survival of early erythroblasts. *Blood.* 2001; 98(12):3261-3273.

Table S1. Selected hematological and biochemical data of patients with *EPAS1*- and *EPOR*-mutated erythrocytosis

	<i>EPAS1 – mutant patients</i>		<i>EPOR – mutant patients</i>			
	<i>EPAS1 mut#1</i>	<i>EPAS1 mut#2</i>	<i>EPOR mut#1</i>	<i>EPOR mut#2</i>	<i>EPOR mut#3</i>	<i>EPOR mut#4</i>
Sex/age (yr)	M/1.5	F/5	F/36	M/10	M/11	M/13
RBC parameters Normal Range						
HCT 2-12 yr [0.35-0.40] Adults [0.35-0.44]	0.52	0.54 ± 0.02	0.51 ± 0.02	0.62 ± 0.05	0.56 ± 0.04	0.57 ± 0.02
MCV (fL) 2-6 yr [72-87] 6-12 yr [76-90]	72.6	89.1 ± 2.3	NA	81.7 ± 0.9	86.3 ± 3.9	89.1 ± 1.1
MCH (pg) 2-6 yr [23.1-29.6] 6-12 yr [27-33]	23.9	31.7 ± 0.7	NA	28.4 ± 0.2	30.6 ± 0.7	31.1 ± 0.8
MCHC (g/L) 2-12 yr [32-37] Adults [27-31]	32.9	35.6 ± 0.1	NA	34.8 ± 0.6	35.5 ± 0.7	35.0 ± 0.7
Iron Status						
sFe (μM) 2-12 yr [8.95-21.5] Female [14.5-26]	16.9	25.7 ± 4.9	NA	15.0 ± 7.6	16.0 ± 8.5	10.5 ± 1.1
Ferritin (ng/mL) 2-12 yr [6-140] Female [20-150]	29.5	27.6 ± 3.9	NA	24.6 ± 0.5	20.0 ± 8.5	11.2 ± 4.2
TSAT (%) [21-48]	13.0	13 ± 1.4	NA	18.6 ± 8.6	14.4 ± 5.1	18.0 ± 2.8
EPO [IU/L] [3.5 - 17.0]	7.3	10.4	< 1	0.3	1.5	2.4
Hepcidin [ng/mL] [1.75 - 4.57]	x	x	3.35	2.07	NA	NA
ERFE [ng/mL] [0.0 - 0.5]	3.29	2.56	x	x	NA	NA

Values indicate means \pm SDs; mut: mutant; yr: years; M: male; F: female; red blood cells (RBCs); HCT: hematocrit; MCV: mean corpuscular volume; MCH: mean corpuscular hemoglobin; MCHC: mean corpuscular hemoglobin concentration; sFe: serum iron; TSAT: transferrin saturation; EPO: erythropoietin; ERFE: erythroferrone; NA: not available; x below detection limit.

Figure S1

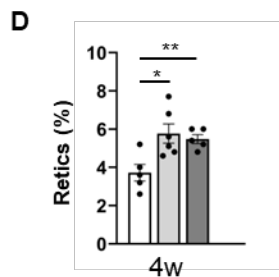
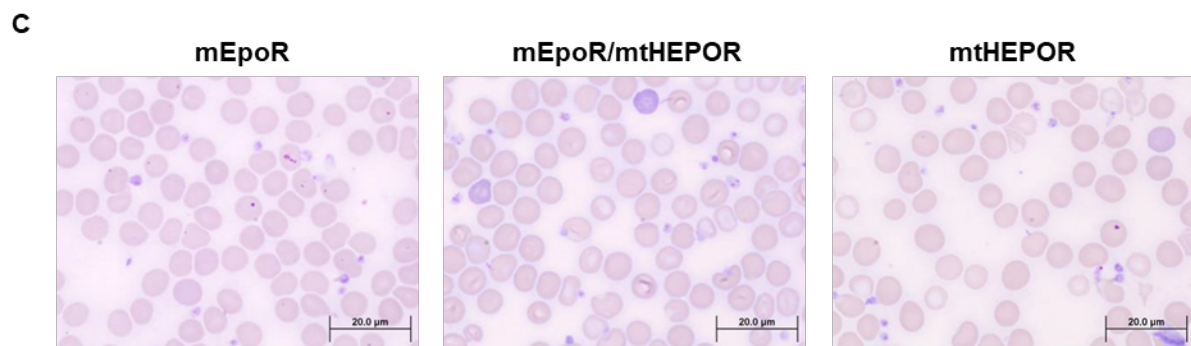
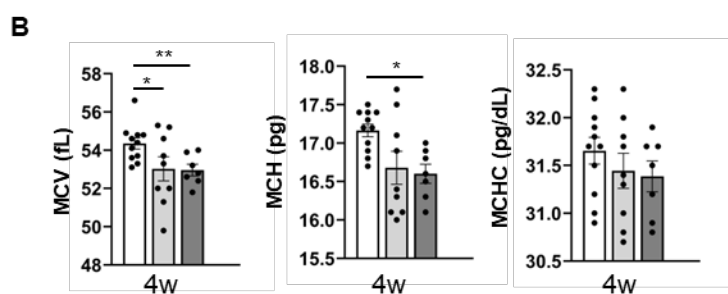
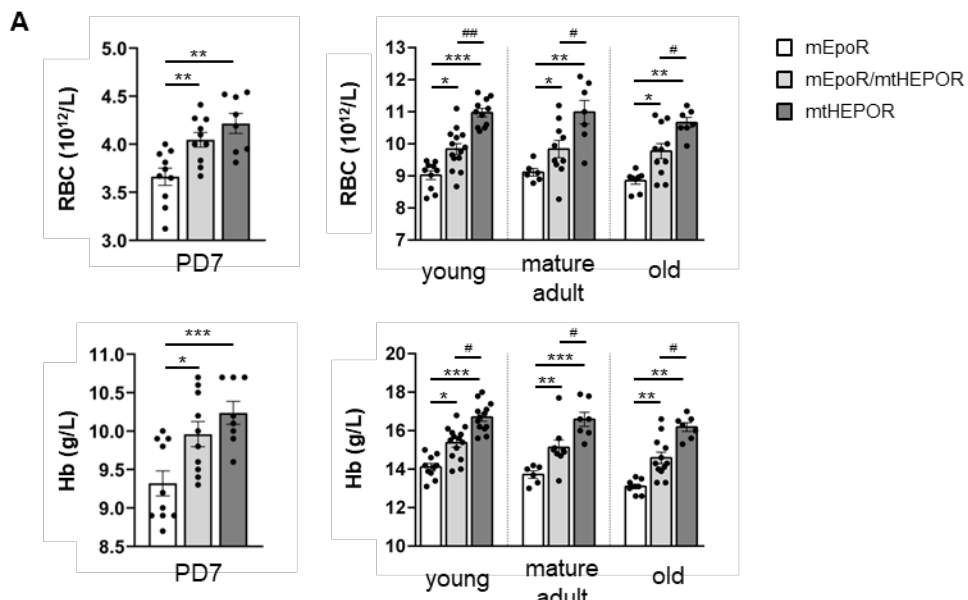


Figure S1. Evaluation of red blood cell (RBC) count and hemoglobin (Hb) levels during perinatal and postnatal period (A) and assessment of red blood cell indices, blood smears, and reticulocytes in four-weeks-old mice (4w) (B-D). RBC and Hb levels in mice of different postnatal age: postnatal day 7 (PD7), ~2.5 months old (young), ~6.5 months old (mature adult), and ~16 months old (old) mice (A). Mean corpuscular volume (MCV), mean corpuscular hemoglobin (MCH), and mean corpuscular hemoglobin concentration (MCHC) (B). Blood smears stained with May-Grünwald–Giemsa stain for assessment of red blood cell morphology (C). The slides were analyzed with an Olympus BX51 light microscope (Olympus); original magnification x1000 (1.4 NA objective), scale bars 20 μ M. Digital images were acquired with an Olympus DP70 camera driven by DP controller software (provided by Olympus). Images were cropped, assembled, and labeled using Adobe Photoshop software (Adobe Systems). Percentage of reticulocytes (Retics) (D). Values indicate mean \pm SEM; * P < 0.05, ** P < 0.01, *** P < 0.001 vs. *mEpoR*; # P < 0.05 and ## P < 0.01, *mtHEPOR* vs. *mEpoR/mtHEPOR* calculated by Welch's correction.

Figure S2

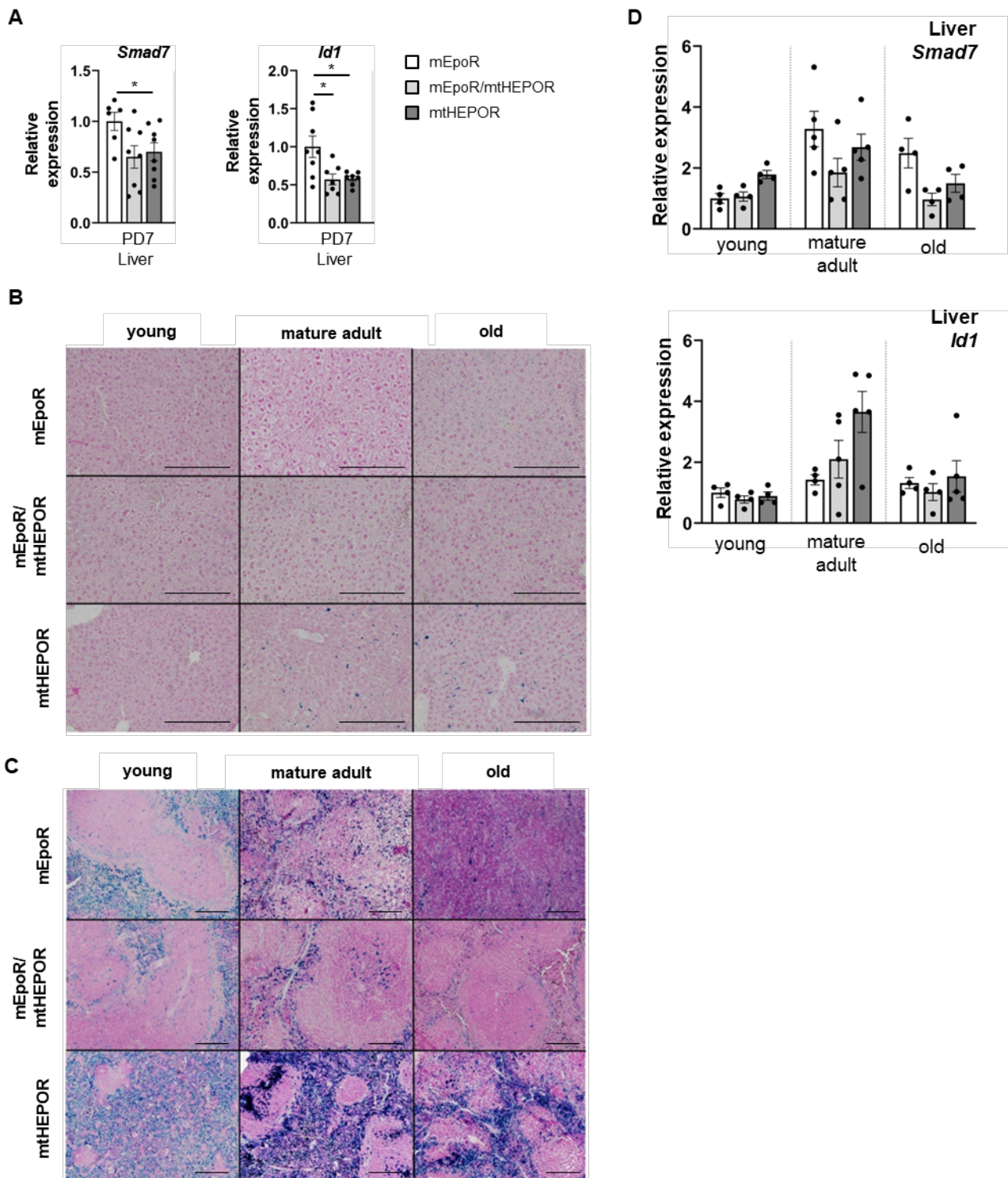


Figure S2. Expression of bone morphogenic protein (Bmp) target genes (A, D) and tissue iron content (B, C). Hepatic mRNA expression of *Smad7* and *Id1* at postnatal day 7 (A, PD7) and during postnatal life (D) was analyzed by q-PCR; β -Actin mRNA expression was used for target gene

expression normalization. In Panel D the expression is presented as fold change relative to young *mEpoR* controls. Error bars indicate mean \pm SEM; * $P < 0.05$ vs. *mEpoR* by unpaired t-test with Welch's correction; n ≥ 4 mice per group and genotype. Tissue iron content was visualized by Perls' staining (blue stain for iron) of liver (**B**) and spleen (**C**) tissue sections. The slides were analyzed using an Olympus BX51 light microscope (Olympus); for liver: original magnification x200 (NA 0.5 objective), scale bars 200 μ M; for spleen original magnification x100 (NA 0.3 objective), scale bars 200 μ M. Digital images were acquired with an Olympus DP70 camera driven by DP controller software (Olympus). Images were cropped, assembled, and labeled using Adobe Photoshop software (Adobe Systems).

Figure S3

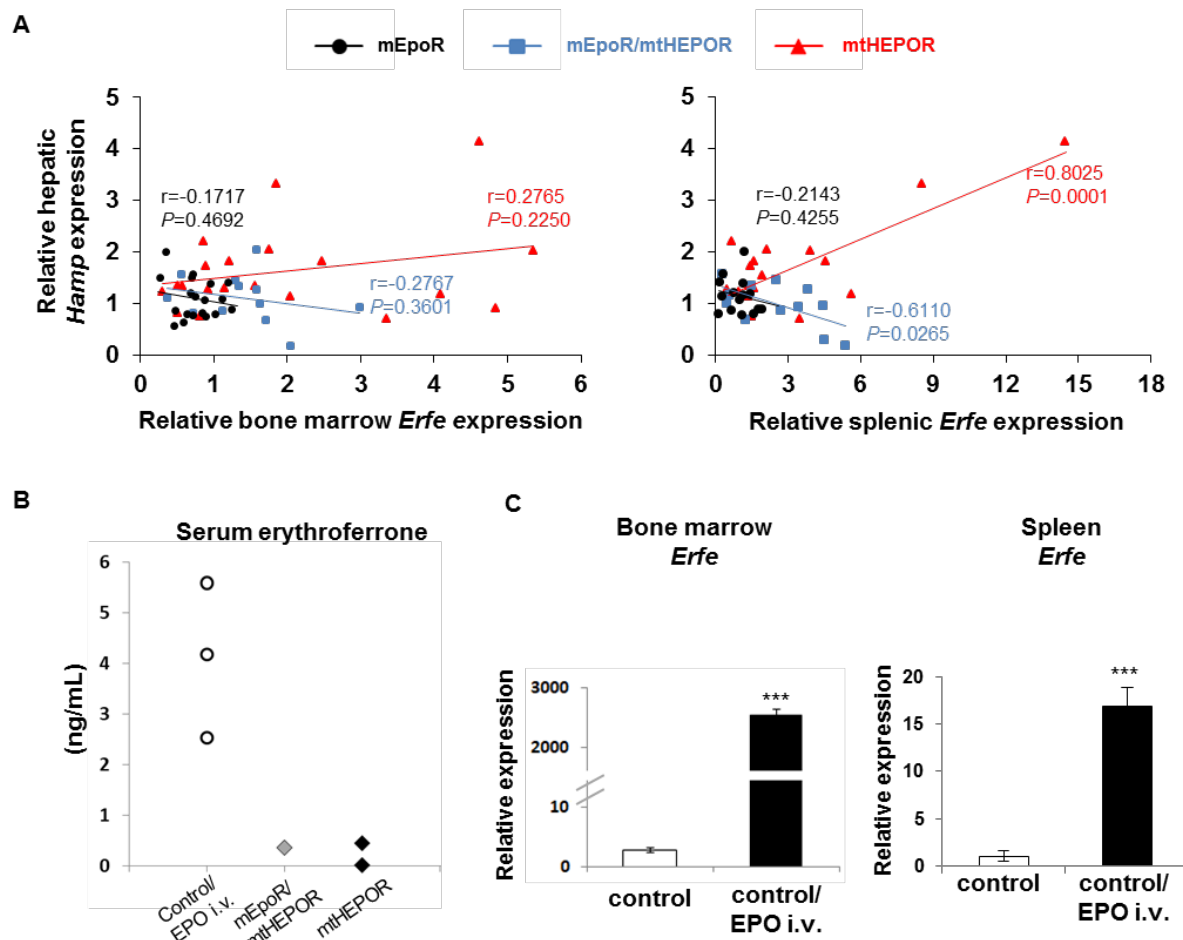


Figure S3. Correlation between erythroferrone (*Erfe*) and hepcidin (*Hamp*) expression (A), quantification of *Erfe* in the serum (B), and *Erfe* mRNA expression in control mice treated with erythropoietin (EPO, C). Correlation analysis (A) was performed between hepatic *Hamp*/ β -Actin mRNA and *Erfe*/ β -Actin mRNA expression in the BM (left panel) and spleen (right panel) of *mEpoR*, *mEpoR/mtHEPOR*, and *mtHEPOR* mice during postnatal life using Pearson correlation coefficient. Serum erythroferrone levels (B) in samples showing values greater than 0 ng/mL: i.e., control mice treated with *i.v.* EPO¹ (n = 3), one young *mEpoR/mtHEPOR* heterozygote and one young and one mature adult *mtHEPOR* homozygote. The assay included *mEpoR* controls (n = 16), *mEpoR/mtHEPOR* (n = 12) and *mtHEPOR* mice (n = 12) of different postnatal age (young, mature adult or old). *Erfe* mRNA expression in the bone marrow and spleen of EPO-treated control mice (C) was analyzed by q-PCR. Relative *Erfe* mRNA expression (normalized to β -Actin) is presented as fold change to non-treated *mEpoR* control group. Error bars indicate mean \pm SEM; n \geq 3 per each group. ***P < 0.001 vs. non-treated controls calculated by Student's t-test.

Figure S4

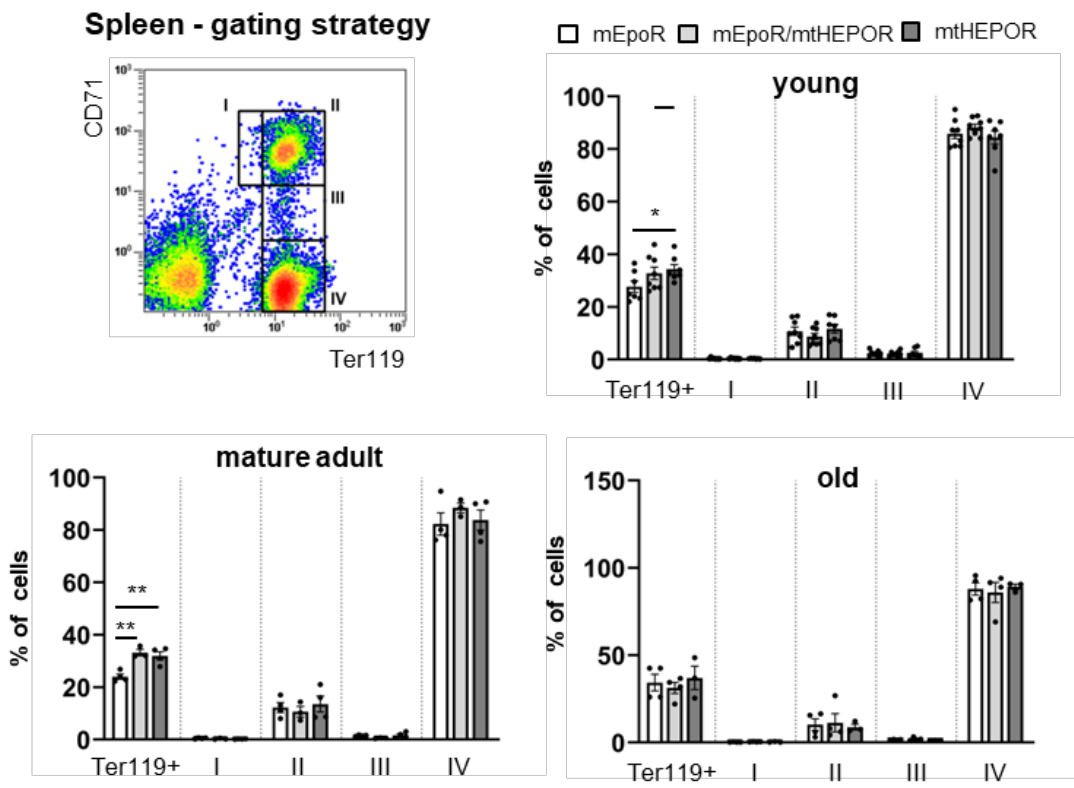


Figure S4. Distribution of maturation stages of erythroid precursors in the spleen during postnatal life. CD71 and Ter119 expression on spleen cells in young, mature adult, and old mice of *mEpoR*, *mEpoR/mtHEPOR*, *mtHEPOR* genotype was quantified by flow cytometry analysis ($n \geq 3$ per each group and genotype). Cells were divided into the regions based on the level of Ter119 and CD71 expression according to Socolovsky et al.⁴ * $P < 0.05$, ** $P < 0.01$ vs. *mEpoR* by unpaired t-test with Welch's correction.

Figure S5

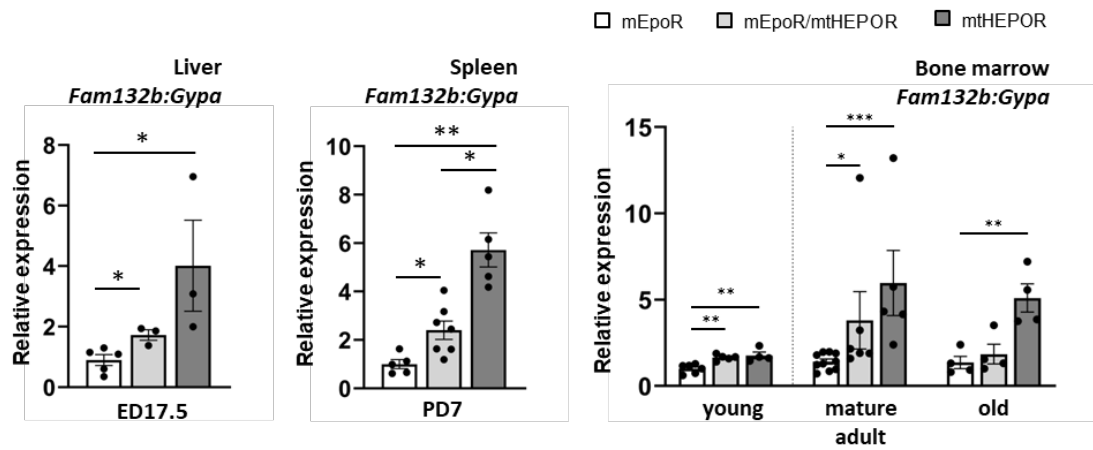


Figure S5. Quantification of erythroferrone (*Erfe*) mRNA expression per individual erythroid cell.
Erfe mRNA expression analyzed by q-PCR at different stages of ontogenesis was normalized to glycophorin A (*Gypa*) expression. The expression at embryonic day (ED)17.5 and postnatal day 7 (PD7) is presented as fold change relative to *mEpoR* controls; for later postnatal stages relative to young *mEpoR* controls. Error bars indicate mean \pm SEM; n \geq 3 per each group. *P < 0.05, **P < 0.01, ***P < 0.001 calculated by Student's t-test.

Figure S6

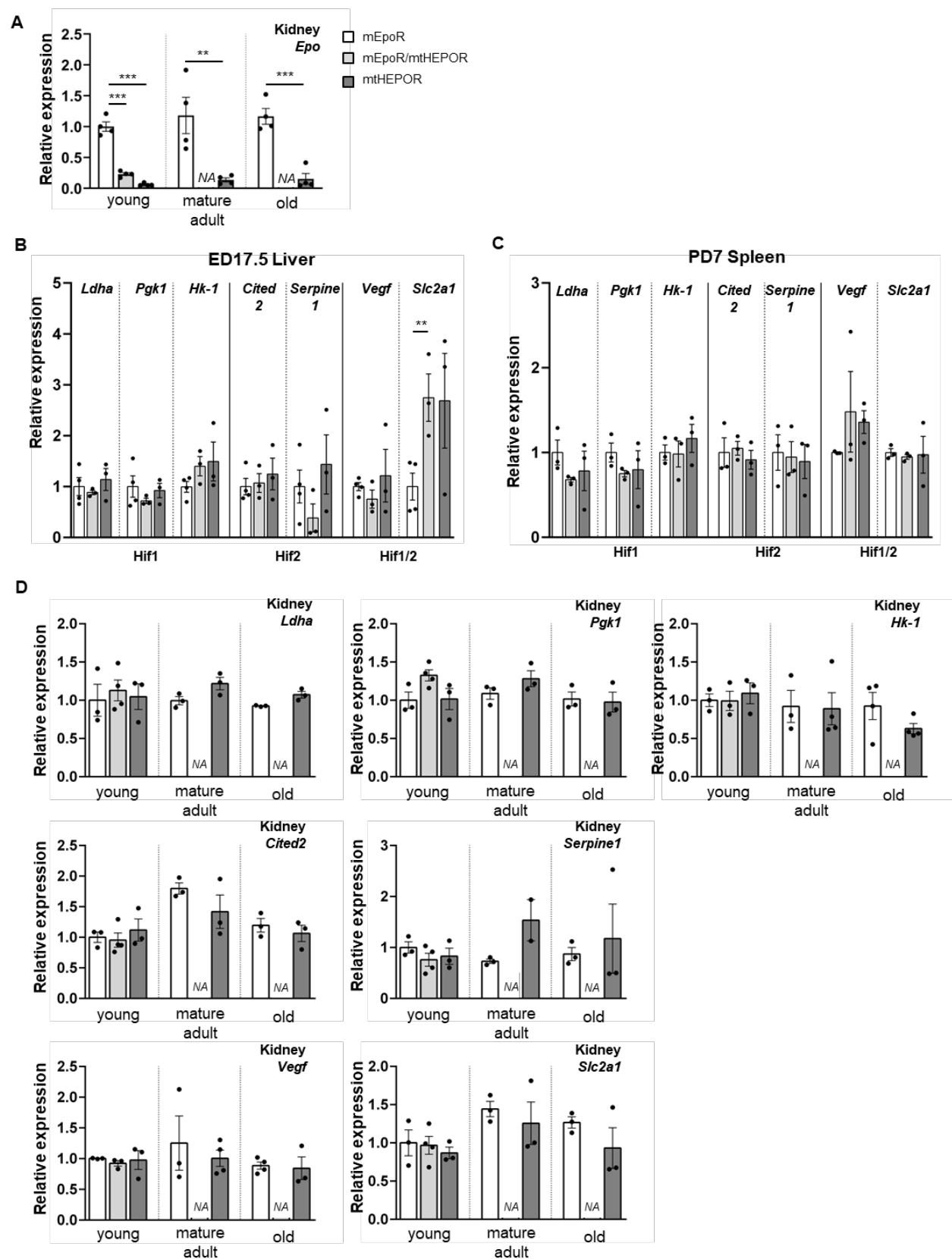


Figure S6. Erythropoietin (*Epo*, A) and hypoxia inducible transcription factors (HIFs) target genes (B – D) expression. Relative mRNA expression of *Epo* (A) in the kidney during different stages of postnatal life was normalized to β -*Actin* and is presented as a fold change relative to young *mEpoR* controls expression. The expression of selected Hif1, Hif2, and Hif1/2 target genes in fetal liver at ED17.5 (B), neonatal spleen at PD7 (C), and kidney of young, mature adult and old mice (D) was normalized to β -*Actin* and to the expression of age-matched *mEpoR* controls (Panels B and C); normalized target gene expression during different stages of postnatal life (Panel D) is presented as fold change relative to young *mEpoR* controls. NA – not available. Error bars indicate mean \pm SEM; n \geq 3 per each group and genotype; ** P < 0.01, *** P < 0.001 vs. *mEpoR* calculated by unpaired t-test with Welch's correction.

Figure S7

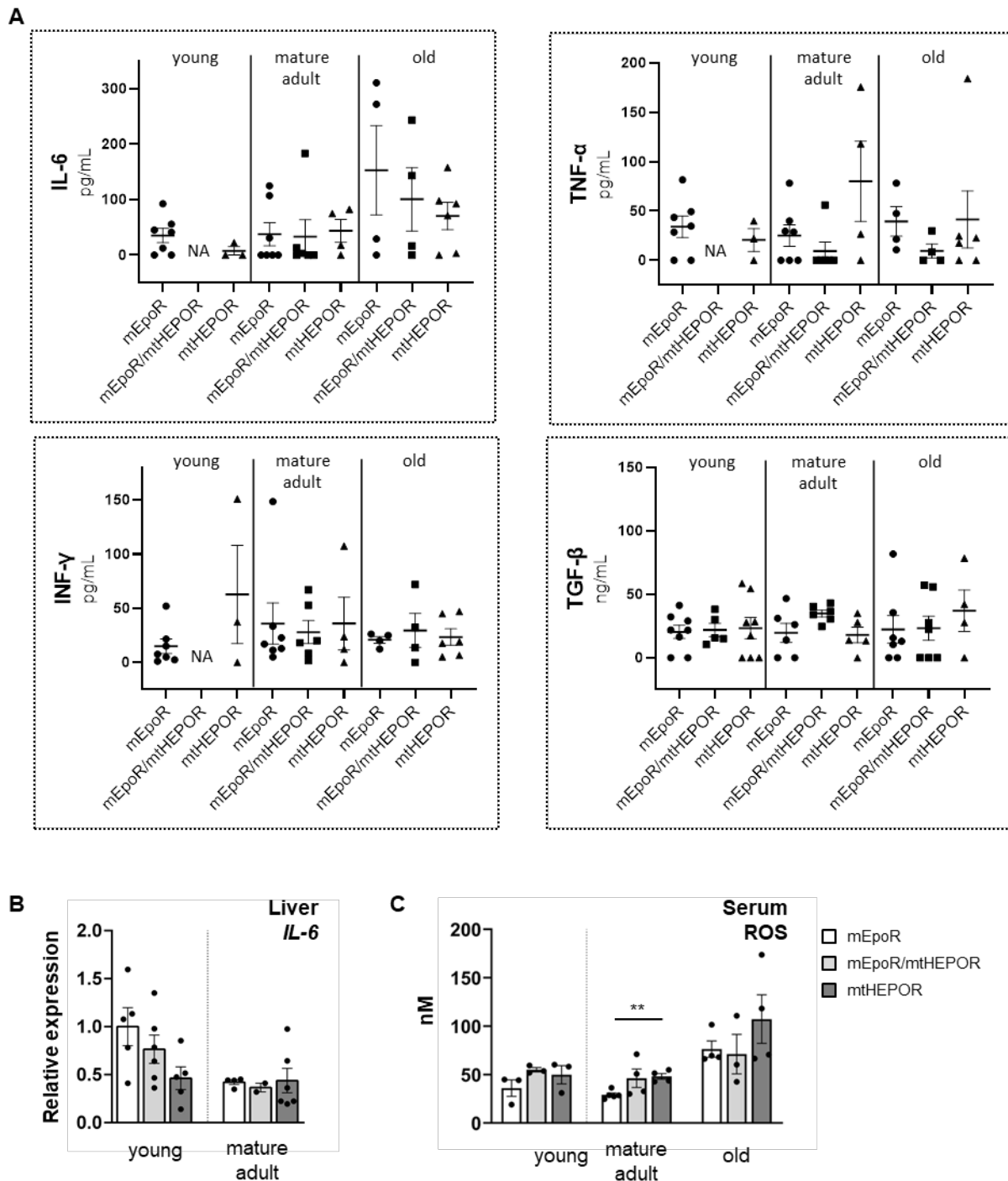


Figure S7. Evaluation of inflammatory cytokines in murine serum (A), IL-6 mRNA expression in the liver (B), and serum reactive oxygen species (ROS) levels (C). Mouse cytokine array for determination of serum concentrations of IL-6, Tnf- α , and Ifn- γ was performed as a custom service by RayBiotech; TGF- β was measured using ELISA (A). Serum samples of young, mature adult, and old mice of *mEpoR*, *mEpoR/mtHEPOR*, and *mtHEPOR* genotype were evaluated.

Individual values are presented in a dot plot depicting mean with error bars showing standard deviations (SDs). NA – not available. Hepatic *IL-6* mRNA expression (**B**), normalized to β -Actin, was analyzed by q-PCR; the expression is presented as fold change relative to young *mEpoR* control group (n ≥ 2 mice per group and genotype). ROS levels (**C**) were measured in serum samples of young, mature adult, and old mice of *mEpoR*, *mEpoR/mtHEPOR*, and *mtHEPOR* genotype. Values in Panels B and C indicate mean ± SEM; **P < 0.01 vs. *mEpoR* by unpaired t-test with Welch's correction. No statistically significant differences were detected for data presented in Panels A and B.

Figure S8

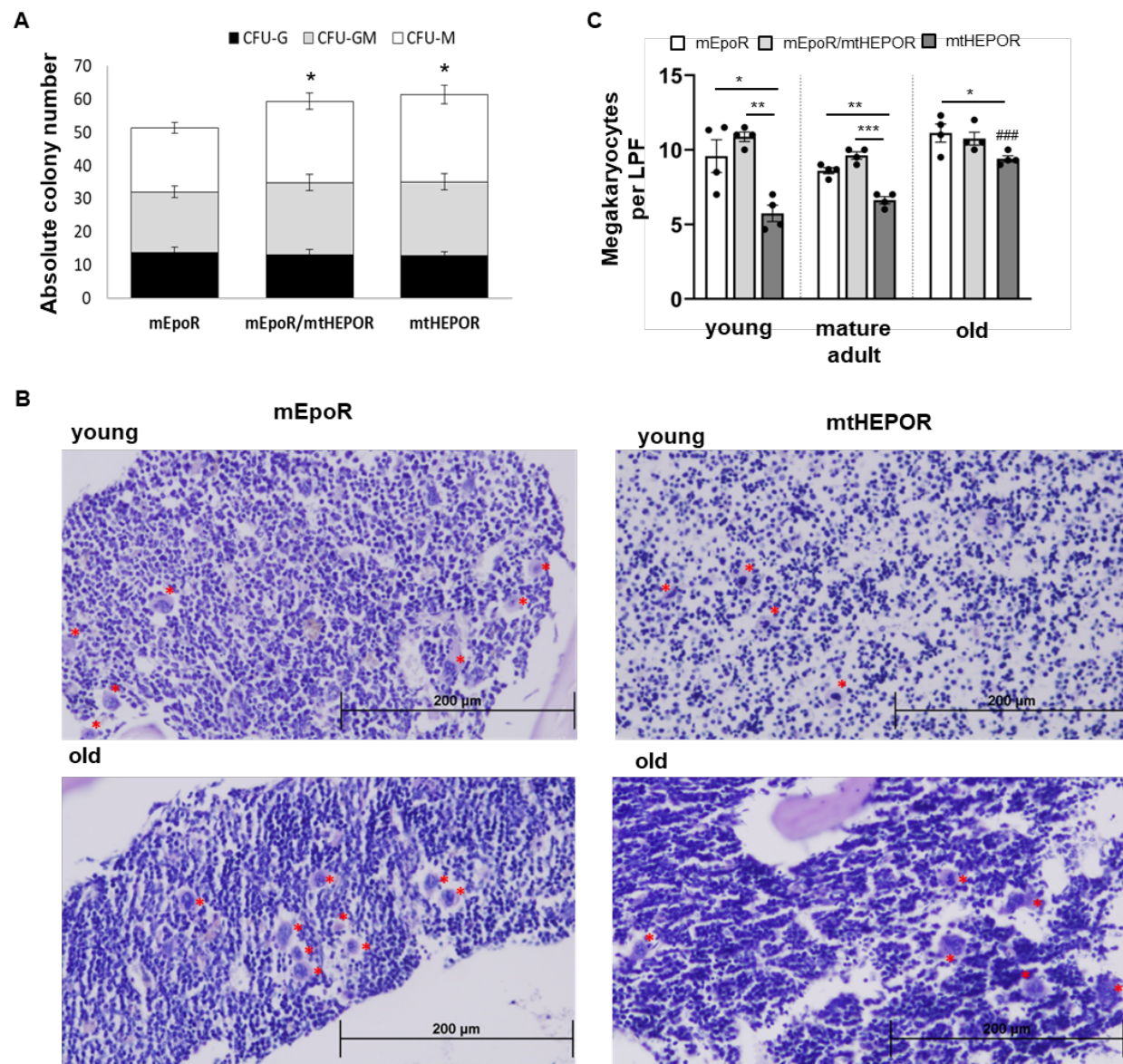


Figure S8. Assessment of non-erythroid bone marrow-derived colonies (A) and detection of megakaryocytes in the bone marrow (B-C). CFU-G, CFU-GM, and CFU-M colonies (A) were enumerated in methylcellulose cultures of bone marrow cells isolated from old mice under an inverted microscope (CKX41, Olympus); ($n = 3$ each group and genotype). Periodic acid-Schiff (PAS) method was used to stain megakaryocytes, marked with an asterisk (B), in the bone marrow of young, mature adult, and old *mEpoR/mtHEPOR*, *mtHEPOR*, and *mEpoR* control mice ($n = 4$ each group and genotype); the slides were counterstained with hematoxylin. The slides were analyzed with an Olympus BX51 light microscope (Olympus); original magnification $\times 200$ (0.5 NA objective), scale bars 200 μm . Digital images were acquired with an Olympus DP70 camera driven by DP

controller software (provided by Olympus). Images were cropped, assembled, and labeled using Adobe Photoshop software (Adobe Systems). The absolute number of megakaryocytes, detected per 20X (low-power) field (LPF) (**C**). Values indicate mean \pm SEM. * $P < 0.05$, ** $P < 0.01$, *** $P < 0.001$; ### $P < 0.001$ young vs. old *mtHEPOR*; both by unpaired t-test with Welch's correction.

Figure S9

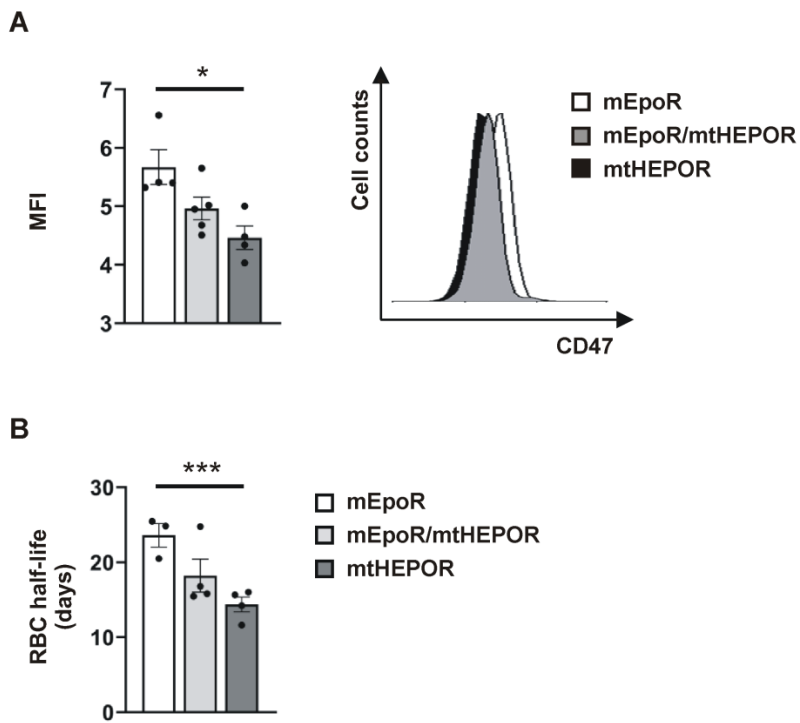


Figure S9. CD47 red blood cell (RBC) surface expression (A) and RBC half-life (B). CD47 expression on the surface of RBCs isolated from young *mEpoR*, *mEpoR/mtHEPOR*, and *mtHEPOR* mice measured by flow cytometry using FITC-labeled anti-CD47 antibody; a representative histogram is shown on the right side (A). RBC half-life. The fluorescence of CFSE-labeled RBCs, injected into the tail veins of *mEpoR* mice (day 0, set 100%), was tracked for 35 days (at day 1, 2, 7, 14, 21, 28, and 35) and the values were plotted against the day of sampling. For each mouse analyzed, an exponential regression equation was determined and used to calculate the RBC half-life presented in the graph (B). Values indicate mean \pm SEM. * $P < 0.05$, *** $P < 0.001$ vs. *mEpoR* by unpaired t-test with Welch's correction; $n \geq 3$ per each genotype.

Figure S10

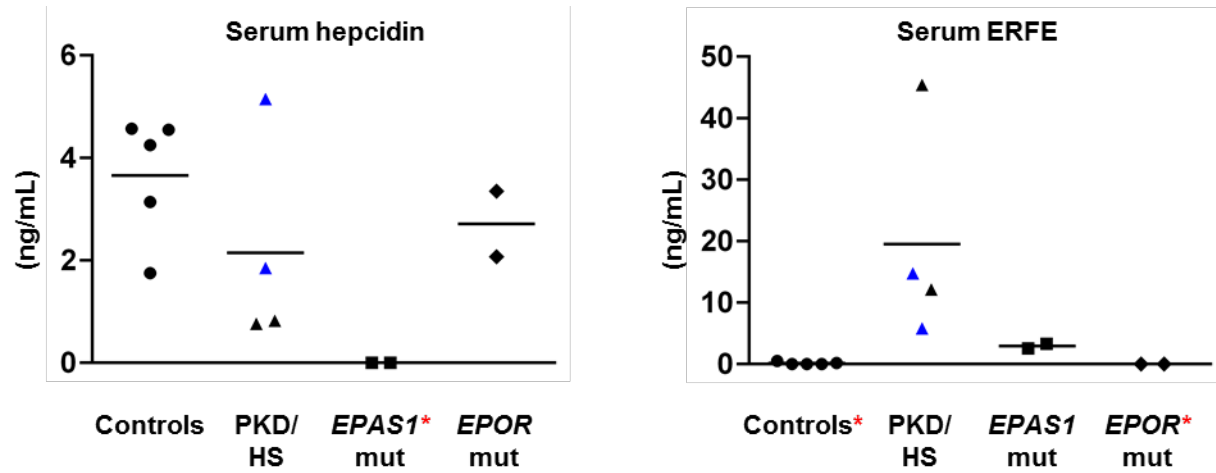


Figure S10. Hepcidin and erythroferrone (ERFE) serum levels in human subjects. Controls (n=5): age-matched to *EPAS1*-mutant (*EPAS1* mut, n=2) and *EPOR*-mutant (*EPOR* mut, n=2) patients (see Table S1); PKD/HS (n=4): patients with pyruvate kinase deficiency or hereditary spherocytosis. Blue triangles denote PKD/HS patients affected by iron overload; *(red asterisks): denote that hepcidin levels in both *EPAS1* mut patients as well as ERFE levels in both *EPOR* mut patients and three out of five controls were below the detection limit.

Príloha 3

Kapralova K, Horvathova M, Pecquet C, Fialova Kucerova J, Pospisilova D, Leroy E,
Kralova B, Milosevic Feenstra JD, Schischlik F, Kralovics R, Constantinescu SN,
Divoky V

Cooperation of germline JAK2 mutations E846D and R1063H in hereditary erythrocytosis
with megakaryocytic atypia.

Blood. 2016; 128(10):1418-1423.

MYELOID NEOPLASIA

Cooperation of germ line JAK2 mutations E846D and R1063H in hereditary erythrocytosis with megakaryocytic atypia

Katarina Kapralova,^{1,3,*} Monika Horvathova,^{1,*} Christian Pecquet,^{2,3,*} Jana Fialova Kucerova,¹ Dagmar Pospisilova,⁴ Emilie Leroy,^{2,3} Barbora Kralova,¹ Jelena D. Milosevic Feenstra,⁵ Fiorella Schischlik,⁵ Robert Kralovics,⁵ Stefan N. Constantinescu,^{2,3} and Vladimir Divoky¹

¹Department of Biology, Faculty of Medicine and Dentistry, Palacký University, Olomouc, Czech Republic; ²Signal Transduction and Molecular Hematology Unit, Ludwig Institute for Cancer Research, Brussels, Belgium; ³de Duve Institute, Université catholique de Louvain, Brussels, Belgium; ⁴Department of Pediatrics, University Hospital and Faculty of Medicine and Dentistry, Olomouc, Czech Republic; and ⁵CeMM Research Center for Molecular Medicine of the Austrian Academy of Sciences, Vienna, Austria

Key Points

- Cells expressing JAK2 E846D or R1063H exhibit pathologic STAT5 activation in the specific context of EPOR.
- Cooperation of germ line JAK2 mutations E846D and R1063H defines a JAK2-signaling threshold for induction of erythrocytosis.

The role of somatic JAK2 mutations in clonal myeloproliferative neoplasms (MPNs) is well established. Recently, germ line JAK2 mutations were associated with polyclonal hereditary thrombocytosis and triple-negative MPNs. We studied a patient who inherited 2 heterozygous JAK2 mutations, E846D from the mother and R1063H from the father, and exhibited erythrocytosis and megakaryocytic atypia but normal platelet number. Culture of erythroid progenitors from the patient and his parents revealed hypersensitivity to erythropoietin (EPO). Using cellular models, we show that both E846D and R1063H variants lead to constitutive signaling (albeit much weaker than JAK2 V617F), and both weakly hyperactivate JAK2/STAT5 signaling only in the specific context of the EPO receptor (EPOR). JAK2 E846D exhibited slightly stronger effects than JAK2 R1063H and caused prolonged EPO-induced phosphorylation of JAK2/STAT5 via EPOR. We propose that JAK2 E846D predominantly contributes to erythrocytosis, but is not sufficient for the full pathological phenotype to develop. JAK2 R1063H, with very weak effect on JAK2/STAT5 signaling, is necessary to augment JAK2 activity caused by E846D above a threshold level leading to erythrocytosis with megakaryocyte abnormalities. Both mutations were detected in the germ line of rare polycythemia vera, as well as certain leukemia patients, suggesting that they might predispose to hematological malignancy. (*Blood*. 2016;128(10):1418-1423)

Introduction

Somatic JAK2 mutations are the most common disease-causing event in patients with myeloproliferative neoplasms (MPNs). In the majority of MPN patients, an acquired gain-of-function V617F JAK2 mutation leads to constitutive activation of the JAK2 kinase and subsequently to excessive activation of JAK/STAT signaling.¹⁻⁴ Recently, germ line JAK2 mutations (different from V617F substitution) have been described in cases with familial MPNs exhibiting hereditary polyclonal thrombocytosis⁵⁻⁷ and triple-negative MPNs.⁸ All of these inherited JAK2 mutations, localized in the kinase and pseudokinase domain of JAK2, signal through the thrombopoietin receptor (MPL) rather than the erythropoietin (EPO) receptor (EPOR), explaining the phenotype of the polyclonal disease. It is proposed that differential signaling of STATs leads to different clinical phenotypes associated with different activating JAK2 mutations: essential thrombocythemia and hereditary thrombocytosis being promoted by MPL/STAT1 signaling; STAT5 activation resulting in excessive erythroid proliferation and polycythemia vera (PV).^{6,9}

Here, we studied a patient who inherited 2 JAK2 mutations and presented with erythrocytosis and abnormal megakaryopoiesis in the

bone marrow (BM), partially resembling PV cases with JAK2 exon 12 mutations.¹⁰ Thus, in contrast to previously studied germ line JAK2 mutations, which were all heterozygous, here mutations on both JAK2 alleles are present. We show that both of these mutations are activating in the context of EPOR, but with different characteristics. Functional analyses of the 2 germ line JAK2 mutations suggested the threshold of JAK2 activity necessary for induction of erythrocytosis.

Study design

Descriptions of assays and tests performed on patient's samples can be found in supplemental Materials and methods (available on the *Blood* Web site).

Ba/F3-EPOR¹¹ JAK2 stable transfectants or γ-2A cells were used in viability and proliferation assays, analyses of JAK2 signal transduction, and dual-luciferase assays for STAT transcriptional activities. Retrovirally transduced mouse BM cells were used for in vitro colony assay. Analysis of x-ray crystallography data was performed using PyMOL software. For detailed descriptions of individual procedures, see supplemental Materials and methods.

Submitted February 10, 2016; accepted June 30, 2016. Prepublished online as *Blood* First Edition paper, July 7, 2016; DOI 10.1182/blood-2016-02-698951.

*K.K., M.H., and C.P. contributed equally to this work.

The online version of this article contains a data supplement.

The publication costs of this article were defrayed in part by page charge payment. Therefore, and solely to indicate this fact, this article is hereby marked "advertisement" in accordance with 18 USC section 1734.

© 2016 by The American Society of Hematology

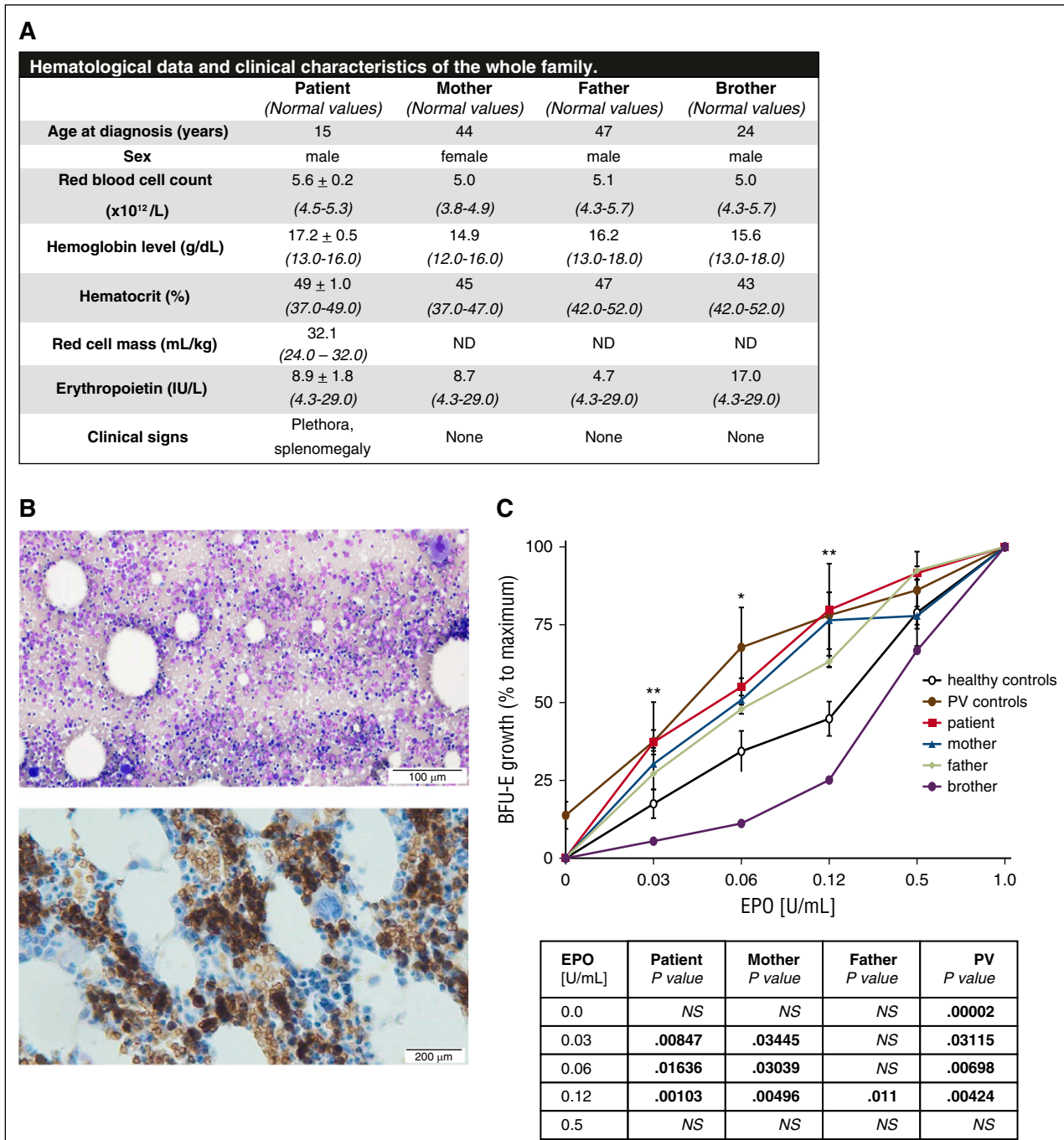


Figure 1. Hematological parameters, clinical data, BM evaluation, and in vitro sensitivity assay of erythroid progenitors to EPO. (A) Hematological and clinical analysis of the propositus and his family members revealed erythrocytosis, plethora, and palpable spleen (splenic length of 12 cm based on ultrasound measurement) in the patient. ND, not done. (B) Patient's BM aspirate (May-Grünwald-Giemsa staining, top) and BM biopsy (glycophorin C staining specific for erythroid lineage, brown color, bottom) showed hypercellularity, erythroid hyperplasia, normal granulopoiesis, and abnormal megakaryopoiesis (for details, see supplemental Figure 1). The images were visualized with an Olympus BX41 light microscope (Hamburg, Germany) and acquired with an Olympus DP73 camera driven by CellSens Entry software. Images were labeled using Adobe Photoshop software (Adobe Systems, San Jose, CA). Top: magnification, $\times 100$; scale bar, 100 μm . Bottom: magnification, $\times 200$; scale bar, 200 μm . (C) The EPO dose-response curves derived from the patient, patient's brother, patient's parents, normal controls, and PV patients. The growth of BFU-E colonies at the indicated concentrations of EPO was expressed as a percentage of maximal EPO stimulation (represented by EPO concentration of 1 U/mL). Erythroid progenitors from the patient (red curve) were hypersensitive to EPO; there was a relatively higher number of BFU-E colonies in comparison with healthy controls (black curve) in low EPO concentrations. The in vitro growth of the erythroid progenitors of both of the patient's parents (blue and green curve, respectively) also showed slightly increased sensitivity to EPO when compared with normal controls (black curve). The progenitors of the patient's brother (purple curve) showed normal growth. Two PV patients, positive for the V617F mutation (brown curve), were used as positive controls for hypersensitivity and formation of EPO-independent colonies (EECs). The table below the graph shows statistical evaluation of the BFU-E colony number at individual concentrations with respect to normal controls. P values were calculated using Origin 6.1 software (OriginLab Corporation, Norhampton, MA, USA). *P < .05; **P < .01. NS, not significant.

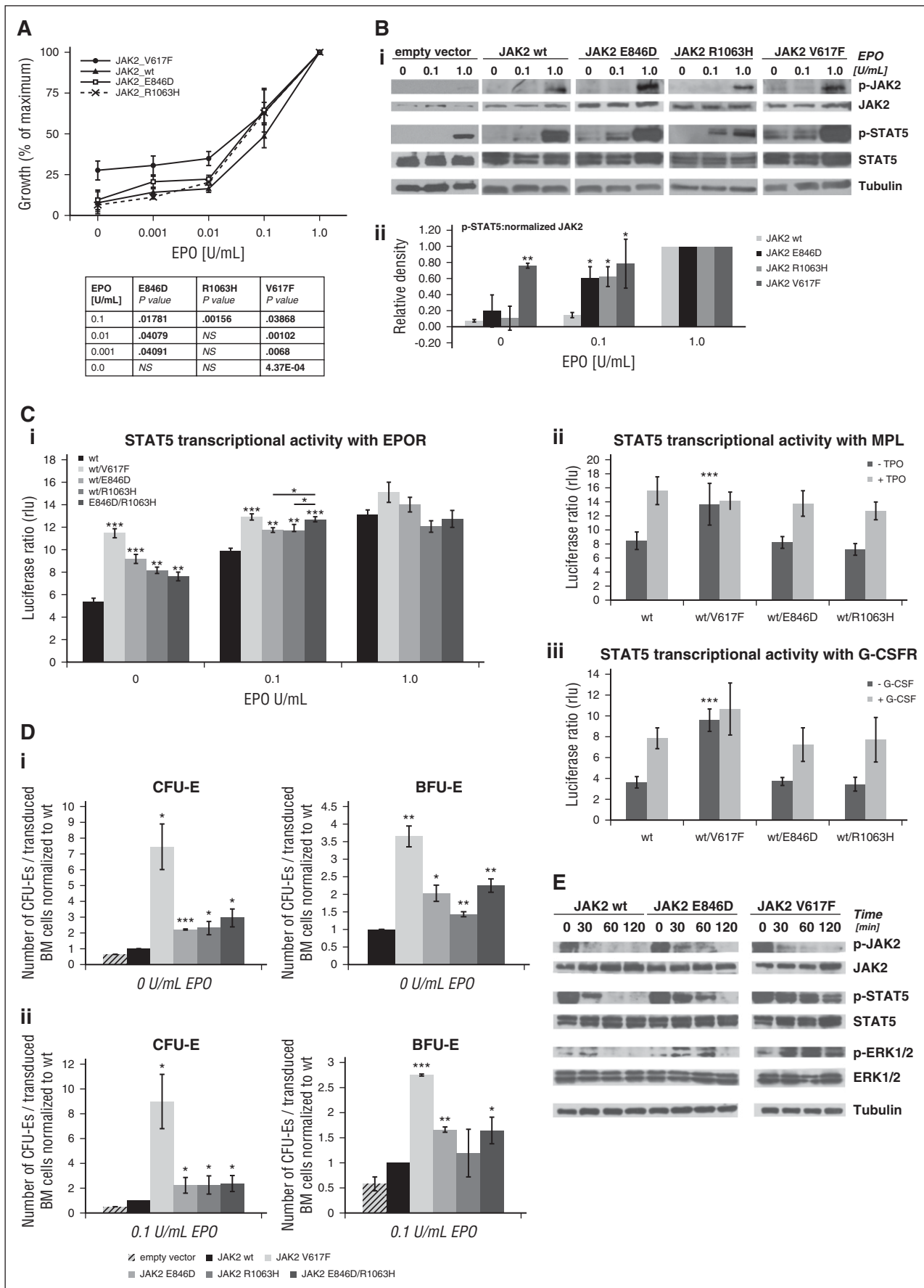


Figure 2.

Results and discussion

Case presentation, EPO hypersensitivity of erythroid progenitors, and mutational analyses

The diagnosis of polycythemia in a 15-year-old boy was based on the hematological and clinical data summarized in Figure 1A. The patient had increased hemoglobin/hematocrit level, higher red blood cell count, plethora, palpable spleen, and normal EPO level. Although the white blood cell differential and platelet count were normal (supplemental Table 1), the BM aspirate and BM biopsy showed hypercellularity, erythroid hyperplasia, and atypical, enlarged, and immature megakaryocytes, likely resulting from the stimulation of the megakaryocytic lineage (Figure 1B; supplemental Figure 1). The iron status parameters were normal (supplemental Table 2). The in vitro colony assay revealed hypersensitivity of the patient's burst-forming unit-erythroid (BFU-E) progenitors to EPO (Figure 1C), a feature characteristic for primary polycythemia states.¹² Both parents and the patient's brother were clinically normal, with normal EPO levels and hematological (Figure 1A) and iron status parameters, with the exception of elevated ferritin in the father and brother likely due to infection (supplemental Table 2). Nevertheless, the sensitivity of BFU-E progenitors to EPO was significantly increased in the mother and slightly also in the father compared with healthy controls and the patient's brother (Figure 1C). In addition, the colony assay revealed significantly increased numbers of circulating BFU-E progenitors in the patient and his parents compared with healthy controls (supplemental Figure 2A). These results suggested the hereditary nature of the propositus's erythrocytosis. No somatic mutations or chromosomal aberrations were uncovered by either whole-exome sequencing or microarray analysis (supplemental Table 3i-ii), suggesting that the hematopoiesis was likely polyclonal. Targeted mutational screening (see supplemental Materials and methods) and search for germ line variants using whole-exome sequencing revealed a E846D substitution in JAK2 in a heterozygous state in the propositus

and his mother and JAK2 R1063H in the propositus and his father (supplemental Results; supplemental Figure 2B); both variants were reported as polymorphisms with very low frequencies (supplemental Table 4). Subsequent screening of a cohort of 99 subjects (including healthy controls, MPN patients, and pediatric patients with essential thrombocythemia or hereditary erythrocytosis) detected JAK2 E846D substitution in 1 CALR⁺/V617F⁺ MPN patient and JAK2 R1063H in 1 V617F⁺ PV patient (supplemental Table 5) and in 1 triple-negative MPN patient (J.D.M.F. and R.K., unpublished data, August 29, 2015). The E846D substitution was previously reported in normal-karyotype acute myeloid leukemia¹³ and the JEG-3 cancer cell line¹⁴; R1063H was reported in 3 JAK2 V617F⁺ PV patients,² as well as in acute myeloid leukemia¹³ and B-cell acute lymphoblastic leukemia cases.¹⁵ Altogether, these data suggest a much higher frequency of these 2 variants in MPN patients than in normal individuals.

JAK2 E846D and R1063H promote survival at low EPO concentrations by increasing EPO-induced phosphorylation of STAT5

Because the germ line JAK2 mutations emerged as the main disease-causing event in our patient, we created a cellular model: Ba/F3-EPOR cells expressing JAK2_E846D and JAK2_R1063H. Ba/F3-EPOR cells transfected with the wild-type human JAK2 (JAK2_wt) and V617F JAK2 were used as a negative and positive control, respectively.¹⁶ As expected, the JAK2_V617F transfectants exhibited survival advantage and supported constitutive proliferation in EPO-free or EPO-limiting conditions^{1,4,17} (supplemental Figure 3A; Figure 2A). The viability of JAK2_E846D and JAK2_R1063H transfectants in EPO-free medium was comparable to the JAK2_wt transfectants (supplemental Figure 3A); neither these transfectants expressing individual JAK2 genetic variants nor double transfectants with both E846D and R1063H (not shown) became growth factor independent. Nevertheless, JAK2_E846D-expressing cells showed significantly increased proliferation in EPO-limiting conditions compared with

Figure 2. Proliferation assay in cytokine-limiting conditions, immunoblot analysis of JAK2 signal transduction, luciferase assay, and colony assay of retrovirally transduced BM cells. (A) MTT (3-[4,5-dimethylthiazol-2-yl]-2,5-diphenyltetrazolium bromide) test in Ba/F3-EPOR-IL-3-dependent cells stably transfected with different JAK2 vectors. The percentage of proliferating cells was calculated as the percentage of the maximal cell growth observed at EPO concentration of 1.0 U/mL. The transfectants were starved for 12 hours in IL-3-free media and then incubated for 48 hours in the media with different EPO concentration. Results are shown as the mean \pm standard deviation (SD) ($n =$ at least 4 tests performed in triplicates). The table below the graph shows statistical evaluation of the growth of individual Ba/F3 transfectants at tested EPO concentrations compared with cell-expressing JAK2 wt. P values were calculated using Origin 6.1 software (OriginLab Corporation). (B) JAK2 downstream signaling in stable Ba/F3-EPOR-IL-3-dependent transfectants. The cells were starved in IL-3-free media for 12 hours and then stimulated with indicated concentrations of EPO for 15 minutes. JAK2_V617F-expressing cells served as a positive control and showed constitutive activation of STAT5 (i-ii). Immunoblot and subsequent densitometry analysis revealed that JAK2_E846D transfectants and also R1063H-expressing cells showed increase in STAT5 activation (i-ii). Each bar represents the ratio of the density of phosphorylated STAT5 (p-STAT5) to the density of normalized total JAK2 and is presented as fold change against the ratio calculated for 1.0 U/mL EPO. For detailed information on JAK2 normalization, see supplemental Materials and methods. Activation of JAK2 and its targets was determined by antibodies recognizing specific phosphorylation sites (as detailed in supplemental Materials and methods); tubulin antibody was used as a loading control. (C) STAT5 transcriptional activity in JAK2-deficient γ-2A cells transfected with various JAK2 complementary DNAs (cDNAs) in the presence of EPOR, MPL, and G-CSF receptor (G-CSFR). The heterozygous configuration was mimicked by cotransfection of JAK2 wt cDNA with JAK2_V617F, JAK2_E846D, or JAK2_R1063H. Four hours after transfection, the cells were stimulated with different concentrations of EPO (i) or stimulated with 10 ng/mL thrombopoietin (ii) or 10 ng/mL G-CSF (iii) and luminescence was detected in cell lysates 24 hours (ii-iii) or 48 hours (i) after transfection using a PerkinElmer Victor X Light analyzer. (i) STAT5 transcriptional activity downstream of JAK2_E846D and R1063H was significantly increased in both EPO-free and EPO-limiting condition in comparison with JAK2 wt in the presence of EPOR; the double mutants expressing both JAK2_E846D and R1063H mutants showed increased STAT5 transcriptional activity over the single mutants in low EPO concentration. (ii-iii) Only JAK2_V617F significantly increased STAT5 transcriptional activity in the presence of MPL and G-CSFR. STAT5 transcriptional activity of JAK2_E846D and JAK2_R1063H cells was comparable to wt cells. The panels show the average of 3 independent experiments \pm standard error of the mean (SEM). * $P < .05$, ** $P < .01$, *** $P < .001$ using the 2-tailed Student t test. rlu, relative light unit. (D) In vitro colony growth of transduced murine BM. Murine BM cells were infected with retroviruses coding for murine JAK2 wt, V617F, E846D, or R1063H for single mutant configuration and with E846D and R1063H retroviral particles for double mutant configuration. Infected murine BM cells were then plated on methylcellulose media in the absence of EPO (i) or in the presence of 0.1 U/mL EPO (ii). After 2 and 7 days, the plates were evaluated for the formation of CFU-E and BFU-E, respectively. The BM cells infected with the virus containing the empty pMEGIX vector were used as a control. JAK2_E846D and JAK2_E846D/R1063H BM cells have significantly higher numbers of CFU-E and BFU-E colonies in both EPO-free and low EPO conditions when compared with JAK2_wt cells. Cells with JAK2_R1063H mutation had significantly increased CFU-E, but not BFU-E colony formation. The highest number of erythroid colonies was detected in the sample derived from JAK2_V617F positive control. Congruent results were obtained by determination of the replating capacity of primary human cells naturally harboring the JAK2_E846D and R1063H mutations (supplemental Figure 6). The panels show the average of 3 independent experiments. The BFU-E and CFU-E colony numbers are expressed as the number of colonies per transduced cells and are normalized to wt values \pm SD. P values were calculated using Origin 6.1 software. * $P < .05$, ** $P < .01$, *** $P < .001$. (E) Immunoblot analysis of prolonged activity of E846D-mutant JAK2 kinase. The JAK2 transfectants were after IL-3 starvation stimulated with 20 U/mL EPO for 15 minutes and then incubated in base Iscove modified Dulbecco medium (IMDM) with no additives for indicated periods of time. JAK2_E846D-expressing cells showed prolonged activation of STAT5 and EKR1/2 similarly to JAK2_V617F transfectants as predicted by in silico modeling (supplemental Figure 7).

JAK2_wt (Figure 2A). Improved proliferation for JAK2_R1063H transfectants was observed only in 0.1 U/mL EPO concentration (Figure 2A). These results suggested that E846D and R1063H substitutions have a weaker effect on the survival and proliferation capacity of cells than the oncogenic V617F mutation, which is consistent with their germ line transmission and with nonclonal hematopoiesis observed in the JAK2 E846D⁺ mother (described in supplemental Materials and methods). This also showed a stronger effect of E846D substitution on improved proliferation in EPO-limiting conditions compared with R1063H.

We then focused on JAK2 downstream signal transduction pathways. Upon interleukin-3 (IL-3) starvation and short incubation in IL-3-free EPO-containing medium, JAK2_E846D- and JAK2_R1063H-expressing cells showed increased STAT5 phosphorylation (Figure 2B). Weak activation of STAT1 was also observed for both mutants (supplemental Figure 3B).

JAK2 E846D and R1063H activate STAT5 transcriptional activity specifically through EPOR

Next, we tested the effect of our JAK2 mutants on STAT transcriptional activity by dual-reporter luciferase assay in JAK2-deficient γ-2A cells.¹⁸ Figure 2Ci shows that JAK2 E846D and R1063H significantly increased STAT5 transcriptional activity in EPO-free and low EPO conditions in the presence of EPOR when compared with cells expressing JAK2 wt. In EPO-limiting conditions, the coexpression of these 2 JAK2 mutants further improved STAT5 transcriptional activity compared with cells expressing a single JAK2 mutant (E846D or R1063H). No effect of JAK2 E846D and R1063H was observed on basal STAT5 activation via MPL or the granulocyte colony-stimulating factor (G-CSF) receptor (Figure 2Cii-iii) or on the activation of other STAT members (supplemental Figure 4). This was in agreement with increased STAT5 phosphorylation in the patient's BM detected by immunohistochemical analysis of STAT5 (supplemental Figure 5) and is consistent with the erythroid phenotype in our patient.

JAK2 E846D-transduced murine BM cells show increased capacity for CFU-E and BFU-E formation whereas JAK2 R1063H increases only CFU-E formation

To assess the effect of JAK2 mutants on primary cells, BM cells from C57BL/6 mice were retrovirally transduced with murine JAK2 expression vectors and used for in vitro colony assay. The cells expressing the E846D mutant formed significantly increased numbers of colony forming unit-erythroid (CFU-E) and BFU-E, when compared with cells with JAK2 wt in EPO-free or EPO-limiting conditions (Figure 2D). The observation that the R1063H mutant induced CFU-E rather than BFU-E colony growth (see also primary father's progenitors in supplemental Figure 6) is reminiscent of the weak activation of EPOR by the anemic strain of the Friend virus complex gp55 envelope protein (gp55-A), which also specifically supported CFU-E formation.^{19,20} For the EPO-free condition, the co-occurrence of the 2 mutations was slightly more effective in colony growth than the single mutants alone (Figure 2D). This assay indicated that JAK2 E846D and R1063H mutations facilitate hypersensitive response of erythroid progenitors from the patient or patient's parents to EPO.

In silico analysis predicted increased activity of JAK2 R1063H-mutant kinase and prolonged activation of JAK2 E846D-mutant kinase after cytokine stimulation

In silico modeling using the x-ray structures of the inactive and active JH1 domain of JAK2^{21,22} suggested that the R1063H mutation

would be presumed to facilitate the active conformation of JH1, whereas the JAK2 E846D mutant would show slower return to the ground state after cytokine stimulation (supplemental Figure 7). The effect of E846D substitution was confirmed by immunoblots analysis in which IL-3-starved JAK2_E846D transfectants showed prolonged activation of STAT5 and extracellular signal-regulated kinase 1/2 (ERK1/2) compared with JAK2_wt after high-dose EPO stimulation and subsequent EPO withdrawal (Figure 2E) resembling signaling downstream EPOR gain-of-function mutants.²³ The prolonged STAT5 and ERK1/2 activation downstream JAK2_E846D can be effectively reduced by JAK2 inhibitors, ruxolitinib or AZ-960, but not by wortmannin, a phosphoinositide-3-kinase inhibitor (supplemental Figure 8).

In summary, we establish that E846D and R1063H are weakly activating mutations and conclude that the cooperation of these activating JAK2 mutations causes a polyclonal hereditary erythrocytosis with megakaryocytic atypia, clinically resembling JAK2 exon 12-positive PV.

Acknowledgments

The authors thank Michael Schuster and Donat Alpar (the Biomedical Sequencing Facility at CeMM) as well as Martin Tichy and Anna Lapcikova (University Hospital and Faculty of Medicine and Dentistry in Olomouc) for their technical assistance, and Srdan Verstovsek (MD Anderson, Houston, TX) for critical reading of the paper and discussions.

This work was supported by Czech Science Foundation Project P301/12/1503 (V.D.). J.F.K. was supported by CZ.1.07/2.3.00/30.0041. Support to S.N.C. was from the Fonds de la Recherche Scientifique–Fonds National de la Recherche Scientifique, Belgium, the Salus Sanguinis Foundation, the Action de Recherche Concertée projects MEXP31C1 and ARC10/15-027 of the University catholique de Louvain, Brussels, the Fondation contre le Cancer, Brussels, the Pôle d'Attraction Interuniversitaire Programs BCHM61B5, and Belgian Medical Genetics Initiative (BeMG). E.L. was supported by a Fonds pour la formation à la Recherche dans l'Industrie et dans l'Agriculture PhD fellowship. The Sonderforschungsbereich grant from the Austrian Science Fund F4702-B20 is acknowledged for its generous support to R.K. J.D.M.F. acknowledges support from L'ORÉAL Österreich, For Women in Science Fellowship.

Authorship

Contribution: K.K. and M.H. designed and performed research, analyzed data, and wrote the paper; C.P. designed and performed research, analyzed data, and reviewed the paper; J.F.K. performed research, analyzed data, and reviewed the paper; D.P. recruited the patient and contributed to the editing of the paper; E.L. performed research and contributed to the writing of the paper; B.K. performed research and analyzed data; J.D.M.F. designed and performed research and analyzed data; F.S. analyzed data; R.K. contributed to study design, analyzed data, reviewed the paper, and provided financial support; S.N.C. contributed to study design, analyzed data, wrote the paper, and provided financial support; and V.D. designed the study, analyzed data, wrote the paper, and provided financial support.

Conflict-of-interest disclosure: The authors declare no competing financial interests.

ORCID profiles: J.F.K., 0000-0002-8808-9411; J.D.M.F., 0000-0001-7420-3298; R.K., 0000-0002-6997-8539.

Correspondence: Vladimir Divoky, Department of Biology, Faculty of Medicine and Dentistry, Palacký University, Hnevotinska 3, Olomouc, 775 15, Czech Republic; e-mail: vladimir.divoky@upol.cz; or Stefan N. Constantinescu, Signal Transduction and Molecular

Hematology Unit, Ludwig Institute for Cancer Research and de Duve Institute, Université catholique de Louvain, Avenue Hippocrate 74, UCL 75-4, Brussels B-1200, Belgium; e-mail: stefan.constantinescu@bru.lircr.org.

References

- James C, Ugo V, Le Couédic JP, et al. A unique clonal JAK2 mutation leading to constitutive signalling causes polycythaemia vera. *Nature*. 2005;434(7037):1144-1148.
- Levine RL, Wadleigh M, Cools J, et al. Activating mutation in the tyrosine kinase JAK2 in polycythemia vera, essential thrombocythemia, and myeloid metaplasia with myelofibrosis. *Cancer Cell*. 2005;7(4):387-397.
- Funakoshi-Tago M, Tago K, Abe M, Sonoda Y, Kasahara T. STAT5 activation is critical for the transformation mediated by myeloproliferative disorder-associated JAK2 V617F mutant. *J Biol Chem*. 2010;285(8):5296-5307.
- Dusa A, Mouton C, Pecquet C, Herman M, Constantinescu SN. JAK2 V617F constitutive activation requires JH2 residue F595: a pseudokinase domain target for specific inhibitors. *PLoS One*. 2010;5(6):e11157.
- Mead AJ, Chowdhury O, Pecquet C, et al. Impact of isolated germline JAK2V617I mutation on human hematopoiesis. *Blood*. 2013;121(20):4156-4165.
- Marty C, Saint-Martin C, Pecquet C, et al. Germline JAK2 mutations in the kinase domain are responsible for hereditary thrombocytosis and are resistant to JAK2 and HSP90 inhibitors. *Blood*. 2014;123(9):1372-1383.
- Etheridge SL, Cosgrove ME, Sangkhae V, et al. A novel activating, germline JAK2 mutation, JAK2R564Q, causes familial essential thrombocytosis. *Blood*. 2014;123(7):1059-1068.
- Milosevic Feenstra JD, Nivarthi H, Gisslinger H, et al. Whole-exome sequencing identifies novel MPL and JAK2 mutations in triple-negative myeloproliferative neoplasms. *Blood*. 2016;127(3):325-332.
- Chen E, Beer PA, Godfrey AL, et al. Distinct clinical phenotypes associated with JAK2V617F reflect differential STAT1 signaling. *Cancer Cell*. 2010;18(5):524-535.
- Lakey MA, Pardanani A, Hoyer JD, et al. Bone marrow morphologic features in polycythemia vera with JAK2 exon 12 mutations. *Am J Clin Pathol*. 2010;133(6):942-948.
- D'Andrea AD, Yoshimura A, Youssoufian H, Zon LI, Koo JW, Lodish HF. The cytoplasmic region of the erythropoietin receptor contains nonoverlapping positive and negative growth-regulatory domains. *Mol Cell Biol*. 1991;11(4):1980-1987.
- Prchal JT. Primary and secondary polycythemias (erythrocytosis). In: Kaushansky K, Lichtman MA, Beutler E, Kipps TJ, Seligsohn U, Prchal JT, eds. *Williams Hematology*. 8th ed. New York, NY: McGraw Hill; 2010:823-838.
- Schnittger S, Bonin M, Schroeder C, et al. Development of an oligonucleotide resequencing array for rapid mutation analysis in acute myeloid leukemia with normal karyotype [abstract]. *Blood*. 2009;114(22). Abstract 705.
- Matthews DJ, Gerritsen ME. Tumor associated mutations in JAK2. In: Matthews DJ, Gerritsen ME, eds. *Targeting Protein Kinases for Cancer Therapy*. Hoboken, NJ: John Wiley & Sons, Inc; 2010.
- Sadras T, Heatley S, Nievergall E, et al. JAK2 mutations are highly enriched in CRLF2-rearranged B-ALL cases with a Ph-like gene signature [abstract]. *Haematologica*. 2015;100(s1):199. Abstract P524.
- Baxter EJ, Scott LM, Campbell PJ, et al; Cancer Genome Project. Acquired mutation of the tyrosine kinase JAK2 in human myeloproliferative disorders. *Lancet*. 2005;365(9464):1054-1061.
- Staerk J, Kallin A, Demoulin JB, Vainchenker W, Constantinescu SN. JAK1 and Tyk2 activation by the homologous polycythemia vera JAK2 V617F mutation: cross-talk with IGF1 receptor. *J Biol Chem*. 2005;280(51):41893-41899.
- Kohlhuber F, Rogers NC, Watling D, et al. A JAK1/JAK2 chimera can sustain alpha and gamma interferon responses. *Mol Cell Biol*. 1997;17(2):695-706.
- Wendling F, Tambourin P, Gallien-Lartigue O, Charon M. Comparative differentiation and numeration of CFUs from mice infected either by the anemia- or polycythemia-inducing strains of Friend viruses. *Int J Cancer*. 1974;13(4):454-462.
- Constantinescu SN, Wu H, Liu X, Beyer W, Fallon A, Lodish HF. The anemic Friend virus gp55 envelope protein induces erythroid differentiation in fetal liver colony-forming units-erythroid. *Blood*. 1998;91(4):1163-1172.
- Andraos R, Qian Z, Bonenfant D, et al. Modulation of activation-loop phosphorylation by JAK inhibitors is binding mode dependent. *Cancer Discov*. 2012;2(6):512-523.
- Lucet IS, Fantino E, Styles M, et al. The structural basis of Janus kinase 2 inhibition by a potent and specific pan-Janus kinase inhibitor. *Blood*. 2006;107(1):176-183.
- Divoky V, Song J, Horvathova M, et al. Delayed hemoglobin switching and perinatal neocytolysis in mice with gain-of-function erythropoietin receptor. *J Mol Med (Berl)*. 2016;94(5):597-608.

Cooperation of germline JAK2 mutations E846D and R1063H in hereditary erythrocytosis with megakaryocytic atypia

Supplemental Materials and Methods, Results, Tables, Figures and References for Kapralova et al.

Supplemental Material and Methods

Patient and sample processing

All human samples were obtained with informed consent and approval from the Ethics Committee of Palacky University Hospital, Olomouc, Czech Republic. Genomic DNA isolated from whole peripheral blood, granulocytes and T-lymphocytes (isolated using Pan T cell kit, Miltenyi Biotec, Bergisch Gladbach, Germany) was used for targeted sequence analysis and whole exome sequencing. Isolated peripheral blood mononuclear cells were used for *in vitro* sensitivity assay to EPO. Bone marrow samples were used for immunohistochemical detection of STAT5 phosphorylation. The serum EPO concentrations were measured by radioimmunoassay (RIA).¹ Red cell mass (RCM) in mL/kg was calculated using ⁵¹Cr RCM in mL and body weight.²

Mutational screening

1. Targeted mutational screening

Genomic DNA was isolated from peripheral blood by the phenol-chloroform method. All amplicons were sequenced on ABI Prism 310 Genetic Analyzer using BigDye Terminator v1.1 Cycle Sequencing kit (Life Technologies, Carlsbad, CA) according to the manufacturer's protocol. List of screened genes (with the respective exons and intron-exon boundaries analyzed through sequencing of genomic DNA) is provided below. The presence of JAK2 V617F mutation in peripheral blood genomic DNA was excluded using highly sensitive allelic discrimination real-time assay.³ The presence of *CALR* exon 9 insertions/deletions was excluded using fragmentation analysis assay as recently described.⁴

Genes screened:

EPOR	exons 7 and 8 ⁵
VHL	complete coding sequence and exon-intron boundaries* (exon 1) ⁶
PHD2 (EGLN1)	complete coding sequence and exon-intron boundaries*

HIF2A (EPAS1)	exons 9* and 12 ⁷
HIF1A	exons 9 and 12*
LNK (SH2B3)	exon 6*
JAK2	exons 12-19 and exon-intron boundaries*

*: primer sequences and reaction conditions available upon request

Reference sequences: EPOR (NM_000121.3), VHL (NM_000551.3), EGLN1 (NM_022051.2), EPAS1 (NM_001430.4), HIF1A (NM_001530.3), JAK2 (NM_004972.3), SH2B3 (NM_005475.2)

2. Whole exome sequencing, data analysis and validation of hits

DNA libraries were generated from genomic DNA isolated from granulocytes and T-lymphocytes of the patient and genomic DNA isolated from the whole blood of the patient's father using the Nextera Rapid Capture Exome kit (Illumina, San Diego, CA) according to the manufacturer's instructions. Due to low sample quality the DNA library could not be generated from the genomic DNA sample of the patient's mother. The 100-bp paired-end sequencing was performed on the Illumina HiSeq 2000 platform, using Illumina v3 reagents. Base calls provided by the Illumina Realtime Analysis software were converted into BAM format using Illumina2bam and demultiplexed using BamIndexDecoder. The next generation sequencing reads for each demultiplexed aliquot were aligned with the BWA MEM algorithm⁸ to the b37 reference sequence supplied with the Genome Analysis Toolkit (GATK).⁹ B37 is a derivative of the GRCh37 reference sequence¹⁰ optimized for variant calling by the 1000 Genomes project¹¹ and includes a human decoy sequence and a copy of the Epstein Barr Virus sequence. PCR duplicates were removed by MarkDuplicates (Picard tools 1.118). Reads suggesting insertion or deletion events were realigned before base quality score recalibration. Collection of alignment summary metrics (Picard tools 1.118) concluded aliquot-level processing. Sample-level processing included merging of refined aliquot alignments, before performing another round of duplicate reads marking, insertion or deletion realignment and collection of alignment summary metrics. Raw variants were characterized with the GATK Haplotype Caller on the individual sample level. On a cohort level, raw variant calls of several samples were merged into a larger cohort, which was then genotyped before recalibration of variant quality scores for SNPs and INDELs. All procedures followed the best practices published by the GATK developers.¹² The resulting, variant calling format files were annotated with functional consequence predictions using Annovar version 2015March22 and custom scripts. The variants annotated as common (>1%) in the dbSNP142

database were removed, as well as variant falling within non-coding regions and synonymous polymorphisms, leaving only exonic and/or splicing mutations. We further removed all variants with low quality scores ($VQSLOD < 0$), variants present in $\geq 3/67$ non-disease control samples, variants annotated as common ($> 1\%$) in 1000 Genomes version 2014Oct, Exome Variant Server versions ESP5400 and ESP6500 databases, and variants covered with < 10 reads.

To detect the presence of potential somatic mutations, following all the above mentioned filtering steps, the variants present in the control tissue of the patient were removed from the list of variants detected in the granulocytes of the patient. To account for potential contamination of control tissue with the tumor tissue we allowed all hits with variant frequency of up to 10% in the control tissue to pass the filtering. This analysis revealed a list of 15 potentially somatic mutations. To validate these hits, PCR primers were designed and Sanger sequencing was performed as previously described,⁴ using the BigDye Terminator v3.1 Cycle Sequencing kit (Life Technologies). The sequencing products were analyzed on the 3130xl Genomic Analyzer (Applied Biosystems) and Sequencher Software 4.9 (Gene Codes) was used for sequence analysis. The primers designed for validation of WES data can be provided upon request.

The efficiency of exome enrichment protocols was assessed as previously described.¹³

Microarray analysis

The DNA sample from granulocytes of the patient was processed according to the manufacturer's instructions and hybridized to Genome-Wide Human SNP 6.0 arrays (Affymetrix). The Genotyping Console version 3.0.2 software (Affymetrix) was used for data analysis.

Transcriptional clonality assay

Patient's mother, who was a carrier of JAK2 E846D mutation, was genotyped for five single nucleotide polymorphisms in genes previously shown to be a subject to X chromosome inactivation (*BTK* dbSNP: rs1135363, *FHL1* dbSNP: rs9018, *G6PD* dbSNP: rs2230037, *IDS* dbSNP: rs1141608 and *MPP1* dbSNP: rs1126762)¹⁴ and was found informative only for the *FHL1* G/A polymorphism. Transcriptional clonality assay involving *FHL1* rs9018 was performed using allele-specific LNA-spiked primers, with sequences described previously

and adapted probe sequence (5' FAM-AGCACTGCAGAACATCTGAGGGGGCT-BHQ 3').¹⁵ Assays were performed on LightCycler 480 using LightCycler 480 Probe Master (both Roche Applied Science, Mannheim, Germany) with recommended conditions and were validated prior to quantification.

White blood cell fraction total RNA from patient's mother was Dnase-treated by TURBO DNA-free (Life Technologies) and reverse-transcribed by Transcriptor First Strand cDNA Synthesis Kit (Roche Applied Science). A pair of quantitative allele-specific PCRs (one for each SNP variant) were performed on DNA (representing the 50:50 ratio) as well as on cDNA (representing the actively transcribed allele) samples and relative quantities were calculated using relative standard curve method, which compensates for different efficiencies of each primer pair. No DNA contamination of RNA sample was detected in the RT-control. The G:A quantity ratio of DNA sample was set to 1 and used to normalize the G:A quantity ratio of cDNA sample.

Screening of the cohort of erythrocytosis patients, MPN patients and controls

Tetra-primer amplification-refractory mutation system (ARMS) PCR was developed using modified Primer1 output.¹⁶ for screening of *JAK2* c.2538G>C (E846D) and *JAK2* c.3188G>A (p.R1063H) mutations in 27 control samples, 17 patients with congenital erythrocytosis, 10 children with ET and 45 MPN patients. Reaction was performed using HotStarTaq Master Mix Kit (QIAGEN, Venlo, Netherlands) as recommended by manufacturer. For detection of E846D mutation: initial denaturation 95°C/15 minutes, then 32 cycles of: 95°C/10 seconds, 60°C/30 seconds, 70°C/30 seconds, with final elongation at 70°C/5 minutes; for R1063H mutation: initial denaturation 95°C/15 minutes, then 30 cycles of: 95°C/10 seconds, 56°C/30 seconds, 72°C/30 seconds, final elongation at 70°C/5 minutes. Sequences of primers and their final concentration in reaction are listed below; in bold is the mutation site on inner primers, a mismatch 2 bp from mutation site is depicted in lowercase. For detection of E846D mutation: size of the outer primer product is 497 bp, sizes of mutated and wild-type sequences are 340 and 211 bp, respectively. For detection of R1063H mutation: size of the outer primer product is 542 bp, sizes of mutated and wild-type sequences are 254 and 341 bp, respectively.

Name	Sequence	Final conc.
E846D		
Outer F	5'-TTATCCTTGCAAAGTCTCTCTGAAGG-3'	0.2μM
Outer R	5'-TTAACACAGCATTCTCAACATCTGAC-3'	0.2μM
Inner F (wt)	5'-ACCGGGATCCTACACAGTTGAAGCAG-3'	0.4μM
Inner R (mut)	5'-CAAGTTGCTGTAGAAATTCAAATGTgTG-3'	0.4μM

Name	Sequence	Final conc.
R1063H		
Outer F	5'-TTGTGTTGAGTTATTACAGCTATGGA-3'	0.2μM
Outer R	5'-AAATGAACACTAAGGGCCATCTT-3'	0.2μM
Inner F (wt)	5'-AAAGTGGGTTGTTAGGAATTATTCG-3'	0.4μM
Inner R (mut)	5'-CCTGTTGTCATTGCCAACATCAGAT-3'	0.4μM

***In vitro* sensitivity assay of erythroid progenitors to EPO**

Isolated peripheral blood mononuclear cells (2.3×10^5) were plated in duplicate in the methylcellulose media (H4531, StemCell Technologies, Vancouver, Canada) with addition of increasing concentrations of EPO (Janssen Pharmaceuticals, Beerse, Belgium): from 0.03 to 1.0 U per mL of media. Cell cultures were maintained in humidified atmosphere at 5% CO₂ and 21% O₂ at 37°C for 14 days. Erythroid burst-forming unit (BFU-E) colonies were scored by standard morphologic criteria using an inverted microscope (Olympus IX 71, Olympus, Hamburg, Germany).

Genotyping of erythroid colonies for JAK2 E846D

Modified nested ARMS PCR protocol (see above) was used to genotype single erythroid colonies derived from the patient (JAK2 E846D/R1063H) and his mother (JAK2 E846D) growing in low EPO concentration (0.03 or 0.06 U/mL). DNA from colonies was precipitated from 100 μL RLT buffer (QIAGEN) with 20 μg/mL linear polyacrylamide carrier (Life Technologies) and used directly in PCR. For the first round of nested PCR only outer primer pair was used for 34 cycles (reaction conditions as above), with final concentration of both primers 0.5 μM and 0.5 μg/μL BSA. Samples positive in the first round were diluted 100x times and used for 30 cycles of tetra-primer ARMS with the same protocol as described above.

Immunohistochemistry on bone marrow samples

Immunohistochemical staining was performed on 3-5-μm-thick slides as previously

described¹⁷ with the primary mouse anti-glycophorin C antibody (1:3000, DAKO, Denmark) or primary rabbit anti-phospho-STAT5 antibody (Y694, 1:50, Cell Signaling, Danvers, MA) and an EnVision+ Dual Link detection System (HRP and DAB+ as a visualization chromogen; both DAKO). The slides were analyzed with an Olympus BX 51 light microscope (Olympus, Hamburg, Germany).

Vector construction and mutagenesis

QuickChange site-directed mutagenesis kit (Agilent Technologies, Santa Clara, CA) was used according to manufacturer instructions to create *JAK2* c.1849G>T (JAK2_V617F), *JAK2* c.2538G>C (JAK2_E846D) and *JAK2* c.3188G>A (JAK2_R1063H) mutants on a human *JAK2* ORF cDNA cloned in pCMV6-Entry plasmid vector (OriGene, Rockville, MD, cat. no. RC520503; *JAK2* sequence accession NM_004972.2). The two mutant and the wild type *JAK2* ORFs were then shuttled by restriction-ligation according to manufacturer instructions to bicistronic pCMV6-AC-IRES-GFP-Puro mammalian expression vector (OriGene, cat. no. PS100059) with C-terminal fusion of Myc-DKK tag. Full-length *JAK2* sequences of final clones were verified by sequencing. The same kit and primers were used to create pMEGIX human and murine *JAK2* mutants.¹⁸

Mutagenesis primers for JAK2

Human

JAK2 V617F sense: 5'-agcattggtttaattatggagtatgttctgtggagacgaga-3'

JAK2 V617F antisense: 5'-tctcgctccacagaaacatactccataattaaaaccaaatgct-3'

JAK2 E846D sense: 5'-cgggatcctacacagttgaagacagacattgaaatttc-3'

JAK2 E846D antisense: 5'-gaaattcaaatgtctgtctcaaactgtgttaggatcccg-3'

JAK2 R1063H sense: 5'-tttgtcattgccaatcatatgcataaattccgctgg-3'

JAK2 R1063H antisense: 5'-ccaccagcggatttatgcatatgattggcaatgacaaa-3'

Mouse

Jak2 E846D sense: 5'-aaactcaagtgtcttcaaactgtgttaggtcc-3'

Jak2 E846D antisense: 5'-ggaccctacacagttgaagacagacacttgaaagg-3'

Jak2 R1063H sense: 5'-cttgttatcattgccaatcatatgcataaattccacgggtggact-3'

Jak2 R1063H antisense: 5'-agtccacccgtggatttatgcatatgattggcaatgataaacaag-3

Ba/F3 cells, electroporation and selection of stable transfectants

Ba/F3-EPOR cells¹⁹ were cultured in IMDM medium containing 10% fetal bovine serum (FBS) (both from Life Technologies) and 1 U/mL of EPO (Janssen Pharmaceuticals, Beerse, Belgium). A total number of 5×10^6 cells were collected for each electroporation. Twenty µg of plasmid DNA: JAK2_E846D (pCMV6-AC-IRES-GFP-PuroJAK2E846D), JAK2_R1063H (pCMV6-AC-IRES-GFP-PuroJAK2R1063H), JAK2_V617F (pCMV6-AC-IRES-GFP-PuroJAK2V617F), JAK2_wt (CMV6-AC-IRES-GFP-PuroJAK2wt) and empty vector (pCMV6-AC-IRES-GFP-Puro) were electroporated under conditions of 420 V and 250 µF using a Gene-Pulser (Bio-Rad, Hercules, CA). Stable transfectants were selected with 2.5 µg/ml puromycin (Life Technologies) for 2 weeks. Individual transfectants expressed similar levels of GFP as determined by flow cytometry (not shown).

Viability and Proliferation Assay

Stably transfected Ba/F3-EPOR cells were washed four times with PBS and plated at a density 1×10^5 cells/mL for viability and 0.4×10^5 cells/well on 96-well plate for proliferation assay. The cells were cultured for 4 days in the absence of EPO or 2 days in descending EPO concentrations in IMDM medium containing 10% FBS. The viability of cells was determined by the exclusion of Trypan blue (0.4% Trypan blue; Sigma-Aldrich, St. Louis, MO). MTT (Thiazolyl Blue Tetrazolium Bromide) proliferation assay was performed according to manufacturer's instructions (Sigma-Aldrich) as we previously described.²⁰ Experiments were done in triplicate. Cell growth is expressed in percentages relative to the proliferation of cells in the media with the highest EPO dose (1 U/mL).

Immunoblotting

For the *in vitro* signal transduction assay stably transfected Ba/F3-EPOR cells were incubated in IMDM with 10% FBS and 2 ng/mL of interleukin-3 (IL-3, ProSpec-Tany TechnoGene Ltd., Rehovot, Israel). Cells were starved of IL-3 for 12 hours; thereafter various concentrations of EPO were added for 15 minutes. Alternatively, after IL-3 starvation the cells were stimulated with 20 U/mL EPO for 15 min and then incubated in base IMDM with no additives for 30, 60 and 120 minutes. For evaluation of the effect of JAK2 inhibitors, the

cells were incubated in plane IMDM with 1 μ M concentration of AZ-960 (Santa Cruz Biotechnology), Ruxolitinib (Jakavi, Novartis, Basel, Switzerland) and Wortmannin (Sigma-Aldrich), or DMSO as a vehicle control. Cells were lysed in 1% NP40 lysis buffer with 100 μ M Na orthovanadate, 100 μ M PMSF and cocktail of protease inhibitors (all from Sigma-Aldrich). The following primary antibodies (all from Cell Signaling, Danvers, MA) were used: phospho-Stat5 (Y694), Stat5, phospho-JAK2 (Y1007/1008), JAK2, phospho-Stat1 (Y701), Stat1, phospho-Stat3 (Y705), Stat3, phospho-p44/42 MAPK (Erk1/2, T202/Y204), and p44/42 MAPK (Erk1/2).

Densitometry quantification

The relative quantification of gel bands from immunoblot analyses was performed by ImageJ software (<http://imagej.nih.gov/ij/>). The levels of JAK2 were first normalized to tubulin and then to JAK2 level detected for the wild type JAK2 transfectants at condition without EPO stimulation. STAT5 activation was calculated as the ratio of phosphorylated STAT5 to the normalized JAK2 level.

Dual luciferase assays for STAT transcriptional activities

The STAT transcriptional activities were measured in JAK2-deficient γ -2A fibrosarcoma cells²¹ by dual luciferase assay (Promega, Madison, WI) with either the Spi-Luc STAT5 reporter²² or pGRR5 STAT1, STAT3 and STAT5 reporter.²³ The cells were transduced with JAK2 cDNA cloned into pMEGIX retroviral vector.¹⁸ The cDNA of murine Jak2 wt, Jak2 V617F, Jak2 E846D or Jak2 R1063H was used for experiments with EPO and TPO receptor and the cDNA of human JAK2 variants for G-CSF receptor. The luciferase assay was performed as previously published.¹⁸

Retroviral mouse bone marrow reconstitution

Viral particles containing murine Jak2 wt, V617F, E846D or R1063H cDNAs (cloned in pMEGIX retroviral vector) were produced in the 293 EBNA cells. Nucleated bone marrow cells from C57BL/6 mice were collected 4 days after 5-fluorouracil treatment, infected 2-

times with the viral particles and the transduction efficiency was determined by flow cytometry analysis for GFP expression. Because of comparable efficiency (around 75%, not shown) unsorted bone marrow cells (10^5 BM cells) were used for *in vitro* colony assay according to manufacturer's instructions (M3534, StemCell Technologies). To simulate double JAK2 mutant configuration presenting in the patient, the murine bone marrow was infected with two different retroviruses containing either E846D or R1063H in ration 1:1.

Modeling based on crystal structures

Molecular graphics were prepared using PyMOL (DeLano Scientific, San Carlos, CA) to compare the X-ray crystal structures of the JAK2 kinase domain (JH1) in the inactive state (PDB: 3UGC)²⁴ and in the active state (PDB: 2B7A).²⁵

Supplemental Results

Targeted mutational screening results

Targeted mutational screening was performed using genomic DNA isolated from whole peripheral blood of all family members. Two germline variants were identified in the patient: the JAK2 E846D mutation inherited from the mother and the PHD2 Q157H mutation inherited from the father (Figure S1B). The PHD2 Q157H variant has been classified as SNP (rs61750991) in several recent publications with the frequency around 2-3 % in normal population;^{26,27} its frequency in the 1000 Genomes database is higher than 1%. This classification is supported by the fact that the Q157 amino acid is neither conserved between species nor within the PHD protein family (PHD1 and 3).²⁶

WES and microarray analysis results

WES was performed on the DNA samples isolated from the granulocytes and T-cells of the patient and they were considered as tumor and control tissue, respectively. In addition WES was applied to the DNA sample isolated from the whole blood of patient's father. The mean number of 208,642,476 unique reads per sample was obtained, which resulted in the mean coverage of 191x across all target regions (Table S3i). Using WES we identified 15 potentially somatic mutations in the patient, however after validation with Sanger sequencing they were all shown to be either false positives or germline variants (Table S3ii). The microarray analysis did not reveal the presence of any acquired chromosomal aberration in the granulocyte DNA sample from the patient. Using the microarray and WES technologies we could not find evidence of somatic mutagenesis in the patient, suggesting that the hematopoiesis was likely polyclonal. The analysis of the germline variants in the patient and subsequent validation using Sanger sequencing revealed the presence of JAK2 E846D inherited from the mother, and JAK2 R1063H inherited from the father. The JAK2 E846D was not annotated in the 1000 Genomes database, while for the JAK2 R1063H variant the presence was detected in 0.18% of subjects reported in the 1000 Genomes database (Table S4). In addition we identified an EPO G84R mutation and a TET2 P174H variant in the patient, both inherited from the father. The EPO G84R mutation was also present in the patient's healthy brother. The TET2 variant was reported with 0.1% frequency in the subjects included in the 1000 Genomes database.

Transcriptional clonality assay results

The results (the mean of duplicate determinations) showed that the G:A ratio in patient's mother cDNA was 63:37, which means her white blood cell fraction is not clonal; assuming the cut-off for clonality as ratio of $\geq 75:25$.^{28,29}

Table S1. Blood differential of the patient

	x10⁹/L <i>(Normal values)</i>	% <i>(Normal values)</i>
White blood cells count	6.9 ± 1.4 (4.0-10.0)	-
Lymphocytes	1.75 ± 0.23 (1.4-3.4)	25.7 ± 5.5 (20.5-51.5)
Monocytes	0.69 ± 0.11 (0-0.59)	11.1 ± 1.5 (1.7-9.3)
Neutrophils	5.02 ± 1.32 (1.4-6.5)	61.1 ± 6.9 (42.2-75.2)
Eosinophils	0.1 ± 0.06 (0-0.7)	1.6 ± 0.8 (0-4.0)
Basophils	0.04 ± 0.01 (0-0.2)	0.6 ± 0.3 (0-4.0)
Platelet count	306 ± 24.3 (150-400)	-

Table S2. Iron status parameters

	Patient <i>(Normal values)</i>	Mother <i>(Normal values)</i>	Father <i>(Normal values)</i>	Brother <i>(Normal values)</i>
Fe (μmol/L)	18.1 (7.2-29)	11.0 (6.6-28)	13.3 (7.2-29)	15.7 (7.2 - 29)
Total iron-binding capacity (μmol/L)	42.8 (22.3 – 61.7)	47.5 (24.2 – 70.1)	38.6 (22.3 – 61.7)	31.6 (22.3 – 61.7)
Ferritin (μg/L)	190.2 (22 – 275)	64.1 (5 – 204)	863.7* (22 – 275)	328.2* (22 – 275)
Transferrin saturation (%)	42 (21-48)	23 (21-48)	34 (21-48)	49 (21-48)

* The most likely cause of elevated ferritin levels was an infection disease as increased number of neutrophils was concomitantly detected.

Table S3i: Whole exome sequencing statistics

SAMPLE ID	SAMPLE ORIGIN	TARGET TERRITORY (bp)	PF UNIQUE READS	% PF UQ READS ALIGNED	MEAN TARGET COVERAGE	% ZERO CVG TARGETS	% TARGET COVERAGE MINIMUM						
							2x	10x	20x	30x	40x	50x	100x
Patient	Granulocytes	37317472	199134945	91.78	191.8	0.08	99.55	98.54	96.77	94.65	92.32	89.84	75.33
	T cells	37317472	251233076	92.37	213.9	0.05	99.70	99.22	98.55	97.62	96.35	94.75	82.31
Patient's father	Whole blood	37317472	175559407	91.88	169.2	0.07	99.54	98.38	96.33	93.86	91.15	88.22	70.86
Mean		37317472	208642476	92.01	191.7	0.07	99.60	98.71	97.22	95.38	93.27	90.93	76.17

PF UNIQUE READS - the number of reads that pass the vendor's filter and are not marked as duplicates; UQ - unique; % ZERO CVG TARGETS - percentage of targets with coverage <2x.

Table S3ii: Outcome of the Sanger sequencing validation of hits detected as somatic by whole exome sequencing

Gene	Chromosome	Position	Amino acid change	Variant frequency in the granulocyte DNA sample	Variant frequency in the T-cells' DNA sample	Validation outcome
<i>PCDHAS5</i>	5	140202859	E500G	14%	not detected	false positive
<i>SRRM1</i>	1	24978928	D243E	21%	not detected	false positive
<i>DHX38</i>	16	72143360	E1143G	14%	not detected	false positive
<i>HIPK4</i>	19	40885573	L591P	18%	not detected	false positive
<i>LMOD1</i>	1	201915330	V47L	50%	1.15%	germline
<i>RPGRIPI</i>	14	21790154	P585S	48%	9.46%	germline
<i>FAMI61A</i>	2	62066986	Q385E	50%	9.45%	germline
<i>DXO</i>	6	31938188	R294C	52%	8.24%	germline
<i>VWDE</i>	7	12397130	P1096A	41%	8.33%	germline
<i>CCDC141</i>	2	179914649	P7L	48%	0.79%	germline
<i>ESPL1</i>	12	53687113	T2073M	44%	8.28%	germline
<i>IL25</i>	14	23845076	R158H	42%	9.09%	germline
<i>ZNF891</i>	12	133698377	M43T	43%	6.99%	germline
<i>ASTN1</i>	1	176853477	T1075I	44%	8.33%	germline
<i>KCP</i>	7	128518682	UNKNOWN	48%	9.09%	germline

Table S4: JAK2 variants frequencies

	E846D	R1063H
CHROMOSOME	9	9
POSITION	5081828	5126343
SNP ID	rs150221602	rs41316003
REFERENCE ALLELE	G	G
ALTERNATIVE ALLELE	C	A
X1000g2014oct_all	-	0.18 %
X1000g2014oct_eur	-	0.40 %
esp6500siv2_all	0.05 %	0.43 %
ESP6500:African_American Allele frequency (count)	G: 0.999773 (4405) C: 0.000226963 (1)	G: 0.998 (4398) A: 0.002 (8)
ESP6500:European_American Allele frequency (count)	G: 0.999 (8595) C: 0.001 (5)	G: 0.994 (8550) A: 0.006 (48)
NHLBI-ESP:ESP_Cohort_Populations Allele frequency (count)	G: 0.999 (4547) C: 0.001 (3)	G: 0.996 (4518) A: 0.004 (16)
CLINSEQ_SNP:CSAgilent Allele frequency (count)	G: 0.999 (1322) C: 0.001 (1)	G: 0.996 (1306) A: 0.004 (5)
EVA_EXAC:ExAc_Aggreated_Populations Allele frequency (count)	G: 0.999531 (121355) C: 0.000469476 (57)	G: 0.996 (120875) A: 0.004 (525)

NHLBI-ESP:ESP_Cohort_Populations - Data derived from population cohorts participating in the NHLBI Exome Sequencing Project; CLINSEQ_SNP:CSAgilent - Population of 662 participants of European descent from the Clinseq project; EVA_EXAC:ExAc_Aggreated_Populations - Populations and size represented in the ExAC data are aggregated from multiple studies listed in exac.broadinstitute.org/faq; X1000g2014oct_eur - European population frequency from 1000 GENOMES database; X1000g2014oct_all - general population frequency from 1000 GENOMES database; esp6500siv2_all - general population frequency from ESP6500 database. Data source: Ensemble genome browser.

Table S5: Screening of the cohort of patients with different etiology

Diagnosis	Total number	Number of JAK2 E846D positive	Number of JAK2 R1063H positive
Healthy controls	n = 27	n = 0	n = 0
MPN – JAK2 V617F+	n = 15	n = 1*	n = 1
MPN – CALR mutation+	n = 31	n = 1*	n = 0
Pediatric ET	n = 10	n = 0	n = 0
Pediatric congenital erythrocytosis	n = 17	n = 0	n = 0

JAK2 mutation analysis was performed either by targeted sequencing or nested ARMS PCR. MPN – myeloproliferative neoplasm, CALR – calreticulin, ET – essential thrombocytemia, *denotes the same MPN patient with both JAK2 V617F and CALR mutations

Table S6: Genotyping of erythroid colonies for JAK2 E846D mutation

	Total number	Number of JAK2 E846D
Patient's BFU-Es	n = 100	n = 0 homozygous n = 100 heterozygous
Mother's BFU-Es	n = 30	n = 0 homozygous n = 30 heterozygous

The genotype of hypersensitive BFU-E colonies, grown in media with EPO concentration of 0.03 or 0.06 U/mL, was performed using nested ARMS PCR as described above.

Figure S1

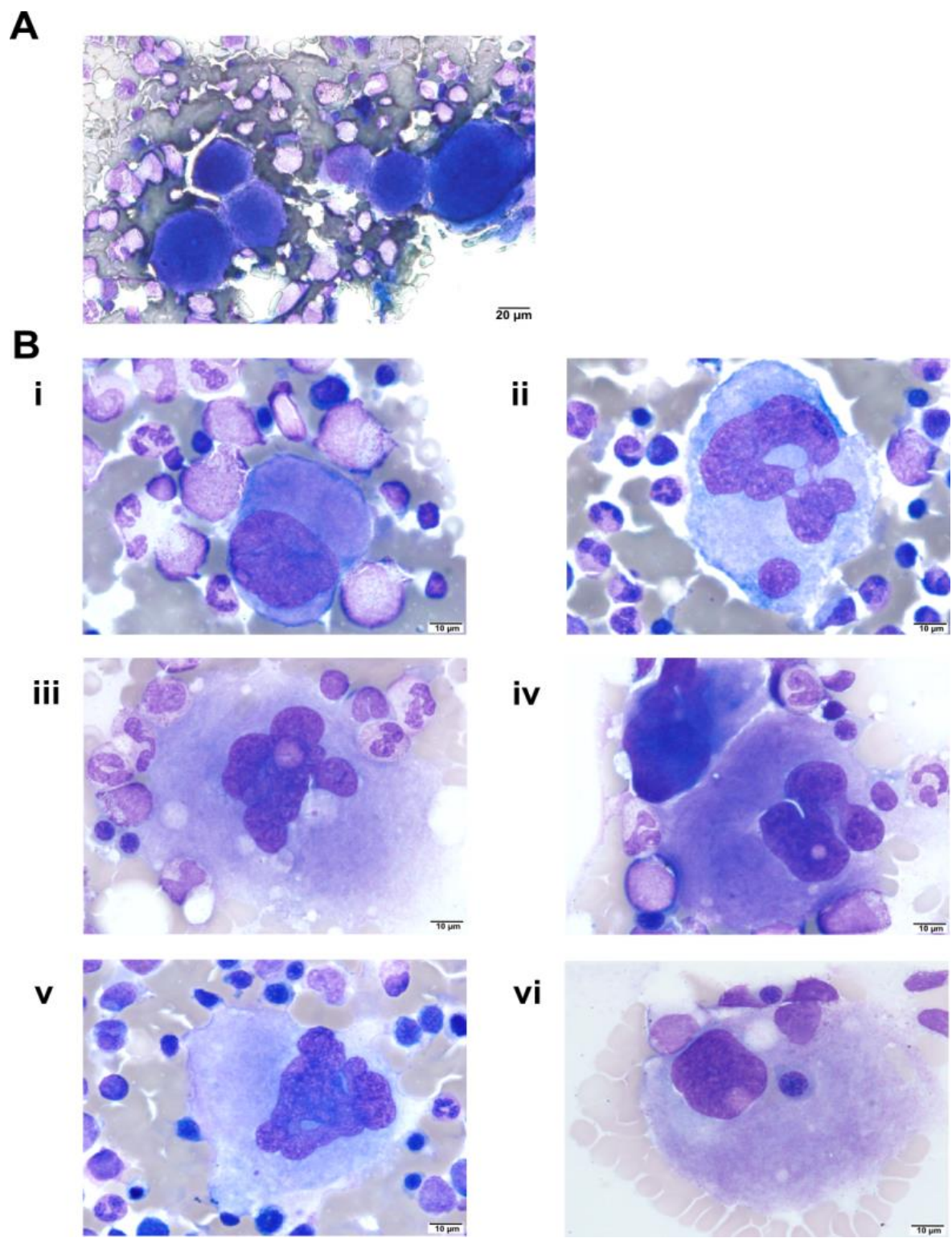
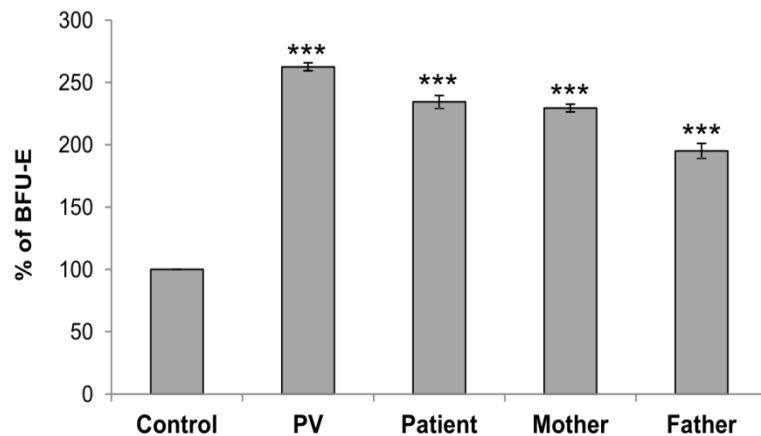


Figure S1. Bone marrow aspirate. Patient's BM aspirate (May Grunwald/Giemsa staining) revealed mild megakaryocytic hyperplasia with polymorphic megakaryocytes of varying cell

size and nuclear lobation, with frequent immature large hypolobulated megakaryocytes. An asynchronous maturation of the nucleus and the cytoplasm with a defect in platelet budding was also noted. Most of the megakaryocytes had hypo- or hyper-lobulated nucleus. Mature megakaryocytes with normally lobulated nucleus and abundant pink cytoplasm diffusely filled with red granules were rarely observed. The megakaryocyte in Panel **Bvi** has mature cytoplasm, but hypo-lobulated nucleus (the budding can also be seen). The images were visualized with an Olympus BX41 light microscope (Olympus, Hamburg, Germany) and acquired with an Olympus DP73 camera driven by CellSens Entry software. Images were labeled using Adobe Photoshop software (Adobe Systems, San Jose, CA). Pictures Panel A: magnification 400 \times , scale bar 20 μm and Panel B, magnification 1000 \times , scale bar 10 μm .

Figure S2

A



B

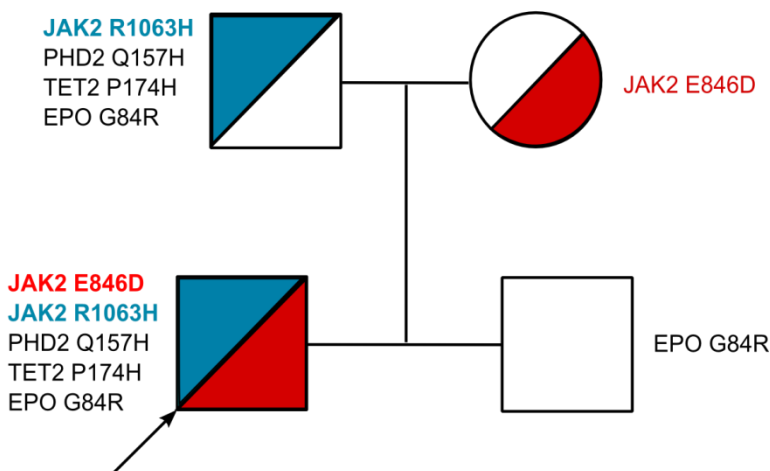
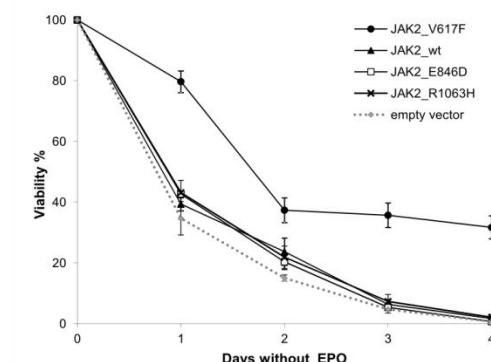


Figure S2. Growth of BFU-E colonies in 1U/mL of EPO, family pedigree. **A.** Mononuclear cells (MNC) from the patient, his parents, three V617F-positive PV patients and three healthy controls were plated in media containing 1.0 U/mL EPO and counted for the BFU-E colonies. As expected, we observed the highest number of BFU-E colonies per 2.3×10^5 viable MNC plated for the PV samples (58.8 ± 3.2)³⁰ and the lowest number of BFU-E colonies for the controls (22.4 ± 1.7); the difference was statistically significant. The number of BFU-E colonies for the patient (52.5 ± 5.1) and his parents' samples reached almost the same value as for the PV samples (mother: 51.4 ± 3.1 ; father: 43.7 ± 6.0), suggesting an increase in the number of circulating progenitors in all three family members. The experiment was repeated two times with the use of patient's and his parents' MNCs isolated from the peripheral blood on two different dates \pm SD; *** for $P < 0.001$. **B.** Family pedigree shows the presence of *JAK2*

c.2538G>C (p.E846D) germline mutation in the patient and his mother and the presence of *JAK2* c.3188G>A (p.R1063H), *PHD2* c.471G>C (p.Q157H), *TET2* c.521C>A (p.P174H), *EPO* c.250G>C (p.G84R) germline mutations in the patient and his father. Patient's brother inherited only the EPO G84R mutation.

Figure S3

A



B

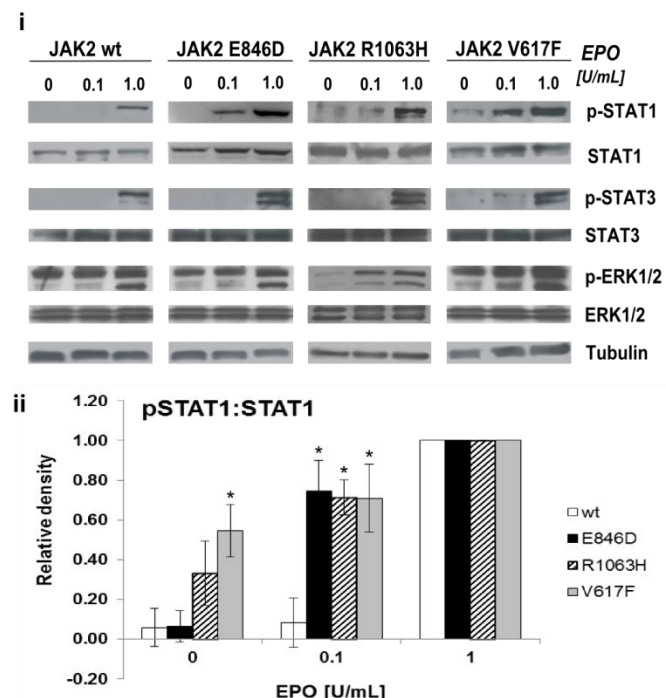


Figure S3. Viability assay of JAK2 E846D and JAK2 R1063H Ba/F3 transfectants, immunoblot analysis of JAK2 downstream signaling. **A.** The percentage of viable Ba/F3-EPOR cells in the absence of EPO was determined at indicated time-points by the exclusion of the Trypan blue from the cells. JAK2 E846D and R1063H do not support growth of stable transfectants in cytokine-free media. Only JAK2_V617F transfectants were able to become EPO-independent. Results are shown as the mean \pm SD ($n = 3$). **Bi.** The stable Ba/F3-EPOR-IL3-dependent transfectants were after IL3 starvation stimulated with indicated concentrations of EPO for 15 minutes. Immunoblot and subsequent densitometry analysis revealed that JAK2_E846D and JAK2_R1063H transfectants showed increase in STAT1 activation (Bi and Bii). Only cells expressing JAK2_V617F increased activation of STAT3 and ERK1/2. **Bii.** The relative quantification of gel bands from immunoblot analyses was performed by ImageJ software (<http://imagej.nih.gov/ij/>). Each bar represents the ratio of the density of phosphorylated Stat1 (p-Stat1) to the density of loading control (total Stat1) and is presented as fold change against the ratio calculated for 1.0 U/mL of EPO. Results are shown as the mean of two independent experiments \pm SD.

Figure S4

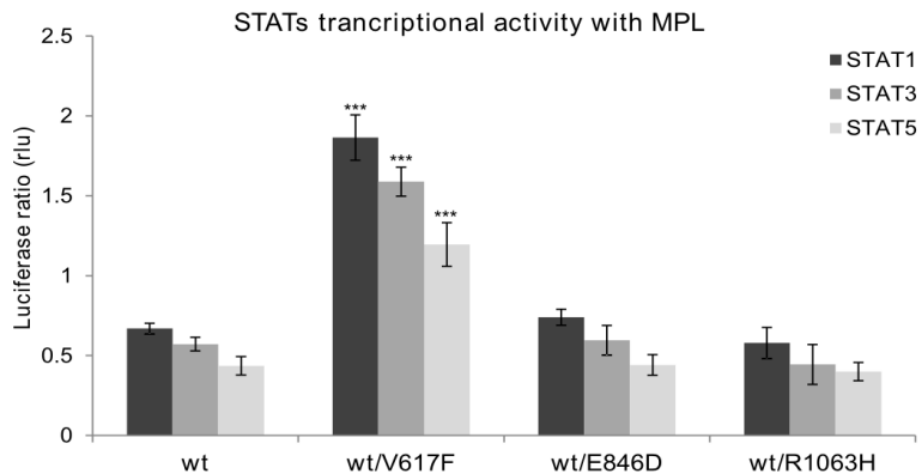


Figure S4. Luciferase assay for STAT1, STAT3 and STAT5 activity with MPL. A, B, C. Luciferase assays were performed in JAK2-deficient γ -2A cells which were transfected using Lipofectamine (Life Technologies) with various JAK2 cDNAs in the presence of MPL. To mimic heterozygous configuration, JAK2 wt cDNA was co-transfected with JAK2 V617F, JAK2 E846D or JAK2 R1063H. Four hours after transfection, the cells were put into cytokine-free media and luminescence was detected in cell lysates 48 hours after transfection using a Perkin-Elmer Victor X Light analyzer (Perkin-Elmer). Only JAK2 V617F significantly increased STAT1, STAT3 and STAT5 transcriptional activity in the presence of MPL. STATs transcriptional activity of JAK2 E846D and JAK2 R1063H cells were comparable to wt cells in the context of MPL. Rlu means relative light unit. The panels show the average of 3 independent experiment \pm SEM; * for $P < 0.05$, ** for $P < 0.01$, *** for $P < 0.001$ using the 2-tailed Student t-test.

Figure S5

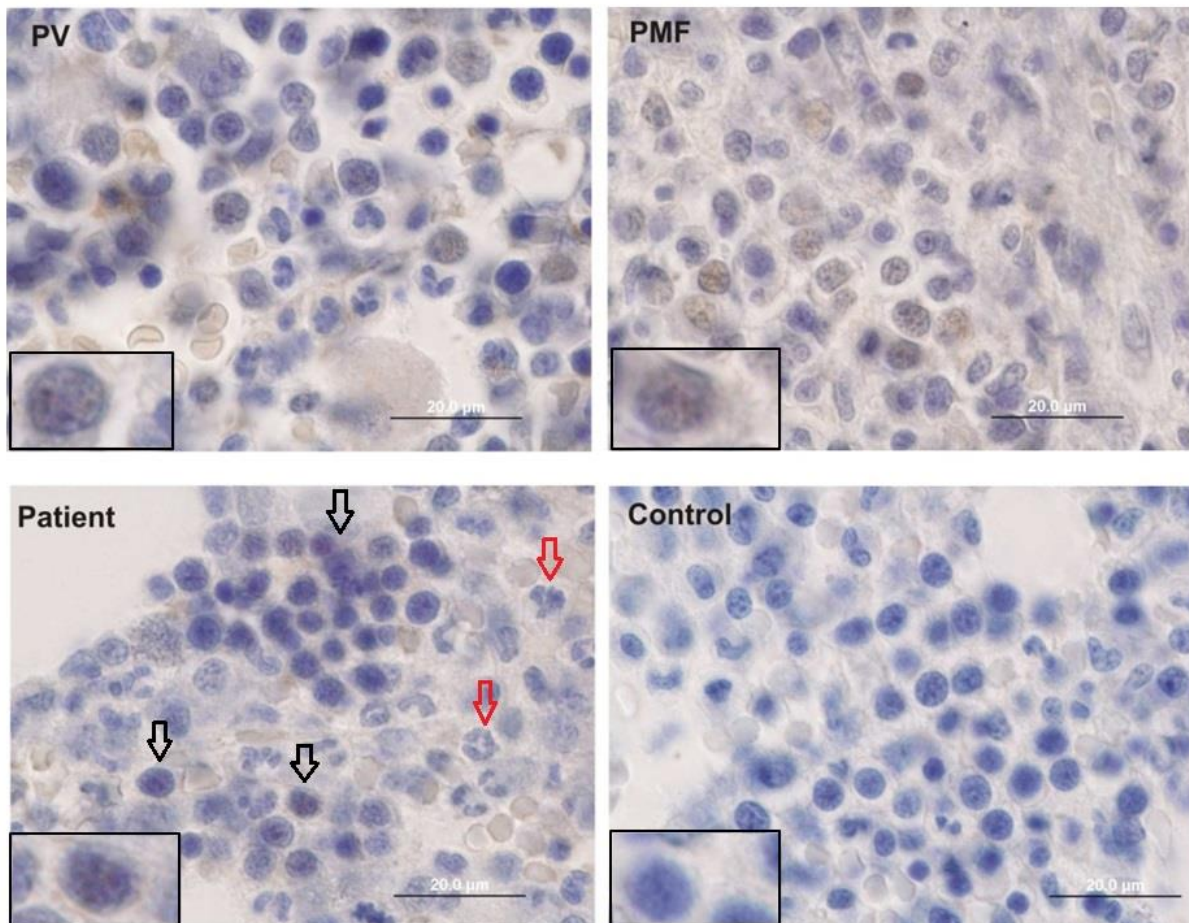


Figure S5. Immunohistochemistry for STAT5 phosphorylation in patient's BM. Specific immunohistochemical staining of BM aspirate confirmed increased phosphorylation of STAT5 (brown nuclear staining) in the JAK2 E846D/R1063H-positive patient's erythroblasts. The slides were analyzed together with samples from JAK2 V617F-positive PV and primary myelofibrosis (PMF) patients (positive controls) and sample from a healthy control. The insets show one cell in detail. The cells of erythroid lineage (mostly polychromatophilic erythroblast), grouped into the clusters and identified according to their morphology, are depicted with black arrows. Red arrows indicate cells of granulocytic lineage with the absence of STAT5 phosphorylation. Immunohistochemical slides were analyzed with an Olympus BX51 light microscope (Olympus), magnification 1000×. Digital images were acquired with an Olympus DP50 camera driven by DP controller software (provided by Olympus). Images were cropped, assembled, and labeled using Adobe Photoshop software (Adobe Systems). Scale bar is 20 μm.

Figure S6.

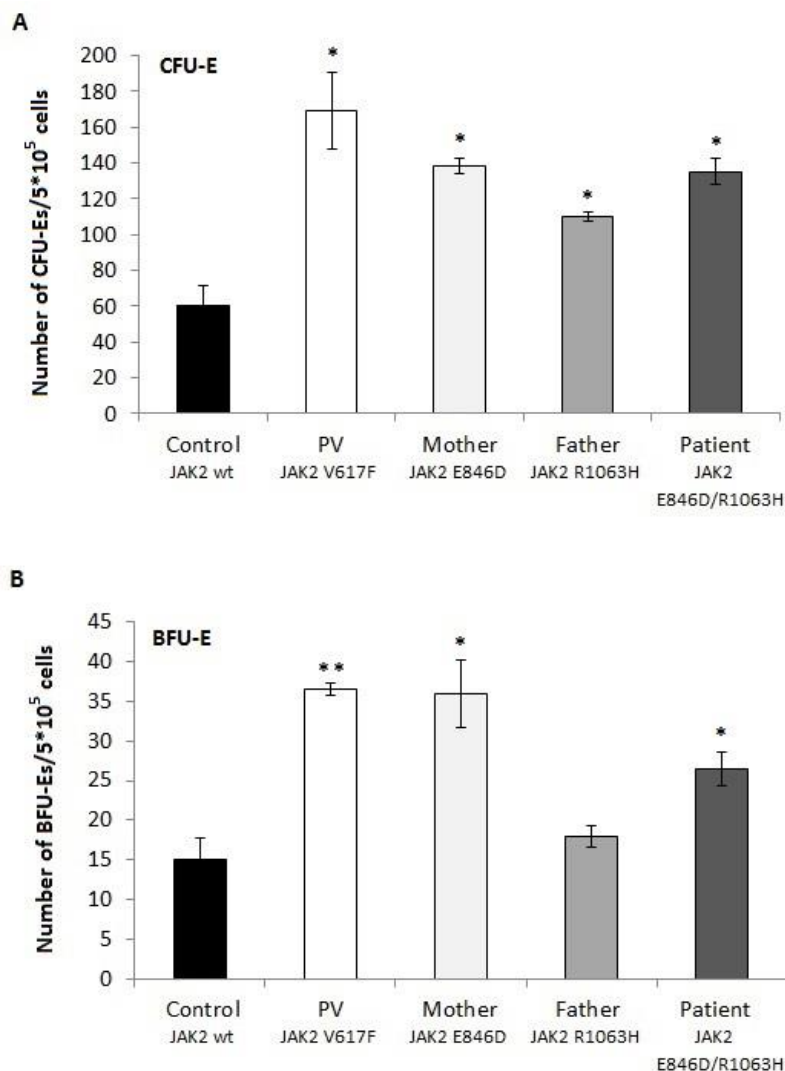
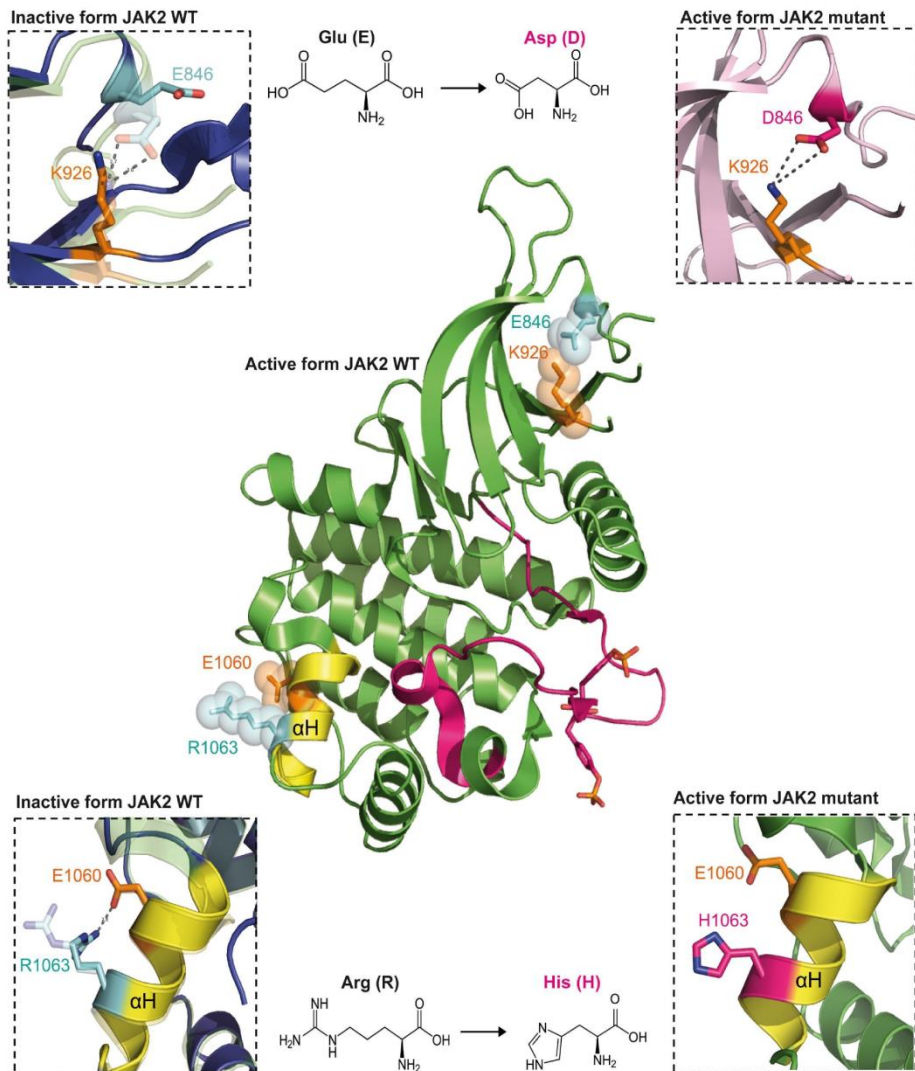


Figure S6. Replating capacity of the primary cells with JAK2 mutations. MNC cells (2.3×10^5) were initially plated in the methylcellulose media with 1.0 U/mL EPO. The initial plates yielded comparable number of BFU-E colonies in the primary culture for the patient and his parents (Figure S1). BFU-E colonies (day 12) were harvested and 5×10^5 cells were seeded in media with low EPO concentration (0.12 U/mL). In secondary EPO-limited cultures we detected: **A**) significantly higher number of CFU-E colonies for the PV samples (JAK2 V617F) and samples of the patient (JAK2 E846D/R1063H), his mother (JAK2 E846D) and father (JAK2 R1063H); **B**) BFU-E colony number was significantly increased for the PV samples (JAK2 V617F) and samples of the patient (JAK2 E846D/R1063H) and his mother (JAK2 E846D). Number of BFU-E colonies derived from JAK2 R1063H sample of patient's father was comparable to number of JAK2 wt BFU-Es. The panels show the average of 2 independent experiments \pm SD. P values were calculated using the Origin 6.1 software

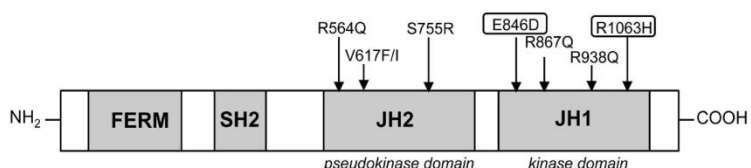
(OriginLab Corporation, Norhampton, MA); * for $P < 0.05$, ** for $P < 0.01$). No homozygotization of the JAK2 E846D mutation was detected for the EPO-hypersensitive BFU-E colonies (see Table S6).

Figure S7

A



B



V617F - Myeloproliferative Neoplasm
V617I - Familial Thrombocytosis (Mead et al., 2012)
R564Q - Familial Thrombocytosis (Etheridge et al., 2014)
S775R/R938Q - Familial Thrombocytosis (Marty et al., 2014)
R867Q - Familial Thrombocytosis (Marty et al., 2014)

Figure S7. *In silico* modeling of JAK2 E846D and JAK2 R1063H and localization of JAK2 germline mutations. **A.** In the active conformation of JAK2 kinase domain (main picture, green; PDB:2B7A),²⁵ E846 forms a salt bridge with K926 located within the β sheet 5 in the N-terminal domain. In the inactive conformation of the kinase domain (square on the upper left, blue cartoon; BDB: 3UGC),²⁴ E846 is rotated out and in that orientation it cannot form a salt bridge with K926. The E846-K926 salt bridge appears to maintain the β sheet 5 in a position exclusively required for the active conformation. Substitution of a E846 by the shorter negatively charged aspartate (D) would predict to promote a tighter salt bridge that would reinforce the active conformation of JH1 (square on the upper right). Indeed, this salt bridge would be more difficult to break when returning to the ground inactive state, and thus activation would be prolonged. R1063 is lying in the so-called “JAK specific insertion” comprising the additional α -helix (α H) (yellow) within the kinase domain.³¹ This motif, only present in JAKs family, is likely involved in intramolecular regulation of JAK2 since its deletion was shown to abolish autophosphorylation in JAK2.³¹ R1063 forms a salt bridge with E1060 in the inactive state of JH1 only (square on the bottom left). This salt bridge is predicted to be broken by the R1063H mutation, consistent with the active conformation (main picture) that does not possess this interaction. Such mutation would be presumed to facilitate the active conformation of JH1 (square on the bottom right). **B.** E846D and R1063H mutations are localized in the JAK2 kinase domain (JH1) close to the positions of germline JAK2 mutations associated with hereditary thrombocytosis.

Figure S8

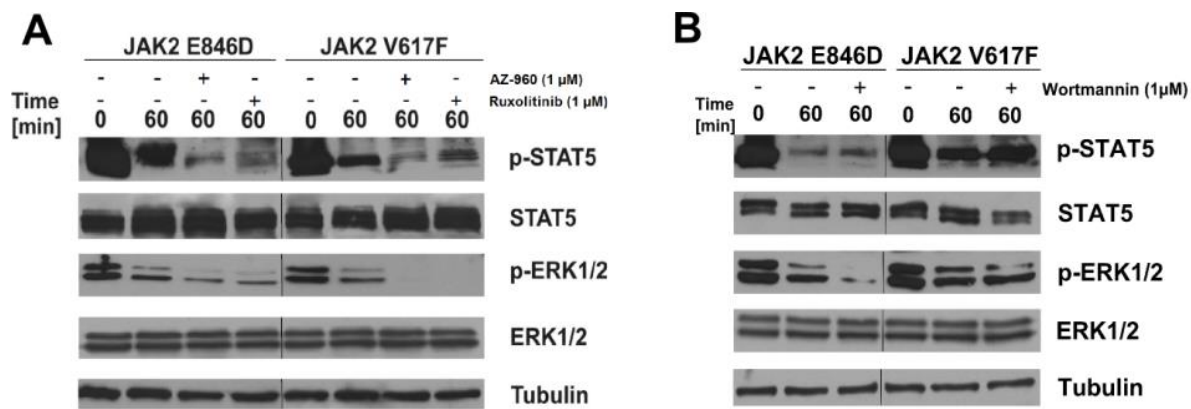


Figure S8. JAK2 inhibitors mitigate the prolonged activation of JAK2 E846D. Stable Ba/F3-EPOR transfectants were starved for IL-3 for 12 hours, then stimulated with 20 U/mL EPO for 15 min and subsequently incubated in IMDM with 1 μM concentration of Ruxolitinib, AZ-960 (**A**) or Wortmannin (**B**) for 60 min. DMSO as vehicle was used in negative controls. Both JAK2 inhibitors, Ruxolitinib and AZ-960, reduced the prolonged activation of STAT5 and ERK1/2 in JAK2_E846D cells, as well as in V617F cells. The PI3K inhibitor, Wortmannin, does not reduce the STAT5 prolonged activation of JAK2_E846D and JAK2_V617F cells and was used as a control to JAK2 inhibitors.

References:

1. Zadrazil J, Horak P, Horcicka V, Zahalkova J, Strebl P, Hruby M. Endogenous erythropoietin levels and anemia in long-term renal transplant recipients. *Kidney Blood Press Res.* 2007;30(2):108-116.
2. Fairbanks VF, Klee GG, Wiseman GA, et al. Measurement of blood volume and red cell mass: re-examination of ⁵¹Cr and ¹²⁵I methods. *Blood Cells Mol Dis.* 1996;22(15):169-186.
3. Veselovska J, Pospisilova D, Pekova S, et al. Most pediatric patients with essential thrombocythemia show hypersensitivity to erythropoietin in vitro, with rare JAK2 V617F-positive erythroid colonies. *Leuk. Res.* 2008;32(3):369-377.
4. Klampfsl T, Gisslinger H, Harutyunyan AS, et al. Somatic mutations of calreticulin in myeloproliferative neoplasms. *N Engl J Med.* 2013;369(25):2379-2390.
5. Kralovics R, Indrak K, Stopka T, et al. Two new EPO receptor mutations: truncated EPO receptors are most frequently associated with primary familial and congenital polycythemias. *Blood.* 1997;90(5):2057-2061.
6. Cario H, Schwarz K, Jorch N, et al. Mutations in the von Hippel-Lindau (VHL) tumor suppressor gene and VHL-haplotype analysis in patients with presumable congenital erythrocytosis. *Haematologica.* 2005;90(1):19-24.
7. Percy MJ, Furlow PW, Lucas GS, et al. A gain-of-function mutation in the HIF2A gene in familial erythrocytosis. *N. Engl. J. Med.* 2008;358(2):162-168.
8. Li H. Aligning sequence reads, clone sequences and assembly contigs with BWA-MEM. arXiv:13033997. 2013.
9. McKenna A, Hanna M, Banks E, et al. The Genome Analysis Toolkit: a MapReduce framework for analyzing next-generation DNA sequencing data. *Genome Res.* 2010;20(9):1297-1303.
10. International Human Genome Sequencing C. Finishing the euchromatic sequence of the human genome. *Nature.* 2004;431(7011):931-945.
11. Genomes Project C, Abecasis GR, Auton A, et al. An integrated map of genetic variation from 1,092 human genomes. *Nature.* 2012;491(7422):56-65.
12. Van der Auwera GA, Carneiro MO, Hartl C, et al. From FastQ Data to High-Confidence Variant Calls: The Genome Analysis Toolkit Best Practices Pipeline. *Current Protocols in Bioinformatics.* 2013;43:11.10.11-11.10.33.
13. Milosevic Feenstra JD, Nivarthi H, Gisslinger H, et al. Whole exome sequencing identifies novel MPL and JAK2 mutations in triple negative myeloproliferative neoplasms. *Blood.* 2016;127(3):325-332.
14. Liu E, Jelinek J, Pastore YD, et al. Discrimination of polycythemias and thrombocytoses by novel, simple, accurate clonality assays and comparison with PRV-1 expression and BFU-E response to erythropoietin. *Blood.* 2003;101(8):3294-3301.
15. Swierczek SI, Agarwal N, Nussenzveig RH, et al. Hematopoiesis is not clonal in healthy elderly women. *Blood.* 2008;112(8):3186-3193.
16. Collins A, and Ke X. Primer1: Primer design Web service for Tetra-Primer ARMS-PCR. *The Open Bioinformatics Journal.* 2012;6:55-58.

17. Pospisilova D, Holub D, Zidova Z, et al. Hepcidin levels in Diamond-Blackfan anemia reflect erythropoietic activity and transfusion dependency. *Haematologica*. 2014;99(7):e118-21.
18. James C, Ugo V, Le Couédic JP, et al. A unique clonal JAK2 mutation leading to constitutive signalling causes polycythaemia vera. *Nature*. 2005;434(7037):1144-1148.
19. D'Andrea AD, Yoshimura A, Youssoufian H, et al. The cytoplasmic region of the erythropoietin receptor contains nonoverlapping positive and negative growth-regulatory domains. *Mol Cell Biol*. 1991;11(4):1980-1987.
20. Koledova Z, Kafkova LR, Calabkova L, et al. Cdk2 inhibition prolongs G1 phase progression in mouse embryonic stem cells. *Stem Cells Dev*. 2010;19(2):181-194.
21. Kohlhuber F, Rogers NC, Watling D, et al. A JAK1/JAK2 chimera can sustain alpha and gamma interferon responses. *Mol Cell Biol*. 1997;17(2):695-706.
22. Wood TJ, Sliva D, Lobie PE, et al. Specificity of transcription enhancement via the STAT responsive element in the serine protease inhibitor 2.1 promoter. *Mol Cell Endocrinol*. 1997;130(1-2):69-81.
23. Dumoutier L., Van Roost E., Colau D, et al. Human interleukin-10-related T cell-derived inducible factor: molecular cloning and functional characterization as an hepatocyte-stimulating factor. *Proc Natl Acad Sci U S A*. 2000; 97(18):10144-10149.
24. Andraos R, Qian Z, Bonenfant D, et al. Modulation of activation-loop phosphorylation by JAK inhibitors is binding mode dependent. *Cancer Discov*. 2012;2(6):512-523.
25. Lucet IS, Fantino E, Styles M, et al. The structural basis of Janus kinase 2 inhibition by a potent and specific pan-Janus kinase inhibitor. *Blood*. 2006;107(1):176-183.
26. Ladroue C, Hoogewijs D, Gad S, et al. Distinct deregulation of the hypoxia inducible factor by PHD2 mutants identified in germline DNA of patients with polycythemia. *Haematologica*. 2012;97(1):9-14.
27. Albiero E, Ruggeri M, Fortuna S, et al. Isolated erythrocytosis: study of 67 patients and identification of three novel germ-line mutations in the prolyl hydroxylase domain protein 2 (PHD2) gene. *Haematologica*. 2012;97(1):123-127.
28. Busque L, Paquette Y, Provost S, et al. Skewing of X-inactivation ratios in blood cells of aging women is confirmed by independent methodologies. *Blood*. 2009;113(15):3472-3474.
29. Swierczek SI, Piterkova L, Jelinek J, et al. Methylation of AR locus does not always reflect X chromosome inactivation state. *Blood*. 2012;119(13):e100-109.
30. Jamieson CH, Gotlib J, Durocher JA, et al. The JAK2 V617F mutation occurs in hematopoietic stem cells in polycythemia vera and predisposes toward erythroid differentiation. *Proc Natl Acad Sci U S A*. 2006;103(16):6224-6229.
31. Haan C, Kroy DC, Wüller S, et al. An unusual insertion in Jak2 is crucial for kinase activity and differentially affects cytokine responses. *J Immunol*. 2009;182(5):2969-2977.

Príloha 4

Mambet C, Babosova O, Defour JP, Leroy E, Necula L, Stanca O, Tatic A, Berbec N,
Coriu D, Belickova M, **Kralova B**, Lanikova L, Vesela J, Pecquet C, Saussoy P,
Havelange V, Diaconu CC, Divoky V, Constantinescu SN.
Co-Occurring JAK2 V617F and R1063H Mutations Increase JAK2 Signaling and
Neutrophilia in MPN Patients.
Blood. 2018; 132(25):2695-2699.

21. Hermine O, Lefrère F, Bronowicki JP, et al. Regression of splenic lymphoma with villous lymphocytes after treatment of hepatitis C virus infection. *N Engl J Med.* 2002;347(2):89-94.
22. da Silva Almeida AC, Abate F, Khiabanian H, et al. The mutational landscape of cutaneous T cell lymphoma and Sézary syndrome. *Nat Genet.* 2015;47(12):1465-1470.
23. Choi J, Goh G, Walradt T, et al. Genomic landscape of cutaneous T cell lymphoma. *Nat Genet.* 2015;47(9):1011-1019.
24. Pomerantz RG, Mirvish ED, Erdos G, Falo LD Jr, Geskin LJ. Novel approach to gene expression profiling in Sézary syndrome. *Br J Dermatol.* 2010;163(5):1090-1094.
25. Jeon YK, Go H, Nam SJ, et al. Expression of the promyelocytic leukemia zinc-finger in T-lymphoblastic lymphoma and leukemia has strong implications for their cellular origin and greater association with initial bone marrow involvement. *Mod Pathol.* 2012;25(9):1236-1245.

DOI 10.1182/blood-2018-07-863381

© 2018 by The American Society of Hematology

TO THE EDITOR:

Cooccurring JAK2 V617F and R1063H mutations increase JAK2 signaling and neutrophilia in myeloproliferative neoplasms

Cristina Mambet,^{1,3,*} Olga Babosova,^{4,*} Jean-Philippe Defour,^{2,5,*} Emilie Leroy,^{1,2} Laura Necula,³ Oana Stanca,^{6,7} Aurelia Tatic,^{7,8} Nicoleta Berbec,^{6,7} Daniel Coriu,^{7,8} Monika Belickova,⁹ Barbora Kralova,¹⁰ Lucie Lanikova,⁴ Jitka Vesela,⁹ Christian Pecquet,^{1,2} Pascale Saussoy,⁵ Violaine Havelange,¹¹ Carmen C. Diaconu,³ Vladimir Divoky,¹⁰ and Stefan N. Constantinescu^{1,3}

¹Ludwig Institute for Cancer Research, Brussels Branch, Brussels, Belgium; ²de Duve Institute, Université Catholique de Louvain, Brussels, Belgium; ³Molecular Profiling of Myeloproliferative Neoplasms and Acute Leukemia (MyeloAL) Program, Stefan S. Nicolau Institute of Virology, Bucharest, Romania; ⁴Department of Cell and Developmental Biology, Institute of Molecular Genetics, Academy of Sciences of the Czech Republic, Prague, Czech Republic; ⁵Department of Clinical Biology, Cliniques Universitaires Saint-Luc, Université Catholique de Louvain, Brussels, Belgium; ⁶Department of Hematology, Coltea Clinical Hospital, Bucharest, Romania; ⁷Department of Radiology, Oncology, and Hematology, Carol Davila University of Medicine and Pharmacy, Bucharest, Romania; ⁸Center of Hematology and Bone Marrow Transplantation, Fundeni Clinical Institute, Bucharest, Romania; ⁹Institute of Hematology and Blood Transfusion, Prague, Czech Republic; ¹⁰Department of Biology, Faculty of Medicine and Dentistry, Palacky University, Olomouc, Czech Republic; and ¹¹Service of Hematology, Cliniques Universitaires Saint-Luc, Brussels, Belgium

Although the concept of somatic driver mutations in myeloproliferative neoplasms (MPNs) represented by polycythemia vera (PV), essential thrombocythemia (ET), and primary myelofibrosis is well established,¹⁻³ the contribution of germline or co-occurring JAK2 variants to a particular MPN phenotype is less well understood.^{4,5} Recently, 2 germline JAK2 mutations, E846D and R1063H, were described in a case of hereditary erythrocytosis;⁶ the same JAK2 R1063H variant was initially reported in 3 of 93 PV patients who were JAK2 V617F⁺.⁷

In this study, we assessed the presence of JAK2 V617F and JAK2 R1063H mutations in a cohort of MPN patients to characterize the double-mutation carriers and gain insight into the functional consequences of coexisting mutations on JAK2 signaling.

Samples from 390 MPN patients positive for JAK2 V617F in Romania ($n = 314$) and Belgium ($n = 76$) were collected for the study. JAK2 R1063H mutation screening was performed using a custom TaqMan SNP Genotyping Assay. Fourteen of 390 JAK2 V617F⁺ MPN patients were found to carry concurrent JAK2 V617F and R1063H mutations. The clinical features and hematological data recorded at disease onset are summarized in supplemental Table 1 (available on the *Blood* Web site). ET was the most frequent diagnosis in double-mutation carriers (9/14). After considering bone marrow histology and the new World Health Organization 2016 criteria for PV diagnosis,⁸ 2 patients were reconsidered to have PV. Our major finding is that a significantly higher white blood cell count ($P = .023$) and, correspondingly, a significantly higher neutrophil count ($P = .025$) were observed in double-mutation carriers compared with MPN

patients harboring only the JAK2 V617F mutation (Figure 1A). When patients with an ET diagnosis were analyzed separately, we found that carriers of both mutations displayed a significantly higher neutrophil count ($P = .031$) and hemoglobin level ($P = .046$) compared with V617F⁺ ET patients (supplemental Figure 1). Furthermore, there was ≥ 1 thrombotic event during the course of the disease in 5 patients, including 2 cases of portal vein thrombosis. Interestingly, in a recent genomic study of patients with venous thromboembolism, JAK2 R1063H was identified in 1 case and was considered a probable disease-causing variant.⁹

To compare the frequency of additional somatic mutations in the analyzed patient groups, we used a targeted NGS panel for the 14 double-mutated patients and for 53 randomly selected patients from the JAK2 V617F cohort without the R1063H variant. Although a trend toward a higher mutational load was observed in the V617F/R1063H group compared with the V617F group, the difference did not reach statistical significance ($P = .092$) (supplemental Tables 2 and 3).

Next, we aimed to characterize the genotype and configuration of JAK2 mutations in the double-positive MPN patients. For these purposes, JAK2 V617F and R1063H allelic burdens were analyzed by quantitative polymerase chain reaction (PCR) and digital droplet PCR (ddPCR), and *cis/trans* configurations of JAK2 V617F and R1063H mutations were established by sequencing single colonies of subcloned JAK2 complementary DNA obtained from peripheral blood leukocytes in 10 of 14 double-mutated patients. *Cis* configuration of the mutations

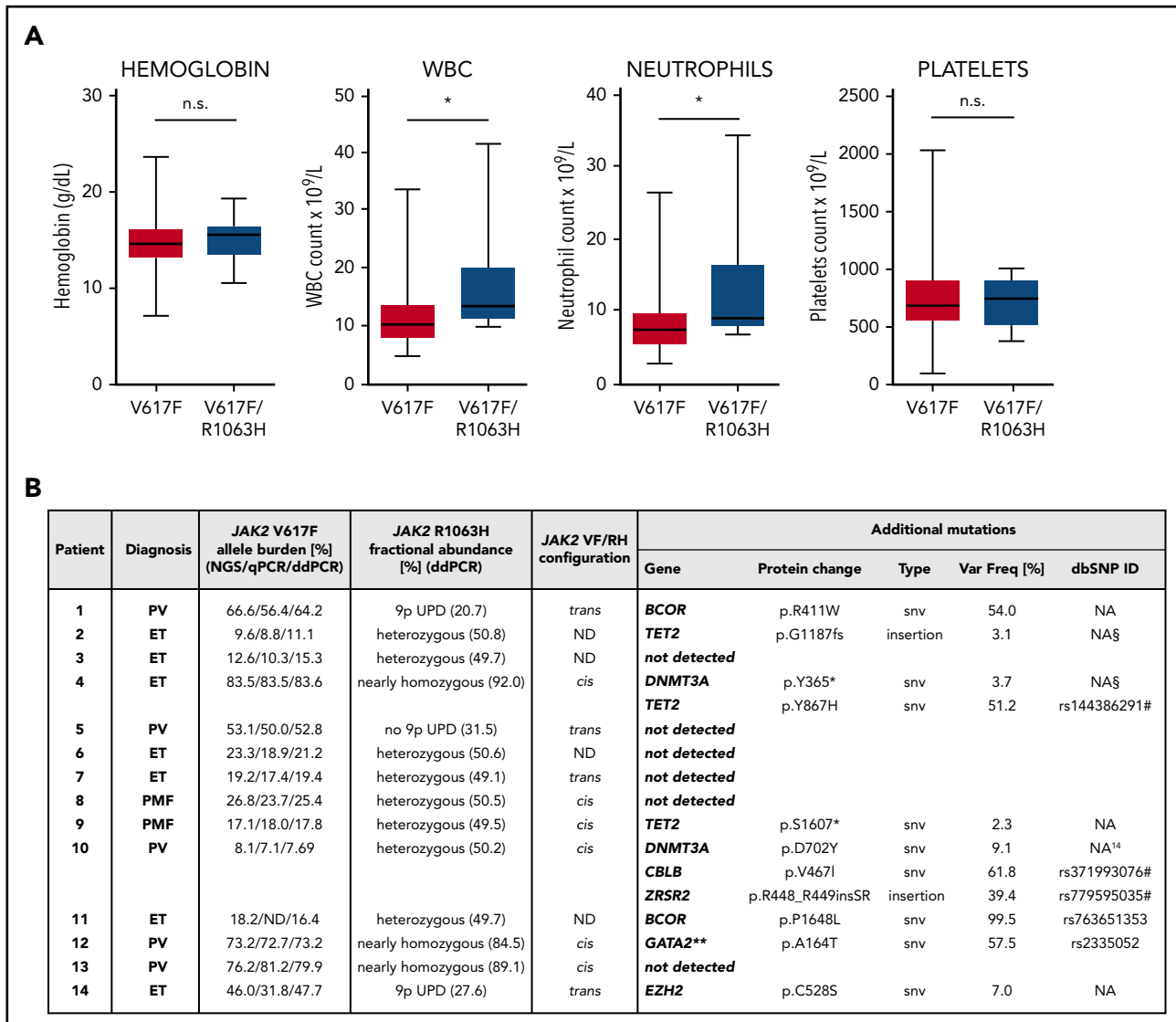


Figure 1. Clinical characteristics, JAK2 analysis, and next-generation sequencing (NGS) screening for MPN patients exhibiting JAK2 V617F and JAK2 R1063H mutations. (A) Hematological data for JAK2 V617F MPN patients ($n = 390$) subdivided according to the JAK2 R1063H mutation status. Data for V617F only ($n = 376$) and for V617F/R1063H double-mutation carriers ($n = 14$) were recorded at diagnosis. For further information, see supplemental Material and methods and supplemental Table 1. The boxes represent the 25% to 75% interquartile range, horizontal lines within the boxes indicate medians, and vertical bars show the range of values (minimum to maximum). P values $< .05$ were considered statistically significant. * $P < .05$, Mann-Whitney U test. (B) JAK2 V617F allele burden, JAK2 R1063H fractional abundance, JAK2 V617F/R1063H mutations configuration, and additional mutations identified by targeted NGS. Third column: JAK2 V617F allele frequency obtained from the NGS study and compared with allele burden determined via quantitative PCR and ddPCR assay. Fourth column: JAK2 R1063H fractional abundance was determined using ddPCR in whole-blood samples collected at the time of diagnosis (see supplemental Material and methods for details). The JAK2 R1063H mutation was considered genuine germline only when the fractional abundance of the JAK2 R1063H variant was 50% ($\pm 1.0\%$). Therefore, 8 patients are confirmed to be heterozygous germline carriers for the JAK2 R1063H variant. JAK2 R1063H in 3 samples with a percentage frequency of the mutant DNA between 20.7% and 31.5% (samples 1, 5, and 14) could be considered an acquired somatic mutation or an inherited variant that was partially lost due to UPD of the V617F–non-R1063H clone. Samples 4, 12, and 13 were nearly homozygous for JAK2 R1063H, and the presence of minor fraction of the WT allele excluded germline homozygosity. See also supplemental Figure 2. Fifth column: Cis/trans JAK2 V617F/R1063H mutations configuration was determined through sequencing of subcloned reverse-transcriptase PCR products spanning exons 14 through 24 of the JAK2 gene (see supplemental Material and methods for details). Sixth column: TruSight Myeloid Sequencing Panel (Illumina, San Diego, CA) was used for targeted mutational screening of JAK2 R1063H⁺ patients. Additional mutations were identified in 8 of 14 screened patients. A total of 11 variants was detected in 7 genes. *Five of these mutations are indexed in the Single Nucleotide Polymorphism database (dbSNP), and 4 of these specific variants are listed in the COSMIC catalog. One additional mutation in DNMT3A was published recently.¹⁴ §Two other mutations (frameshift in TET2 and premature stop codon in DNMT3A) do not have SNP/COSMIC IDs but are documented in the VarSome genomic variant database. **The GATA2 (A164T) allele (patient 12) was recently detected in a higher-than-expected frequency in myelodysplastic syndrome, suggesting a possible predisposing function in myeloid malignancies.¹⁵ Two patients harbor unique undescribed variants: patient 1 in BCOR and patient 9 in TET2. The BCOR variants were identified in 2 patients (both are missense mutations); their variant frequency was 54% for patient 1 and 99.5% for patient 11. They could be germline variants; both were estimated to be “damaging” or “probably damaging” by 2 algorithms (Sift, PolyPhen). *Indicates translation termination (stop) codon. All mutations were identified in DNA collected at the time of diagnosis; acquisition of additional mutations during disease evolution was not performed. For further information see supplemental Table 2. NA, not available; ND, not done; n.s., not significant; PMF, primary myelofibrosis; qPCR, quantitative PCR; snv, single nucleotide variant; Var Freq, variant allele frequency.

was detected in 6 cases, and trans configuration was found in 4 cases (Figure 1B). Quantification of the R1063H allele in the genomic DNA samples indicated that the variant was heterozygous

in 8 cases, likely inherited, as shown previously⁶ (R1063H percentage $\sim 50\%$). In 3 patients with high V617F allelic burden, R1063H was nearly homozygous (fractional abundance $> 80\%$),

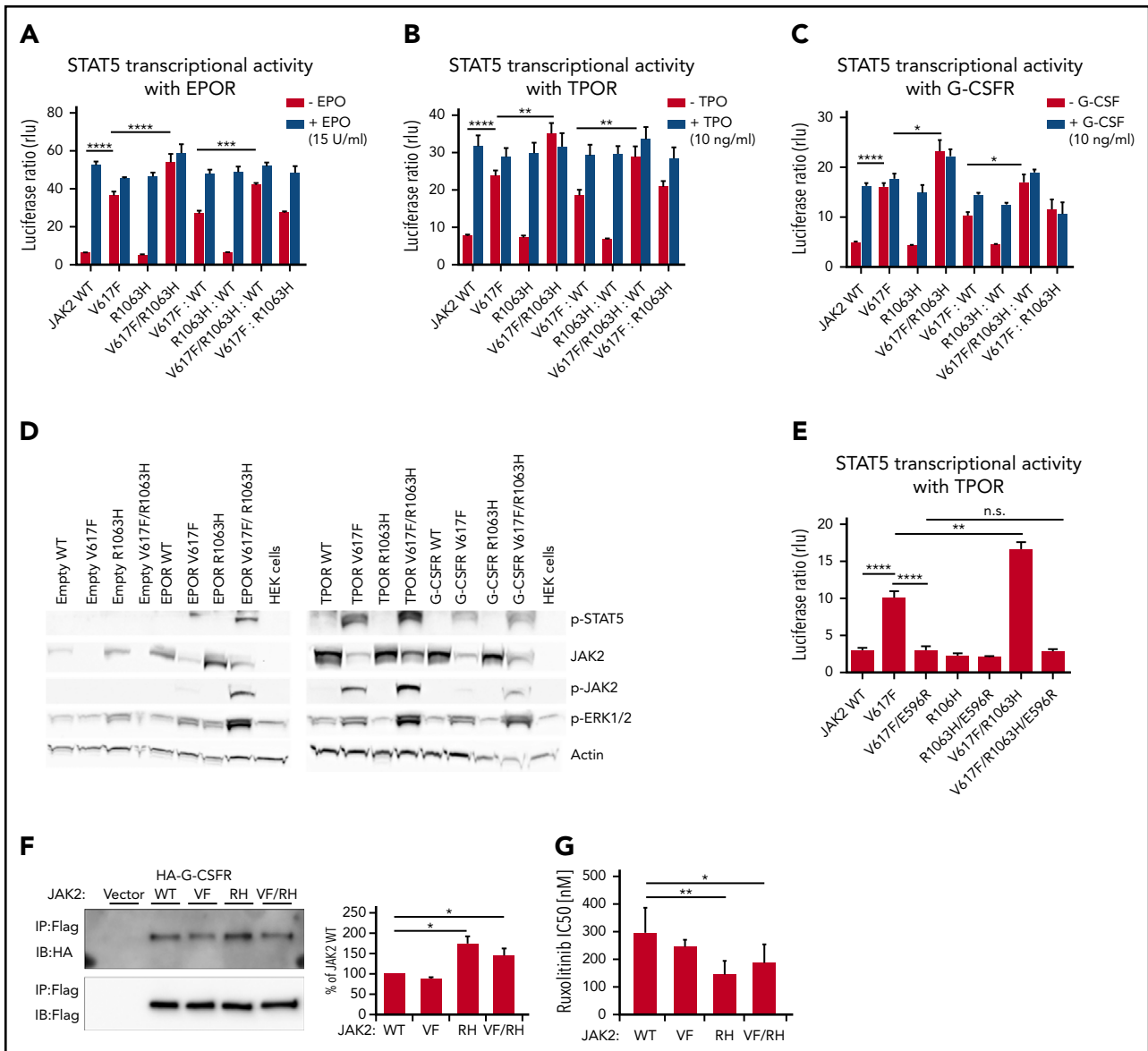


Figure 2. STAT5 transcriptional activity, the status of activation of downstream signaling by human JAK2 V617F and R1063H in the presence of dimeric myeloid cytokine receptors, the binding affinities of JAK2 mutants to G-CSFR and in vitro drug sensitivity assay. Constitutive and cytokine-dependent STAT5 transcriptional activity, as assessed by dual-luciferase assay, in γ2A cells transfected with JAK2 WT, JAK2 V617F, JAK2 R1063H, and JAK2 V617F/R1063H double mutant in the presence of EPOR (A), TPOR (B), and G-CSFR (C). Homozygous and heterozygous states of JAK2 mutants are mimicked. Shown are the averages of 9 replicates from 3 independent experiments ± standard error of the mean (SEM). *P < .05, **P < .01, ***P < .001, ****P < .0001, 1-way analysis of variance (ANOVA), followed by the post hoc Tukey test. (D) Western blot analysis of constitutive JAK2, STAT5, and ERK 1/2 phosphorylation levels (indicative of activated status) induced by human JAK2 mutants coexpressed with empty vector/ cytokine receptors in HEK 293T cells. β-actin antibody was used as a loading control. Higher levels of p-JAK2 (p-Tyr1007/1008), p-STAT5 (p-Tyr694), and p-ERK 1/2 (p-Thr202/ p-Tyr 204) are observed in cells expressing the JAK2 V617F/R1063H double mutant in comparison with JAK2 V617F. Image shown is representative of 3 independent experiments. (E) The effect of E596R mutation on constitutive STAT5 activation induced by JAK2 V617F and JAK2 V617F/R1063H, as evaluated by dual-luciferase assay, in γ2A cells in the presence of TPOR. Both mutated proteins exhibit a similar decline in constitutive activity. The graph displays the averages of 9 replicates from 3 independent experiments ± SEM. **P < .01, ****P < .0001, 1-way ANOVA, followed by the post hoc Tukey test. (F) JAK2 mutants bind to the cytokine receptor G-CSFR with different affinities. Flag-tagged JAK2 mutants were transiently expressed in HEK 293 cells in which hemagglutinin-tagged G-CSFR was stably expressed. Interaction was examined by coimmunoprecipitation with anti-Flag affinity gel. Immunoblot band intensity was quantified by ImageJ software and normalized to a loading control, and WT JAK2 intensity was set to 100%. The data represent the mean of 3 independent experiments; T bars designate SEM. See also supplemental Figure 4. P values < .05 were considered statistically significant. *P < .05, Student paired t test with equal variance. (G) In vitro drug sensitivity assay. Stably transfected Ba/F3/EPOR cells expressing JAK2 WT, JAK2 V617F, JAK2 R1063H, and JAK2 V617F/R1063H were cultivated for 72 hours with decreasing concentrations of the JAK2 inhibitor ruxolitinib (1, 0.5, 0.25, 0.1, 0.05, 0.01, and 0 μM). IC₅₀ was defined as the drug concentration needed to inhibit 50% of cell growth (using GraphPad Prism 6.01 software). The data represent the mean of 7 independent experiments performed in triplicates (see also supplemental Material and methods for details). T bars designate the standard deviation. When the ruxolitinib sensitivity of mutant cells is compared with WT cells, the sensitivity of V617F⁺ cells is not statistically significant, whereas R1063H⁺ and V617F/R1063H double-mutant cells are significantly more sensitive to ruxolitinib compared with WT cells. Experiments with AZ-960 revealed comparable results (data not shown). P < .05 was considered statistically significant. *P < .05, **P < .01, 1-way ANOVA, followed by the post hoc Tukey test. IB, immunoblot; IP, immunoprecipitation; RH, R1063H; rlu, relative light unit; VF, V617F; VF/RH, V617F/R1063H.

suggesting that 1 R1063H allele was inherited and the second allele was acquired by uniparental disomy (UPD). Low R1063H allele burden was found (allele percentage between 20.7% and 31.5%) in 3 other patients who exhibited *trans* configuration of JAK2 mutations (Figure 1B; supplemental Figure 2), raising the hypotheses that R1063H was acquired during the course of the disease or was partially lost due to UPD of the V617F–non-R1063H clone that, when amplified, decreased R1063H allelic burden. Because non-myeloid tissue DNA was not available for the study, we used a combined array-comparative genomic hybridization/single-nucleotide polymorphism assay to detect unbalanced chromosomal changes and copy number neutral loss of heterozygosity in DNA samples with low R1063H allele burden. We detected UPD on chromosome 9p in 2 of 3 samples, suggesting that both hypotheses could be valid (supplemental Figure 3). However, without germline DNA, the origin of the R1063H mutation cannot be unequivocally established.

Later, cellular models were used to assess the functional consequences of the coexisting JAK2 mutations in *cis* or *trans*. Using site-directed mutagenesis, we generated JAK2 mutants (V617F, R1063H, and V617F/R1063H) on the background of JAK2 complementary DNA cloned into a pMEGIX–IRES–GFP bicistronic vector. STAT5 transcriptional activity of the JAK2 wild-type (WT) and JAK2 mutants in the presence of myeloid dimeric cytokine receptors (erythropoietin receptor [EPOR], thrombopoietin receptor [TPOR], and granulocyte-macrophage colony-stimulating factor receptor [G-CSFR]), as measured by dual-luciferase assay, revealed significantly higher constitutive activity of JAK2 V617F/R1063H (*cis* mutant) compared with JAK2 V617F in homozygous and heterozygous configurations and with each cytokine receptor (Figure 2A–C). Also, western blot analysis demonstrated a higher level of constitutive activation of JAK2 and STAT5 induced by the V617F/R1063H mutant vs V617F (Figure 2D). We then asked whether R1063H enhances the same conformational circuit used by V617F or triggers a different one. We introduced the E596R mutation in V617F/R1063H, because this mutation was previously found to block V617F constitutive, but not ligand-induced, JAK2 activity.¹⁰ The constitutive STAT5 transcriptional activities of V617F and V617F/R1063H mutants were decreased to the same extent by E596R (Figure 2E). Thus, R1063H amplifies signaling via the same circuit as V617F.

The enhancement of G-CSFR signaling, which regulates neutrophilic granulocyte formation, by V617F/R1063H might be relevant for the neutrophilia, which is not seen in all MPN patients with JAK2 V617F. Neutrophilia is detected in JAK2-double mutant patients, irrespective of *cis*- or *trans*-configuration. For the latter, we could not see enhanced activation by R1063H and V617F vs WT JAK2 and V617F via cytokine receptors (Figure 2A–C), possibly because small changes are difficult to detect in overexpression systems. We assessed whether R1063H changes the association of JAK2 with G-CSFR. Using coimmunoprecipitation, we detected a significantly higher biochemical association between JAK2 R1063H and JAK2 V617F/R1063H with G-CSFR compared with JAK2 V617F or JAK2 (Figure 2F). This might have a significant impact on signaling at low receptor levels *in vivo*, as well as in a *trans*-configuration, because R1063H alone enhances the association of JAK2 with G-CSFR. Linking neutrophilia to the increased association of JAK2 V617F/R1063H with G-CSFR is in agreement with a recent study in which differential coupling of JAK2 mutants to different receptors impacted the *in vivo* phenotypes induced by the different mutants.¹¹ In ET double-mutant carriers, the higher

level of hemoglobin that accompanied the higher neutrophil count supports the hypothesis that the co-occurrence of JAK2 V617F and R1063H mutations would lead to an ET phenotype with PV-like features, as a result of a cumulative effect on JAK2 signaling.¹² Furthermore, the ruxolitinib sensitivity of JAK2 V617F/R1063H-expressing cells may have therapeutic implications (Figure 2G).

The frequency of R1063H in our JAK2 V617F⁺ MPN cohort (14/390) is consistent with the initial report (3/93 PV patients).⁷ The frequency of R1063H cited in the normal population in the Exome Aggregation Consortium database¹³ is much lower (0.004377). More studies on large patient populations, as well as on families with MPNs, would be necessary for determining whether JAK2 R1063H predisposes to acquisition of the JAK2 V617F mutation, as well as to assess its role in MPN progression, given the involvement of G-CSFR in leukemia.

Acknowledgments

The authors gratefully acknowledge funding from the Competitiveness Operational Program A1.1.4. ID: P_37_798, contract 149/26.10.2016 (MySMIS2014+: 10674), Molecular Profiling of Myeloproliferative Neoplasms and Acute Leukemia Project. S.N.C. received support from the Ludwig Institute for Cancer Research, Fondation contre le cancer, Salus Sanguinis, Fondation Les Avions de Sébastien, the Action de Recherche Concertée Project, and the Walloon Excellence in Lifesciences & Biotechnology project, Belgium. O.B., B.K., L.L., and V.D. received research funding from the Czech Science Foundation (project GACR 17-05988S) and from the Ministry of Education, Youth and Sports, Czech Republic (projects LO1200 [O.B.] and LTAUSA17142 [B.K., L.L., and V.D.]). M.B. and J.V. received support from the Ministry of Health of Czech Republic—conceptual development of research organization (00023736).

Authorship

Contribution: C.M., O.B., and J.-P.D. designed and performed research, analyzed data, and wrote the manuscript; L.N., O.S., A.T., N.B., D.C., V.H., P.S., and C.C.D. recruited the patients, performed research, and contributed to the editing of the manuscript; E.L., B.K., M.B., J.V., L.L., and C.P. performed research, analyzed data, and reviewed the manuscript; and S.N.C. and V.D. designed the study, wrote the manuscript, and provided financial support.

Conflict-of-interest disclosure: The authors declare no competing financial interests.

ORCID profiles: O.B., 0000-0001-7036-6807; M.B., 0000-0002-9158-881X; C.C.D., 0000-0002-2259-1425; V.D., 0000-0003-0202-245X.

Correspondence: Stefan N. Constantinescu, Ludwig Institute for Cancer Research, Ave Hippocrate 74, UCL, 75-4, 1200 Brussels, Belgium; e-mail: stefan.constantinescu@bru.licr.org; and Vladimir Divoky, Department of Biology, Faculty of Medicine and Dentistry, Palacky University, Hnevotinska 3, CZ-775 15 Olomouc, Czech Republic; e-mail: vladimir.divoky@upol.cz.

Footnotes

*C.M., O.B., and J.-P.D. are joint first authors.

The online version of this article contains a data supplement.

REFERENCES

- Vainchenker W, Kralovics R. Genetic basis and molecular pathophysiology of classical myeloproliferative neoplasms. *Blood*. 2017;129(6):667-679.
- Skoda RC, Duek A, Grisouard J. Pathogenesis of myeloproliferative neoplasms. *Exp Hematol*. 2015;43(8):599-608.

3. Rumi E, Cazzola M. Diagnosis, risk stratification, and response evaluation in classical myeloproliferative neoplasms. *Blood*. 2017;129(6):680-692.
4. Harutyunyan AS, Kralovics R. Role of germline genetic factors in MPN pathogenesis. *Hematol Oncol Clin North Am*. 2012;26(5):1037-1051.
5. Lanikova L, Babosova O, Swierczek S, et al. Coexistence of gain-of-function JAK2 germ line mutations with JAK2V617F in polycythaemia vera. *Blood*. 2016;128(18):2266-2270.
6. Kapralova K, Horvathova M, Pecquet C, et al. Cooperation of germ line JAK2 mutations E846D and R1063H in hereditary erythrocytosis with megakaryocytic atypia. *Blood*. 2016;128(10):1418-1423.
7. Levine RL, Wadleigh M, Cools J, et al. Activating mutation in the tyrosine kinase JAK2 in polycythaemia vera, essential thrombocythaemia, and myeloid metaplasia with myelofibrosis. *Cancer Cell*. 2005;7(4):387-397.
8. Arber DA, Orazi A, Hasserjian R, et al. The 2016 revision to the World Health Organization classification of myeloid neoplasms and acute leukemia. *Blood*. 2016;127(20):2391-2405.
9. Lee EJ, Dykas DJ, Leavitt AD, et al. Whole-exome sequencing in evaluation of patients with venous thromboembolism. *Blood Adv*. 2017;1(16):1224-1237.
10. Leroy E, Dusa A, Colau D, et al. Uncoupling JAK2 V617F activation from cytokine-induced signalling by modulation of JH2 α C helix. *Biochem J*. 2016;473(11):1579-1591.
11. Yao H, Ma Y, Hong Z, et al. Activating JAK2 mutants reveal cytokine receptor coupling differences that impact outcomes in myeloproliferative neoplasm. *Leukemia*. 2017;31(10):2122-2131.
12. Campbell PJ, Scott LM, Buck G, et al; Australasian Leukaemia and Lymphoma Group. Definition of subtypes of essential thrombocythaemia and relation to polycythaemia vera based on JAK2 V617F mutation status: a prospective study. *Lancet*. 2005;366(9501):1945-1953.
13. Lek M, Karczewski KJ, Minikel EV, et al; Exome Aggregation Consortium. Analysis of protein-coding genetic variation in 60,706 humans. *Nature*. 2016;536(7616):285-291.
14. van den Akker EB, Pitts SJ, Deelen J, et al; Genome of The Netherlands Consortium. Uncompromised 10-year survival of oldest old carrying somatic mutations in DNMT3A and TET2. *Blood*. 2016;127(11):1512-1515.
15. Hahn CN, Babic M, Schreiber AW, et al. Rare and common germline variants contribute to occurrence of myelodysplastic syndrome. *Blood*. 2015;126(23):1644.

DOI 10.1182/blood-2018-04-843060

© 2018 by The American Society of Hematology

Supplemental Materials and Methods, Tables, Figures and References for Mambet et al.

SUPPLEMENTAL MATERIAL AND METHODS

Patients and samples

Screening for the presence of *JAK2* R1063H was performed in 390 *JAK2* V617F-positive DNA samples, previously obtained by standard methods from peripheral blood granulocytes of MPN patients and stored in the biobanks of Stefan S Nicolau Institute of Virology, Bucharest, Romania, and Cliniques Universitaires Saint-Luc, Université catholique de Louvain, Belgium. The Romanian patients received an MPN diagnosis at the Hematology Services of Coltea and Fundeni Hospitals and were consequently referred to Stefan S Nicolau Institute of Virology for *JAK2* V617F mutation testing. All the patients included in the study provided informed consent at the time of blood drawing. Clinical data were analyzed retrospectively from the medical records of Coltea and Fundeni Hospitals and Cliniques Universitaires Saint-Luc, respectively.

Real-time PCR assay for *JAK2* R1063H mutation screening

To detect the *JAK2* R1063H mutation in the samples of genomic DNA (gDNA) we employed a custom TaqMan SNP Genotyping Assay (Applied Biosystems, Carlsbad, CA) with PCR primers flanking the mutant region and two allele-specific Taqman minor groove-binding (MGB) real-time PCR probes, performed on StepOnePlus Real-Time PCR System (Applied Biosystems).

Real-time quantitative PCR (qPCR) for *JAK2* V617F

The quantification of *JAK2* V617F mutation was performed using the ready-to-use ipsogen JAK2 MutaQuant Kit (Qiagen, Hilden, Germany) with a measured limit of detection of 0.1% on LightCycler® 480 Real-Time PCR instrument (Roche, Basel, Switzerland).

Next-generation sequencing for targeted mutational screening

In order to detect additional mutations of potential clinical relevance in MPN patients and to compare mutational load of patients harboring both *JAK2* V617F and R1063H mutations and *JAK2* V617F mutation only, we employed a targeted next-generation sequencing (NGS) panel (TruSight Myeloid Sequencing Panel, Illumina, San Diego, CA) for 14 *JAK2* V617F/R1063H double positive patients and for 53 randomly selected patients from the *JAK2* V617F cohort. The DNA libraries were generated from patients' granulocyte DNA according to the manufacturer instructions. The panel targeted 54 genes and covered full coding sequence of 15 genes and exonic hotspots of 39 genes. Targeted sequencing was performed on the Illumina MiSeq or NextSeq500 System using Illumina v3 Reagent Kit (600cycles) and V2 Mid OutPut Kit, respectively. We identified sequence alterations with a variant allele frequency (VAF) of $\geq 2\%$. The FASTQ files were analyzed by NextGENe V2.4.2.1 (SoftGenetics, State College, PA). The analysis included read quality trimming, alignment to the human hg19 reference genome, calling of single-nucleotide variants and short insertions or deletions. Read alignment and variant calling were also performed using the MiSeq Reporter (MSR) V2.6.3 software (Illumina), and annotated using VariantStudio V2.2 (Illumina). *JAK2* V617F allele frequency

was also obtained from NGS to allow comparison with digital droplet PCR (ddPCR) assay and qPCR.

Digital droplet PCR for *JAK2* R1063H and *JAK2* V617F allele burden measurement

To calculate the *JAK2* R1063H/wild type and *JAK2* V617F/wild type allele ratios, ddPCR was employed. One reaction of ddPCR was performed using 100 ng of genomic DNA, 1 µl of ddPCR™ Mutation Detection Assay mix for human *JAK2* R1063H/WT (20x assay mix, custom designed: dHsaMDS460320799; Biorad) or 1 µl of each probe PrimePCR™ ddPCR™ Mutation Assay for human *JAK2* V617F/WT (*JAK2* WT for p.V617: dHsaCP2000062 and *JAK2* p.F617: dHsaCP2000061; Biorad), 10 µl ddPCR™ Supermix for Probes (No dUTP; Biorad) and 1 µl of restriction enzyme *HindIII* (Thermo Scientific™) in total of 20 µl of reaction. Droplets were created using Droplet Generation Oil for Probes in QX200™Droplet Generator. PCR was performed in C1000 Touch™Thermal Cycler using conditions as follows, 95 °C for 10 min, 40 cycles of 30 s at 94 °C and 1 min at 55 °C, and a final step at 98 °C for 10 min. The ramp rate was always limited for 2 °C/sec. After the PCR reaction, droplet fluorescence was measured by QX200 Droplet Reader. Data were analyzed using QuantaSoft (Bio-Rad, V1.7.4).

***Cis/trans* configuration of *JAK2* V617F and R1063H mutations**

Patients' DNA-free RNA isolated either from whole blood or from peripheral blood leukocytes using Aurum™ Total RNA Mini Kit; Biorad and TRIzol method, respectively, was reverse transcribed by High Capacity cDNA Reverse Transcription Kit (Thermo Fisher Scientific). The position of V617F mutation relative to R1063H mutation was determined by amplifying a region spanning exons 14 – 24 of *JAK2* gene. The semi-nested PCR using primers (1st round, F1 5' ACGGTCAACTGCATGAAACA 3', R1 5' AGGAGGGGCG TTGATTACA 3'; 2nd round, R2 5' ATCTCATCTGGGCATCCATC 3') was performed. The amplicon was gel-purified using Zymoclean™ Gel DNA Recovery Kit (Zymo Research) and cloned into pGEM-T easy vector (Promega). Single colonies positive for the recombinant plasmid were picked after overnight incubation, plasmid DNA was purified using the High Pure Plasmid Isolation Kit (Roche) and the PCR insert was sequenced at SEQme company, Czech Republic. At least 20 colonies per each amplicon (patient sample) were analyzed.

Microarray analysis for detection of chromosomal changes

Microarray analysis (array-comparative genomic hybridization/single-nucleotide polymorphism [aCGH/SNP]) was performed with SurePrint G3 Cancer CGH+SNP Microarray, 4x180K (Agilent Technologies, Santa Clara, CA) to detect unbalanced chromosomal changes and copy number neutral loss of heterozygosity (CN-LOH). The minimal resolution for the detection of CN-LOH was a region of ~3 Mb, which was achieved with approximately 20 SNP probes per Mb. The final product was scanned with the Agilent G2565CA Microarray Scanner System (Agilent) and analyzed with Agilent Cytogenomics v4.0.3.12 (Agilent).

Mutagenesis and vector construction

QuickChange II site-directed mutagenesis kit (Agilent Technologies, Santa Clara, CA) was used to introduce the *JAK2* c.1849G>T (V617F), and *JAK2* c.3188G>A (R1063H) point mutations into a human *JAK2* WT cDNA cloned in pMEGIX-IRES-GFP plasmid vector and also to generate double mutant *JAK2* c.1849G>T/*JAK2* c.3188G>A (V617F/R1063H), following the manufacturer instructions. Similarly, we introduced the suppressive E596R mutation for *JAK2* V617F into pMEGIX coding for human *JAK2* V617F, R1063H, and V617F/R1063H constructs. All *JAK2* cDNA constructs were verified for accuracy by Sanger sequencing.

Dual luciferase assays for STAT5 transcriptional activity assessment

STAT5 transcriptional activity of the *JAK2* WT and *JAK2* mutants in the presence of myeloid dimeric cytokine receptors was measured in *JAK2*-deficient γ -2A fibrosarcoma cells¹ where we can reconstitute *JAK2* or mutants, thereof. Dual luciferase assays were employed, using the firefly luciferase reporter Spi-Luc responding to STAT5 and p-RLTK renilla luciferase for normalizing transfection efficiencies, as previously described.² Briefly, γ -2A cells were transiently transfected with cDNA of *JAK2* WT or mutants, Spi-Luc, STAT5, p-RLTK and either EPOR, TPOR or Granulocyte Colony-Stimulating Factor receptor (G-CSFR), at a 3:3:1:1:3 ratio, using Lipofectamine 2000 (Thermo Fisher Scientific, Waltham, MA). At the same time, to mimic heterozygous status encountered in patients, *JAK2* V617F, R1063H, or V617F/R1063H mutants were co-transfected in γ -2A cells with an equal amount of *JAK2* WT cDNA. Four hours after transfection, cell culture medium was changed and cells were incubated with the corresponding cytokine: 15 U/ml erythropoietin (EPO), 10 ng/ml thrombopoietin (TPO) or 10 ng/mL granulocyte colony-stimulating factor (G-CSF). 24 hours post-transfection the luciferase production was quantified in cell lysates with Dual-Luciferase® Reporter Assay kit (Promega, Madison, WI) on a Victor X luminescence microplate reader (Perkin Elmer, Waltham, MA). Firefly: Renilla luciferase ratios were calculated for each condition in order to assess the STAT5 transcriptional activity of different *JAK2* constructs. In a similar manner, γ -2A cells were transfected with *JAK2* E596R constructs and TPOR and dual-luciferase assay was applied to evaluate STAT5 constitutive activation.

Western blotting for signaling studies

Signaling studies were also performed in human embryonic kidney (HEK) 293T cells co-transfected with *JAK2* WT or *JAK2* mutants and one of the cytokine receptors, using TransIT®-LT1 Transfection Reagent (Mirus Bio, Madison, WI). After obtaining cell extracts, the levels of total *JAK2* as well as the phosphorylation status of *JAK2*, STAT5, and extracellular signal-regulated kinase 1/2 (ERK1/2) were analyzed by western blotting with the following primary antibodies (all from Cell Signaling Technology, Danvers, MA): *JAK2*, phospho-Jak2 (p-Tyr1007/1008), phospho-Stat5 (p-Tyr694) and phospho-p44/42 MAPK (Erk1/2, p-Thr202/p-Tyr204).

Generation of cells stably expressing HA-tagged receptor

HA-tagged human G-CSFR cDNA was cloned in the retroviral pMX-IRES-GFP vector, as described previously.^{4,5} The construct was co-transfected into retroviral producing cells HEK

293T together with the envelope encoding construct pCMV-VSV and Gag-Pol construct. Retroviral particles were collected at 48 and 72 hours after transfection and concentrated using filtration system Vivaspin® 20 (Sartorius). HEK 293 cells were then infected two times sequentially with the concentrated viral media overnight. Cells were GFP-sorted 72 hours after the second infection and the expression of G-CSFR was confirmed by Western blot.

Immunoprecipitation

HA-tagged receptor expressing HEK 293 cells cultured in DMEM + 10 % FBS and no additional cytokines, were transfected with pCMV-Puro-JAK2 variants using Lipofectamine 2000 (Thermo Fisher Scientific). 48 hours post transfection cells were lysed using lysis buffer (NaCl, Tris, Triton-X, CaCl₂, MgCl₂, EDTA) and a cocktail of proteinase inhibitors. For immunoprecipitation EZview™ Red ANTI-FLAG® M2 Affinity Gel (Sigma) was used according to the manufacturer's instructions. For maximal specificity elution using 3X FLAG® Peptide (Sigma) was performed. Receptors were detected using anti-HA rabbit monoclonal antibody (Cell Signalling, #3724) and JAK2 using anti-FLAG rabbit monoclonal antibody (Cell Signalling, #14793). Total cell lysates (TCL) were immunoblotted alongside the immunoprecipitated samples, anti-HA and anti-FLAG antibodies used for the detection are listed above, and a loading control anti-CtBP (Santa Cruz, sc-17759) was used.

***In vitro* Ruxolitinib sensitivity assay**

QuickChange II site-directed mutagenesis kit (Agilent Technologies, Santa Clara, CA, USA) was used to introduce *JAK2* c.1849G>T (V617F), *JAK2* c.3188G>A (R1063H) and combination of both *JAK2* c.1849G>T/*JAK2* c.3188G>A (V617F/R1063H) mutations into human *JAK2* WT ORF cDNA cloned in pCMV6-AC-IRES-GFP-Puro mammalian expression vector (OriGene, cat. no. PS100059). Ba/F3-EPOR cells cultured in IMDM medium containing 10% fetal bovine serum (FBS; both from Life Technologies) and 2 ng/mL of IL-3 (Sigma) were transfected with all the variants of pCMV-Puro-JAK2 vector by electroporation under conditions of 420 V and 250 µF using a Gene-Pulser (Bio-Rad, Hercules, CA). Stable transfectants were selected with 1 µg/ml puromycin (Life Technologies) for 2 weeks. *In vitro* drug sensitivity was determined using the MTT cytotoxicity assay, as described previously.³

Statistical analysis

Statistical tests were performed using GraphPad Prism 6.01 for Windows. Mann–Whitney U test was used to compare the differences in blood counts between the two groups of patients (double-mutation carriers and patients harboring only *JAK2* V617F mutation). One-way ANOVA followed by post-hoc Tukey's allowed for multiple comparisons between the measurements obtained by dual luciferase assays and *in vitro* Ruxolitinib sensitivity assay. Student's paired t test with equal variance was employed for assessing binding affinities of JAK2 mutants to G-CSFR. NGS data were compared and analyzed by the two-tailed Fisher exact test. Statistical significance was defined as P <0.05.

SUPPLEMENTAL TABLES AND FIGURES

Table S1. Clinical data of *JAK2* V617F MPN patients (n = 390) subdivided according to the *JAK2* R1063H mutation status. Data for V617F only (n = 376) and V617F/R1063H double mutation carriers (n = 14) were recorded at diagnosis. Abbreviations: PV, Polycythemia Vera; ET, Essential Thrombocythemia; PMF, Primary Myelofibrosis; MPN-U, MPN Unclassifiable; WBC, White Blood Cell.

Variables	Patients JAK2 V617F/R1063H positive (n=14)	Patients JAK2 V617F positive (n=376)	P value
Sex ratio (male/female)	5/9	157/219	
Age, years, median (range)	60 (34-80)	61(16-92)	
MPN subtype (PV/ET/PMF/MPN-U)	5/7/2/0	115/205/34/22	
Hemoglobin g/dL, median (range)	15.8 (10.6 - 19.5)	14.7 (7.3 - 24.0)	0.43
WBC count × 10 ⁹ /L, median (range)	13.3 (9.9 - 41.6)	10.2 (4.6 - 31.6)	0.023
Neutrophil count × 10 ⁹ /L, median (range)	9.0 (6.9 - 34.2)	7.4 (2.6 – 26.8)	0.025
Platelet count × 10 ⁹ /L, median (range)	730 (363 - 1000)	670 (74 - 2025)	0.87
JAK2 V617F allele burden %, median (range)	21.3 (7.1 - 83.5)	32.0 (5.5 - 89.9)	0.78

Table S2. Detailed information about mutations identified by TruSight Myeloid Sequencing Panel for the MPN patients exhibiting *JAK2* V617F and *JAK2* R1063H mutations.

** Denotes likely inherited *GATA2* (A164T) variant, recently associated with increased risk of developing myeloid malignancy.⁶

Abbreviations: D, deleterious; PD, probably damaging; T, tolerated; B, benign; NA, not available. DbSNP ID: ID in The Single Nucleotide Polymorphism database. (1) This variant does not have SNP/COSMIC ID, but has been repeatedly viewed on VarSome.

SUPPLEMENTAL TABLE 2. for Mambet et al.

Patient	Diagnosis	Additional mutations										
		Gene	CDS mutation	Protein change	Chr	Type	Var Freq [%]	Var Type	Sift	PolyPhen	dbSNP ID	References
1	PV	<i>BCOR</i>	c.1231C>T	p.R411W	X	snv	54.0	missense	D	PD	NA	
2	ET	<i>TET2</i>	c.3556_3557insA	p.G1187fs	4	insertion	3.1	frameshift	NA	NA	NA	(1) www.varsome.com/variant
3	ET	<i>not detected</i>										
4	ET	<i>DNMT3A</i>	c.1095C>G	p.Y365*	2	snv	3.7	stop	NA	NA	NA	(1) www.varsome.com/variant
		<i>TET2</i>	c.2599T>C	p.Y867H	4	snv	51.2	missense	D	PD	rs144386291	COSM327337
5	PV	<i>not detected</i>										
6	ET	<i>not detected</i>										
7	ET	<i>not detected</i>										
8	PMF	<i>not detected</i>										
9	PMF	<i>TET2</i>	c.4820C>A	p.S1607*	4	snv	2.3	stop	NA	NA	NA	
10	PV	<i>DNMT3A</i>	c.2104G>T	p.D702Y	2	snv	9.1	missense	D	PD	NA	PMC4797027
		<i>CBLB</i>	c.1399G>A	p.V467I	3	snv	61.8	missense	T	B	rs371993076	COSM1035961
		<i>ZRSR2</i>	c.1314_1315insAGCCGG	p.R448_R449insSR	X	insertion	39.4	in-frame	NA	NA	rs779595035	COSM5762985
11	ET	<i>BCOR</i>	c.4943C>T	p.P1648L	X	snv	99.5	missense	D	PD	rs763651353	
12	PV	<i>GATA2**</i>	c.490G>A	p.A164T	3	snv	57.5	missense			rs2335052	
13	PV	<i>not detected</i>										
14	ET	<i>EZH2</i>	c.1582T>A	p.C528S	7	snv	7.0	missense			NA	

Table S3. Detailed information about mutations identified by TruSight Myeloid Sequencing Panel for the JAK2 V617F-positive/R1063H-negative patients in our cohort.

Additional mutations were identified in 12 out of 53 screened patients (after the exclusion of *GATA2* (A164T) SNP). A total of 17 variants in 8 genes were detected. Two of these mutations are indexed in the dbSNP database, and 7 of these specific variants are listed in the COSMIC catalogue (#). Seven patients harbor unique undescribed variants. ** Denotes likely inherited *GATA2* (A164T) variant (11 times in heterozygous and 2 times in homozygous configuration), recently associated with increased risk of developing myeloid malignancy.⁶ In this cohort of 53 patients, the variant comprises 14% of allele frequency, which is consistent with the expected frequency (European non-Finnish 15% allelic frequency - <http://gnomad.broadinstitute.org/variant/3-128204951-C-T>; European 18% allelic frequency - https://www.ncbi.nlm.nih.gov/projects/SNP/snp_ref.cgi?rs=2335052). All mutations were identified in the genomic DNA collected at the time of diagnosis; acquisition of additional mutations during the disease evolution was not studied.

Abbreviations: PV, Polycythemia Vera; ET, Essential Thrombocythemia; PMF, Primary Myelofibrosis; NA, not available; dbSNP ID: ID in The Single Nucleotide Polymorphism database.

SUPPLEMENTAL TABLE 3. for Mambet et al.

Patient	Diagnosis	JAK2 V617F allele burden [%]	Gene	Protein change	Type	Var Freq [%]	dbSNP ID
1	ET	4.0	not detected				
2	PMF	38.9	not detected				
3	PV	51.8	GATA2**	p.A164T	snv	58.7	rs2335052# COSM445531
4	ET	5.9	not detected				
5	PV	10.2	ETV6	p.R14*	snv	5.5	NA
			GATA2**	p.A164T	snv	56.7	rs2335052# COSM445531
6	PMF	38.6	GATA2**	p.A164T	snv	50.0	rs2335052# COSM445531
7	PV	32.3	not detected				
8	PMF	19.5	GATA2**	p.A164T	snv	99.1	rs2335052# COSM445531
9	PV	83.1	not detected				
10	ET	10.6	GATA2**	p.A164T	snv	48.9	rs2335052# COSM445531
11	ET	5.4	JAK2	p.N542_E543del	deletion	10.0	NA# COSM1757322
12	PV	54.7	not detected				
13	ET	34	not detected				
14	PV	46.6	GATA2**	p.A164T	snv	56.3	rs2335052# COSM445531
15	ET	18.6	GATA2**	p.A164T	snv	47.5	rs2335052# COSM445531
16	ET	8.4	not detected				
17	ET	14.9	not detected				
18	ET	38.9	not detected				
19	ET	19.8	GATA2**	p.A164T	snv	49.0	rs2335052# COSM445531
20	ET	18.1	not detected				
21	PMF	26.3	not detected				
22	ET	29.2	not detected				
23	PV	49.4	not detected				
24	PV	70.1	not detected				
25	ET	14.7	GATA2**	p.A164T	snv	50.6	rs2335052# COSM445531
26	PV	46.8	not detected				
27	PV	65.3	not detected				
28	ET	11.6	ASXL1	p.P805fs	deletion	6.8	NA
29	ET	26.6	KDM6A	p.Q1377*	snv	4.6	NA# COSM255009
30	PMF	41.2	ZRSR2	p.E362*	snv	89.1	NA# COSM211059
			TET2	p.N377fs	deletion	10.4	NA
31	PMF	91.6	not detected				
32	ET	18.6	not detected				
33	PMF	4.4	KRAS	p.R68S	snv	15.5	NA# COSM183929
			SRSF2	p.H63P	snv	5.5	NA
34	ET	12.3	not detected				
35	PV	22.1	not detected				
36	ET	13.5	GATA2**	p.A164T	snv	56.8	rs2335052# COSM445531
37	ET	28.0	not detected				
38	ET	32.8	DNMT3A	p.A884fs	deletion	35.3	NA
39	PMF	19.9	ASXL1	p.P647fs	insertion	12.0	NA
40	ET	13.8	not detected				
41	PMF	27.8	not detected				
42	PV	41.6	TET2	p.Q1030*	snv	45.8	rs780043982# COSM4766113
43	ET	16.0	GATA2**	p.A164T	snv	97.5	rs2335052# COSM445531
44	early PV	23.3	GATA2**	p.A164T	snv	48.4	rs2335052# COSM445531
45	PV	80.3	TET2	p.D1384G	snv	18.2	NA# COSM6023668
			DNMT3A	p.V897D	snv	17.8	NA# COSM87000
46	PV	30.8	not detected				
47	ET	11.1	not detected				
48	ET	21.4	GATA2**	p.A164T	snv	53.8	rs2335052# COSM445531
49	PV	45.4	TET2	p.P1536fs	insertion	32.5	NA
			TET2	p.L1065fs	deletion	12.8	NA
			ASXL1	p.Q757*	snv	5.3	rs779078826# COSM132979
50	PV	16.4	not detected				
51	ET	54.0	not detected				
52	PV	59.6	not detected				
53	ET	28.1	TET2	p.L1515*	snv	34.7	NA# COSM5945064

Figure S1. Hematological data of *JAK2* V617F ET patients (n = 212) subdivided according to the *JAK2* R1063H mutation status. Data for V617F only (n = 205) and V617F/R1063H double mutation carriers (n = 7) were recorded at diagnosis. The boxes represent 25% to 75% interquartile range, horizontal lines inside the boxes indicate medians, and vertical bars show the range of values (minimum to maximum). Mann-Whitney U test was used to assess the statistical significance. P values <0.05 were considered statistically significant.

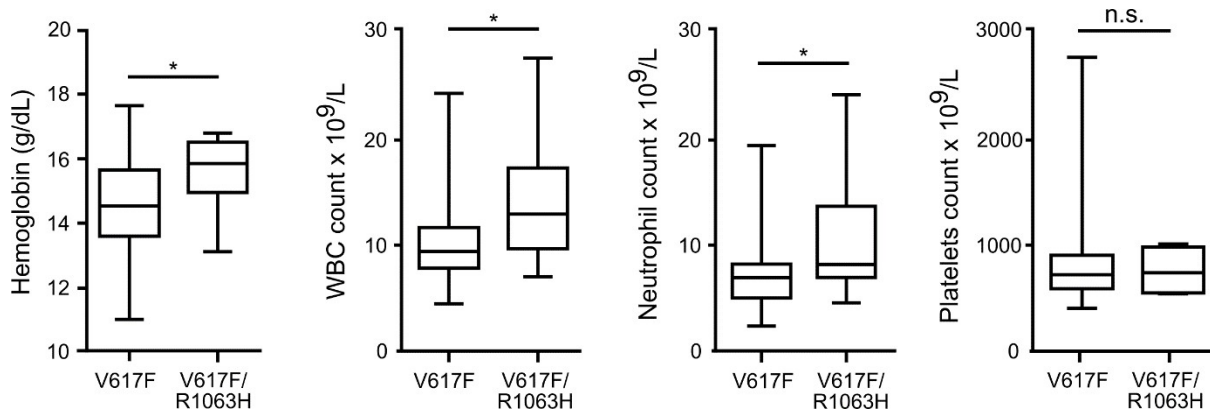


Figure S2. Quantification of *JAK2* R1063H allele in MPN patient samples using digital droplet PCR.

Single-well measurements of hybridization probes FAM/HEX specific for *JAK2* R1063H and *JAK2* WT were analyzed by QuantaSoft software and the count collection areas were held constant for each sampling.

(A) Comparison of number of events (amount of FAM- and HEX-positive droplets) of all analyzed patients. FAM fluorescence specific for the mutant allele is shown in blue while the HEX fluorescence specific for WT allele is shown in green.

(B) 2-D fluorescence amplitude plot generated by QuantaSoft software shows single-well measurement of a sample from one patient. The black cluster on the plot represents the negative droplets, the blue FAM cluster represents the droplets that are positive for the mutant DNA only, the green HEX cluster is specific for wild-type DNA only, and the orange cluster represents the droplets that are positive for both mutant and wild-type DNA. Patient 2 is presented as an example of a heterozygous sample compared to nearly homozygous sample obtained from Patient 4.

(C) Fractional abundance plot shows the percentage frequency of the mutant DNA in a wild-type DNA background. As presented in the boxplot, patients 1, 5 and 14 have low *JAK2* R1063H mutation allelic burden (20.7%, 31.5% and 27.6% of template copies detected carried

the mutation, respectively) and were examined for the presence of 9p UPD (see also Figure S3). Patients 4, 12 and 13 are nearly homozygous since 92.01%, 84.50% and 89.13% template copies carry the *JAK2* R1063H mutation, respectively. We hypothesize that one allele was inherited while the second one was acquired by UPD. This is also supported by the fact that allelic burden of *JAK2* V617F mutation in these patients is 83.5%, 73.2% and 76.2%, respectively. All the rest of the patients analyzed are heterozygous. All error bars generated by QuantaSoft software represent the 95% confidence interval.

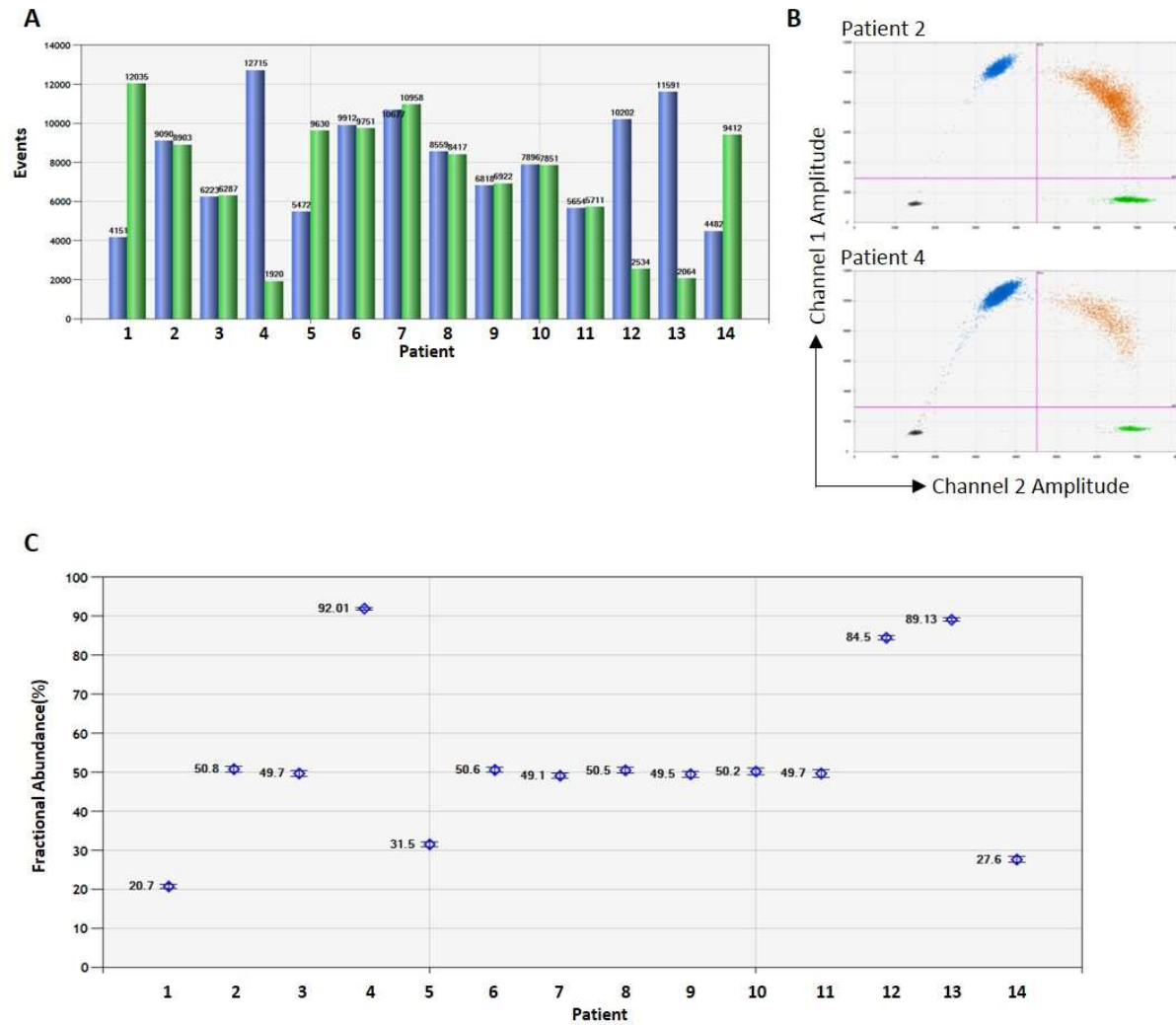


Figure S3. Determination of uniparental disomy for chromosome 9 of *JAK2* V617F positive MPN patients with low *JAK2* R1063H fractional abundance.

SNP-A based karyotypic analysis of chromosome 9 for patients with reduced fractional abundance of the *JAK2* R1063H was used to test hypothesis that the R1063H heterozygous germline variant carried by the non-V617F allele (*in trans* configuration) could have been lost due to mitotic recombination generating *JAK2* UPD of the V617F-non-R1063H clone which then could have been amplified thus leading to decreased R1063H allelic burden. Analysis was performed for patient #4 (nearly homozygous for both V617F and R1063H mutations, used as a positive control for UPD) and for patients #1, #5 and #14 with reduced fractional abundance

of the *JAK2* R1063H. Patient #4 (A) had cnLOH/UPD 9pterp21.3, patient #1 (B) carried cnLOH/UPD 9pterp21.2, patient #14 (C) carried cnLOH/UPD 9pterp21.1 at the detection limit and patient #5 (D) did not have detectable cnLOH/UPD 9p.

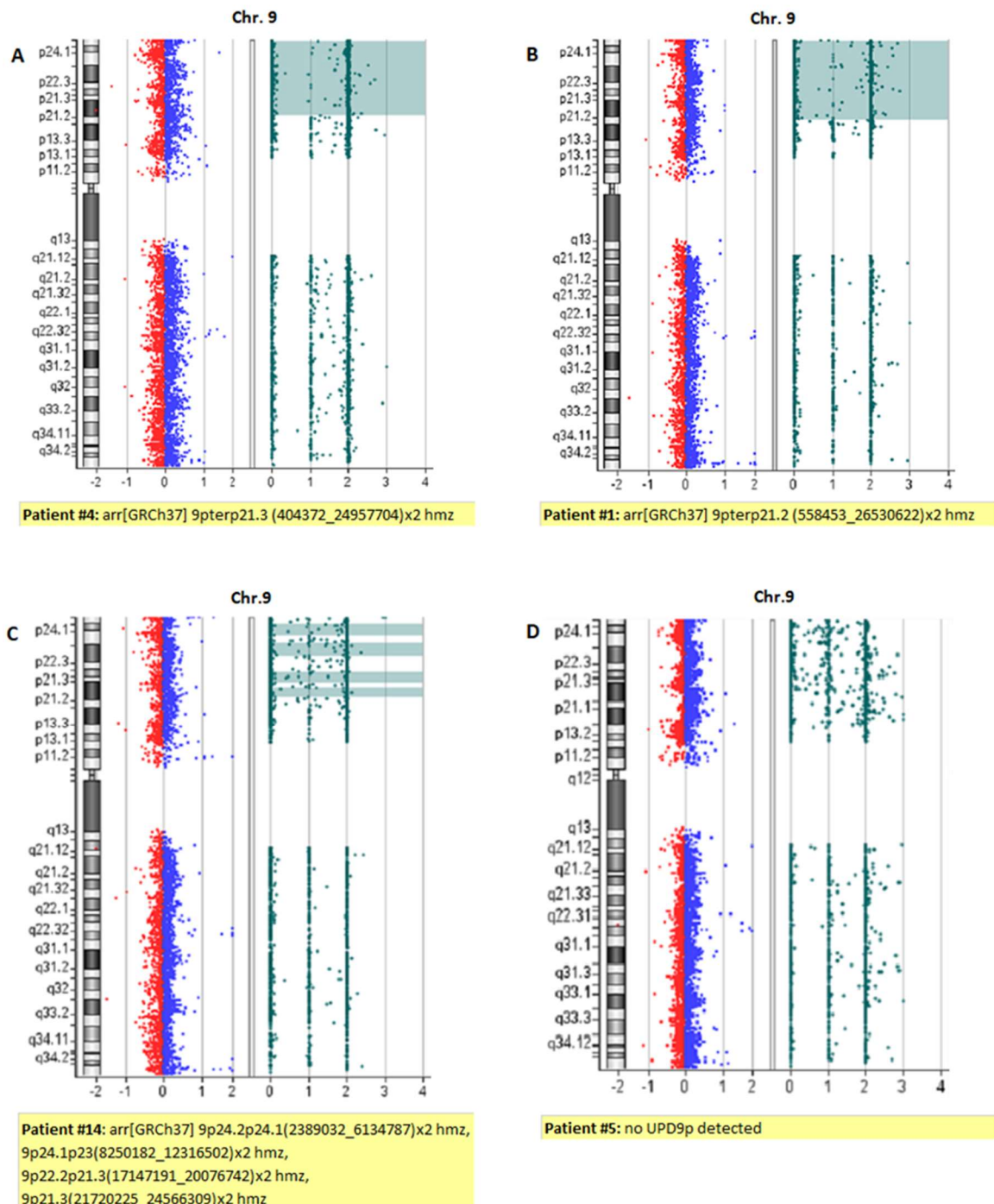
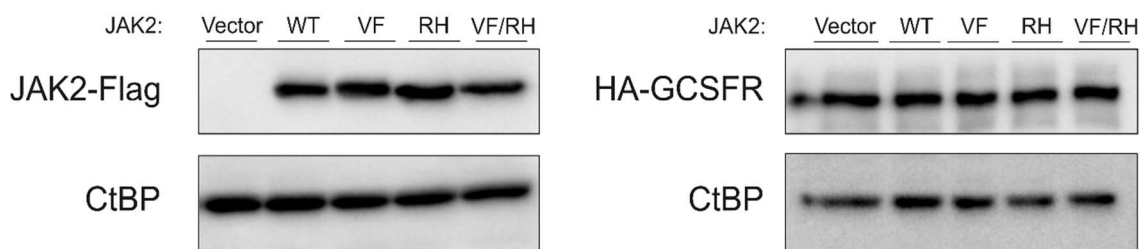


Figure S4. Levels of HA-tagged G-CSFR and FLAG-tagged JAK2 in lysates are comparable when different JAK2 mutants are expressed in HEK 293 cells.

HEK 293 cells stably expressing HA-tagged G-CSFR were transfected with FLAG-tagged JAK2 variants and the total cell lysates (TCL) were extracted 24 hours post-transfection. TCL were immunoblotted alongside the immunoprecipitated samples. As a loading control CtBP protein was detected. WT: wild type, VF: V617F, RH: R1063H, VF/RH: V617F/R1063H.



SUPPLEMENTAL REFERENCES

1. Kohlhuber F, Rogers NC, Watling D, et al. A JAK1/JAK2 chimera can sustain alpha and gamma interferon responses. *Mol. Cell. Biol* 1997; **17**: 695–706.
2. Defour J-P, Chachoua I, Pecquet C, Constantinescu SN. Oncogenic activation of MPL/thrombopoietin receptor by 17 mutations at W515: implications for myeloproliferative neoplasms. *Leukemia* 2016; **30**: 1214–1216.
3. Koledova Z, Kafkova LR, Calabkova L, et al. Cdk2 inhibition prolongs G1 phase progression in mouse embryonic stem cells. *Stem Cells Dev* 2010; **19**: 181-194.
4. Constantinescu SN, Liu X, Beyer W, et al. Activation of the erythropoietin receptor by the gp55-P viral envelope protein is determined by a single amino acid in its transmembrane domain. *EMBO J* 1999; **18**: 3334-3347.
5. Liu X, Constantinescu SN, Sun Y, et al. Generation of mammalian cells stably expressing multiple genes at predetermined levels. *Anal Biochem* 2000; **280**: 20-28.
6. Hahn CN, Babic M, Schreiber AW, Kutyna MM, Wee LA, Brown AL, et al. Rare and common germline variants contribute to occurrence of myelodysplastic syndrome. *Blood* 2015; **126**: 1644 (ASH Meeting Abstract).

Príloha 5

Kráľová B., Hlušičková Kapralová K, Divoký V, Horváthová M.

Nové poznatky v patofyziológií Ph-negatívnych myeloproliferatívnych neoplázií.

Transfuze a Hematologie Dnes. 2021; 27 (3): 208-217.

Nové poznatky v patofyziológií Ph-negatívnych myeloproliferatívnych neoplázií

New insights into the pathophysiology of Ph-negative myeloproliferative neoplasms

Kráľová B., Hlušičková Kapraľová K., Divoký V., Horváthová M.

Ústav biologie, LF UP v Olomouci

SÚHRN: Myeloproliferatívne neoplázie (MPN) tvoria skupinu príbuzných klonálnych hematologických porúch s prekryvajúcim sa fenotypom. Hlavným znakom MPN je nadprodukcia plne diferencovaných myeloidných buniek, chronický zápal a riziko transformácie do sekundárnej akútnej myeloidnej leukémie. Klonálna proliferácia je riadená rôznymi somatickými mutáciami, najčastejšie mutáciami v géne kódujúcom Janusovu kinázou 2 (JAK2). Fenotypová diverzita, špecifická pre MPN, však nemôže prameniť len zo súčinnosti rôznych riadiacich mutácií s mutáciami prídavnými, ktoré sú popisované u pacientov s MPN. Naopak, za heterogenitou MPN stojí celý rad genetických ako aj negenetických faktorov. Ako významný determinant, predovšetkým rozvoja klonálnej hematopoézy, sa ukazuje genetická predispozícia. Násuhrnný článok prináša prehľad najnovších poznatkov týkajúcich sa komplexnosti patobiológie chromozóm Filadelfia (Ph)-negatívnych MPN.

KEÚČOVÉ SLOVÁ: myeloproliferatívne neoplázie – JAK2 – CALR – MPL – genetická predipozícia – heterogenita MPN

SUMMARY: Myeloproliferative neoplasms (MPNs) represent a group of related clonal haematological disorders with overlapping phenotypes. The main typical features are excessive production of fully differentiated myeloid cells, chronic inflammation and a tendency to transform to acute myeloid leukaemia. Clonal proliferation in MPN is driven by various somatic mutations, most notably involving Janus kinase 2 (JAK2). However, MPN phenotypic diversity cannot be explained only by cooperation of acquired driver mutations with additional somatic mutations detected in MPN patients. Indeed, MPN initiation and clinical phenotype is a product of complex interactions involving both genetic and non-genetic factors. Recently, genetic predisposition appeared as an important determinant of MPN pathophysiology, particularly of clonal expansion. This review provides insights into complex, newly emerging factors contributing to Philadelphia chromosome (Ph)-negative MPN pathobiology.

KEY WORDS: myeloproliferative neoplasms – JAK2 – CALR – MPL – genetic predisposition – MPN heterogeneity

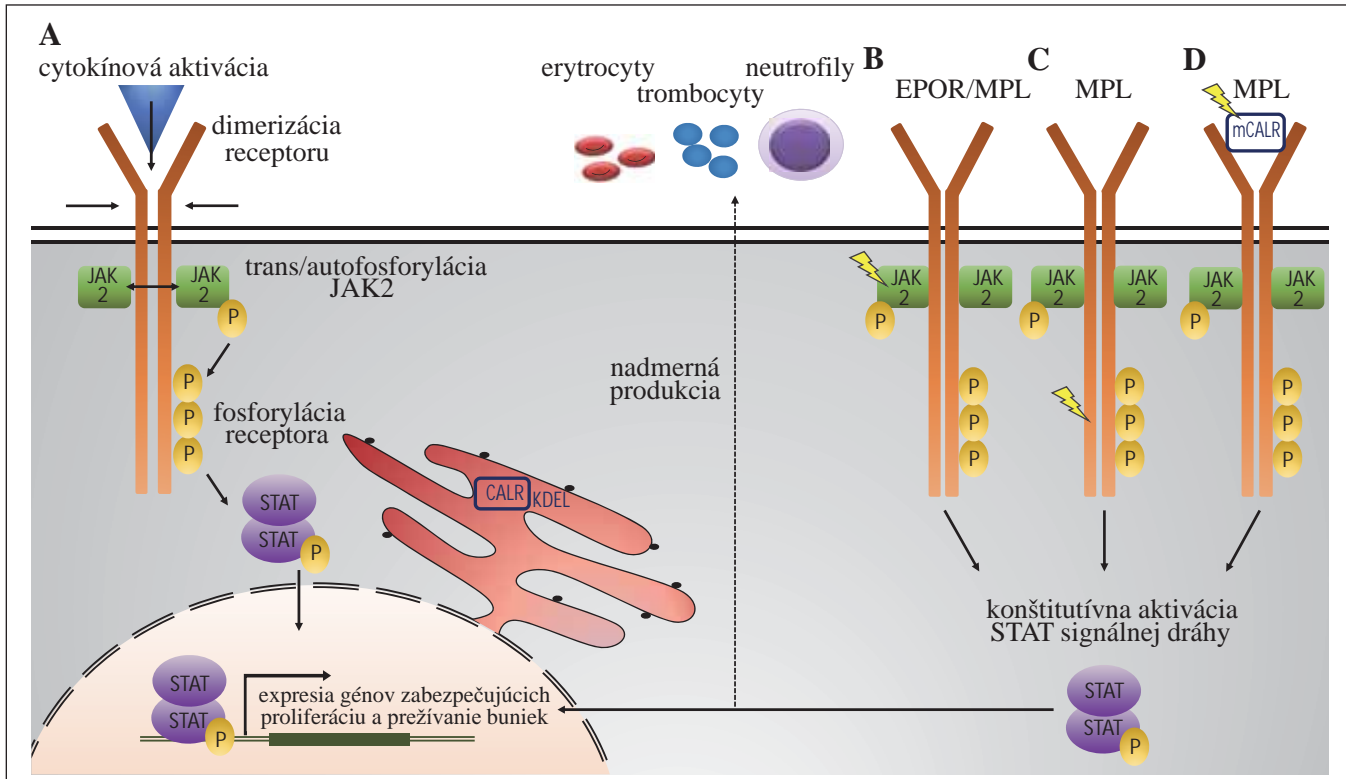
ÚVOD

Myeloproliferatívne neoplázie (MPN), popísané už v roku 1951 Dameshekom, sú fenotypovo rôznorodou skupinou klonálnych chorôb, ktorá je charakterizovaná zvýšenou proliferáciou aspoň jedného z myeloidných vývojových radov (erytrocytového, granulocytového alebo megakaryocytového) v kostnej dreni. Nadmerne produkované plne diferencované bunky si zachovávajú svoju typickú funkciu a nevykazujú známky rozsiahlej dysplázie [1]. Avšak najväčším rizikom MPN je, že postupom času môže dôjsť k poruche terminálnej diferenciácie

a maturácie progenitorov, kedy pretrvávajúci chronický zápal, remodelácia mikroprostredia kostnej dreny a postupná akumulácia genetických a epigenetických zmien vedú k blastickému zvratu a transformáciu inak chronického ochorenia do sekundárnej akútnej myeloidnej leukémie (sAML). Hlavným genetickým faktorom tejto leukemickej transformácie sú prídavné mutácie vznikajúce spontánne alebo ako dôsledok mutagénnej liečby [2]. MPN ochorenia vznikajú na podklade mutácií v hematopoietickej kmeňovej bunke (*hematopoietic stem cell* – HSC) a podľa klinických, histopato-

logických a molekulárnych charakteristik sa rozdeľujú do 7 rozdielnych entít: chronická myeloidná leukémia (CML), chronická neutrofilná leukémia (CNL), polycytémia vera (PV, pravá polycytémia), primárna myelofibróza (PMF), esenciálna trombocytémia (ET), chronická eosinofílna leukémia (bližšie nešpecifikovaná) a neklasifikovateľné MPN [3].

Dameshekova koncepcia pôvodu MPN je postavená na neznámom myelostimulačnom faktore, ktorý je zodpovedný za vznik týchto ochorení. Odvtedy sa vďaka pokrokom v technológiách molekulárnej biológie do veľkej



Obr. 1. Všeobecný mechanizmus JAK2 signálnej dráhy za fyziologických podmienok (A): po väzbe cytokínu k receptoru dochádza k jeho dimerizácii, následnej trans- a autofosforylácii JAK2 kinázy, ktorá ďalej fosforyluje tyrozínové zvyšky receptora. Tie poskytujú väzbové miesta pre STAT signálne molekuly, ktoré dimerizujú a vo fosforylovanej forme sa presúvajú do jadra, kde pôsobia ako transkripcné faktory génov zabezpečujúcich proliferáciu a prežívanie buniek. **Patofyziologická JAK2 signalizácia** v prípade JAK2 mutácií (B) a mutácií MPL receptora (C) vede ku konformačným zmenám JAK2 alebo MPL receptora, následnej konštitutívnej aktivácii JAK2/STAT signálnej dráhy a nadmernej produkcií rôznych krvných elementov. Naopak, sekretovaný mutovaný CALR (mCALR) sa ako „falošný“ cytokín viaže na MPL (D), aktivuje ho, čo u buniek exprimujúcich MPL a súčasne mCALR vede k trvalej aktivácii JAK2/STAT5 signalizácie.

P – fosforylácia, symbol blesku – mutácia

miery objasnila molekulárna podstata MPN a vytvorila sa komplexná knižnica kauzálnych alebo tzv. „driver“ (riadacích) mutácií vedúcich k MPN. Väčšina MPN sa javí ako sporadičká a býva obvykle diagnostikovaná v piatej až šiestej dekáde života. Avšak pribúdajúce štúdie ukazujú, že existuje skupina MPN pacientov, u ktorých nástup ochorenia nastáva v podstatne mladšom veku a že rôzne hematologické malignity sa môžu častejšie vyskytovať v rámci rodonomea jednej rodiny [4,5]. Zdá sa, že toto klastrovanie MPN v rámci rodín nie je náhodné; až 7,6 % zdanlivu sporadičkých MPN má naopak familiárne pozadie [6]. Diskutovaným javom je aj fenomén tzv. anticipácie, ktorý popisuje stav, kedy sa v každej nasledujúcej generácii ochore-

nie objavuje v skoršom veku ako v generácii predchádzajúcej [6,7]. Táto kohorta pacientov môže niesť jednu alebo niekoľko dedičných kooperujúcich mutácií s neúplnou penetranciou, čím je podporovaná existencia predispozičného faktora prispievajúceho nielen k prepuknutiu MPN ale aj jeho modulačného efektu na celkový fenotyp ochorenia.

Medzi klasické MPN patrí CML. Jej typickým cytogenetickým nálezom je chromozóm Filadelfia (Ph) vznikajúci recipročnou translokáciou t(9;22) [8]. Dôsledkom tejto výmeny vzniká fúzny onkogén BCR-ABL1 kódajúci konštitutívne aktívnu tyrozínovú kinázu aktivujúcu spletité signálne dráhy, ktoré zvyšujú proliferáciu potenciál mutovaných buniek a zároveň znižujú ich adhezívnu schopnosť a apo-

ptickú odpovedeť [9]. Zvýšená produkcia kyslíkových radikálov BCR-ABL1-pozičnými bunkami vede k nestabilite genómu a leukemogenéze [10].

Do klasických, avšak Ph-negatívnych MPN (BCR-ABL1 negatívne MPN), sa zaraďujú PV, ET a PMF. U väčšiny prípadov sú identifikované „driver“ mutácie v génoch kódajúcich Janusovu kinázu 2 (JAK2) [11–14], kalretikulín (CALR) [15,16] alebo trombopoetínový receptor (TPOR, označovaný aj ako MPL z angl. *myeloproliferative leukemia virus*) [17,18]; mutácie CALR a MPL sa vyskytujú u ET a PMF a len výnimcoľ u PV. Napriek niektorým spoločným klinickým, patologickým a molekulárny charakteristikám sa PV, ET a PMF vyznačujú veľkou variabilitou s ohľadom na možné

riziká trombotických a krváčavých komplikácií ako aj na riziko progresie do leúkémie. Heterogenita MPN podľa všetkého ovplyvňuje celý rad faktorov zahŕňajúci: prídavné somatické mutácie (vrátane poradia v akom boli získané), genetickú predispozíciu, charakteristiky samotného pacienta a zmeny v mikroprostredí kostnej drene [19].

SOMATICKÉ „DRIVER“ MUTÁCIE U Ph-NEGATÍVNYCH MPN

Somatické „driver“ mutácie v JAK2, [11–14], CALR [15,16] a MPL [17,18] vznikajú v HSC a vedú k neadekvátnnej aktivácii JAK2/STAT (*signal transducer and activator of transcription*) signálnej dráhy (obr. 1), čo poskytuje bunkám myeloidnej línie selektívnu proliferáčnu výhodu. Iniciačná mutácia v JAK2 géne, ktorá je najčastejšou „driver“ mutáciou u Ph-negatívnych MPN, pritom vzniká podľa novo publikovaných poznatkov veľmi skoro, v detskom alebo adolescentnom veku alebo dokonca prenátalne („pre-diagnostická“ fáza ochorenia) a môže trvať desiatky rokov, než dôjde k rozvoju signifikantnej klonálnej frakcie a nástupu „diagnostickej“ fázy MPN [20,21].

JAK2 V617F a JAK2 exón 12 mutácie

JAK2 je súčasťou rodiny nereceptorových tyrozínových kináz. Väzbou ligandu na cytokínové receptory: erytropoetínový receptor (EPOR), MPL a receptor pre kolónie granulocytov stimulujúci faktor (G-CSFR) sa prostredníctvom fosforylácie JAK2 aktivuje signálna dráha odovzdávajúca signál prevažne cez transkripcné faktory rodiny STAT (predovšetkým STAT1, 3 a 5), ktoré v jadre spúšťajú expresiu rôznych génov ovplyvňujúcich diferenciáciu, proliferáciu a prežívanie hematopoetických buniek [22] (obr. 1). Bodová mutácia v exóne 14 JAK2 génu vedúca k aminokyselinovej zámene V617F spôsobuje konštitutívnu aktiváciu JAK2 kinázy aj v neprítomnosti cytokínov a tým stimuluje klonálnu ex-

panziu buniek [11–14]. JAK2 V617F mutácia je prítomná u 95 % pacientov s PV a u približne 50–60 % pacientov s ET a PMF. Klinická a fenotypová heterogenita pacientov nesúcich JAK2 V617F mutáciu, v rozmedzí od často asymptomatickej ET, cez chronickú myeloproliferačiu až po agresívnejšiu formu PMF so zlou prognózou, je veľmi pozoruhodný a doposiaľ nie celkom ozrejmený aspekt. Svoju úlohu hrá čiastočne podiel mutovanej JAK2 V617F k celkovej JAK2, označovaný aj ako alelová záťaž (*allele burden*) [23]. Nižšia V617F alelová záťaž (zvyčajne okolo 25 %) je typická pre ET, vyššia ($\geq 50\%$) pre PV. Úplná V617F homozygozita (alelová záťaž 100 %), ktorá vzniká mitotickou rekombináciou a viedie tak k získanej uniparentálnej dizómi (aUPD) chromozómu 9, je spájaná s PV, post-PV a post-ET myelofibrózou. Prítomnosť nízkej frekvencie JAK2 V617F mutácie ($\leq 2\%$) u zdravých jedincov bez preukázaných hematologických abnormalít (s tzv. klonálnou hematopoézou s neurčitým potenciáлом, *clonal hematopoiesis of indeterminate potential* – CHIP), s incidenciou až 0,2 %, je ďalším ukazovateľom komplexnej patofyziológie MPN [24].

U 1–2 % PV pacientov, väčšinou JAK2 V617F negatívnych, sa vyskytujú mutácie v exóne 12 JAK2 génu [25]. Doteraz bolo v exóne 12 identifikovaných vyše 40 rôznych mutácií, zahŕňajúcich delécie, inzercie, duplikácie a zámeny, ktoré spôsobujú zvýšenú aktiváciu JAK2/STAT signálnej dráhy. Tieto mutácie sú výlučne asociované s izolovanou erytrocytú. Ukazuje sa však, že riziko vzniku trombózy ako aj transformácie do PMF alebo sAML je u tejto podskupiny PV porovnatelné s PV pacientmi s mutáciou JAK2 V617F [25].

CALR mutácie

Kalretikulín je chaperónový proteín, ktorý reguluje homeostázu vápnika a zbaľovanie novosyntetizovaných proteínov [26]. Mutácie v CALR géne sa vyskytujú približne v 30 % prípadov ET a PMF a výnimcoľne u pacientov s PV.

Dôsledkom mutácií dochádza k strate KDEL motívu zodpovedného za organelovo-špecifickú lokalizáciu kalretikulínu v endoplazmatickom retikule. Mutovaný kalretikulín (mCALR) sa naopak viaže na MPL, aktivuje ho a následne tak sprostredkováva nadmernú aktiváciu JAK2/STAT signálnej dráhy (obr. 1). Mutovaný kalretikulín vykazuje slabú väzbu s G-CSFR, ale neviaže sa na EPOR, čo má za následok špecifickú asociáciu CALR mutácií s ET a PMF, ale nie s PV. CALR mutácie sa rozdeľujú do dvoch typov. Nadmernú väčšinu tvoria mutácie typu 1 (delécia 52 bázových párov) prevládajúce u pacientov s diagnostikovanou PMF, naopak mutácie typu 2 (inzercia 5 bázových párov) sa vo veľkej miere vyskytujú u pacientov s ET [15,16]. Mutácie typu 1 majú agresívnejší ráz vzhľadom na robustnejší zásah do DNA; ET pacienti s týmito mutáciami častejšie pre redujú do myelofibrózy na rozdiel od ET pacientov s mutáciami typu 2, ktoré sú spájané s miernejším priebehom ochorenia [27].

MPL mutácie

Najmenej frekventovanými „driver“ mutáciami u klasických Ph-negatívnych MPN sú aktivujúce mutácie v géne kódujúcom MPL [17,18]. MPL viaže na povrchu buniek trombopoetín a zohráva tak kľúčovú úlohu v procese megakaryopoézy a tvorbe krvných dosťičiek [28,29]. MPL mutácie vedú ku konformačným zmenám receptora, ktoré vyústia do jeho aktivácie a následnej konštitutívnej aktivácie JAK2/STAT signálnej dráhy a k cytokínom-nezávislému rastu buniek (obr. 1) [17,18]. Najčastejšími mutáciami sú zámeny tryptofánu v pozícii 515 (MPL W515), ktoré sa vyskytujú výhradne u ET a PMF s prevalenciou 1, resp. 5 % [18] a sú spájané so zvýšeným rizikom myelofibrotickej transformácie u ET [30]. Iná mutácia postihujúca MPL, MPL S505N, bola popísaná ako vrozená mutácia asociovaná s familiárnu trombocytózou a následne aj ako získaná mutácia vo vzácných prípadoch ET [31,32].

Tab. 1. NGS (next generation sequencing) myeloidný panel. Prehľad génov, rozdelených podľa ich funkcie, ktoré sú indikované k vyšetreniu u pacientov s MPN.

(zdroj: <https://www.illumina.com/products/by-type/clinical-research-products/trusight-myeloid.html#gene-list>)

Úloha kódovaného proteínu	Analyzované gény
DNA metylácia	<i>DNMT3A, IDH1, IDH2, TET2</i>
Remodelácia chromatínu	<i>ASXL1, ATRX, BCOR, BCORL1, EZH2, KDM6A, MLL, NPM1</i>
Zostrih mRNA	<i>SF3B1, SRSF2, U2AF1, ZRSR2</i>
Regulácia transkripcie	<i>CEBPA, CUX1, ETV6/TEL, GATA1, GATA2, IKZF1, RUNX1, SETBP1</i>
Bunková signalizácia	<i>ABL1, BRAF, CALR, CBL, CBLB, CBLC, CSF3R, FLT3, JAK2, JAK3, KIT, KRAS, MPL, MYD88, NOTCH1, NRAS, PDGFRA, PTPN11</i>
Tumorové supresory	<i>CDKN2A, FBXW7, PHF6, PTEN, TP53, WT1</i>
Protoonkogény	<i>GNAS, HRAS</i>
Kohezínový komplex	<i>RAD21, SMC1A, SMC3, STAG2</i>

„Triple“ negatívne a biklonálne MPN

Asi 10 % pacientov s MPN, predovšetkým s ET a PMF, je negatívnych na prítomnosť výšie uvedených „driver“ mutácií v JAK2, CALR a MPL. Tieto prípady označujeme ako tzv. „*triple*“ negatívne MPN [2]. Zatial čo „*triple*“ negatívna ET je skôr benígnym ochorením, „*triple*“ negatívna PMF má veľmi agresívny klinický priebeh a zlú prognózu s viac ako 30 % pravdepodobnosťou leukemickej transformácie. V malej časti „*triple*“ negatívnych MPN boli popísané nekanonické mutácie v JAK2 (napr. V625F, F556V), MPL (napr. S204P, Y591N) alebo v géne *SH2B3* (napr. E208Q, D231fs), ktorý kôduje negatívny regulátor aktivácie JAK2. Často sa však jedná o vrodené varianty a nie o varianty získané [33–35].

Vo väčšine prípadov MPN s identifikovanými „driver“ mutáciami v JAK2, CALR alebo MPL sa ich koexistencia u jednotlivca vylučuje. Existujú však aj pacienti, u ktorých bol popísaný súčasný výskyt mutácií JAK2 V617F/JAK2 exón 12 [36], JAK2/CALR [37], JAK2/MPL [36,37] a ojedinele i CALR/MPL [38]. Jedná sa o biklonálne MPN, vyznačujúce sa prítomnosťou dvoch „driver“ mutácií v dvoch nezávislých klonoch [39]. Toto zistenie spoločne s popisovanými rozdielmi v klinických prejavoch u jednotlivých členov rodín s familiárnym výskytom MPN, ktorí často nesú aj rôzne „driver“ mutá-

cie, poukazuje na úlohu dedičného faktora u MPN. Tento faktor sám o sebe nevedie k vzniku MPN, ale predisponuje k zisku somatických MPN mutácií a/alebo mení vývoj a finálny fenotyp MPN [34].

Postupne sa tak odhaluje komplexné pozadie MPN biológie, kedy genetická predispozícia v súčinnosti s ďalšími genetickými a negenetickými faktormi ovplyvňuje riziko vzniku a fenotyp MPN.

GENETICKÉ FAKTORY OVPLYVŇUJÚCE HETEROGENITU Ph-NEGATÍVNYCH MPN

Somatické mutácie kooperujúce s „driver“ mutáciami

Okrem „driver“ mutácií sa u MPN pacientov popisuje aj výskyt prídavných somatických mutácií, ktoré nie sú špecifické pre MPN, ale objavujú sa aj u iných hematologických malignít (ako napr. myelodysplastický syndróm – MDS a AML). Jedná sa o získané mutácie génov kôdujúcich epigenetické modifikátory, faktory dôležité pre zostrih mRNA, niektoré transkripcné faktory alebo signálne molekuly [40,41]. Súčasný výskyt rôznych prídavných mutácií u jedného pacienta je možný, pričom platí, že zvyšujúci sa počet prídavných mutácií negatívne ovplyvňuje prežívanie a zvyšuje riziko leukemickej transformácie [42]. Príklad panelu génov vyšetrovaných u MPN pa-

cientov pomocou sekvenovania novej generácie (*next generation sequencing – NGS*) je uvedený v tab. 1.

Jednými z najčastejších mutácií, vyskytujúcich sa u všetkých subtypov MPN, sú mutácie génov kôdujúcich epigenetické modifikátory DNA: Tet metylcytozin dioxygenázu 2 (TET2) [43] a DNA (cytozin-5)-metyltransferázu 3A (DNMT3A) [44]. Tieto mutácie zvyšujú potenciál sebaobnovy HSCs. Ich prognostický význam u MPN nie je celkom objasnený. Ukázalo sa však, že poradie ich získania s ohľadom na zisk „driver“ mutácie JAK2 V617F, ovplyvňuje fenotyp MPN. Ak JAK2 V617F mutácia vzniká ako prvá, s väčšou pravdepodobnosťou dôjde k rozvoju PV ako ET. Naopak, ak mutácie v TET2 a DNMT3 predchádzajú vzniku JAK2 V617F mutácie, pravdepodobnejší je fenotyp ET [45, 46]. Prídavné mutácie ďalších epigenetických regulátorov remodelujúcich chromatín ako ASXL1 (*additional sex comb-like 1*) a EZH2 (*enhancer of zeste homolog 2*) sú častejšie u PMF a bývajú asociované s horšou prognózou a zvýšeným rizikom transformácie do sAML [41].

Prídavné mutácie faktorov kontroloujúcich zostrih mRNA (napr. SF3B1, SRSF2 a U2AF1) sa vyskytujú u PMF a ET, zriedkavo u PV. Ich úloha v patogenéze MPN nie je zrejmá, ale pravdepodobne súvisí s narušením normálneho zostrihu mRNA celého spektra génov. Mutácie

SF3B1 zvyšujú riziko progresie ET do myelofibrózy [47]; mutácie SRSF2 sú u pacientov s PMF asociované so zníženým prežíváním a zvýšeným rizikom transformácie do sAML [48].

Mutácie transkripcívnych faktorov ako napr. tumorového proteínu 53 (TP53) [40], (*runt-related transcription factor 1*) [49] alebo NF-E2 (*nuclear factor erythroid-2*) [50] sú vo väčšine prípadov asociované s leukemickou transformáciou MPN. Kým mutácie TP53 narúšajú jeho fyziológickú úlohu v indukcii opravy poškodenej DNA a apoptózy, mutácie NF-E2, ktorý reguluje diferenciáciu a maturáciu buniek erytroidnej a megakaryocytárnej línie, poskytujú bunkám ďalšiu proliferačnú výhodu. Rovnako tak somatické mutácie v génoch kódajúcich ďalšie signálne molekuly (napr. NRAS) sú typické pre MPN progredujúce do leukémie [51].

Genetická predispozícia

Je dlhodobo známe, že riziko vývoja MPN sa u prvostupňových príbuzných pacienta s MPN zvyšuje 5–7× [5], čo indikuje prítomnosť vrodeného genetického faktora podielajúceho sa na rozvoji ochorenia. Predpokladá sa pritom, že vrodená predispozícia zohráva svoju úlohu pred ale aj po získaní somatických „driver“ mutácií.

Prvým predispozičným faktorom identifikovaným u MPN bol haplotyp JAK2 46/1 [52]. Haplotyp JAK2 46/1 sa rozkladá na chromozóme 9, zahŕňa sadu génov spoločne s JAK2 génom a obsahuje niekoľko polymorfizmov vo väzbovej nerovnováhe. Minimálne jednu rizikovú alelu tohto haplotypu nesie 56 % MPN pacientov [53]. Ďalšie identifikované predispozičné polymorfizmy, ktoré zvyšujú riziko MPN boli popísané v génoch zapojených napr. do bunkového starnutia (*TERT*), epigenetickej regulácie (*TET2*), kontroly bunkového cyklu a opravy DNA (*CHEK2*, *ATM*), JAK2/STAT signálnej transdukcie (*SH2B3*) a regulácie transkripcie (*GFI1B*, *PINT*, *MECOM* a *HBS1L-MYB*) [54–56]. V niektorých z týchto génov sú pritom popisované aj prídavné somatické mutácie, čo pod-

trhuje ich biologický význam v regulácii hematopoézy a patogenéze MPN. Presné biologické mechanizmy, ktoré spojujú vyššie zmienené vrodené polymorfizmy s vývojom MPN sú predmetom intenzívneho výskumu.

Najnovšie štúdie ukazujú, že genetická predispozícia u MPN má polygénny charakter [57,58]. Rozsiahla celogenómová asociačná štúdia (*genome-wide association study – GWAS*) odhalila celkom 17 nezávislých rizikových lokusov, s mnohými rizikovými variantami identifikovanými v kódujúcich, nekódajúcich alebo regulačných oblastiach génov [57]. Niektoré rizikové varianty pritom priamo ovplyvňujú biologické vlastnosti HSCs súvisiace s dĺžkou telomér (v *TERT*), odpovedou na poškodenú DNA (v *ATM*, *CHEK2*) a s potenciáлом sebaobnovy (v *GFI1B*). Ďalej bolo ukázané, že v dôsledku mitotickej rekombinácie a straty heterozygozity sú rizikové varianty dostávajú do homozygotného stavu, ktorý môže znamenať proliferáčnu výhodu a podporovať tak následnú klonálnu selekciu [58]. Viac ako 50 vzácnych vrodených variant lokalizovaných v 7 rôznych lokusoch (*MPL*, *ATM*, *TM2D3*, *FH*, *NBN*, *MRE11* a *SH2B3*) vykazuje asociáciu so zvýšenou náchylosťou ku klonálnej hematopoéze [58].

Zárodočné mutácie v JAK2 géne

Vďaka celogenómovému sekvenovaniu boli v JAK2 géne odhalené vzácne zárodočné varianty, ktoré sa vyskytujú samostatne alebo spoločne s JAK2 V617F mutáciou u pacientov s PV, myelofibrózou alebo neutrofiliou [59–61]. Ukazuje sa, že tieto varianty kooperujú s JAK2 V617F mutáciou, amplifikujú kinázovú aktivitu mutovaného JAK2 enzymu, čo môže taktiež prispievať k fenotypovej heterogenite. Nedávna štúdia kohorty asi 2 000 MPN a AML pacientov z MD Anderson Cancer Center odhalila prítomnosť 35 rôznych variant JAK2 distribuovaných v rámci celého génu; u väčšiny z nich bol potvrdený dedičný pôvod [62]. Výskyt týchto variant bol pritom častejší u pacientov s MPN a AML než v zdravej popu-

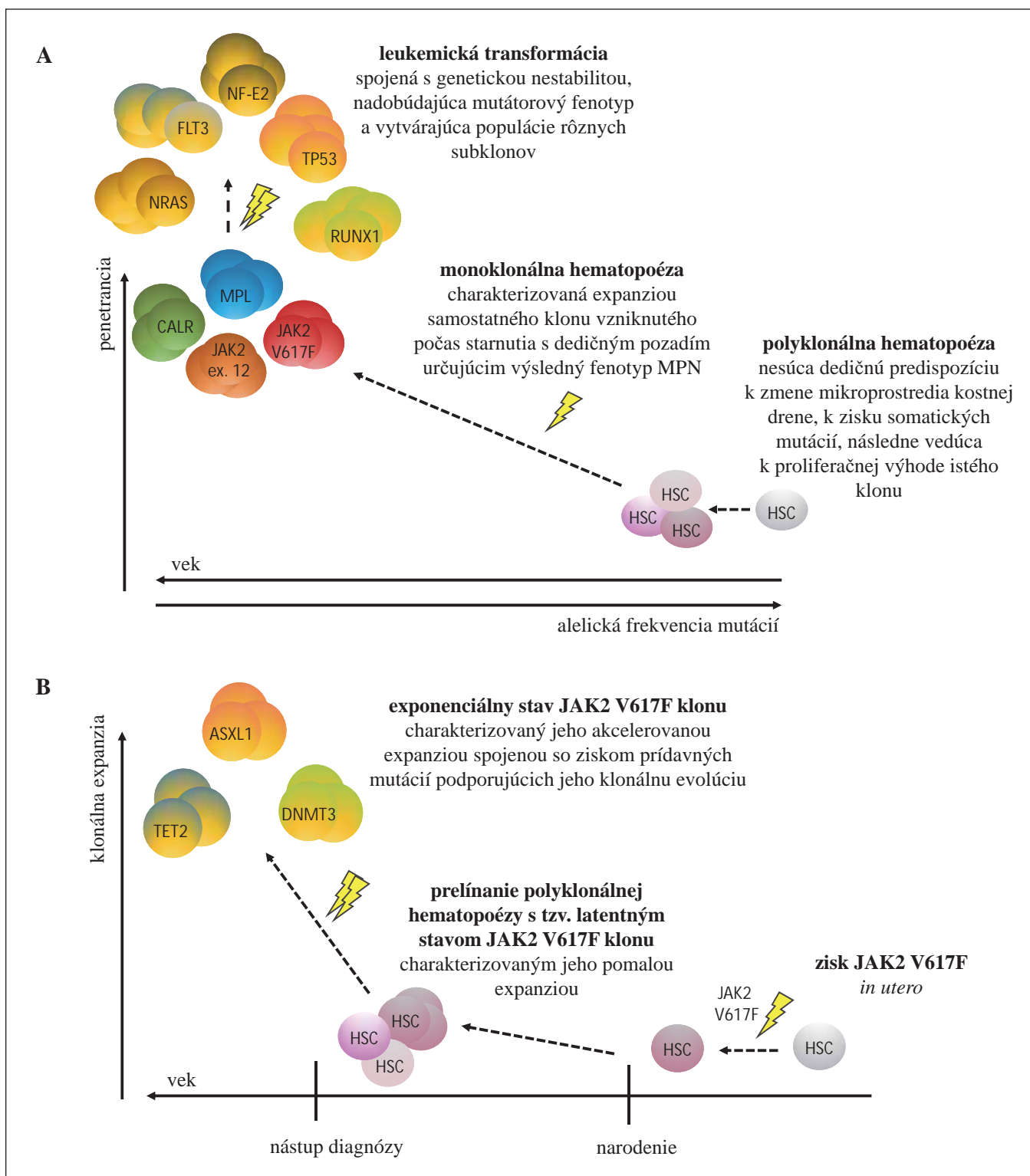
lácii. Najčastejšimi zámenami boli L393V, R1063H a N1108S. Autori zároveň ukázali, že prítomnosť dodatočných variant v JAK2 géne u JAK2 V617F pozitívnych pacientov výrazne zvyšuje kumulatívne riziko progresie do sAML v porovnaní so skupinou JAK2 V617F pozitívnych pacientov bez týchto variant.

Zaujímavosťou je, že niektoré z identifikovaných variant boli už predtým popísané samostatne alebo v kooperácii s inou JAK2 mutáciou vo vzácných prípadoch hereditárnej trombocytózy (napr. S593C [63], S755R/R938Q [63] a L815P/V1123G [64]) alebo erytrocytózy (E846D/R1063H [65]). Funkčná štúdia E846D a R1063H JAK2 mutácií ukázala, že každá mutácia samostatne má mierny dopad na aktiváciu JAK2/STAT signalizácie a k rozvoju patologického fenotypu dochádza až pri ich vzájomnej kooperácii [65]. Rozdielny klinický fenotyp (erytroidná hyperplázia vs. trombocytóza) pravdepodobne pramení z kvalitatívnych rozdielov v následnej JAK2/STAT signalizácii, napr. z odlišnej miery aktivácie jednotlivých molekúl STAT (STAT5 vs. STAT1) alebo z prípadnej aktivácie alternatívnych signálnych dráh.

ĎALŠIE FAKTORY OVPLYVŇUJÚCE HETEROGENITU Ph-NEGATÍVNÝCH MPN

Charakteristiky pacienta

Fenotyp MPN a jeho prognóza sú ovplyvnené aj vekom, pohlavím a komorbidityou pacienta. Výskyt MPN sa všeobecne zvyšuje s vekom, pričom medián veku nástupu PV je 65 rokov, 68 rokov u ET a 70 rokov u PMF [66]. So zvyšujúcim sa vekom zároveň stúpa riziko trombotických komplikácií a progresie ochorenia. To pravdepodobne súvisí s celkovým vplyvom starnutia a hromadenia volných radikálov (teória oxidačného stresu a starnutia) na akumuláciu somatických mutácií a rozvoj klonálnej hematopoézy [67,68]. Nie je prekvapením, že bola popísaná významná asociácia medzi fajčením a rozvojom MPN [69]. V priebehu



Obr. 2. Dynamický proces vývoja MPN. Dospelý prezentovaný, klasický model, model (A), ktorý popisuje, že penetrancia MPN závisí od veku jedinca, typu mutácií a komplexných interakcií dedičného faktora, mikropredstredia kostnej dreny a environmentálneho prostredia, ktoré sa spoločne podielajú na konverzii polyklonálnej hematopoézy na monoklonálnu, s možným medzistupňom v podobe CHIP. Nadmerná klonálna expanzia so sebou prináša riziko vzniku ďalších mutácií (napr. v génoch špecifických pre AML – NRAS, FLT3, TP53, RUNX1, NF-E2 a ľ.). [49]) a transformácie do sAML. Nový model (B) založený na retrospektívnej analýze buniek krvotvorných linií dospelých pacientov až po embryogenézu [20,21]. Model ukazuje, že získanie „driver“ JAK2 V617F (príp. DNMT3A) mutácie sa dá vystopovať až do prenatálneho obdobia. Následne dochádza k veľmi pomalej expanzii mutovaného klonu a trvá desiatky rokov, než klonálna frakcia dosiahne 1 %. Rýchlosť klonálnej expanzie a akvizície ďalších mutácií rozhoduje o klinickej manifestácii ochorenia.

starnutia dochádza vplyvom chronickej zápalu a prepínania metabolizmu krvotvorných kmeňových buniek z glykolýzy na oxidatívnu fosforyláciu, ako aj vplyvom myeloidného posunu krvotvorby k rozvoju klonálnych pre-leukemických stavov označovaných ako CHIP [70–72]. CHIP je kľúčový rizikový faktor vedúci k získaniu JAK2 V617F somatickej mutácie (obr. 2A) alebo zrýchlenej (sub)klonálnej expanzie preexistujúceho minoritného klonu u MPN (obr. 2B) a/alebo prípadnej transformácie do sAML.

Pohlavie sa taktiež ukazuje ako významný činiteľ fenotypu a progresie MPN. U žien sa častejšie vyskytuje ET, kým PV a PMF prevládajú u mužského pohlavia. Priebeh ochorenia býva miernejší u žien ako u mužov; navyše ženy majú všeobecne lepšiu prognózu ako muži, u ktorých je pozorované aj vyšie riziko myelofibrotickej transformácie [73]. Ďalšou zložkou prispievajúcou k heterogenite MPN je aj úroveň zásob železa v organizme. Kedže železo je nevyhnutné pre erytropoézu a tvorbu hemoglobínu, jeho počiatočný deficit je spájaný skôr s rozvojom ET ako PV [41].

Heterogenita HSC

V posledných rokoch sa ukazuje, že populácia HSCs nie je homogénnou skupinou buniek, ale obsahuje frakcie HSCs s rozdielnym líniom potenciálov (tzv. „lineaged biased“ HSCs), ktoré už sú časťou líniovo zamerané. Fenotypová špecifikácia MPN môže preto závisieť aj od toho, v akom líniovo predeterminovanom type HSC JAK2 V617F mutácia nastane [19]. U PV pacientov vzniká JAK2 V617F mutácia pravdepodobne v HSC umiestnenej na vrchole hematopoetickej hierarchie (s väčším multi-potentným potenciáлом), keďže jej prítomnosť bola zachytená aj v lymfoidnej líni. Tiež sa predpokladá, že stredne vysoká biochemická aktivita JAK2 V617F potláča MPL signalizáciu, a preto je skôr asociovaná s PV fenotypom; pri nízkej aktivite JAK2 V617F zostávajú aktívne

signály z TPOR/MPL receptorov, ktoré vedú k rozvoju ET [74].

Mikroprostredie kostnej drene a zápalové cytokíny

Mikroprostredie kostnej drene zohráva klúčovú úlohu v regulácii hematopoézy a jeho narušenie sa podieľa na rozvoji mnohých hematologických malignít. Ukazuje sa, že aj u MPN, rôzne nehematopoetické bunky kostnej drene, ako napr. endoteliálne bunky alebo mesenchymálne stromálne bunky, kooperujú s mutovanými MPN klonmi a spoločne vytvárajú niku podporujúcu propagáciu a progresiu MPN [19]. Nie je však úplne jasné, nakolko je aberantné mikroprostredie kostnej drene priamo zodpovedné za heterogenitu MPN alebo je len jej odzrkadlením.

Janusove kinázy sú kritickými mediátormi cytokínovej a chemokínovej signalizácie a signalizácie rastovými faktormi [75]. Dysregulácia JAK2/STAT signalizácie u MPN podporuje tvorbu mikroprostredia v kostnej dreni, ktoré sa vyznačuje aberantnou syntézou zápalových cytokínov a chemokínov (napr. interferónu γ – IFN- γ , tumor nekrotizujúceho faktora α – TNF- α , transformujúceho rastového faktora β – TGF- β alebo interleukínu 1b – IL-1b) [76–78]. Tieto následne spúšťajú systémovú a chronickú zápalovú odpoveď spojenú so zvýšenou koncentráciou zápalových markerov v cirkulácii. Myšie modely ukázali, že zápalové cytokíny prispievajú k tejto remodelácii mikroprostredia kostnej drene, ktorá potláča normálnu hematopoézu a podporuje transformáciu do myelofibózy a leukémie. Napriek výraznému chronickému zápalu je však kumulatívny výskyt blastickej transformácie u PV a ET (v porovnaní s transformáciou CML) relatívne nízky. Nedávna štúdia ukázala, že JAK2 V617F-mutantné bunky si v zápalovom prostredí indukujú ochranný program, sprostredkovany fosfatázou DUSP1 (*dual specificity phosphatase 1*), ktorý udržuje ich proliferačnú schopnosť a zároveň ich chráni pred akumáciou poškodenia DNA a myelofibotickou a leukemickou transformáciou [79].

ZÁVER

Rozvoj MPN a ich prípadná progresia do sAML je dlhotrvajúci a niekoľkostupňový proces asociovaný s klonálnou selekciami mutovaných HSCs (obr. 2). Molekulárna diagnostika a biológia spolu s rozsiahlymi epidemiologickými štúdiami významným spôsobom rozšírili naše poznatky o patogenéze MPN. Ukažuje sa, že genetické pozadie jedinca vytvára základ pre familiárnu predispozíciu k rozvoju MPN. Vrodené rizikové alely môžu modulovať biologické vlastnosti HSCs a tým im poskytovať selekčnú výhodu. Na podklade mitotickej rekombinácie a homozygotizácie rizikových alel a v súčinnosti so získanými somatickými mutáciami môže postupne dochádzať k rozvoju CHIP. So zvyšujúcim sa vekom a získaním somatickej „driver“ mutácie sa následne naplno rozvíja klonálna hematopoéza, ktorá sa môže manfestovať vo forme chronickej myeloproliferácie a v tomto stave pretrvávať aj roky (obr. 2A). Podľa nového, alternatívneho modelu vzniku MPN dochádza k získaniu somatickej „driver“ mutácie veľmi skoro (dokonca pred narodením), ale k signifikantnej klonálnej expanzii dôjde až po desiatkach rokov v súvislosti so zmienenými rizikovými faktormi spojenými so starnutím krvotvorby (obr. 2B). K transformácii do sAML dochádza v dôsledku akumulácie ďalších mutácií, ktoré zvyšujú onkogénny potenciál klonu. Paralelne môže vznikať aj niekoľko rôznych klonov, nesúcich odlišné somatické mutácie. Tieto klony môžu mať aj odlišné fenotypové charakteristiky a vyzkoušať rôznu citlivosť na liečbu a schopnosť vyvolať relaps ochorenia.

Faktory, ktoré vedú k rozvoju MPN a tie, ktoré prispievajú k ich výraznej fenotypovej variabilite sú heterogénné a doposiaľ nie dostatočne vysvetlené. Ďalší intenzívny výskum je preto nevyhnutný, aby sme lepšie pochopili patogenézu MPN a mohli nové poznatky úspešne integrovať do klinickej praxe s cieľom spresniť diagnostiku, prognostiku a liečbu MPN.

ZOZNAM POUŽITÝCH SKRATIEK

AML – akútnej myeloidnej leukémie
aUPD – získaná uniparentálna dizómia
ATM – *ataxia telangiectasia mutated*
ASXL1 – *additional sex comb-like 1*
BCR:ABL1 – *breakpoint cluster region: Abelson*
CALR – kalretikulín
CHEK2 – checkpoint kináz 2
CHIP – klonálna hematopoéza s neurčitým potenciáлом
CML – chronická myeloidná leukémia
CNL – chronická neutrofílna leukémia
DNMT3 – DNA (cytozín-5)-metyltransferáza 3A
DUSP1 – *dual specificity phosphatase 1*
EPOR – erytropoetínový receptor
ET – esenciálna trombocytémia
EZH2 – *enhancer of zeste homolog 2*
FH – fumarát hydratáza
FLT3 – *Fms related receptor tyrosine kinase 3*
G-CSFR – receptor pre kolónie granulocytov stimulujúci faktor
GFI1B – *growth factor independence 1b*
GWAS – celogenómová asociačná štúdia
HBS1L-MYB – intergénová oblasť medzi HBS1L a MYB
HSC – hematopoetická kmeňová bunka
IFN γ – interferón γ
IL-1b – interleukín 1b
JAK2 – Janusova kináz 2
mCALR – mutovaný CALR
MDS – myelodysplastický syndróm
MECOM – *MDS1 and EVI1 complex locus*
MPL (TPOR) – trombopoetínový receptor
MPN – myeloproliferatívne neoplázie
MRE11 – *meiotic recombination 11 homolog*
NF-E2 – *nuclear factor erythroid-2*
NBN – nibrín
NGS – *next generation sequencing*
NRAS – *neuroblastoma RAS viral oncogene homolog*
Ph – chromozóm Filadelfia
PINT – *p53 induced transcript*
PMF – primárna myelofibróza
PV – polycytémia vera
RUNX1 – *runt-related transcription factor 1*
sAML – sekundárna akútnej myeloidnej leukémia
SF3B1 – *splicing factor 3b subunit 1*
SH2B3 – SH2B adaptoričkový proteín 3
SRSF2 – *serine and arginine rich splicing factor 2*
STAT – *signal transducer and activator of transcription*
TERT – telomerázová reverzná transkriptáz
TET2 – tet metylcytozín dioxygenáza 2
TGF β – transformujúci rastový faktor β
TNF α – tumor nekrotizujúci faktor α
TM2D3 – *TM2 domain containing 3*
TPOR (MPL) – trombopoetínový receptor
TP53 – tumorový protein p53
U2AF1 – *U2 small nuclear RNA auxiliary factor 1*

Literatúra

1. Dameshek W. Some speculation on the myeloproliferative syndromes. *Blood*. 1951;6:372–375.
2. Rumi E, Cazzola M. Diagnosis, risk stratification, and response evaluation in classical myeloproliferative neoplasms. *Blood*. 2017;129:680–692.
3. Arber DA, Orazi A, Hasserjian R, et al. The 2016 revision to the World Health Organization classification of myeloid neoplasms and acute leukemia. *Blood*. 2016;127:2391–2405.
4. Kralovics R, Stockton DW, Prchal JT. Clonal hematopoiesis in familial polycythemia vera suggests the involvement of multiple mutational events in the early pathogenesis of the disease. *Blood*. 2003;102:3793–3796.
5. Landgren O, Goldin LR, Kristinsson SY, Helgadottir EA, Samuelsson J, Bjorkholm M. Increased risks of polycythemia vera, essential thrombocythemia, and myelofibrosis among 24,577 first-degree relatives of 11,039 patients with myeloproliferative neoplasms in Sweden. *Blood*. 2008;112:2199–2204.
6. Rumi E, Passamonti F, Della Porta MG, et al. Familial chronic myeloproliferative disorders: clinical phenotype and evidence of disease anticipation. *J Clin Oncol*. 2007;25:5630–5635.
7. Tegg EM, Thomson RJ, Stankovich JM, et al. Anticipation in familial hematologic malignancies. *Blood*. 2011;117:1308–1310.
8. Nowell PC, Hungerford DA. Chromosome studies on normal and leukemic human leukocytes. *J Natl Cancer Inst*. 1960;25:85–109.
9. Ren, R. Mechanisms of BCR-ABL in the pathogenesis of chronic myelogenous leukaemia. *Nat Rev Cancer*. 2005;5:172–183.
10. Nieborowska-Skorska M, Kopinski PK, Ray R, et al. Rac2-MRC-cIII-generated ROS cause genomic instability in chronic myeloid leukemia stem cells and primitive progenitors. *Blood*. 2012;119:4253–4263.
11. Baxter E, Scott L, Cambell P, et al. Acquired mutation of the tyrosine kinase JAK2 in human myeloproliferative disorder. *Lancet*. 2005;365:1054–1061.
12. Kralovics R, Passamonti F, Buser A, et al. A gain-of-function mutation of JAK2 in myeloproliferative disorders. *N Engl J Med*. 2005;352:1779–1790.
13. James C, Ugo V, Le Couedic J, et al. A unique clonal JAK2 mutation leading to constitutive signalling causes polycythaemia vera. *Nature*. 2005;434:1144–1148.
14. Levine RL, Wadleigh M, Cools J, et al. Activating mutation in the tyrosine kinase JAK2 in polycythemia vera, essential thrombocythemia, and myeloid metaplasia with myelofibrosis. *Cancer Cell*. 2005;7(4):387–397.
15. Klampfl T, Gisslinger H, Harutyunyan AS, et al. Somatic mutations of calreticulin in myeloproliferative neoplasms. *N Engl J Med*. 2013;369:2379–2390.
16. Nangalia J, Massie CE, Baxter EJ, et al. Somatic CALR mutations in myeloproliferative neoplasms with nonmutated JAK2. *N Eng J Med*. 2013;369:2391–2405.
17. Defour JP, Chachoua I, Pecquet C, Constantinescu SN. Oncogenic activation of MPL/thrombopoietin receptor by 17 mutations at W515: implications for myeloproliferative neoplasms. *Leukemia*. 2016;30:1214–1216.
18. Pardanani AD, Levine RL, Lasho T, et al. MPL515 mutations in myeloproliferative and other myeloid disorders: a study of 1182 patients. *Blood*. 2006;108:3472–3476.
19. O'Sullivan J, Mead AJ. Heterogeneity in myeloproliferative neoplasms: Causes and consequences. *Adv Biol Regul*. 2019;71:55–68.
20. Van Egeren D, Escabi J, Nguyen M, et al. Reconstructing the lineage histories and differentiation trajectories of individual cancer cells in myeloproliferative neoplasms. *Cell Stem Cell*. 2021;28:514–523.
21. Williams N, Lee J, Moore L, et al. Phylogenetic reconstruction of myeloproliferative neoplasm reveals very early origins and lifelong evolution. *bioRxiv*; publikováno elektronicky 9. novembra 2020. doi:10.1101/2020.11.09.374710.
22. Jatiani SS, Baker SJ, Silverman LR, Reddy EP. JAK/STAT pathways in cytokine signaling and myeloproliferative disorders. *Genes Cancer*. 2010;1:979–993.
23. Takahashi K, Patel KP, Kantarjian H, et al. JAK2 p.V617F detection and allele burden measurement in peripheral blood and bone marrow aspirates in patients with myeloproliferative neoplasms. *Blood*. 2013;122:3784–3786.
24. Jaiswal S, Fontanillas P, Flannick J, et al. Age-related clonal hematopoiesis associated with adverse outcomes. *N Engl J Med*. 2014;371:2488–2498.
25. Scott L. The JAK2 exon 12 mutations: a comprehensive review. *Am J Hematol*. 2011;86:668–676.
26. Gold LI, Eggleton P, Sweetwyne MT, et al. Calreticulin: non-endoplasmic reticulum functions in physiology and disease. *Faseb J*. 2010;24:665–683.
27. Pietra D, Rumi E, Ferretti VV, et al. Differential clinical effects of different mutation subtypes in CALR-mutant myeloproliferative neoplasms. *Leukemia*. 2016;30:431–438.
28. Kaushansky K. Thrombopoietin. *N Engl J Med*. 1998;339:746–754.
29. Staerk J, Lacout C, Sato T, Smith SO, Vainchenker W, Constantinescu SN. An amphipathic motif at the transmembrane-cytoplasmic junction prevents autonomous activation of the thrombopoietin receptor. *Blood*. 2006;107:1864–1871.
30. Haider M, Elala YC, Gangat N, Hanson CA, Tefferi A. MPL mutations and palpable splenomegaly are independent risk factors for fibrotic progression in essential thrombocythemia. *Blood Canc J*. 2016;10:e347.
31. Ding J, Komatsu H, Wakita A, et al. Familial essential thrombocythemia associated with

- a dominant-positive activating mutation of the c-MPL gene, which encodes for the receptor for thrombopoietin. *Blood*. 2004;103:4198–4200.
- 32.** Beer PA, Campbell PJ, Scott LM, et al. MPL mutations in myeloproliferative disorders: analysis of the PT-1 cohort. *Blood*. 2008;112:141–149.
- 33.** Milosevic Feenstra JD, Nivarthi H, Gisslinger H, et al. Whole-exome sequencing identifies novel MPL and JAK2 mutations in triple-negative myeloproliferative neoplasms. *Blood*. 2016;127:325–332.
- 34.** Harutyunyan AS, Kralovics R. Role of germline genetic factors in MPN pathogenesis. *Hematol/Oncol Clin North Am*. 2012;1037–1051.
- 35.** Cabagnols X, Favale F, Pasquier F, et al. Presence of atypical thrombopoietin receptor (MPL) mutations in triple-negative essential thrombocythemia patients. *Blood*. 2016;127:333–342.
- 36.** Beer PA, Jones AV, Bench AJ, et al. Clonal diversity in the myeloproliferative neoplasms: independent origins of genetically distinct clones. *Br J Haematol*. 2009;144:904–908.
- 37.** Usseglio F, Beaufils N, Calleja A, Raynaud S, Gebart J. Detection of CALR and MPL mutations in low allelic burden JAK2 V617F essential thrombocythemia. *J Mol Diagn*. 2017;19:92–98.
- 38.** Bernal M, Jiménez P, Puerta J, Ruiz-Cabello F, Jurado M. Co-mutated CALR and MPL driver genes in a patient with myeloproliferative neoplasm. *Ann Hematol*. 2017;96:1399–1401.
- 39.** Thompson ER, Nguen T, Kankanige Y, et al. Clonal independence of JAK2 and CALR or MPL mutations in comutated myeloproliferative neoplasms demonstrated by single cell DNA sequencing. *Haematologica*. 2021;106:313–315.
- 40.** Lundberg P, Karow A, Nienhold R, et al. Clonal evolution and clinical correlates of somatic mutations in myeloproliferative neoplasms. *Blood*. 2014;123:2220–2228.
- 41.** Grinfeld J, Nangalia J, Green AR. Molecular determinants of pathogenesis and clinical phenotype in myeloproliferative neoplasms. *Haematologica*. 2017;102:2–12.
- 42.** Guglielmelli P, Lasho TL, Rotunno G, et al. The number of prognostically detrimental mutations and prognosis in primary myelofibrosis: an international study of 797 patients. *Leukemia*. 2014;28:1804–1810.
- 43.** Delhommeau F, Dupont S, Della Valle V, et al. Mutation in TET2 in myeloid cancers. *N Engl J Med*. 2009;360:2289–2301.
- 44.** Stegelmann F, Bullinger L, Schlenk RF, et al. DNMT3A mutations in myeloproliferative neoplasms. *Leukemia*. 2011;25:1217–1219.
- 45.** Ortmann CA, Kent DG, Nangalia J, et al. Effect of mutation order on myeloproliferative neoplasms. *N Engl J Med*. 2015;372:601–612.
- 46.** Nangalia J, Nice FL, Wedge DC, et al. DNMT3A mutations occur early or late in patients with myeloproliferative neoplasms and mutation order influences phenotype. *Haematologica*. 2015;100:e438–e442.
- 47.** O'Sullivan J, Panchal A, Yap C, et al. The mutational landscape in hydroxycarbamide-resistant/intolerant essential thrombocythemia

- treated on the MAJC-ET study. *Hemisphere*. 2018;2:714.
- 48.** Zhang SJ, Rampal R, Manhouri T, et al. Genetic analysis of patients with leukemic transformation of myeloproliferative neoplasms shows recurrent SRSF2 mutations that are associated with adverse outcome. *Blood*. 2012;119:4480–4485.
- 49.** Rampal R, Ahn J, Abdel-Wahab O, et al. Genomic and functional analysis of leukemic transformation of myeloproliferative neoplasms. *Proc Natl Acad Sci USA*. 2014;111:E5401–E5410.
- 50.** Jutzi JS, Bogeska R, Nikoloski G, et al. MPN patients harbor recurrent truncating mutations in transcription factor NF-E2. *J Exp Med*. 2013;210:1003–1019.
- 51.** Ward AF, Braun BS, Shannon KM. Targeting oncogenic Ras signaling in hematologic malignancies. *Blood*. 2012;120:3397–3406.
- 52.** Jones AV, Chase A, Silver RT, et al. JAK2 haplotype is a major risk factor for the development of myeloproliferative neoplasms. *Nat Genet*. 2009;41:446–449.
- 53.** Hermouet S, Vilaine M. The JAK2 46/1 haplotype: a marker of inappropriate myelomonocytic response to cytokine stimulation, leading to increased risk of inflammation, myeloid neoplasm, and impaired defense against infection? *Haematologica*. 2011;96:1575–1579.
- 54.** Jäger R, Harutyunyan AS, Rumi E, et al. Common germline variation at the TERT locus contributes to familial clustering of myeloproliferative neoplasms. *Am J Hematol*. 2014;89:1107–1110.
- 55.** Iapper W, Jones AV, Kralovics R, et al. Genetic variation at MECOM, TERT, JAK2 and HBS1L-MYB predisposes to myeloproliferative neoplasms. *Nat Commun*. 2015;6:6691.
- 56.** Hinds DA, Barnolt K, Mesa RA, et al. Germ line variants predispose to both JAK2 V617F clonal hematopoiesis and myeloproliferative neoplasms. *Blood*. 2016;128:1121–1128.
- 57.** Loh PR, Genovese G, McCarroll SA. Monogenic and polygenic inheritance become instruments for clonal selection. *Nature*. 2020;584:136–141.
- 58.** Bao EL, Nandakumar SK, Liao X. Inherited myeloproliferative neoplasm risk affects hematopoietic stem cells. *Nature*. 2020;586:769–775.
- 59.** Mambet C, Babosova O, Defour JP, et al. Cooccurring JAK2 V617F and R1063H mutations increase JAK2 signaling and neutrophilia in myeloproliferative neoplasms. *Blood*. 2018;132:2695–2699.
- 60.** Lanikova L, Babosova O, Swierczek S, et al. Coexistence of gain-of-function JAK2 germ line mutations with JAK2V617F in polycythemia vera. *Blood*. 2016;128:2266–2270.
- 61.** Schulze S, Stengel R, Jaekel N, et al. Concomitant and noncanonical JAK2 and MPL mutations in JAK2V617F- and MPLW515 L-positive myelofibrosis. *Genes Chromos Cancer*. 2019;58:747–755.
- 62.** Benton CB, Prajwal CB, DiNardo CD, et al. Janus Kinase 2 variants associated with the transformation of myeloproliferative neoplasms into acute myeloid leukemia. *Cancer*. 2019;125:1855–1866.
- 63.** Marty C, Saint-Martin C, Pecquet C, et al. Germ-line JAK2 mutations in the kinase domain are responsible for hereditary thrombocytosis and are resistant to JAK2 and HSP90 inhibitors. *Blood*. 2014;123:1372–1383.
- 64.** Ricci K, Huber E, Raj A, et al. Compound heterozygosity of two novel JAK2 mutations in hereditary essential thrombocythemia implicates important monomer-monomer interactions in thrombopoiesis signaling. *Blood*. 2016;128:3137.
- 65.** Kapralova K, Horvathova M, Pecquet C, et al. Cooperation of germline JAK2 mutations E846D and R1063H in hereditary erythrocytosis with megakaryocytic atypia. *Blood*. 2016;128:1418–1423.
- 66.** Srour SA, Devesa SS, Morton LM, et al. Incidence and patient survival of myeloproliferative neoplasms and myelodysplastic/myeloproliferative neoplasms in the United States, 2001–12. *Br J Haematol*. 2016;174:382–396.
- 67.** Harman D. The free radical theory of aging: effect of age on serum copper levels. *J Gerontol*. 1965;20:151–153.
- 68.** Kurosawa S, Iwama A. Aging and leukemic evolution of hematopoietic stem cells under various stress conditions. *Inflamm Regen*. 2020;40:29.
- 69.** Sørensen AL, Hasselbalch HC. Smoking and Philadelphia-negative chronic myeloproliferative neoplasms. *Eur J Haematol*. 2016;97:63–69.
- 70.** Schultz MB, Sinclair DA. When stem cells grow old: phenotypes and mechanisms of stem cell aging. *Development*. 2016;143:3–14.
- 71.** Kovtonyuk LV, Fritsch K, Feng X, et al. Inflamm-aging of hematopoiesis, hematopoietic stem cells, and the bone marrow microenvironment. *Front Immunol*. 2016;7:502.
- 72.** Ho YH, Méndez-Ferrer S. Microenvironmental contributions to hematopoietic stem cell aging. *Haematologica*. 2020;105:38–46.
- 73.** Barraco D, Mora B, Guglielmelli P, et al. Gender effect on phenotype and genotype in patients with post-polycythemia vera and post-essential thrombocythemia myelofibrosis: results from the MYSEC project. *Blood Cancer J*. 2018;8:89.
- 74.** Pecquet C, Diaconu CC, Staerk J, et al. Thrombopoietin receptor down-modulation by JAK2 V617F: restoration of receptor levels by inhibitors of pathologic JAK2 signaling and of proteasomes. *Blood*. 2012;119:4625–4635.
- 75.** Parganas E, Wang D, Stravopodis D, et al. Jak2 is essential for signaling through a variety of cytokine receptors. *Cell*. 1998;93:385–395.
- 76.** Hasselbalch HC, Bjørn RnME. MPNs as inflammatory diseases: the evidence, consequences, and perspectives. *Mediators Inflamm*. 2015;2015:e102476.
- 77.** Vaidya R, Gangat N, Jimma T, et al. Plasma cytokines in polycythemia vera: phenotypic correlates, prognostic relevance, and comparison with myelofibrosis. *Am J Hematol*. 2012;87:1003–1005.

78. Pourcelot E, Trocme C, Mondet J, Bailly S, Toussaint B, Mossuz P. Cytokine profiles in polycythemia vera and essential thrombocythemia patients: clinical implications. *Exp Hematol.* 2014;42:360–368.

79. Stetka J, Vyhliadlova P, Lanikova L, et al. Addiction to DUSP1 protects JAK2V617F-driven polycythemia vera progenitors against inflammatory stress and DNA damage, allowing chronic proliferation. *Oncogene.* 2019;38:5627–5642.

PODIEL AUTOROV NA PRÍPRAVE RUKOPISU

BK – príprava rukopisu a obrázkovej dokumentácie

KHK – podiel na príprave rukopisu
VD a MH – korekcia a revízia rukopisu

článku nebolo podporené žiadou farmaceutickou firmou.

Do redakce doručeno dne 7. 5. 2021.

Přijato po recenzi dne 13. 5. 2021.

doc. Mgr. Monika Horváthová, Ph.D.

Ústav biologie

LF UP v Olomouci

Hněvotínská 3

775 15 Olomouc

e-mail: monika.horvathova@upol.cz

POĎAKOVANIE

Práca vznikla za podpory Ministerstva zdravotníctva Českej republiky (NU21-03-00338) a Interného grantu Univerzity Palackého (IGA_LF_2021_004). Ďakujeme prof. MUDr. Dagmar Pospišilovej, Ph.D. za cenné pripomienky pri príprave rukopisu.

ČESTNÉ PREHLÁSENIE AUTOROV

Autori práce potvrdzujú, že v súvislosti s téhou, vznikom a publikovaním tohto článku nie sú v strete záujmov a vznik ani publikovanie